

Synthesis of Parasite Related Carbohydrates and their Use as Probes for Glycobiology

Inaugural-Dissertation

to obtain the academic degree

Doctor rerum naturalium (Dr. rer. nat.)

Submitted to the Department of Biology, Chemistry and Pharmacy
of Freie Universität Berlin

by

Sebastian Andreas Götze

December 2013

The work in this PhD thesis was performed between March 2010 and November 2013 in the Department of Biomolecular Systems, Max Planck Institute of Colloids and Interfaces and Institute of Chemistry and Biochemistry, Freie Universität Berlin under the guidance of Prof. Dr. Peter H. Seeberger.

1st Reviewer: Prof. Dr. Peter H. Seeberger

2nd Reviewer: Prof. Dr. Rudolf Tauber

Date of oral defense: 24.03.2014

Acknowledgements

At first I want to thank Prof. Dr. Peter H. Seeberger and Dr. Daniel Varón Silva for their support over the last years.

I would like to thank Prof. Dr. Rudolf Tauber for agreeing to review this thesis and his thoughtful comments.

My deepest thanks go to Felix Bröcker, Andreas Geißner, Reka Kurucz, Stefan Matthies, Eike Wamhoff and Markus Weishaupt not only for carefully proofreading this thesis but also for their constant help and excellent troubleshooting skills over the last years.

I would like to express my gratefulness to Yu-Hsuan Tsai for sharing his experience in regard to GPI chemistry and many valuable late stage intermediates as well as Dr. Marie-Lyn Hecht who familiarized me with the laboratory and glycobiology. I am also much obliged to Dr. Nahid Azzouz who introduced me to the wonderful field of parasitology and *T. gondii* infection biology.

In addition, I want to thank my collaboration partners Felix Wojcik, Dr. Alexander G. O'Brien, Dr. Ivan Vilotijevic, Maurice Grube, Anika Reinhardt, Annette Wahlbrink, Dr. Jonathan Hudon, Dr. Yan Liu, Prof. Dr. Ten Feizi, Dr. Yoshiki Yamaguchi, Dr. Shinya Hanashima, Akemi Ikeda, Prof. Dr. Minoru Fukuda, Dr. Motohiro Nonaka, Prof. Dr. Uwe Groß, Prof. Dr. Paul A. MacAry and Dr. Conrad E. Chan for their hard work and commitment.

I thank past and current members of the Seeberger group for valuable discussions and precious carbohydrates.

Finally I want to thank my family, my roommate Dustin Nielow and my close friends for supporting me during this unique period of life.

*Nur wer von Herzen negativ denkt,
kann positiv überrascht werden.*

Albert Einstein

Summary

Carbohydrates are a class of structurally diverse biomolecules that surround every cell of all living organisms. Glycans found on mammalian cells differ significantly from saccharides presented on the surface of pathogenic organisms. Therefore the immune system of higher animals can differentiate self from non-self by interacting with sugars displayed on plasma membranes and consequently raise an immune response against foreign carbohydrate structures to eliminate pathogens. Investigating the immunogenicity of a sugar or its interaction with a carbohydrate binding protein to assess structure-activity relationships is difficult, because an amplification method for glycans does not exist and isolation of reasonable quantities of single molecular species remains challenging. Chemical synthesis of oligosaccharides has emerged as a strategy to overcome the aforementioned obstacles. The goal of this thesis was the generation of a library of pathogen related carbohydrates and their employment in different *in vitro* and *in vivo* essays to analyze their interaction with the immune system or single components thereof.

In the first part of this thesis (Chapter 2) a general and convergent method, which features a set of fully orthogonal protecting groups allowing the introduction of late stage modifications, was used to prepare derivatives of glycosylphosphatidylinositol (GPI) anchors and their corresponding substructures. The synthesized compounds resemble the phosphoglycan moiety of GPIs presented on the plasma membrane of the apicomplexan parasite *Toxoplasma gondii*. All synthetic carbohydrates were equipped with either a thiol or amine linker that enables fabrication of neoglycoconjugates and carbohydrate microarrays.

In the second part of this thesis (Chapter 3) two *T. gondii*-specific GPI glycans were coupled to the carrier protein CRM₁₉₇ to form two neoglycoconjugates, which were evaluated for their immunogenic properties in an animal model. The IgG immune response elicited by the glycoconjugates in mice was highly specific towards the full phosphoglycans exhibiting no cross-reactivity towards a structurally closely related mammalian GPI or corresponding substructures. Furthermore, it was shown that the polyclonal mouse serum recognized *T. gondii* tachyzoites revealing distinct differences in the surface localization of the two glycolipids. Carbohydrate microarray analysis of sera from humans suffering from toxoplasmosis confirmed that GPIs of *T. gondii* are immunogenic and capable of inducing an

early IgM response in infected individuals (in collaboration with Prof. Dr. Uwe Groß, Universitätsklinikum Göttingen). Taken together these results form the basis for the development of a GPI-based vaccine against this obligate parasite and a diagnostic tool for the detection of toxoplasmosis in humans. However, further tests and challenge studies will be required to evaluate the protective properties of this potential carbohydrate conjugate vaccine.

In the last part of this thesis (Chapter 4) the binding preferences of the human lectin ZG16p, which may be involved in innate immunity, were defined by using glycan microarray and NMR studies (in collaboration with Prof. Ten Feizi, Glycosciences Laboratory, Imperial College, London and Dr. Yoshiki Yamaguchi, Structural Glycobiology Team, RIKEN, Tokyo). A glycan microarray analysis identified phosphatidylinositol mannosides (PIMs), which are major cell wall components of some pathogenic bacteria including *Mycobacterium tuberculosis*, as novel ZG16p ligands. On this account analogs of these glycolipids were synthesized and employed in STD-NMR experiments to define binding epitopes. These findings raise the possibility that human lectin ZG16p is involved in the mucosal immune response by ‘opsonizing’ mycobacteria *via* an interaction with PIMs on the cell surface of the pathogen. This hypothesis is subject for future investigations.

Zusammenfassung

Kohlenhydrate gehören zu einer Klasse strukturell diverser Biomoleküle, die jede Zelle aller lebenden Organismen umgeben. Glykane die auf Säugetierzellen vorhanden sind unterscheiden sich signifikant von Sacchariden die auf der Oberfläche von pathogenen Erregern vorkommen. Auf Grund dieser Differenz kann das Immunsystem höherer Tiere durch Interaktionen mit Zuckern, die auf der Plasmamembran präsentiert sind, Fremdorganismen von eigenen Körperzellen unterscheiden und eine Immunantwort, die Pathogene eliminiert, gegen körperfremde Kohlenhydrate erzeugen. Die Untersuchung der Immunogenizität von Zuckern oder ihre Wechselwirkung mit Kohlenhydrat-bindenden Proteinen, um Struktur-Wirkungsbeziehungen zu erstellen, ist schwierig, da keine Vervielfältigungsmethode für Glykane existiert und die Isolierung angemessener Mengen reiner Saccharide anspruchsvoll ist. Die chemische Synthese von Oligosacchariden wurde deshalb als Strategie gewählt um die obengenannten Hürden zu umgehen. Das Ziel dieser Doktorarbeit war die Generierung einer pathogen-assoziierten Kohlenhydratbibliothek und deren Verwendung in verschiedenen *in vitro* und *in vivo* Experimenten, um ihre Wechselbeziehung mit dem Immunsystem oder einzelnen Komponenten davon zu untersuchen.

Im ersten Teil dieser Dissertation (Kapitel 2) wurde eine generelle und konvergente synthetische Methode, welche als Besonderheit einen Satz an vollkommen orthogonalen Schutzgruppen aufweist und eine Einführung von verschiedenen Modifizierungen im späten Stadium der Synthese ermöglicht, genutzt, um Derivate von Glycosylphosphatidylinositol (GPI)-Ankern und deren entsprechenden Substrukturen darzustellen. Die synthetischen Kohlenhydrate spiegeln die Phosphoglykanstruktur von GPIs wieder, welche auf der Plasmamembran des Parasiten *Toxoplasma gondii*, der zu den Apicomplexa gehört, vorliegen. Alle Verbindungen wurden entweder mit einem Thiol- oder Amino-Linker versehen, der die Anfertigung von Glykanmicroarrays oder Neoglycoproteinen erlaubt.

Im zweiten Teil dieser Dissertation (Kapitel 3) wurden zwei *T. gondii* spezifische GPI-Glykane kovalent mit dem Carrier Protein CRM₁₉₇ verknüpft, um zwei Neoglycoproteine herzustellen, deren Immunogenizität in einem Tiermodell evaluiert wurde. Die IgG Immunreaktion, welche durch die Glykoconjugate ausgelöst wurde, war hochspezifisch und

gegen die komplette Phosphoglycanstruktur gerichtet. Kreuzreaktionen gegen unterschiedliche Substrukturen oder einen strukturell eng verwandten GPI-Anker, der in Säugetierzellen vorkommt, konnten nicht festgestellt werden. Des Weiteren konnte gezeigt werden, dass das erhaltene polyklonale Mausserum *T. gondii* Tachyzoiten erkennt und es deutliche Unterschiede in der Lokalisierung der GPIs auf der Oberfläche des Parasiten gibt. Eine Glykanmicroarrayanalyse von Blutseren, welche von Menschen stammen, die an einer Toxoplasmose leiden, bestätigte, dass GPIs von *T. gondii* immunogen sind und eine frühe IgM Immunreaktionen in Menschen hervorrufen (in Zusammenarbeit mit Prof. Dr. Uwe Groß, Universitätsklinikum Göttingen). Zusammenfassend lässt sich sagen, dass diese Resultate die Basis für die Entwicklung eines GPI-basierten *T. gondii* Impfstoffes und diagnostischen Tests, der eine Toxoplasmose in Menschen nachweisen kann, darstellen. Allerdings müssen noch weitere Untersuchungen und Challenge Studien durchgeführt werden um die protektiven Eigenschaften dieser potentiellen Kohlenhydratimpfstoffe bewerten zu können.

Im letzten Teil dieser Dissertation (Kapitel 4) wurde die Bindungspräferenz des humanen Lectins ZG16p, welches möglicherweise einen Teil der angeborenen Immunantwort darstellt, mit Hilfe von Glykanmicroarrays und NMR-Experimenten bestimmt (in Zusammenarbeit mit Prof. Ten Feizi, Glycosciences Laboratory, Imperial College, London und Dr. Yoshiaki Yamaguchi, Structural Glycobiology Team, RIKEN, Tokyo). Eine Glykanmicroarrayanalyse konnte Phosphatidylinositol Mannoside (PIMs), die einen Hauptbestandteil der Zellwand von verschiedenen pathogenen Bakterien wie beispielsweise *Mycobacterium tuberculosis* ausmachen, als neue Liganden von ZG16p identifizieren. Aus diesem Grund wurden Analoga dieser Glycolipide synthetisiert und in STD-NMR Experimenten verwendet, um deren Bindungsepitope zu bestimmen. Die erhaltenen Ergebnisse unterstützen die Hypothese, dass dieses Lectin eine Rolle während der Immunabwehr in der Darmschleimhaut spielt, in dem es Mykobakterien durch die Interaktion mit den PIMs auf deren Oberfläche “opsonisiert“. Diese Theorie ist Gegenstand zukünftiger Forschung.

Table of Contents

Acknowledgements.....	i
Summary.....	iii
Zusammenfassung.....	v
Table of Contents.....	vii
Abbreviations.....	ix
Chapter 1 General Introduction to Glycosciences.....	1
1.1 Structure, Biosynthesis and Function of Carbohydrates.....	2
1.2 Surface Organization of Pathogenic Microbial Agents.....	12
1.3 Methods in Glycosciences.....	17
1.4 Aim and Outline of the Thesis.....	19
Chapter 2 Chemical Synthesis of GPI Derivatives and their Corresponding Substructures.....	21
2.1 GPIs of <i>T. gondii</i> – Potential Vaccine Candidates against Toxoplasmosis.....	21
2.2 Retrosynthetic Analysis of GPI Derivatives.....	24
2.3 Synthesis of the Pseudodisaccharide Building Block.....	27
2.4 Preparation of GPI Derivatives.....	30
2.5 Synthesis of GPI Substructures.....	36
2.6 Conclusions and Perspectives.....	41
2.7 Experimental Part.....	42
Chapter 3 Synthetic GPIs for Medical Applications.....	108
3.1 Preparation of GPI-Based Glycoconjugates.....	108
3.2 Immunological Evaluation of GPI-Based Glycoconjugates.....	111
3.3 Diagnostic Potential of Synthetic GPI Glycans.....	115
3.4 Conclusion and Outlook.....	120
3.5 Experimental Part.....	121
Chapter 4 Defining the Interaction of Human Lectin ZG16p and Mycobacterial PIMs.....	129
4.1 The Human Lectin ZG16p.....	129

4.2 Identification of Novel Binding Partners of ZG16p Using a Carbohydrate Microarray.....	132
4.3 Chemical Synthesis of PIM Glycans.....	134
4.4 STD-NMR Analysis of the Interaction between PIM1/2 and ZG16p.....	136
4.5 Possible Role of ZG16p in Mucosal Immune Response.....	141
4.6 Experimental Part.....	143
List of References.....	157
List of Publications.....	166
<i>Curriculum vitae</i> – Sebastian Götze.....	167
Appendix.....	170
A. Characterization of the Interaction between the Chemokine CCL20 and Synthetic Heparins.....	170
B. Determination of the Binding Motif of the Monoclonal Antibody my2F12.....	177
C. Development of a Fully Synthetic Glycolipid Vaccine Targeted against the Cancer Associated T _N -antigen.....	182
D. Synthetic Substructures of GPI-Anchors as NMR probes for the Investigation of the Torsion of the Conserved GPI Core.....	198




















Abbreviations

$[\alpha]^{20}_D$	Specific rotation
Å	Angstrom
AAG	2-Acyl-1-alkyl- <i>sn</i> -glycerol
Ac	Acetyl
ADP	Adenosine-5'-diphosphate
AF	Amplification factor
ALG	1-Alkyl-2- <i>lyso</i> - <i>sn</i> -glycerole
AO	<i>N</i> -aminoxyacetyl-1,2-dihexadecyl- <i>sn</i> -glycero-3-phosphoethanolamine
Ara	D-Arabinose
Arg	L-Arginine
Asn	L-Asparagine
Asp	L-Aspartic acid
ATP	Adenosine-5'-triphosphate
ATR	Attenuated total reflectance
Bn	Benzyl
Boc	<i>tert</i> -Butyloxycarbonyl
BSA	Bovine serum albumin
Bu	Butyl
c	centi
calcd	calculated
CAN	Cer(IV)-ammoniumnitrat
Cbz	Carboxybenzyl
CD	Cluster of differentiation
Cer	Ceramide
CFA	Complete Freund's Adjuvant
COD	1,5-Cyclooctadiene
Con A	Concanavalin A
COSY	Correlation spectroscopy
CRD	Carbohydrate recognition domain
CSA	Camphorsulfonic acid
D	L-Aspartic acid
Da	Dalton
DAG	1,2-Diacyl- <i>sn</i> -glycerole
DAPI	4',6-Diamidino-2-phenylindole
DBU	1,8-Diazabicyclo[5.4.0]undec-7-ene
DCM	Dichloromethane
DC-SIGN	Dendritic cell-specific intercellular adhesion molecule-3-grabbing non-integrin
DDQ	2,3-Dichloro-5,6-dicyano-1,4-benzoquinone
DHAP	2',4',-Dihydroxyacetophenone
DHPE	1,2-Dihexadecyl- <i>sn</i> -glycero-3-phosphoethanolamine
DIPEA	<i>N,N</i> -Diisopropylethylamine
DMEM	Dulbecco's Modified Eagle's Medium
DMF	Dimethylformamide
DMSO	Dimethylsulfoxide
DNA	Deoxyribonucleic acid
Dol	Dolichol
DTT	Dithiothreitol
<i>E. coli</i>	<i>Escherichia coli</i>

ELISA	Enzyme Linked Immunosorbent Assay
equiv.	Equivalent
ESI	Electrospray ionization
Et	Ethyl
f	femto
<i>f</i>	Furanoside
FcR γ	Fc receptor common γ signaling chain
FI	Fluorescence intensity
FITC	Fluorescein isothiocyanate
FTIR	Fourier transform infrared spectroscopy
Fuc	L-Fucose
g	gram
GAG	Glycosaminoglycan
Gal	D-Galactose
GalT	Galactosyltransferase
Glc	D-Glucose
GlcNAc	D- <i>N</i> -Acetylglucosamine
GlcNH ₂	D-Glucosamine
GlcUA	D-Glucuronic acid
Gly	Glycine
GPI	Glycosylphosphatidylinositol
GPI-GnT	GPI-GlcNAc transferase
GSL	(2S,3S,4R)-1- <i>O</i> -(α -D-galactosyl)- <i>N</i> -hexacosanoyl-2-amino-1,3,4-octadecanetriol
GST	Glutathione- <i>S</i> -transferase
h	hour
HBTU	<i>N,N,N',N'</i> -Tetramethyl- <i>O</i> -(1 <i>H</i> -benzotriazol-1-yl)uronium hexafluorophosphate
HEV	High endothelial venules
HFF	Human foreskin fibroblast
HMBC	Heteronuclear multiple bond correlation
HOBt	Hydroxybenzotriazole
HSQC	Heteronuclear single quantum correlation
HV	High vacuum
Hyl	L-Hydroxylysine
Hyp	L-Hydroxyproline
IFA	Incomplete Freund's Adjuvant
Ig	Immunoglobulin
Ino	Inositol
ITC	Isothermal titration calorimetry
k	kilo
K_D	Dissociation constant
L	liter
LAM	Lipoarabinomannan
Leu	L-Leucine
Lev	Levulinyl
LM	Lipomannan
LPS	Lipopolysaccharide
LTA	Lipoteichoic acids
Lys	L-Lysine
M	mol·L ⁻¹

m	milli
μ	micro
mAGP	Mycolyl-arabinogalactan–peptidoglycan
MALDI	Matrix-assisted laser desorption/ionization
Man	D-Mannose
Man-LAM	Mannose-capped lipoarabinomannan
ManT	Mannosyltransferase
MBL	Mannose-binding lectin
<i>M. bovis</i>	<i>Mycobacterium bovis</i>
Me	Methyl
min	minute
Mincle	Macrophage inducible C-type lectin
MS	Molecular sieves or Mass spectroscopy
<i>M. smegmatis</i>	<i>Mycobacterium smegmatis</i>
<i>M. tuberculosis</i>	<i>Mycobacterium tuberculosis</i>
MDO	Membrane-derived oligosaccharides
mol	mole
MRC	Macrophage mannose receptor
MurNAc	<i>N</i> -Acetylmuramic acid
N	<i>L</i> -Asparagine
n	nano
NAP	2-Naphthylmethyl
NMR	Nuclear magnetic resonance
NHS	<i>N</i> -Hydroxysuccinimide
<i>o</i>	<i>ortho</i>
obsd	Observed
p	pico
<i>p</i>	<i>para</i>
P or P _i	Phosphate
PCR	Polymerase chain reaction
Pd/C	Palladium on charcoal
PEtn	Phosphoethanolamine
PI	1- <i>O</i> -(2-acyl-1-alkyl- <i>sn</i> -glyceryl-phosphonato)-D-myo-inositol
PIM	Phosphatidylinositol mannoside
PIG	Phosphatidylinositol glycan
PI-LAM	Phospho inositol-capped lipoarabinomannan
Piv	Pivaloyl
<i>P. falciparum</i>	<i>Plasmodium falciparum</i>
PMB	<i>p</i> -Methoxybenzyl
PP _i	Pyrophosphate
ppm	Parts per million
<i>p</i> -TsOH	<i>p</i> -Toluenesulfonic acid
Py	Pyridine
Reg	Regenerating islet-derived
R _f	Retention factor
Rha	L-Rhamnose
RNA	Ribonucleic acid
ROC	Receiver operating characteristic
ROESY	Rotating frame nuclear Overhauser effect spectroscopy
rpm	Rounds per minute
r.t.	Room temperature

s	second
S	Sulfate
SAG1	Surface Antigen 1
SAG2	Surface Antigen 2
sat.	Saturated
SEC	Size exclusion chromatography
Ser	L-Serine
Sia	General term for <i>O</i> - and <i>N</i> -derivatives of neuraminic acid
SIGLEC	Sialic acid binding Ig-like lectin
SPPS	Solid phase peptide synthesis
SPR	Surface plasmon resonance
STD	Saturation transfer difference
Sulfo-GMBS	Sodium <i>N</i> -(γ -maleimidobutyryloxy)-sulfosuccinimide ester
TA	Teichoic acid
TB	Tuberculosis
TBAF	Tetra- <i>n</i> -butylammonium fluoride
TBAI	Tetra- <i>n</i> -butylammonium iodide
TBDPS	<i>tert</i> -Butyldiphenylsilyl
TBS	<i>tert</i> -Butyldimethylsilyl
TCEP	Tris(2-carboxyethyl)phosphine
TDM	Trehalose 6,6'-dimycolate
TEA	Triethylamine
<i>tert</i>	<i>tertiary</i>
Tf	Trifluoromethanesulfonyl
TFA	Trifluoroacetic acid
THF	Tetrahydrofuran
Thr	L-Threonine
TIPS	Triisopropylsilyl
TMM	Trehalose monomycolate
TMS	Trimethylsilyl
TNF- α	Tumor necrosis factor alpha
TOCSY	Total correlation spectroscopy
TOF	Time of flight
Trp	L-Tryptophan
Ts	Tosyl
Tyr	L-Tyrosine
UTP	Uridine-5'-triphosphate
VSG	Variant Surface Glycoprotein
Xxx	random amino acid
Xyl	D-Xylose
XylT	Xylosyltransferase

 = Xyl	 = Rha
 = Gal	 = Ara
 = Rha	 = GlcUA
 = Sia	 = MurNAc
 = GalNAc	 = <i>myo</i> -Ino
 = Man	 = Mycolic acid
 = GlcNH ₂	 = generic complex sugar
 = Glc	   } = generic proteins
 = GlcNAc	

Chapter 1 – General Introduction to Glycosciences

1.1 Structure, Biosynthesis and Function of Carbohydrates

Carbohydrates are next to proteins, lipids and DNA, which is a glycan itself since it is composed of the sugar 2-deoxy-D-ribose, one of the four major classes of biomolecules. They are the end product of photosynthesis and constitute the biggest part of biomass in the world. Polysaccharides such as amylose, glycogen or amylopectin and their respective metabolites play a central role as physiological energy sources in all living organisms (Figure 1.1, page 2). In addition to this fundamental function carbohydrate based biopolymers also serve as important structural components. Chitin for example amounts for the main part of the exoskeleton of arthropods and cellulose in combination with pectin is utilized for the construction of green plant cell walls.¹ Linear and highly charged GAGs, whose disaccharide repeating unit consists of an amino sugar and a uronic acid or Gal, are employed by nature as gelators to build up extracellular structures like the synovial fluid or the vitreous humour, which contain up to 99% of water.²

However, a considerable amount of glycans is not found in a free form in cell organelles or the extracellular matrix but covalently attached to peptides, proteins and lipids. Those glycoconjugates are defined according to the nature of the glycosidic bond that connects the glycoside to the aglycone (Figure 1.2, page 4). To date five glycan-types have been reported in nature, which are posttranslationally added to proteins.³

In eukaryotic cells complex *N*-glycans are attached to proteins⁴ or peptides⁵ *via* a β -glycosylamine linkage of GlcNAc to the Asn side chain of peptide backbones containing

¹ B. G. Davis, A. J. Fairbanks, in *Carbohydrate Chemistry*, (Ed: S. G. Davies), OXFORD UNIVERSITY PRESS, New York (NY), 2008, Chapter 9.

² V. Hascall, J. D. Esko, in *Essentials of Glycobiology 2nd Ed.*, (Eds: A. Varki, R. D. Cummings, J. D. Esko, H.H. Freeze, P. Stanley, C. R. Bertozzi, G. W. Hart, M. E. Etzler), Cold Spring Harbor Laboratory Press, Cold Spring Harbor (NY), 2009, Chapter 15.

³ R. G. Spiro, *Glycobiology* **2002**, *12*, 43-56.

⁴ R. G. Spiro, *Glycoproteins. Adv. Protein Chem* **1973**, *27*, 349-467.

⁵ A. Seko, M. Kotetsu, M. Nishizono, Y. Enoki, H. R. Ibrahim, L. R. Juneja, M. Kim, T. Yamamoto, *Biochim. Biophys. Acta.* **1997**, *1335*, 23-32.

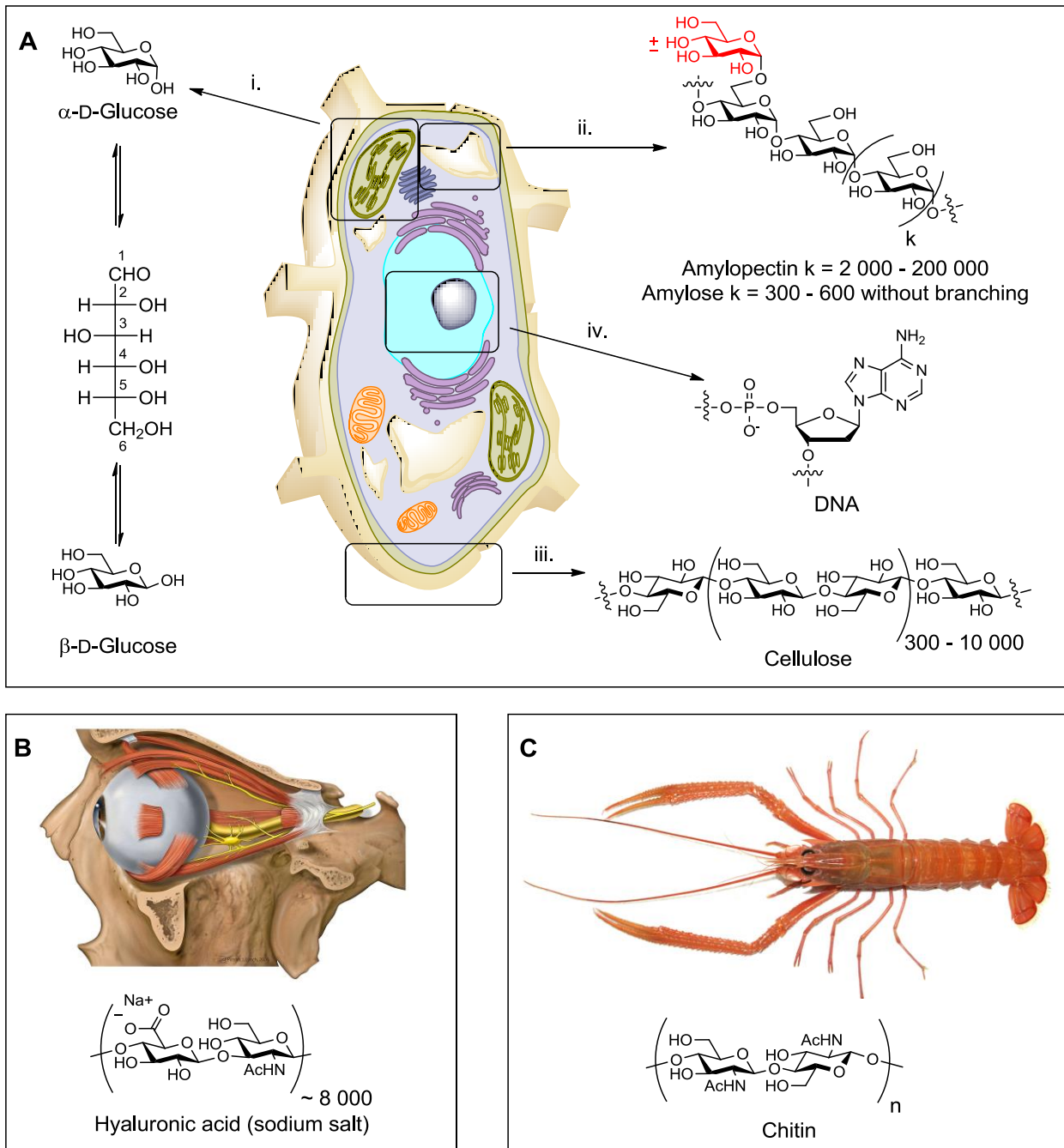


Figure 1.1: Common carbohydrates and their occurrence in nature. (A) Schematic presentation of a green plant cell. i. Glucose is produced during photosynthesis in chloroplasts. In solution the pyranose form of this hexose can interconvert *via* an open ring intermediate into two diastereoisomers called anomers. ii. Starch is an energy storage compound found in plants that consists of amylose and amylopectin. It is accumulated in starch granules or amyloplasts. iii. Cellulose a polysaccharide made of several hundred to over ten thousand β 1 \rightarrow 4 linked D-glucose units. It is synthesized at the plasma membrane and can form microfibrils that are used for building up cell walls. iv. The backbone of DNA, which encodes the genetic instruction, is comprised of a polyphosphodiester of 2-deoxy-D-ribose. (B) Hyaluronic acid is a member of the GAG family and is a major component of the vitreous humour in the eye. Up to 25 000 disaccharide repeating units of GlcUA β 1 \rightarrow 3GlcNAc β 1 \rightarrow 4 form linear and highly charged polysaccharides, which can bind approximately one hundred gram of water per gram of dry hyaluronic acid. (C) Crustaceans use chitin together with calcium carbonate as a composite material to produce tough exoskeletons. It is closely related to cellulose, but contains an *N*-acetyl-group at the C2 position instead of a hydroxyl function, which increases hydrogen bonding between adjacent polymers.

the consensus sequence Asn-X-Ser/Thr. *O*-glycans are more diverse in their structure, because all amino acids or lipids containing a hydroxyl function can potentially be glycosylated with various mono- or oligosaccharides. Prominent examples for *O*-glycans are: 1. GalNAc- α -Ser/Thr, which occurs in clusters on mucins and contributes considerably to the biophysical properties of this protein class⁶; 2. GlcNAc- β -Ser/Thr, a transient protein modification comparable to phosphorylation that occurs in cytoplasmic and nuclear proteins⁷; and 3. Glc β Cer, a biosynthetic precursor for different glycosphingolipids that are enriched in special membrane compartments called lipid rafts⁸. α -C-Mannosylation of the C2 indol carbon of Trp was initially discovered in RNase 2 and represents the only known posttranslational protein modification employing a C-glycan today.⁹ Investigation of IL-12 and various components of the human complement system¹⁰ revealed Trp-X-X-Trp¹¹ as a sequence motif (glycosylation occurs at the first Trp), which is commonly found in protein databases. Therefore C-glycosylation is maybe not a rare but rather neglected event. Phosphoglycosyl bonds represent a form of protein modification found only in lower eukaryotes, especially protozoan parasites. To give an example, Man- α -1-O-(P=O)OH-O-Ser has been observed in several major proteins of different *Leishmania* species, but the biological role of this glycan is still under debate.¹² The process of adding a GPI *via* a Man- α -6-PEt amide linkage to the C-terminus of a protein is termed glypiation. The primary biological role of this among eukaryotes ubiquitous mode of anchoring is to localize the attached protein to the outer surface of the plasma membrane bilayer¹³ and associate it with lipid rafts¹⁴. GPI-anchored proteins are involved in diverse biological processes such as regulation of innate immunity¹⁵, protein trafficking¹⁶ and antigen presentation¹⁷. In addition, their biogenesis is essential for fertilization¹⁸ and homeostasis of blood coagulation as well as neurological function¹⁹.

⁶ M. A. Hollingsworth, B. J. Swanson, *Nat. Rev. Cancer* **2004**, *4*, 45-60.

⁷ G. W. Hart, C. Slawson, G. Ramirez-Correa, O. Lagerlof, *Annu. Rev. Biochem* **2011**, *80*, 825-858.

⁸ K. Jacobson, O. G. Mouritsen, R. G. W. Anderson, *Nat. Cell Biol.* **2007**, *9*, 7-14.

⁹ T. Debeer, J. F. G. Vliegthart, A. Loffler, J. Hofsteenge, *Biochemistry* **1995**, *34*, 11785-11789.

¹⁰ P. Lafite, R. Daniellou, *Nat. Prod. Rep.* **2012**, *29*, 729-738.

¹¹ K. Julenius, *Glycobiology* **2007**, *17*, 868-876.

¹² P. A. Haynes, *Glycobiology* **1998**, *8*, 1-5.

¹³ M. G. Low, *Biochim. Biophys. Acta* **1989**, *988*, 427-454.

¹⁴ Y. Maeda, Y. Tashima, T. Houjou, M. Fujita, T. Yoko-o, Y. Jigami, R. Taguchi, T. Kinoshita, *Mol. Biol. Cell* **2007**, *18*, 1497-1506.

¹⁵ I. A. Rooney, J. E. Heuser, J. P. Atkinson, *J. Clin. Invest.* **1996**, *97*, 1675-1686.

¹⁶ M. Fujita, Y. Maeda, M. Ra, Y. Yamaguchi, R. Taguchi, T. Kinoshita, *Cell* **2009**, *139*, 352-365.

¹⁷ M. A. Ferguson, *J. Cell Sci.* **1999**, *112*, 2799-2809.

¹⁸ Y. Ueda, R. Yamaguchi, M. Ikawa, M. Okabe, E. Morii, Y. Maeda, T. Kinoshita, *J. Biol. Chem.* **2007**, *282*, 30373-30380.

¹⁹ A.M. Almeida, Y. Murakami, D.M. Layton, P. Hillmen, G.S. Sellick, Y. Maeda, S. Richards, S. Patterson, I. Kotsianidis, L. Mollica, D.H. Crawford, A. Baker, M. Ferguson, I. Roberts, R. Houlston, T. Kinoshita, A. Karadimitris, *Nat. Med.* **2006**, *12*, 846-851.

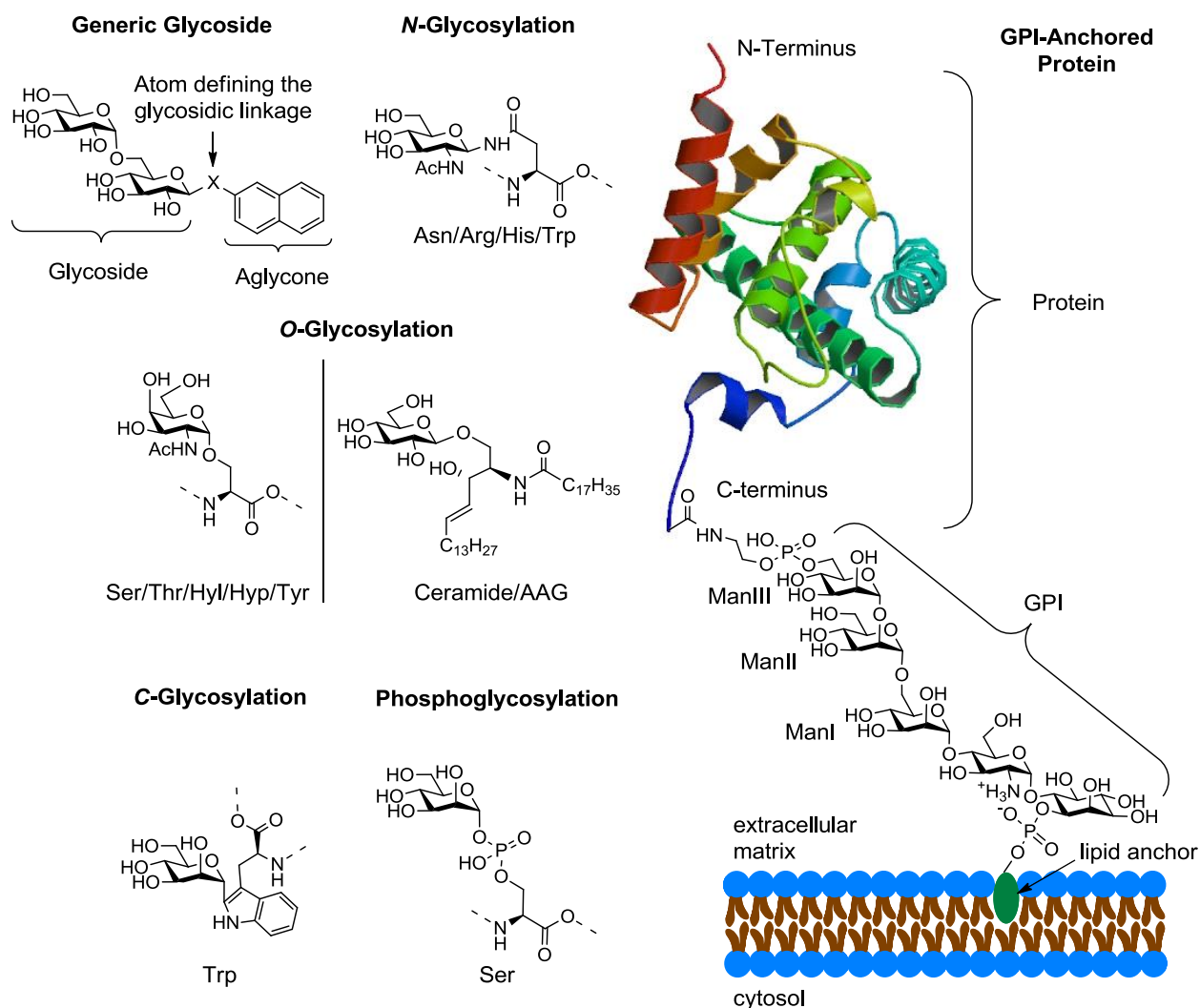


Figure 1.2: A selection of glycoconjugate linkages occurring in nature. Aglycones, which are non-sugar compounds remaining after replacement of the glycosyl group from a glycoside by a hydrogen atom, for different types of glycosylations are listed beneath the examples. The lipid moiety of a GPI can consist of a Cer, AAG, DAG and ALG. Glycosylated natural products are not covered.²⁰

The biosynthesis of glycoconjugates, poly- and oligosaccharides requires a transformation of carbohydrates into high-energy donors (Figure 1.3, page 5).²¹ Nature employs nucleotide sugars as primary glycosylation agents that are generated in the cytoplasm and transported *via* different membrane transporters to other organelles.²² Hence, sugars are first phosphorylated at the anomeric position by a kinase using ATP as a phosphate source, before a pyrophosphorylase under consumption of the corresponding nucleoside triphosphate synthesizes the nucleotide sugar in a condensation reaction.

²⁰ J. S. Thorson, V. Thomas, in *Carbohydrate-Based Drug Discovery*, (Ed. C.-H. Wong), Wiley-VCH Verlag GmbH & Co. KGaA, Weinheim, 2005, Chapter 25.

²¹ E. F. Neufeld, V. Ginsburg, *Annu. Rev. Biochem.* **1965**, *34*, 97-312.

²² C. B. Hirschberg, P. W. Robbins, C. Abeijon, *Annu. Rev. Biochem.* **1998**, *67*, 49-69.

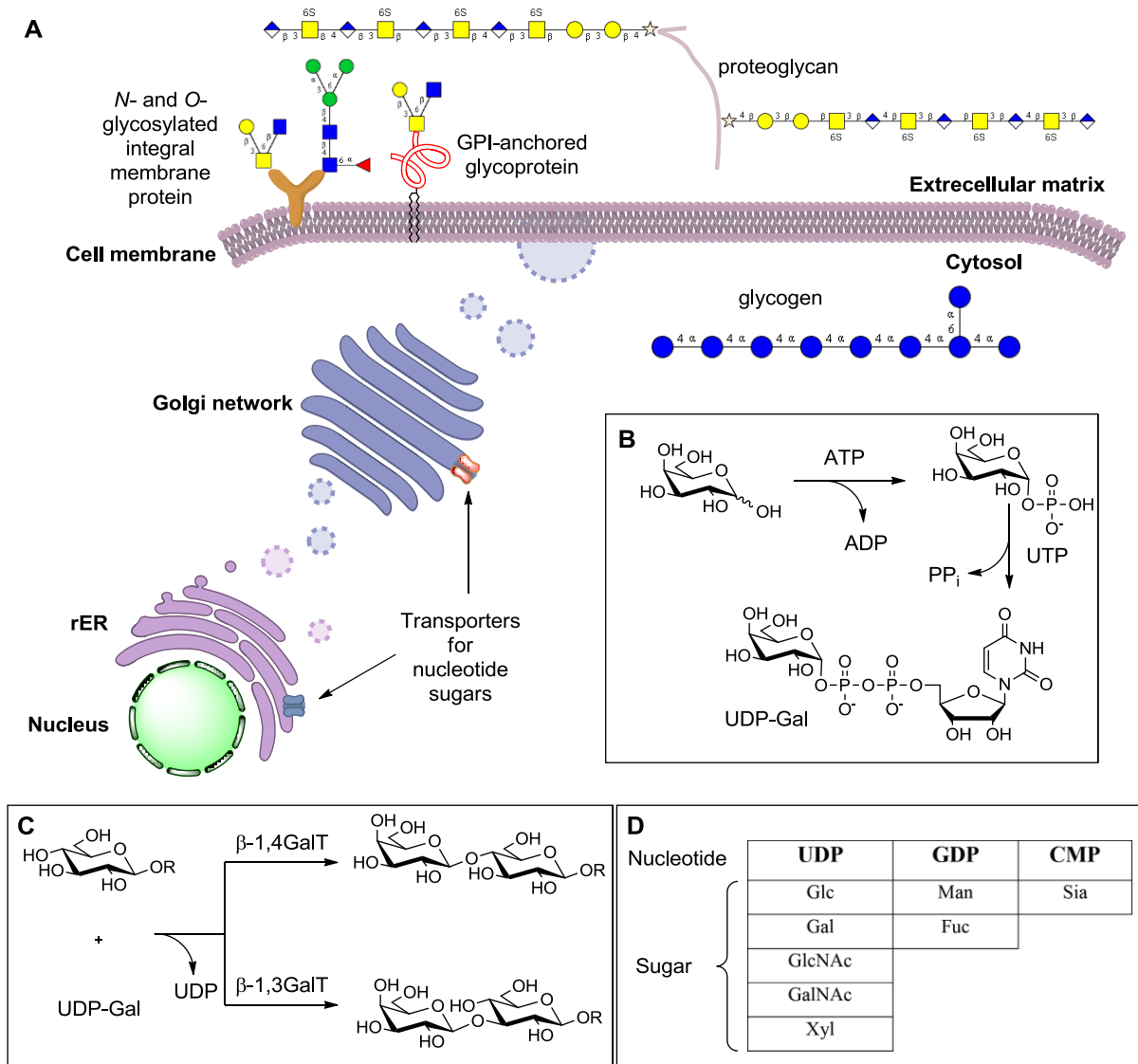


Figure 1.3: (A) Cell compartments, which take part in the anabolism of polysaccharides and glycoconjugates in eukaryotes. (B) Random example for the conversion of a monosaccharide into a nucleotide sugar. (C) Generic examples of glycosyltransferase catalyzed glycosyl bond formations. The specific regioisomer and stereoisomer produced depends on the enzyme employed. (D) The most common nucleotide sugars found in animal cells. Further donors are generated *via* enzyme catalyzed transformations of the depicted metabolic intermediates.^{21,23}

Nine activated sugar donors are known in animal cells, which are added to an aglycone or already existing glycoside in glycosyltransferase-catalyzed glycosylation reactions.²⁴ With the exception of homopolysaccharides such as glycogen, chitin or hyaluronan as well as nuclear and cytoplasmic *O*-glycosylated proteins⁷, which are synthesized in the cytosol, the majority of carbohydrates is assembled in the ER and Golgi network in the form of glycoconjugates. In animal cells the five major types of glycoconjugates originate in the ER, are further modified in the Golgi network and finally secreted into the extracellular matrix or associated

²³ L. V. Bindschedler, E. Wheatley, E. Gay, J. Cole, A. Cottage, G. P. Bolwell, *Plant Mol. Biol.* **2005**, *57*, 285-301.

²⁴ J. C. Paulson, K. J. Colley, *J. Biol. Chem.* **1989**, *264*, 17615-17618.

to the outer leaflet of the plasma membrane (Figure 1.4, page 8). The biosynthesis of *N*-glycans, which all share the biantennary core sequence $\text{Man}\alpha 1\rightarrow 6(\text{Man}\alpha 1\rightarrow 3)\text{Man}\beta 1\rightarrow 4\text{GlcNAc}\beta 1\rightarrow 4\text{GlcNAc}\beta 1\text{-Asn}$, begins on the cytoplasmic side of the ER. GlcNAc- P_i from UDP-GlcNAc is transferred to the isoprene Dol- P_i to generate Dol- PP_i -GlcNAc, which is sequentially extended into a heptasaccharide. Afterwards the heptasaccharide is flipped across the membrane to the luminal side of the ER where it is further elongated into a tetradecasaccharide ($\text{Glc}_3\text{Man}_9\text{GlcNAc}_2\text{-PP}_i\text{-Dol}$) using Dol- P_i -Glc and Dol- P_i -Man as glycosyl transfer agents.²⁵ Subsequently the branched 14-mer is transferred *en bloc* to an Asn-X-Ser/Thr sequon in the nascent protein and is further remodeled in the ER and Golgi by a complex series of reactions catalyzed by membrane-bound glycosidases and glycosyltransferases to finally yield one of the three types (oligomannose, complex or hybrid) of *N*-glycans.²⁶

The assembly of all mucine type *O*-glycans starts in the lumen of the ER. Serine or threonine side chains are glycosylated by ppGalNAcTs employing the corresponding nucleotide sugar as a donor to form the so called T_N -antigen⁶ (GalNAc- α -Ser/Thr), which is the core structure shared by all mucine type *O*-glycans. This glycan is further elongated in the Golgi network by various glycosyltransferases to form a plethora of different oligosaccharides like the ABO blood group antigens. In contrast to *N*-glycans a general consensus sequence that promotes mucine type *O*-glycosylation is not known, only nucleotide sugars are used as glycosylation agents in their biosynthesis and glycosidases are not involved in further processing of GalNAc- α -glycans inside the Golgi network.²⁷

Addition of β -Xyl to Ser in the ER catalyzed by a XylT using UDP-Xyl as a donor displays the starting point for the formation of proteoglycans carrying heparan sulfate and chondroitin sulfate polysaccharides. This type of glycoconjugate consists of a linear core protein, which is linked to one or more covalently attached GAGs, *via* the aforementioned *O*-glycosidic Xyl- β -Ser motif. The first sugar is then extended by three different glycosyltransferases in the Golgi network to form the core tetrasaccharide $\text{GlcUA}\beta 1\rightarrow 3\text{Gal}\beta 1\rightarrow 4\text{Gal}\beta 1\rightarrow 4\text{Xyl}\beta 1\text{-Ser}$ that is further glycosylated, sulfated and epimerized in a cell and tissue dependent manner.²⁸ Given that a consensus sequence for the imperfect process of xylosylation does not exist and sulfotransferases as well as epimerases are acting in a complex, sequential and sometimes competing interplay GAGs from the same proteoglycan can vary tremendously in their

²⁵ C. J. Waechter, *Annu. Rev. Biochem.* **1976**, *45*, 95-112.

²⁶ H. Schachter, *Glycoconjugate J.* **2000**, *17*, 465-483.

²⁷ L. A. Tabak, *Annu. Rev. Physiol.* **1995**, *57*, 547-564.

²⁸ J. D. Esko, S. B. Selleck, *Annu. Rev. Biochem.* **2002**, *71*, 435-471.

chemical structure. Alongside these classes of proteoglycans there exists another type of GAG, namely keratan sulfate, whose disaccharide repeating unit consists of a sulfated poly-*N*-acetylglucosamine, which is not linked to the peptide backbone over a xylose, but is added to terminal residues of *N*- and *O*-glycans *via* specific glycosyltransferases in an alternating fashion.²⁹

Biosynthesis of GPIs in mammals commences on the cytosolic side of the ER with the addition of GalNAc to PI. This reaction is catalyzed by the enzyme GPI-GnT, which consists of six different proteins encoded by the PIG gene family and the dolichol phosphate-mannose biosynthesis regulatory protein, using UDP-GlcNAc as a donor substrate.³⁰ Afterwards the protein PIG-L de-*N*-acetylates the GlcNAc and the sugar is flipped to the luminal side of the ER. Subsequently GPI specific ManTs add further sugars, which are phosphorylated by different ethanolamine phosphate transferases to generate the mature GPI- precursor (PEt→6)Manα1→2(PEt→6)Manα1→6(PEt→2)Manα1→4GlcNH₂α1→6-*myo*-Ino. In the next step proteins containing a GPI-attachment signal peptide at the C-terminus are unified with this precursor by the GPI transamidase. This multi-subunit enzyme cleaves the signal peptide and replaces it with the GPI-precursor by forming an amide bond between the C-terminus of the protein and the PEt attached to the C6-position of ManIII. Further modifications of the carbohydrate moiety of GPIs, e.g. dephosphorylation or glycosylation, are performed in the ER and Golgi network, while fatty acid remodeling of the lipid anchor takes place mostly in the Golgi apparatus.³¹

Glycosphingolipids, the last class of glycoconjugates discussed in this introduction, are synthesized from Cer. Glycosylation of Cer with UDP-Gal in the presence of the corresponding glycosyltransferase on the cytoplasmic side of the ER yields β-linked GalCer that flips to the luminal side and trafficks through the Golgi network where it can be sulfated or sialylated at the C3-position of Gal. In contrast, β-linked GlcCer can be either synthesized on the cytoplasmic face of the ER or early Golgi apparatus, before it flips to the lumen of these organelles. There GlcCer is elongated by various glycosyltransferases, which are substrate specific for nucleotide sugars, to form a large variety of different and mainly sialylated oligosaccharides.³²

²⁹ J. L. Funderburgh, *IUBMB Life* **2002**, *54*, 187-194.

³⁰ T. Kinoshita, M. Fujita, Y. Maeda, *J. Biochem.* **2008**, *144*, 287-294.

³¹ Y. Maeda, T. Kinoshita, *Prog. Lipid Res.* **2011**, *50*, 411-424.

³² T. Kolter, R. L. Proia, K. Sandhoff, *J. Biol. Chem.* **2002**, *277*, 25859–25862.

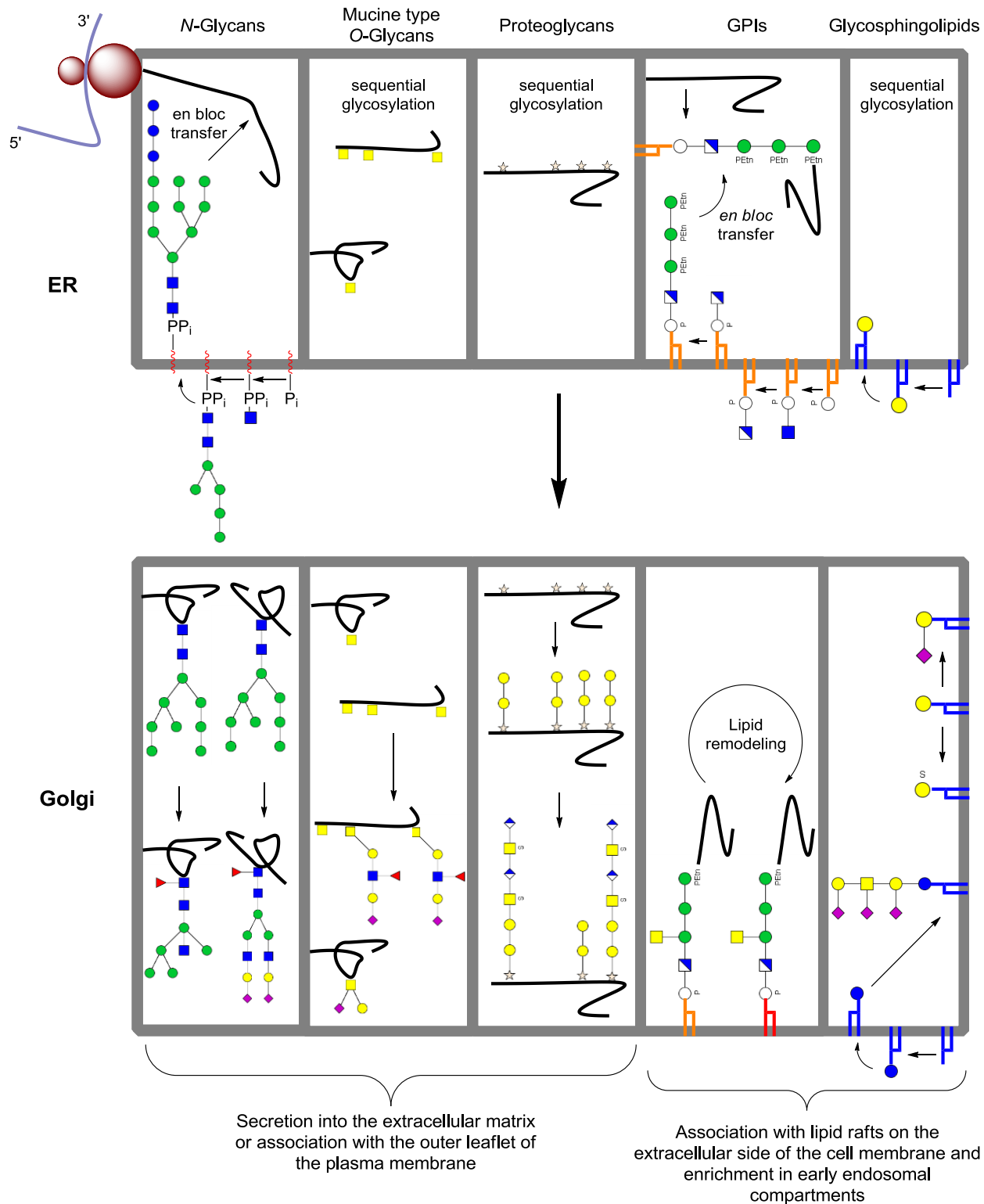


Figure 1.4: Simplified presentation of the biosynthesis of the major types of eukaryotic glycoconjugates in relation to sub-cellular trafficking in the ER-Golgi-plasma membrane pathway. *N*-glycan- and GPI- precursor are built up first in the ER in a stepwise manner, before they are transferred *en bloc* to proteins and further modified in the ER and Golgi apparatus by glycosyltransferases and glycosidases. Mucine type *O*-glycans, proteoglycans and glycosphingolipids are directly assembled *via* a sequential addition of monosaccharides to the corresponding aglycone. Elongation as well as modification of these glycans mainly takes place in the Golgi network.

Given that the majority of glycoconjugates is either secreted or associated with the side of the plasma membrane that faces the extracellular matrix, the surface of all cells existing in nature is covered with a dense layer of carbohydrates, the so-called glycocalyx (Figure 1.5).³³ This sugar coat has the function of a barrier that protects the cell and simultaneously stabilizes and organizes the cell membrane. Carbohydrates covalently linked to proteins not only ensure correct folding of the polypeptide during biosynthesis in the ER, but also preserve their solubility and conformation outside the cell.³⁴ In addition, glycans can provide a shield that protects the subjacent proteins from proteolytic digest or recognition of antibodies.

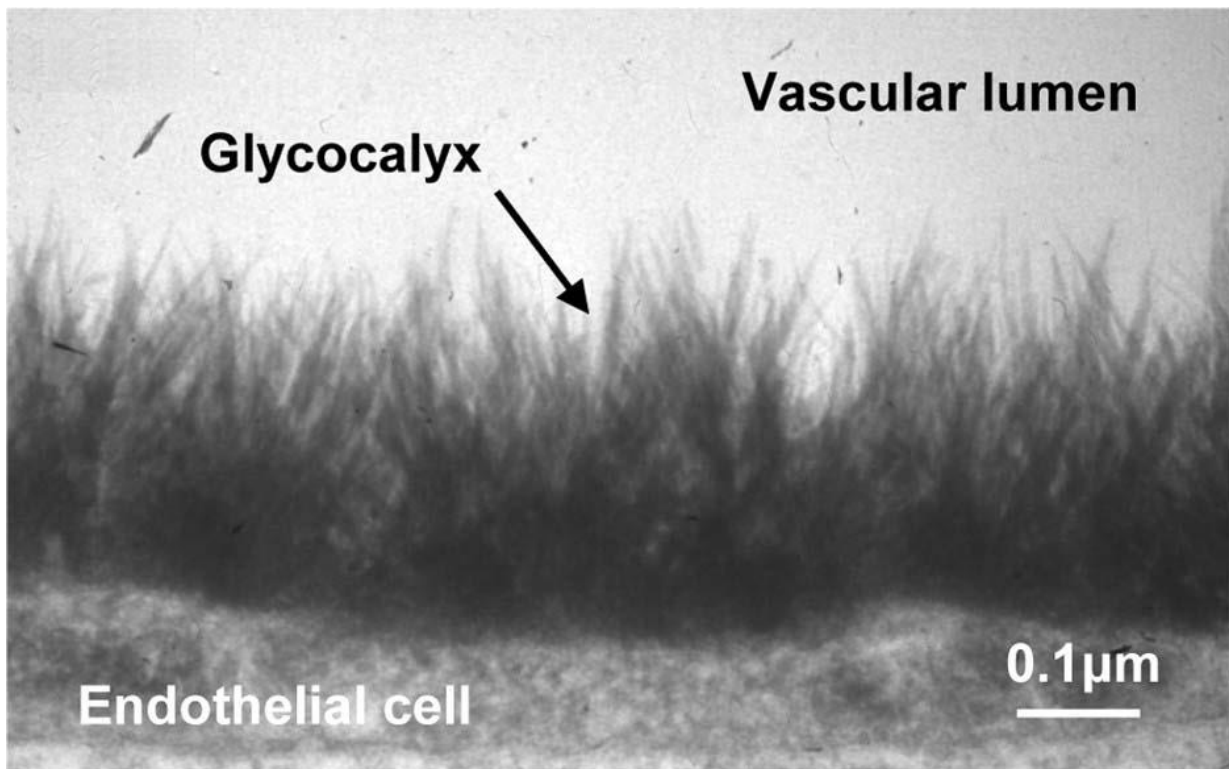


Figure 1.5: Electron microscopy image of an intact glycocalyx of guinea pig heart cells stained with lanthanum nitrate.³⁵

Besides their structure giving and modulatory functions saccharides also serve as ligands for glycan-binding proteins, which are present throughout all biological domains and consist of two major groups termed lectins and glycosaminoglycan-binding proteins.³⁶ The main purpose of animal lectins, which can serve as receptors³⁷, adhesion molecules³⁸ or

³³ A. Varki, *Glycobiology* **1993**, 3, 97-130.

³⁴ A. Helenius, M. Aebi, *Annu. Rev. Biochem.* **2004**, 73, 1019-1049.

³⁵ D.Chappell, M. Jacob, K. Hofmann-Kiefer, M. Rehm, U. Welsch, P. Conzen, B. F. Becker, *Cardiovasc. Res.* **2009**, 83, 388-396.

³⁶ A. Varki, T. Angata, *Glycobiology* **2006**, 16, 1-27.

³⁷ K. Drickamer, M. E. Taylor, *Annu. Rev. Cell Biol.* **1993**, 9, 237-264.

³⁸ M. L. Phillips, E. Nudelmann, F. C. Gaeta, M. Perez, A. K. Singhal, S. I. Hakomori, J. C. Paulson, *Science*, **1990**, 250, 1130-1132.

antibiotics³⁹, is to distinguish between endogenous and exogenous carbohydrates presented on the surface of cells. The glycosylation pattern of microbial invaders is significantly different from animals and therefore a feature that can be used to distinguish between self and non-self cell surface structures on a molecular level. A well-studied example describing an endogenous recognition is CD22, a membrane receptor belonging to the family of SIGLECs that is found on antibody producing B-cells of the mammalian immune system (Figure 1.6, page 11).⁴⁰ B-cell receptors, present on the surface of B-cells, recognize antigenic structures from pathogenic organisms whereupon they get activated, proliferate and produce antibodies against the encountered antigen. CD22 is not involved in this process, because it interacts with its own ligand (a α 2,6-sialylated *N*-acetyllactosamine moiety) that is presented by other glycoconjugates on the cell surface of the B-cell. This binding mode is called *cis* interaction, because the receptor and ligand are displayed on the same cell membrane. However, once the B-cell receptors interact with an auto antigen, which is presented by a neighboring cell that carries the sialylated ligand of CD22 on other membrane proteins, the B-cell is not activated but apoptosis is initiated. Due to the binding of CD22 to its natural ligand on the neighboring cell, which is called a *trans* interaction, this receptor locates next to the B-cell receptors where it is able to blunt the activation of the B-cell and induce programmed cell death. The interaction between a carbohydrate and a lectin is therefore used to identify self-antigens and prevent an autoimmune response by elimination of the cell, displaying the auto reactive B-cell receptor, from the B-cell population.⁴¹ In contrast, lectins like the MRC directly mediate binding and internalization of single-celled pathogens by macrophages through the interaction of exogenous carbohydrate ligands terminating in Man, Fuc or GlcNAc with this membrane receptor.³⁷ MRC is involved in the clearance of foreign serum proteins and neutralization of pathogens such as fungi, viruses and bacteria and discriminates self from non-self *via* binding to sugars of possible pathogenic origin.⁴²

³⁹ H. L. Cash, C. V. Whitham, C. L. Behrendt, L. V. Hooper, *Science* **2006**, *313*, 1126-1130.

⁴⁰ A. H. Courtneya, E. B. Puffera, J. K. Pontrellob, Z.-Q. Yangb, L. L. Kiessling, *Proc. Natl. Acad. Sci.* **2009**, *106*, 2500-2505.

⁴¹ M. S. Macauley, F. Pfrengle, C. Rademacher, C. M. Nycholat, A. J. Gale, A. von Drygalski, J. C. Paulson, *J. Clin. Invest.* **2013**, *123*, 3074-3083.

⁴² G. Szolnoky, Z. Bata-Csörgö, A. S. Kenderessy, M. Kiss, A. Pivarcsi, Z. Novák, K. N. Newman, G. Michel, T. Ruzicka, L. Maródi, A. Dobozy, L. Kemény, *J. Invest. Dermatol.* **2001**, *117*, 205-213.

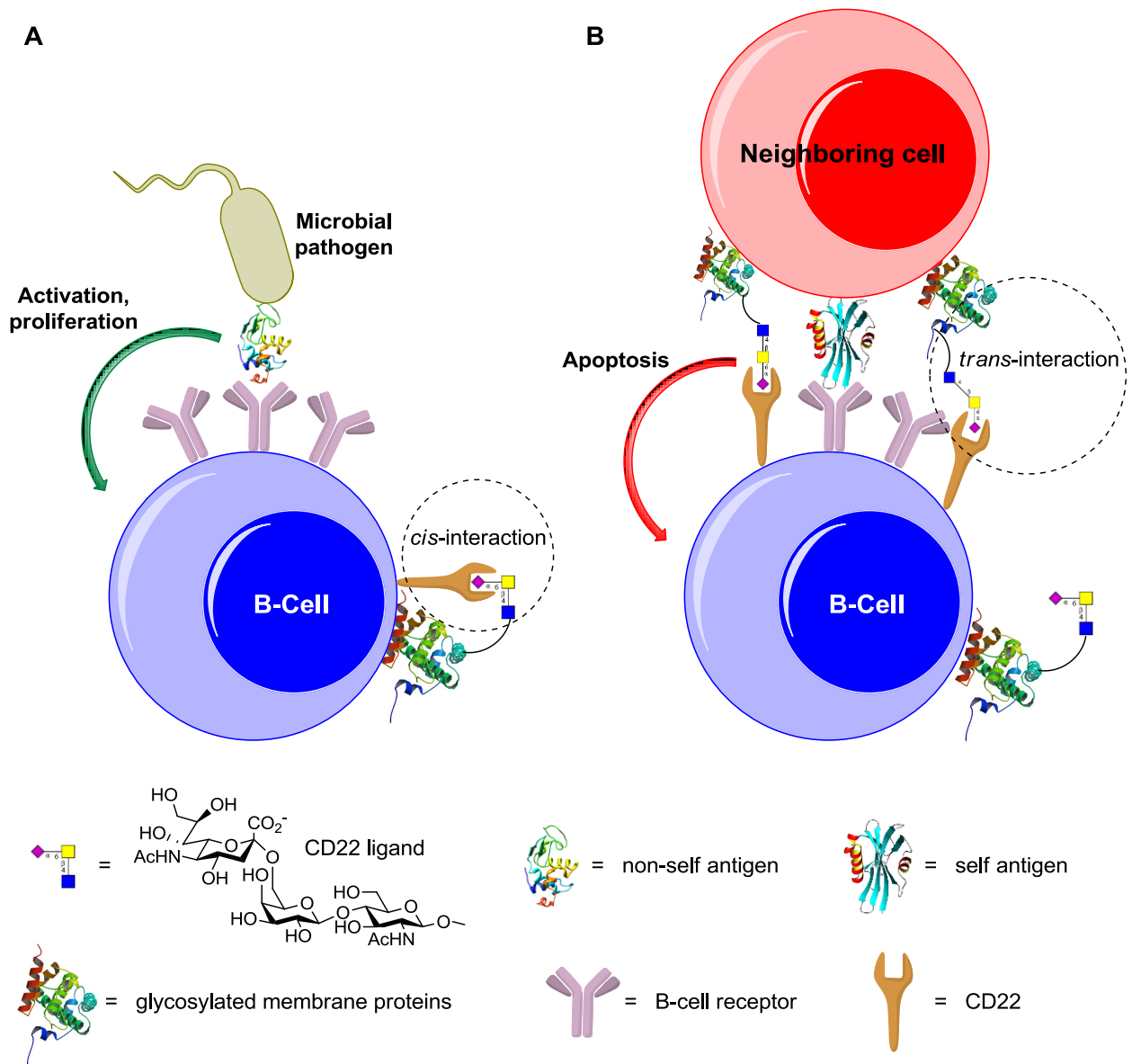


Figure 1.6: Simplified interaction model between a B-cell and (A) a microbial pathogen and (B) a neighboring cell. In both cases the B-cell receptors interact with an antigen displayed by one of the two different cell types. In case (A) the foreign protein causes B-cell activation that leads to proliferation, activation and production of antibodies against the antigen. In case (B) apoptosis is triggered, because the membrane receptor CD22 is translocated to the antigen-B-cell receptor complex *via* a *trans* interaction with its natural sialylated ligand that is displayed by glycoconjugates of the neighboring cell. The carbohydrate ligand interaction is used to discriminate between foreign antigens and possible auto antigens that are displayed by cells of the own organism.

To circumvent an immune reaction or phagocytosis some microbial pathogens even evolve and decorate their surface with sugars that are typical of their hosts. This phenomenon driven by selective forces is called “molecular mimicry”.⁴³

⁴³ L. S. Kreisman, B. A. Cobb, *Glycobiology* **2012**, *22*, 1019-1030.

1.2 Surface Organization of Pathogenic Microbial Agents

The cell surface of eubacteria, mycobacteria and parasitic protozoa differs significantly from animals. Bacteria are divided in Gram-positive and Gram-negative organisms based on their behavior, which depends on the composition of the cell wall, in retaining crystal violet dye during a Gram staining procedure. Gram-negative bacteria like *E. coli* possess a cell wall consisting of inner and outer membranes that are separated by the so-called periplasm.⁴⁴ The outer membrane is asymmetric and contains mainly LPS, which is anchored through the glycolipid Lipid A, in the outer leaflet (Figure 1.7, page 13). In addition mucoid bacteria also synthesize capsular polysaccharides that form the outmost layer of the cell. The inner membrane of all bacteria is surrounded by a polysaccharide composed of the disaccharide unit GlcNAc β 1 \rightarrow 4MurNAc β 1 \rightarrow 4 known as peptidoglycan or murein.⁴⁵ The different layers of peptidoglycan are cross-linked *via* short peptides, which are covalently linked to the lactic acid moiety of the MurNAc unit. Gram-positive bacteria lack the outer membrane, but have a much thicker peptidoglycan layer containing either TA or LTA, which constitute highly charged polymers.⁴⁶

All these polysaccharide components fulfill important structural and functional tasks. Gram-positive bacteria use the peptidoglycan to create a structural barrier to prevent rupture of the cell membrane by osmotic swelling. Gram-negative bacteria use highly charged membrane-derived oligosaccharides (MDO) to create an osmotic buffer in the periplasm, which compensates for their thin peptidoglycan layer, to protect themselves from extreme differences in osmolarity in the environment. The outer membrane is stabilized by divalent cations, which coordinate to Lipid A, and form a dense layer of LPS that is not permeable to proteins. Lipid A is also a potent toxin, which can trigger the secretion of proinflammatory mediators like TNF- α and NO that, in high concentrations, cause fever and septic shock.⁴⁷ During mammalian infection the capsular polysaccharide and LPS can shield bacteria against complement-mediated lysis. In some cases the structure of the capsular polysaccharide is actually identical to carbohydrates produced by the host animal rendering the bacteria resistant against the specific immune system.⁴⁸

⁴⁴ C. R. Raetz, C. M. Reynolds, M.S. Trent, R.E. Bishop, *Annu. Rev. Biochem.* **2007**, 76, 295-329.

⁴⁵ J. van Heijenoort, *Glycobiology* **2001**, 11, 25-36.

⁴⁶ C. Weidenmaier, A. Peschel, *Nat. Rev. Microbiol.* **2008**, 6, 276-287.

⁴⁷ C. Raetz, C. Whitfield, *Annu. Rev. Biochem.* **2002**, 71, 635-700.

⁴⁸ I. S. Roberst, *Annu. Rev. Biochem.* **1996**, 50, 285-315.

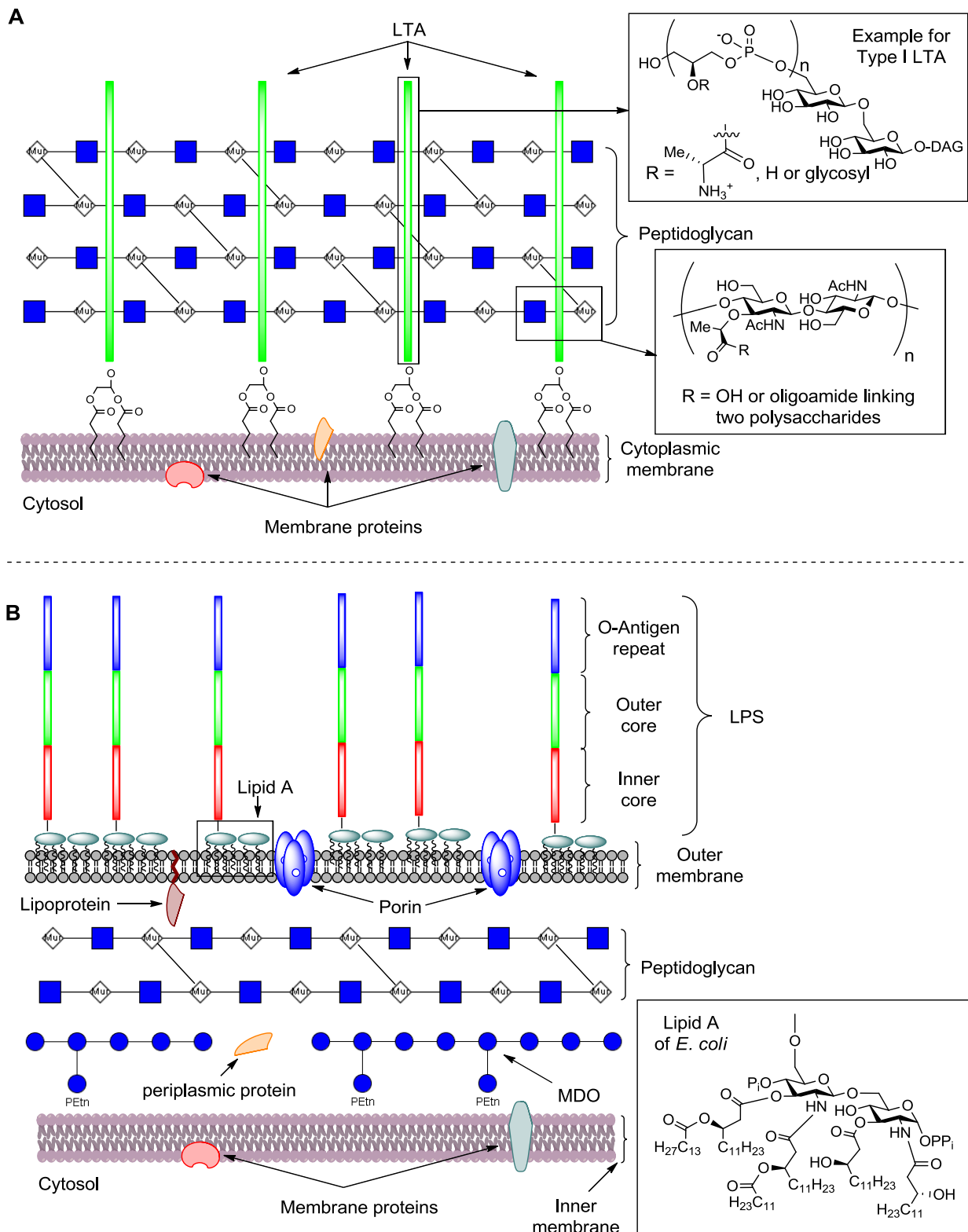


Figure 1.7: Schematic representation of cell walls from (A) Gram-positive and (B) Gram-negative bacteria. Capsular polysaccharides are anchored into the membranes by covalent attachment to different lipids and are omitted for clarity. Capsular polysaccharides⁴⁸, LPS⁴⁷ as well as TA and LTA⁴⁹ feature a high structural diversity.

⁴⁹ J. W. Greenberg, W. Fischer, K. A. Joiner, *Infect. Immun.* **1996**, *64*, 3318-3325.

Mycobacteria are classified as acid-fast Gram-positive bacteria despite the fact that they lack an outer cell membrane. The term acid-fast originates from the fact that after staining mycobacteria with concentrated crystal violet or other dyes these organisms cannot be discolored with standard methods e.g. diluted acids or ethanol-based procedures.⁵⁰ All mycobacterium species share a characteristic cell wall, which is thicker than in almost all other bacteria and has a high content of lipids that constitute up to 60% of their dry weight (Figure 1.8, page 15). The peptidoglycan layer is linked *via* a diglycosyl-phosphodiester bridge ($\text{Rha}\alpha 1 \rightarrow 3\text{GlcNAc}\alpha 1 \rightarrow \text{P} \rightarrow 6\text{MurNAc}$) to arabinogalactan and forms a structure known as the mAGP complex (Figure 1.8). The galactan moiety consists of a linear polygalactofuranoside with an alternating $\beta 1 \rightarrow 5$ and $\beta 1 \rightarrow 6$ linkage pattern. Approximately two to three branched polyarabinofuranosides are attached *via* an $\text{Araf}\alpha 1 \rightarrow 5$ linkage to the 6-linked galactofuranoside residues of one polygalactoside. A hexaarabinose motif that is esterified with four mycolic acids, which are α -alkyl- β -hydroxy fatty acids with a chain length of C60-C90, terminates the non-reducing end of the arabinan part. Lipids like TDM and TMM are intercalated into the terminal mycolates of the mAGP complex and form the mycolic acid layer, which is enclosed by capsule like polysaccharides.⁵¹ In addition to this complex surface organisation different types of mycobacteria like the causative agent of tuberculosis *M. tuberculosis* possess amphipathic lipoglycans, which are inserted into the mycolic acid layer and the plasma membrane. The common precursors of all LAM structures are PIMs (PIM2 and PIM6), which are found as glycoconjugates on the surface of *M. tuberculosis* and other related pathogens. They are partially elongated by $\text{Man}\alpha 1 \rightarrow 6$ homooligosaccharides that have a length of 17-19 residues and carry up to 9 singular $\text{Man}\alpha 1 \rightarrow 2$ branches to create LM. Mature LAM is synthesized by further extension of LM by an unknown linkage with a multiple branched polyarabinofuranoside that consists of about 70 monosaccharaides. LAM can be capped in a species dependent fashion by either mannose or phospho inositol to yield the corresponding Man-LAM (*M. tuberculosis*) or PI-LAM (*M. smegmatis*). The parasite *M. tuberculosis* uses Man-LAM to facilitate the infection of mononuclear phagocytes and to prevent fusion of the phagosome with lysosomal organelles inside the host cell, which protects the pathogen from digestion.⁵²

⁵⁰ N. Ahmad, W. L. Drew, J. J. Plorde, in *Sherrie Medical Microbiology 5th Ed.*, (Eds: K. J. Ryan, C. G. Ray), McGraw-Hill Companies, Inc., New York (NY), 2010, Chapter 27.

⁵¹ V. Bhowruth, L. J. Alderwick, A. K. Brown, A. Bhatt, G. S. Besra, *Biochem. Soc. Trans.* **2008**, *36*, 555-565.

⁵² A. K. Mishra, N. N. Driessen, B. J. Appelmelk, G. S. Besra, *FEMS Microbiol. Rev.* **2011**, *35*, 1126-1157.

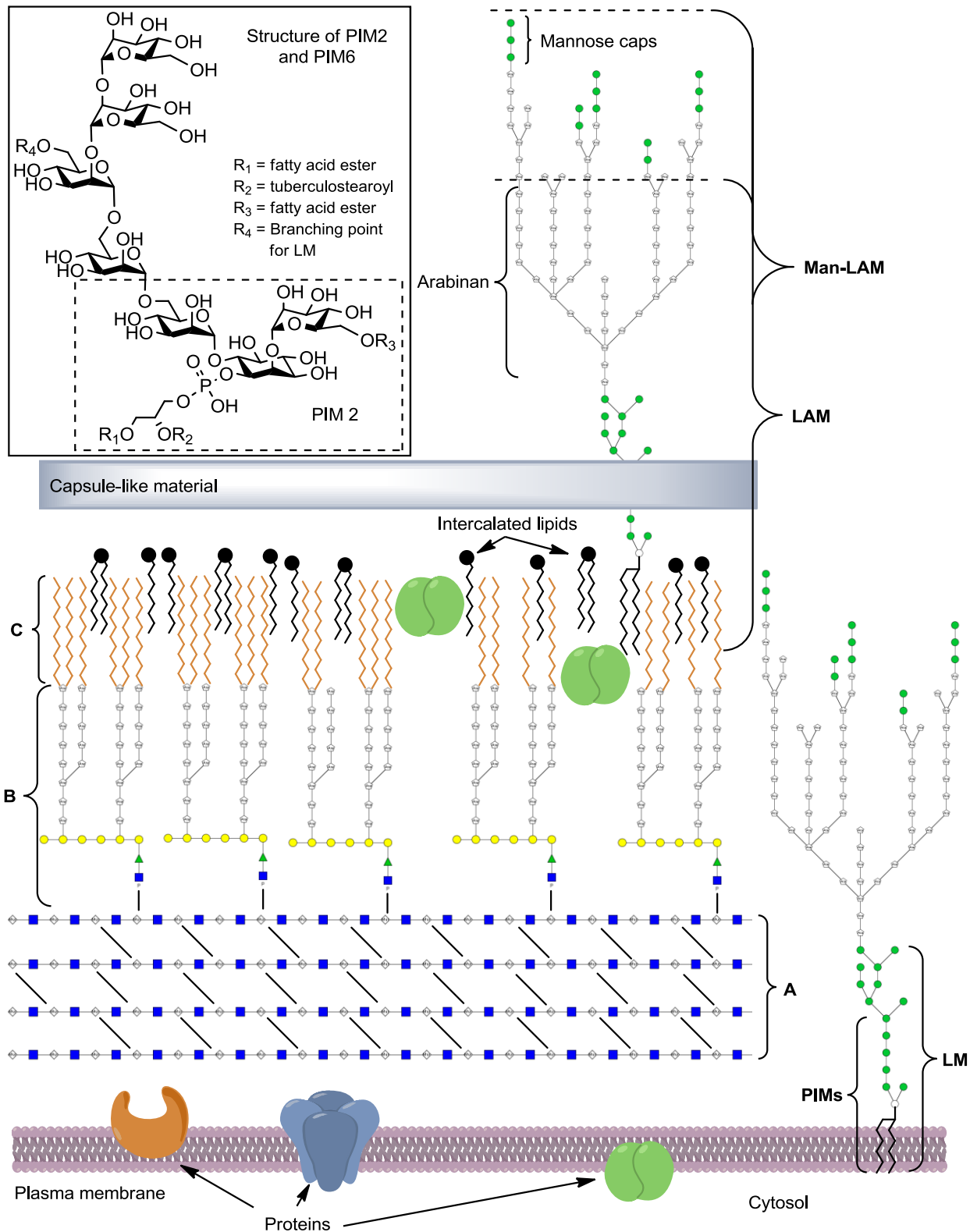


Figure 1.8: Schematic picture of the cell wall of *M. tuberculosis*. (A) Peptidoglycan; (B) arabinogalactan; (C) mycolic acid layer.

In contrast to mammalian cells, which exhibit approximately 10^{4-5} GPI-anchored proteins and glycoproteins per cell, the cell surface of parasitic protozoa like *T. brucei* or *T. gondii* is

covered with up to 5×10^6 GPIs and their corresponding glycoconjugates (Figure 1.9). *T. brucei* uses a dense coat of GPI-anchored heterodimers called VSG to prevent the host immune system from accessing the plasma membrane. The only immunologic response against the parasite is therefore directed against the N-terminus of the VSG, which are all identical. Given that *T. brucei* varies the structure of the VSG in a periodic interval the generated immune response is ineffective against the new glycoprotein coat.⁵³ *T. gondii* in contrast anchors different proteins *via* glypiation to the outer leaflet of the cell membrane, which are crucial for binding (SAG3) and invasion (SAG1) of host cells.⁵⁴

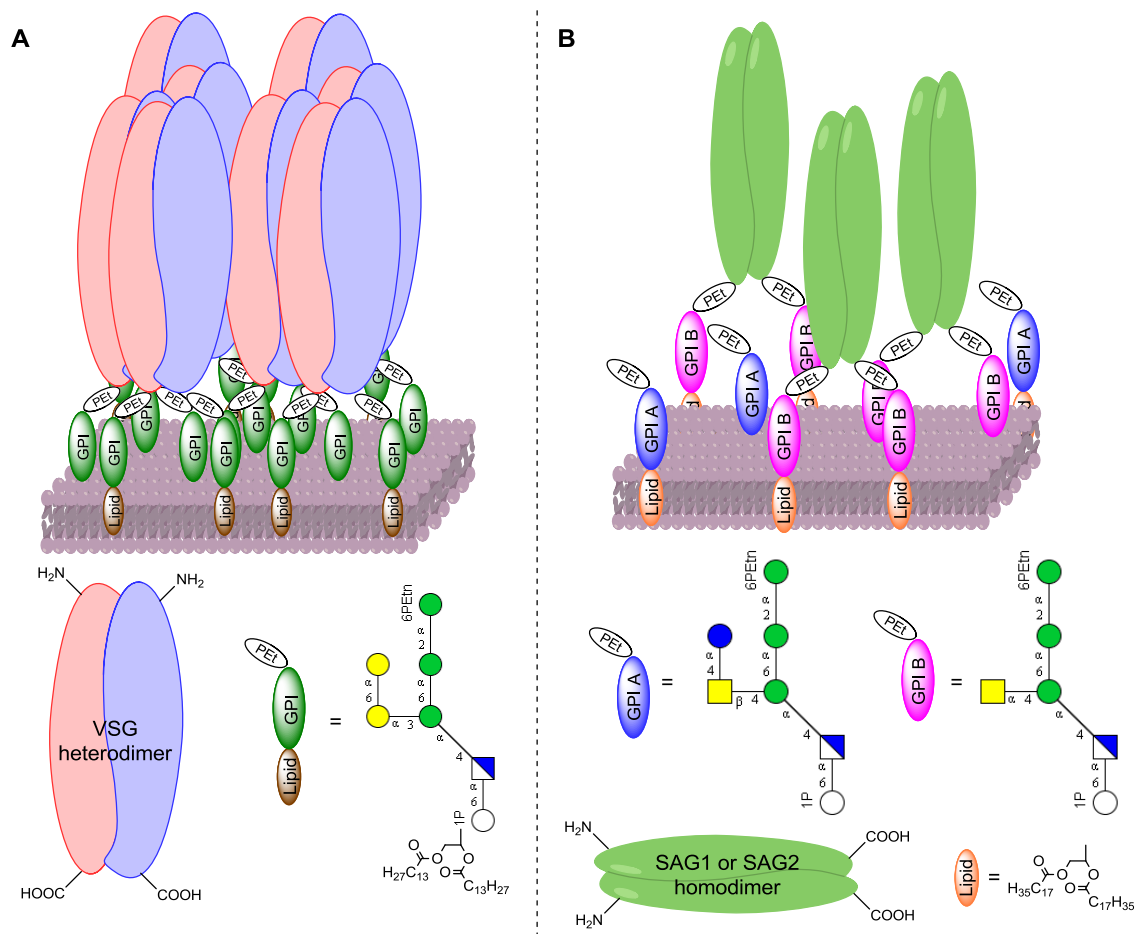


Figure 1.9: Representation of the plasma membrane of (A) *T. brucei* and (B) *T. gondii*. *T. gondii* also possesses GPI A, which is not covalently linked to proteins and induces an early IgM response in humans as well as TNF- α production in macrophages.⁵⁵

⁵³ J. D. Barry, R. McCulloch, *Adv. Parasitol.* **2001**, *49*, 1-70.

⁵⁴ X.-L. He, M. E. Grigg, J. C. Boothroyd, K. C. Garcia, *Nat. Struct. Biol.* **2002**, *9*, 606-611.

⁵⁵ N. Azzouz, H. Shams-Eldin, S. Niehus, F. Debierre-Grockiego, U. Bieker, J. Schmidt, C. Mercier, M. F. Delauw, J.-F. Dubremetz, T. K. Smith, R. T. Schwarz, *Int. J. Biochem. Cell. Biol.* **2006**, *38*, 1914-1925.

1.3 Methods in Glycosciences

Investigating carbohydrate-protein interactions is a fundamental aspect of glycobiology, which is the study of the biological function of glycans. Different NMR techniques and X-ray crystallography in combination with molecular modeling can give insights into the binding mode of proteins with their sugar ligand/s on a molecular level in solution as well as in solid state.⁵⁶ Carbohydrate microarrays have the ability to serve as high-throughput platforms for binding studies, because the interaction of one protein can be investigated with thousands of different glycans in one single experiment.⁵⁷ In addition SPR⁵⁸ and ITC⁵⁹ are methods used for the determination of thermodynamic and kinetic parameters of a binding event between a biomacromolecule and a sugar. A requirement that certainly has to be fulfilled to conduct the aforementioned experiments is access to pure carbohydrates and their corresponding derivatives.

Given that the biosynthesis of sugars is not under genetic control and a proofreading mechanism compared to protein and DNA biosynthesis is nonexistent, isolated glycans and glycoconjugates are usually heterogeneous mixtures of closely related compounds that sometimes cannot be further separated, because their physical properties are too similar. Moreover, amplification procedures for carbohydrates, which are comparable to protein expression in *E. coli* or PCR techniques, have not been developed yet. Therefore the only approach providing sufficient amounts of well-defined oligosaccharides is chemical⁶⁰, chemoenzymatic⁶¹ or enzymatic synthesis⁶². Other advantages of these methods are conformational locking of the reducing end, which simplifies signal assignment in NMR experiments, and site selective introduction of orthogonal linkers. Additionally, synthetic procedures provide substructures, regioisomers or unnatural mimetics, which are used for the

⁵⁶ A. Imberty, H. Lortat-Jacob, S. Pérez, *Carbohydr. Res.* **2007**, *342*, 430–439.

⁵⁷ T. Horlacher, P. H. Seeberger, *Chem. Soc. Rev.* **2008**, *37*, 1414–1422.

⁵⁸ G. Safina, *Anal. Chim. Acta.* **2012**, *712*, 9–29.

⁵⁹ A. Velázquez-Campoy, H. Ohtaka, A. Nezami S. Muzammil, E. Freire, *Curr. Protoc. Cell Biol.* **2004**, *17*, 1–24.

⁶⁰ A. Koizumi, I. Matsuo, M. Takatani, A. Seko, M. Hachisu, Y. Takeda, Y. Ito, *Angew. Chem. Int. Ed.* **2013**, *52*, 7426–7431.

⁶¹ Z. Wang, Z. S. Chinoy, S. G. Ambre, W. Peng, R. McBride, R. P. de Vries, J. Glushka, J. C. Paulson, G.-J. Boons, *Science* **2013**, *341*, 379–383.

⁶² T.-I Tsai, H.-Y. Lee, S.-H. Chang, C.-H. Wang, Y.-C. Tu, Y.-C. Lin, D.-R. Hwang, C.-Y. Wu, C.-H. Wong, *J. Am. Chem. Soc.* **2013**, *135*, 14831–14839.

development of high affinity ligands⁶³ or mapping of immunogenic carbohydrate epitopes in polysaccharides⁶⁴.

⁶³ C. D. Rillahan, E. Schwartz, R. McBride, V. V. Fokin, J. C. Paulson, *Angew. Chem. Int. Ed.* **2012**, *51*, 11014-11018.

⁶⁴ M. A. Johnson, D. R. Bundle, *Chem. Soc. Rev.* **2013**, *42*, 4327-4344.

1.4 Aim and Outline of the Thesis

Surface carbohydrates of microorganisms are important structural motifs that are recognized by different components of the mammalian immune system. Interplay of foreign glycans with lectin receptors can lead to endocytosis of the respective pathogen or initiates a protective immune response. To establish structure-activity relationships of glycan-dependent bacterial infections and host defense mechanisms, different methodologies from physics to biology have to be combined with synthetic organic chemistry.

The aim of this thesis was the preparation of various carbohydrates, which are displayed on the surface of the parasites *T. gondii* and *M. tuberculosis*. Once the structural motifs were generated, biophysical and immunological experiments would allow gaining insight into biological processes related to the interaction of the mammalian immune system with the aforementioned synthetic glycans (Figure 1.10, page 20).

For *T. gondii*, species-specific GPIs were chosen as target structures to investigate the potential of those carbohydrates as antigens for anti-parasitical vaccines or a diagnostic test to identify toxoplasmosis in patients. Therefore, the synthesis of the phosphoglycan moieties reflecting the two major GPI glycoforms of *T. gondii* as well as their corresponding substructures was investigated (Chapter 2). The obtained carbohydrate antigens were coupled to a carrier protein and their immunological properties were evaluated in a mouse model. The diagnostic feasibility of the phosphoglycans was studied by their capability of detecting antibodies directed against GPIs in reference sera from individuals suffering from toxoplasmosis using carbohydrate microarray analysis (Chapter 3).

PIMs display major cell wall components of *M. tuberculosis* and were found to bind human soluble lectin ZG16p, which is present in the intestines. Given that tuberculosis can be transmitted *via* ingestion, this lectin could act as a first line of defense of the innate immune system by “opsonizing” mycobacteria in the digestive tract. To study this glycan-protein interaction on the molecular level, a synthesis was developed that gives access to PIM structures suitable for STD-NMR and chemical shift perturbation experiments (Chapter 4).

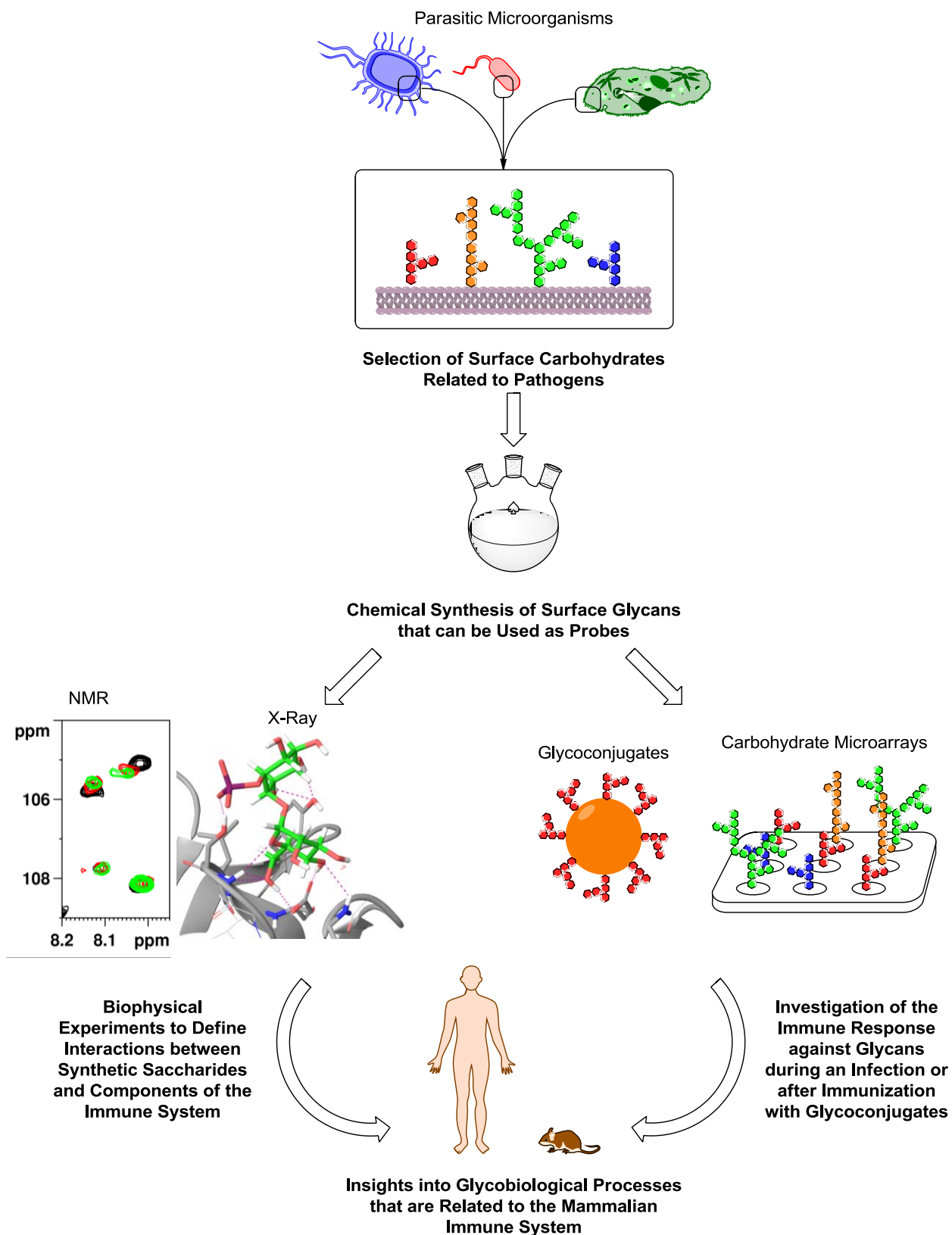


Figure 1.10: Schematic diagram of the general aim of this thesis.

Chapter 2 – Chemical Synthesis of GPI Derivatives and their Corresponding Substructures

2.1 GPIs of *T. gondii* – Potential Vaccine Candidates against Toxoplasmosis

The apicomplexan *T. gondii* is a worldwide distributed pathogen and capable of infecting all warm-blooded animals.⁶⁵ Infection occurs through the ingestion of contaminated raw meat or oocysts shed by cats that serve as the definite host of the parasite in which it replicates *via* a sexual reproduction cycle.⁶⁶ Although infection with *T. gondii* is the third leading cause of food-borne infections requiring hospitalization in the USA⁶⁷, it is not perceived as a large public health problem in developed countries, because of its benign ethiopathology.⁶⁸ In immunocompetent persons, toxoplasmosis is a disease causing no or mild flu-like symptoms leading to a lifelong immunity.⁶⁹ However, the human immune system is unable to prevent the formation of tissue cysts enclosing *T. gondii* parasites during the acute phase of infection and incapable of eradicating them afterwards. In immunocompromised individuals this latent toxoplasmosis is a dangerous medical condition. AIDS or lymphoma patients for example are prone to develop toxoplasmosis encephalitis, a severe inflammation of the brain, because the weakened immune system is not able to eliminate liberated parasites from reactivated cysts in brain and nervous tissue.⁷⁰ Furthermore, primary infection during pregnancy can cause a transmission of the parasite from the mother to the unborn child, leading to formation of hydrocephalus or abortion.⁷¹ Taken together, the health burden caused by toxoplasmosis calls for the development of a vaccine capable of inducing sterile immunity against this parasite. In the last sixty, years numerous studies have been conducted to develop a vaccine against *T.*

⁶⁵ F. Debierre-Grockiego, *Trends Parasitol.* **2010**, *26*, 404-411.

⁶⁶ F. A. Hunter, L. D. Sibley, *Nat. Rev. Microbiol.* **2012**, *10*, 766-778.

⁶⁷ P. S. Mead, L. Slutsker, V. Dietz, L. F. McCaig, J. S. Bresee, C. Shapiro, P. M. Griffin, R. V. Tauxe, *Emerg. Infect. Dis.* **1999**, *5*, 607-625.

⁶⁸ C. Silveira, N. Gargano, A. Kijlstra, E. Petersen, *Expert Rev. Anti Infect. Ther.* **2009**, *7*, 905-908.

⁶⁹ F. Debierre-Grockiego, R. T. Schwarz, *Glycobiology* **2010**, *20*, 801-811.

⁷⁰ B. J. Luft, J. S. Remington, *Clin. Infect. Dis.* **1992**, *2*, 211-222.

⁷¹ J. S. Remington, in *Infectious Diseases of the Fetus and Newborn Infant (6th edition)*, (Ed: J. S. Remington, J. O. Klein, C. B. Wilson, C. J. Baker), Elsevier Saunders, Philadelphia (PA), 2006, Chapter 31.

gondii. All these approaches based on live or inactivated parasites, isolated as well as recombinant proteins and plasmids failed to induce a protective immunity in rodents.⁷² Therefore our attention was drawn to GPIs, which are a class of immunogenic carbohydrates found in high abundance on the cell surface of this pathogen. *T. gondii* uses GPIs to anchor the majority of its enzymes and surface antigens to the extracellular side of the plasma membrane. The two main GPI glycoforms of the parasite contain a branch connected to the O4-position of ManI (Figure 2.1).⁷³ Whereas GPI 1 bears a Glc α 1 \rightarrow 4GalNAc β side chain GPI 2 lacks the glucose. Furthermore, both molecules not only differ in their structure but also in their function. While GPI 2 serves as a membrane anchor for proteins, GPI 1 is displayed on the cell surface without being covalently attached to any macromolecule.⁵⁵ In particular GPI 1 is an immunological active compound that induces TNF- α production in macrophages and an early IgM response in humans after infection with *T. gondii*.⁷⁴ Consequently, it was hypothesized that the phosphoglycan moieties of GPIs 1 and 2 constitute valuable antigens for the development of a vaccine against this pathogen and a diagnostic tool for the detection of toxoplasmosis in humans.

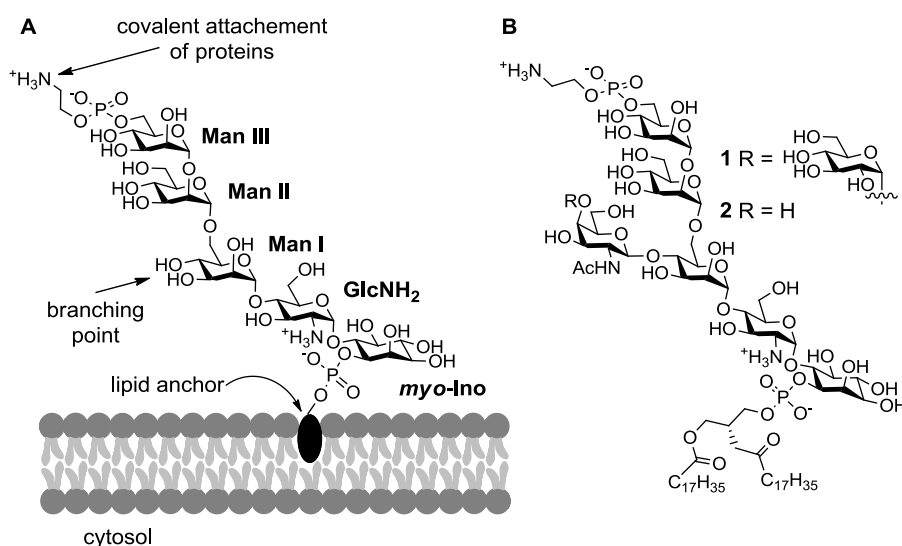


Figure 2.1: (A) The conserved pseudopentasaccharide core structure of GPIs. Arrows indicate potential sites of modification. (B) The structures of the two major GPIs 1 and 2 of *T. gondii*.⁷⁵

To boost the immunogenicity of the antigens, it was envisioned to conjugate the sugars of parasitic origin to a carrier protein to prepare neoglycoconjugates (Figure 2.2, page 23).⁷⁶ Hence, the lipid of the GPIs was exchanged for a 6-mercaptohexan-1-ol linker that allows for

⁷² E. Jongert, C. W. Roberts, N. Gargano, E. Förster-Waldl, E. Petersen, *Mem. I. Oswaldo Cruz* **2009**, *104*, 252-266.

⁷³ B. Striepen, C. F. Zinecker, J. B. Damm, P. A. Melgers, G. J. Gerwig, M. Koolen, J. F. Vliegthart, J. F. Dubremetz, R. T. Schwarz, *J. Mol. Biol.* **1997**, *266*, 797-813.

⁷⁴ S. D. Sharma, J. Mullenax, F. G. Araujo, H. A. Erlich, J. S. Remington, *J. Immunol.* **1983**, *131*, 977-983.

⁷⁵ Y.-H. Tsai, X. Liu, P. H. Seeberger, *Angew. Chem. Int. Ed.* **2012**, *51*, 11438-11456.

⁷⁶ O. T. Avery, W. F. Goebel, *J. Exp. Med.* **1929**, *50*, 533-550.

chemically orthogonal conjugation of phosphoglycans **3** and **4** to proteins or surfaces and ensures correct orientation of the antigens without alternating immunogenic epitopes.^{77,78} In addition, mammalian phosphoglycan⁷⁹ **5** as well as substructures of all GPIs were prepared to investigate the immune response against the carbohydrate conjugates in great detail. Especially cross-reactivity against the mammalian structure **5**, which is closely structurally related to both antigens, could lead to an auto immune response that would render a GPI-based vaccine approach against *T. gondii* unsuccessful.⁸⁰

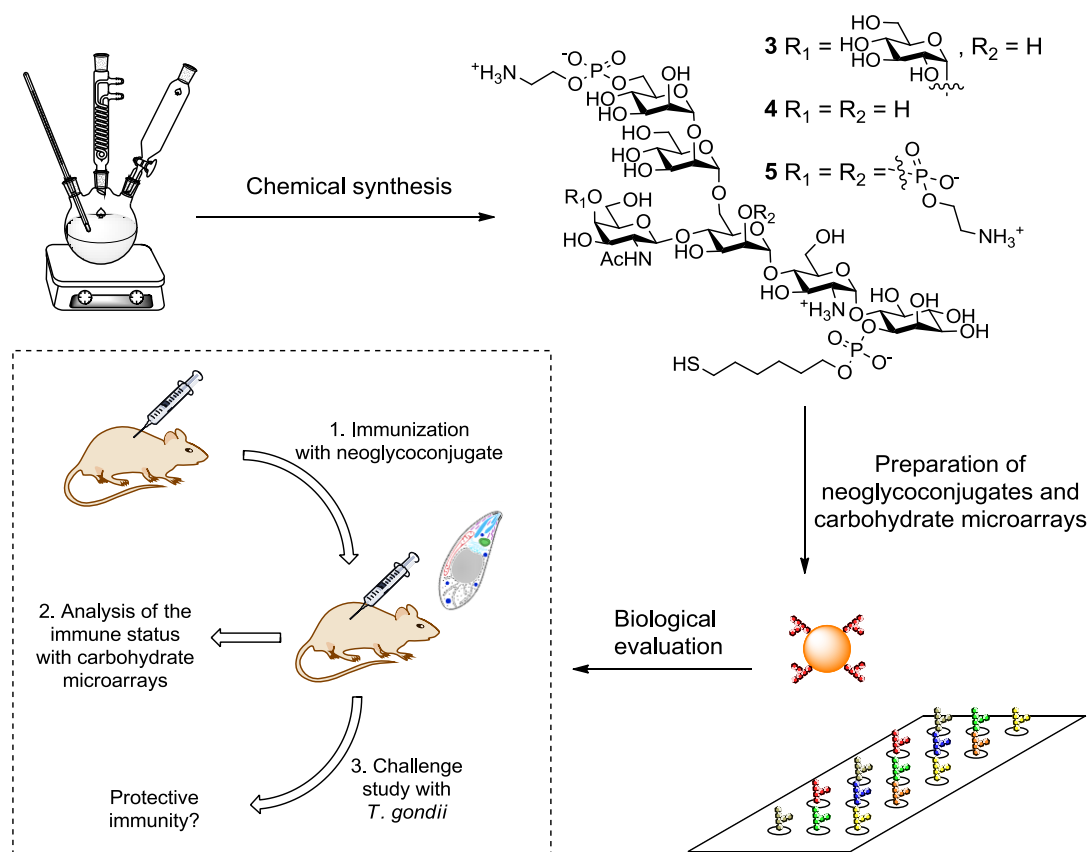


Figure 2.2: General sequence of experiments to decipher the potential of GPI based vaccines against *T. gondii*. Chemical synthesis supplies unnatural GPI derivatives and substructures, which are selectively conjugated to prepare carbohydrate microarrays and neoglycoconjugates. The conjugates are afterwards evaluated in a mouse model.

⁷⁷ P. H. Seeberger, R. L. Soucy, Y. U. Kwon, D. A. Snyder, T. Kanemitsu, *Chem. Commun.* **2004**, 1706-1707.

⁷⁸ F. Kamena, M. Tamborrini, X. Y. Liu, Y. U. Kwon, F. Thompson, G. Pluschke, P. H. Seeberger, *Nat. Chem. Biol.* **2008**, *4*, 238-240.

⁷⁹ N. Stahl, M. A. Baldwin, R. Hecker, K. M. Pan, A. L. Burlingame, S. B. Prusiner, *Biochemistry* **1992**, *31*, 5043-5053.

⁸⁰ Y.-L. Huang, C.-Y. Wu, *Expert Rev. Vaccines* **2010**, *9*, 1257-1274.

2.2 Retrosynthetic Analysis of GPI Derivatives

In most of the reported synthetic routes to GPIs the target molecules are built from individual monosaccharides in a linear stepwise manner.⁸¹ The oligomannoside, in particular, has often been constructed in a linear fashion applying a participating group at O2 position to facilitate stereoselective α -mannosylations. Even the branched structures have been predominantly produced in a linear fashion adding one monosaccharide to the growing glycan at a time. Although convergent synthetic routes require less protecting group manipulations and transformations that include large oligosaccharide intermediates, only a few such routes have been reported. The notable work in this area was reported by Guo^{82,83}, Ley^{84,85} and Fraser-Reid⁸⁶ typically using the disconnections around ManI to achieve convergence. With no exception, the reported synthetic routes to GPIs are target oriented and although such approaches typically result in shorter synthetic schemes, these routes are not readily amenable to modifications that would allow for efficient production of analogues or other GPIs. With this in mind, a synthetic strategy was developed to address the need for a diverse set of homogeneous GPI analogues as a basis for structure-activity studies.

The retrosynthetic analysis of the GPI derivatives identified phosphodiester as the natural point for initial bond disconnections (Figure 2.3, page 25). The late stage phosphorylations that would install the anticipated GPI phosphorylation pattern, thus, emerged as one of the key challenges that served as a template for the design of a comprehensive protecting group strategy with special emphasis on the orthogonal protection of phosphorylation sites. In light of this analysis, only three orthogonal protecting groups are sufficient to introduce any of the chosen GPI phosphorylation patterns if arranged in an appropriate, target dependent manner: one protecting group for the O6 position of ManIII, one for the O1 position of *myo*-inositol and one for the positions carrying the additional phosphoethanolamine at O2 of ManI. These groups are, naturally, required to be: orthogonal to the benzyl ethers chosen for permanent protection of hydroxyls, stable under the phosphorylation conditions, and removable in the presence of already introduced phosphodiester. To allow for more flexibility in the design of

⁸¹ A. V. Nikolaev, N. Al-Maharik, *Nat. Prod. Rep.* **2011**, 28, 970-1020.

⁸² Z. W. Guo, J. Xue, *J. Am. Chem. Soc.* **2003**, 125, 16334-16339.

⁸³ X. M. Wu, Z. W. Guo, *Org. Lett.* **2007**, 9, 4311-4313.

⁸⁴ S. V. Ley, D. K. Baeschlin, A. R. Chaperon, V. Charbonneau, L. G. Green, U. Lucking, E. Walther, *Angew. Chem. Int. Ed.* **1998**, 37, 3423-3428.

⁸⁵ S. V. Ley, D. K. Baeschlin, A. R. Chaperon, L. G. Green, M. G. Hahn, S. J. Ince, *Chem.-Eur. J.* **2000**, 6, 172-186.

⁸⁶ U. E. Udodong, R. Madsen, C. Roberts, B. Fraser-Reid, *J. Am. Chem. Soc.* **1993**, 115, 7886-7887.

the synthetic route, the groups that are labile only under a specific set of conditions were selected.⁸⁷ A Lev ester that is known to be relatively stable under mildly basic conditions but is easily cleaved in the presence of other esters *via* hydrazinolysis was preferred over generally base sensitive groups such as acetyl or benzoyl esters. For similar reasons, allyl and TIPS ethers were selected to complete the fully orthogonal set of protecting groups.

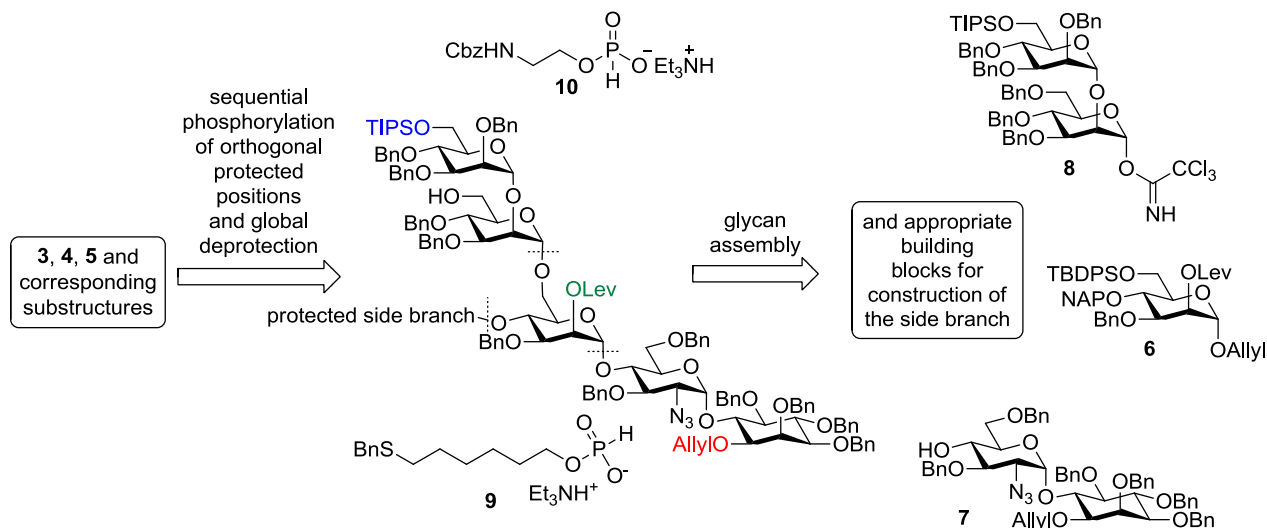


Figure 2.3: General retrosynthetic analysis of GPI derivatives 3-5. The orthogonal protecting groups that mark the phosphorylation sites on the protected glycan are highlighted in different colors.

The specific pattern for protecting group placement within the fully protected glycan was created in a way that either enables these substituents to control stereoselectivity of glycosylation reactions during the assembly of the glycan (e.g., Lev at O2 of ManI) or simplifies the synthesis of the required building blocks (e.g., TIPS ether at the C6 of ManIII). The orthogonal protecting group strategy designed for late stage phosphorylations was fully integrated into the plan for assembly of the GPI glycans. A simple matching of the protecting groups between the position of the glycosyl acceptor and the corresponding glycosylating agent was followed in order to avoid coexistence of multiple temporary protecting groups of the same type in the growing glycan. Incorporation of all protecting groups into a single, central building block would simplify synthesis of the building blocks and result in the most convergent route. Following this logic, two bond disconnections were made at the glycosidic bonds around the ManI giving rise to the fully orthogonally protected central mannose building block **6** and a simple set of building blocks **7** and **8**, which contain protecting groups that enable the introduction of the respective saccharide branches or phosphodiester. These disconnections emerged as a reasonable choice considering the variety of glycosylation

⁸⁷ P. G. M. Wuts, T. W. Greene, in *Greene's Protective Groups in Organic Synthesis* (4th edition), John Wiley & Sons, Inc., Hoboken (NJ), 2007, Chapter 2.

protocols that reliably produce α -mannosides⁸⁸ and the appropriate positioning of the directing protecting groups.⁸⁹

Phosphitylation of hydroxyl functions with the H-phosphonates **9**⁹⁰ and **10**⁸⁸ activated *via* transient formation of a mixed anhydride with pivaloyl chloride followed by oxidation with iodine in wet pyridine was chosen as a method to introduce the phosphorylation moieties. This procedure was adopted from well-established protocols for the synthesis of oligonucleotides and has the advantage over the phosphoramidite approach that reagents used in these reactions are cheap, easy to prepare and stable under normal storage conditions. Even though activation and oxidation of phosphoramidites usually proceeds under milder conditions the general yield for both methodologies is high and comparable.⁹¹

⁸⁸ C. Murakata, T. Ogawa, *Tetrahedron Lett.* **1991**, 32, 671-674.

⁸⁹ A. Ali, R. A. Vishwakarma, *Tetrahedron* **2010**, 66, 4357-4369.

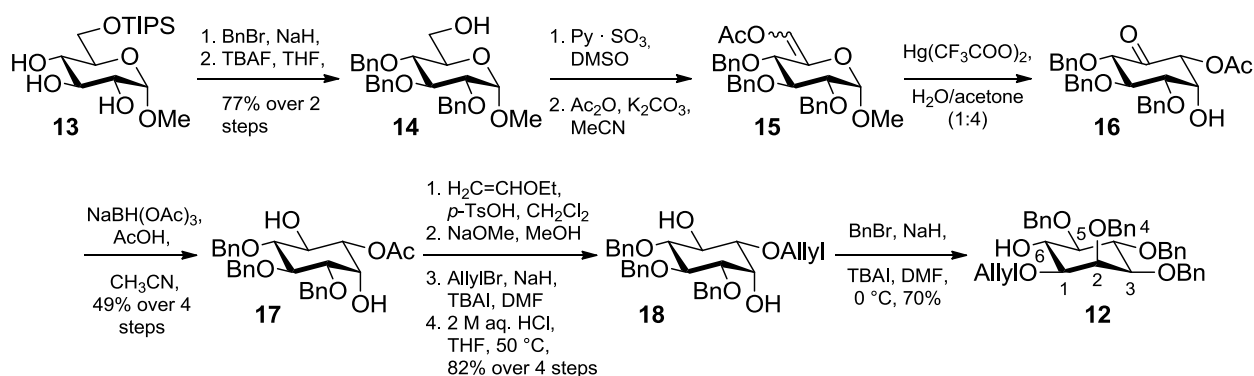
⁹⁰ Y.-U. Kwon, R. L. Soucy, D. A. Snyder, P. H. Seeberger, *Chem. Eur. J.* **2005**, 11, 2493-2504.

⁹¹ S. L. Beaucage, R. P. Iyer, *Tetrahedron* **1992**, 48, 2223-2311.

2.3 Synthesis of the Pseudodisaccharide Building Block

Preparation of pseudodisaccharide building block **7**^{84,85} was achieved by coupling of the known trichloroacetimidate **11**⁹² (Scheme 2.2, page 28) with *myo*-Ino **12** (Scheme 2.1), which is accessible through a *de novo* synthesis developed by the groups of Fraser-Reid⁹³ and Seeberger^{94,95}. The synthesis of **12** commenced with triol **13** that was benzylated and subsequently treated with TBAF to remove the silyl ether (Scheme 2.1). Afterwards the O6 position of alcohol **14** was oxidized and converted into enol acetate **15**, which underwent a Ferrier carbocyclization⁹⁶ to yield ketone **16**. Reduction using sodium triacetoxyborohydride gave access to enantiomerically pure *myo*-Ino **17**⁹⁷ in 49% yield over 4 steps.

The acetyl group of **17** was exchanged for an allyl ether in a high yielding four step reaction sequence starting with the formation of acetals at O2 and O6 employing ethyl vinyl ether and *p*-TsOH as an acid.⁹⁴ Deacetylation under Zemplén⁹⁸ conditions followed by allylation of the O1 position and final hydrolysis of the remaining acetals yielded diol **18** in 82% yield starting from **17**. Selective benzylation of the O2 position completed the synthesis of aglycone **12**.



Scheme 2.1: *De novo* synthesis of *myo*-inositol building block **12**. Atom numbers are indicated.

Imidate **11** was prepared from commercial available D-glucosamine hydrochloride (**19**) (Scheme 2.2). A diazotransfer reaction⁹⁹ using *in situ* generated trifluoromethanesulfonyl

⁹² G. Grundler, R. R. Schmidt, *Liebigs Ann. Chem.* **1984**, 1826-1847.

⁹³ Z. J. Jia, L. Olsson, B. Fraser-Reid, *J. Chem. Soc., Perkin Trans. 1* **1998**, 631-632.

⁹⁴ X. Liu, B. L. Stocker, P. H. Seeberger, *J. Am. Chem. Soc.* **2006**, *128*, 3638-3648.

⁹⁵ S. Boonyarattanakalin, X. Liu, M. Michieletti, B. Lepenies, P. H. Seeberger, *J. Am. Chem. Soc.* **2008**, *130*, 16791-16799.

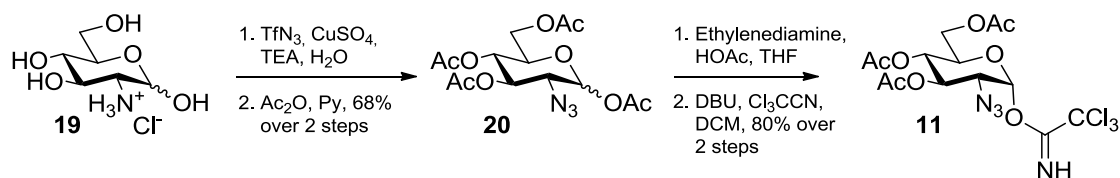
⁹⁶ R. J. Ferrier, S. Middleton, *Chem. Rev.* **1993**, *93*, 2779-2831.

⁹⁷ H. Takahashi, H. Kittaka, S. Ikegami, *J. Org. Chem.* **2001**, *66*, 2705-2716.

⁹⁸ G. Zemplén, E. Pacsu, *Ber. Dtsch. Chem. Ges.* **1929**, *62*, 1613-1614.

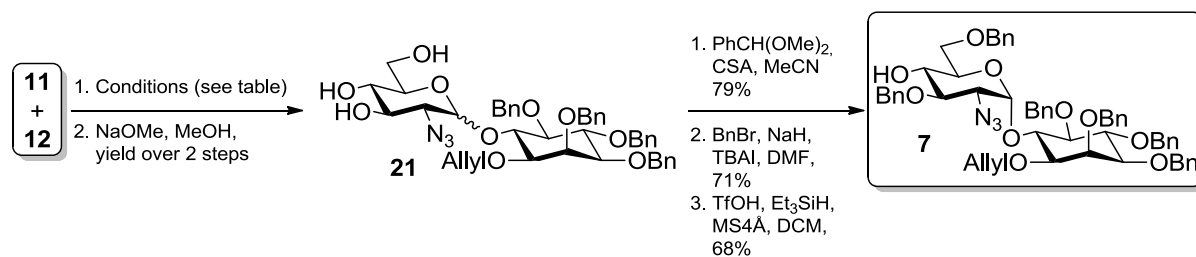
⁹⁹ R.-B. Yan, F. Yang, Y. Wu, L.-H. Zhang, X.-S. Ye, *Tetrahedron Lett.* **2005**, *46*, 8993-8995.

azide converted the amine functionality into an azide that is not involved in neighbouring group participation and hence crucial for achieving α -selectivity in the impending glycosylation reaction. Acetylation of the remaining free hydroxyl groups gave azide **20** in 68% over 2 steps. Selective deacetylation of the anomeric position with ethylenediamine and acetic acid in THF¹⁰⁰ provided the corresponding lactol that was transformed into glycosylation agent **11** using standard protocols¹⁰¹.



Scheme 2.2: Synthesis of imidate **11**.

To optimize the yield of the glycosylation reaction between **11** and **12** different conditions were investigated (Scheme 2.3).



Catalyst	Solvent	Temperature	Thiophene	Yield(%)	α/β ratio
TMSOTf	DCM	-40 °C	-	82	4:1
TMSOTf	DCM	r.t.	10 equiv.	86	11:2
TMSOTf	DCM	r.t.	3 equiv.	72	5:1
TMSOTf	Et ₂ O	0 °C	-	65	7:2
BF ₃ ·OEt ₂	DCM	r.t.	-	decomposition	-

Scheme 2.3: Final steps in the synthesis of building block **7** and tested conditions for the glycosylation reaction (2 equiv. of **11** and 1 equiv. of **12** were used in all reactions at a concentration of 36 mM based on the aglycone). Anomeric ratios were calculated by integration of the anomeric signals in ¹H-NMR spectra. Yields are given after purification. The best condition is highlighted in red.

A protocol established by the Boons group, which uses thiophene as a promoter for the formation of 1,2-*cis* glycosides, gave an anomeric ratio that was superior to standard protocols (DCM, -40 °C or Et₂O, 0 °C) without affecting the general good yields that were obtained in glycosylations using TMSOTf as a catalyst. Based on NMR data and theoretical calculations Boons *et al.* proposed that during the reaction a β -linked sulfonium ion intermediate of the activated glycosylation agent, which is detectable even at 0° C, is formed and only allows

¹⁰⁰ J. Zhang, P. Kováč, *J. Carbohydr. Chem.* **1999**, *18*, 461-469.

¹⁰¹ R. R. Schmidt, J. Michel, *Angew. Chem. Int. Ed.* **1980**, *19*, 731-732.

nucleophilic attack from the α -anomeric site.¹⁰² The received anomeric mixture was inseparable by column chromatography and therefore directly deacetylated to form triol **21**. Introduction of a 4,6-benzylidene acetal, subsequent benzylation of the O3 position and final regioselective ring opening afforded the desired pseudodisaccharide **7** in 38% yield over 3 steps starting from **21**, which could be finally separated from its β -isomer at this stage.

¹⁰² J. Park, S. Kawatkar, J.-H. Kim, G.-J. Boons, *Org. Lett.* **2007**, *9*, 1959-1962.

2.4 Preparation of GPI Derivatives

According to the general retrosynthetic scheme, the fully protected direct precursor of the GPI derivatives **4**, **5** and **22** can be prepared *via* sequential phosphorylation using H-phosphonates **9** and **10**, and the fully protected GPI glycan **23** (Figure 2.4). Glycan **23** was envisioned to arise from the building blocks **6**, **7**, **8**, and **24**¹⁰³ *via* sequential deprotection/glycosylation cycles.

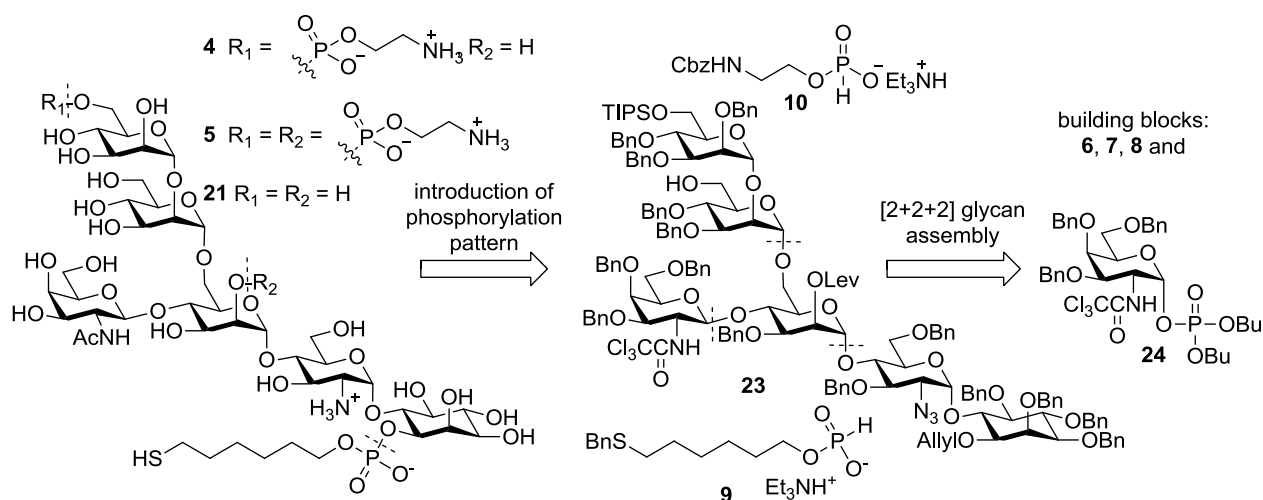


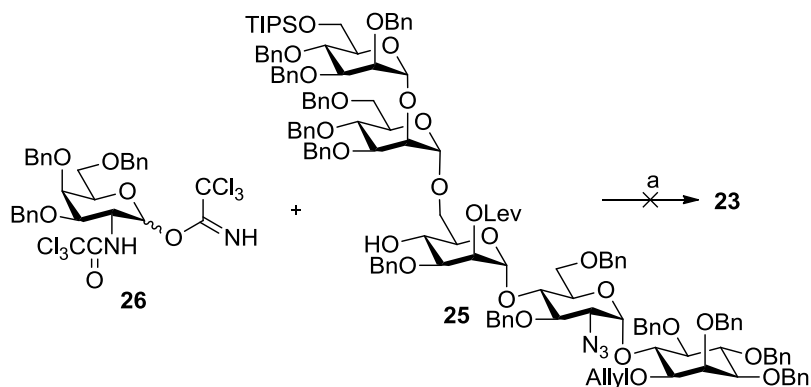
Figure 2.4: Retrosynthetic analysis of GPI derivatives containing the simple GalNAc β side branch connected to the O4 position of ManI.

The order of phosphorylation reactions is inconsequential owing to the fully orthogonal character of the protecting group set. In contrast, the order in which the saccharide building blocks are assembled cannot be chosen freely.

It was already demonstrated that a [1+5] glycosylation strategy, which introduces the side branch as the final step in the assembly sequence of glycan **23** and displays the most efficient route in generating diverse GPI structures, is unsuccessful, because the steric crowding in pseudopentasaccharide **25** renders the O4 hydroxyl of ManI only weakly nucleophilic allowing for competitive decomposition of the activated glycosylating agent during the reaction (Scheme 2.4, page 31).¹⁰⁴

¹⁰³ Y.-U. Kwon, X. Y. Liu, P. H. Seeberger, *Chem. Commun.* **2005**, 2280-2282.

¹⁰⁴ Experiments were carried out by Y.-H. Tsai. For more information see Y.-H. Tsai, S. Götze, I. Vilotijevic, M. Grube, D. Varón Silva, P. H. Seeberger, *Chem. Sci.* **2013**, *4*, 468-481.



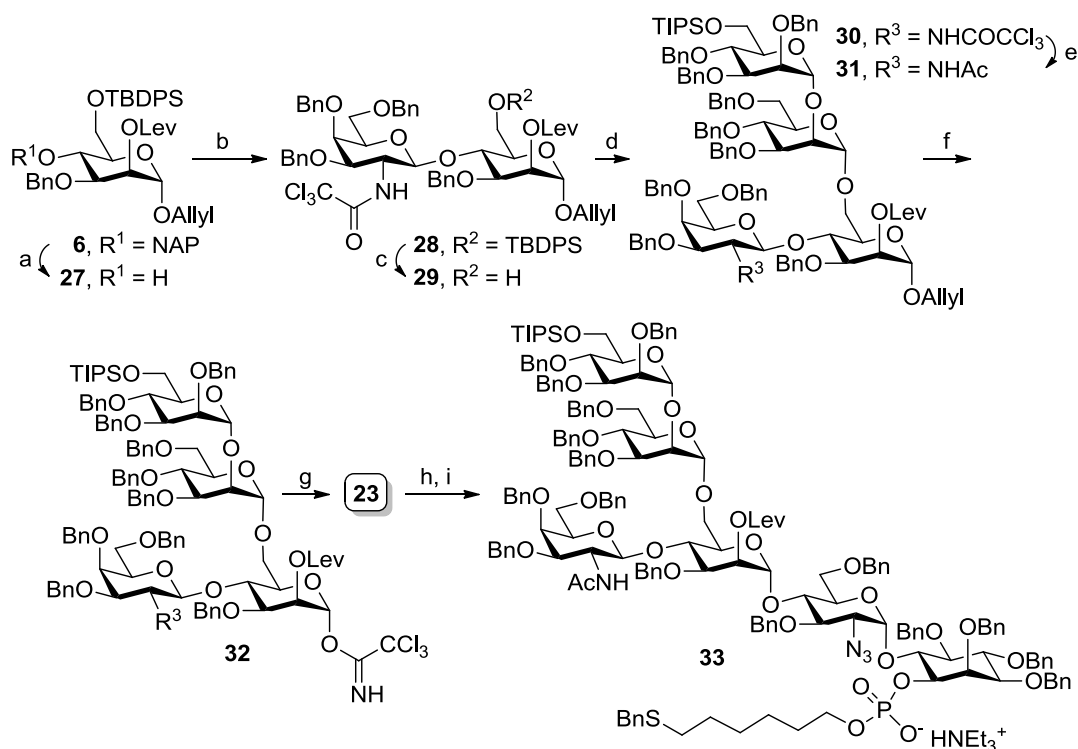
Scheme 2.4: Key step in the formation of fully protected glycan **23** using a [1+5] glycosylation strategy. Glycan **25** was built up using compounds **6**, **7** and **8**. *Reagents and conditions:* (a) Phosphate **24** or the corresponding imidate **26**, TMSOTf, DCM, $-40\text{ }^{\circ}\text{C}$, no reaction.

Based on this result the synthesis of the desired pseudohexasaccharide **23** was performed utilizing a [2+2+2] glycosylation strategy (Scheme 2.5, page 32). The glycan assembly commenced with the removal of the NAP ether of mannoside **6** using DDQ. Glycosylation of **27** with phosphate **24** in the presence of TMSOTf in DCM at $-40\text{ }^{\circ}\text{C}$ went smoothly to produce the corresponding disaccharide **28** in 82% yield. The TBDPS ether was cleaved using HF•Py in THF to yield alcohol **29**, which was glycosylated with trichloroacetimidate **8** to afford the desired tetrasaccharide **30** in 59% yield over two steps, isolated as a single diastereomer. Reduction of the trichloroacetamide with zinc in acetic acid produced acetamide **31**. Isomerization of the allyl ether using *in situ* prepared iridium hydride catalyst¹⁰⁵ and subsequent hydrolysis of the resulting enol ether¹⁰⁶ followed by formation of the trichloroacetimidate under standard conditions provided glycosylating agent **32** in 61% yield over 3 steps. TBSOTf catalyzed glycosylation of the pseudodisaccharide **7** with trichloroacetimidate **32** furnished the desired pseudohexasaccharide **23** in 81% yield with complete stereocontrol.

With pseudohexasaccharide **23** in hand, the TIPS/Lev/Allyl set of protecting groups was used for the introduction of the sulfhydryl handle and the desired phosphorylation status. Cleavage of the allyl ether at the O2 position of *myo*-Ino *via* the Ir-catalyzed isomerization followed by the mercury(II) promoted hydrolysis of the resulting enol ether, unveiled the site for conjugation with H-phosphonate **9**. Formation of the H-phosphonate diester from the *in situ* generated mixed anhydride of **9** and pivalic acid followed by iodine promoted oxidation produced the corresponding phosphodiester **33** in 82% yield.

¹⁰⁵ J. J. Oltvoort, C. A. A. van Boeckel, J. H. De Koning, J. H. van Boom, *Synthesis* **1981**, 305-308.

¹⁰⁶ B. M. Swarts, Z. W. Guo, *J. Am. Chem. Soc.* **2010**, *132*, 6648-6650.

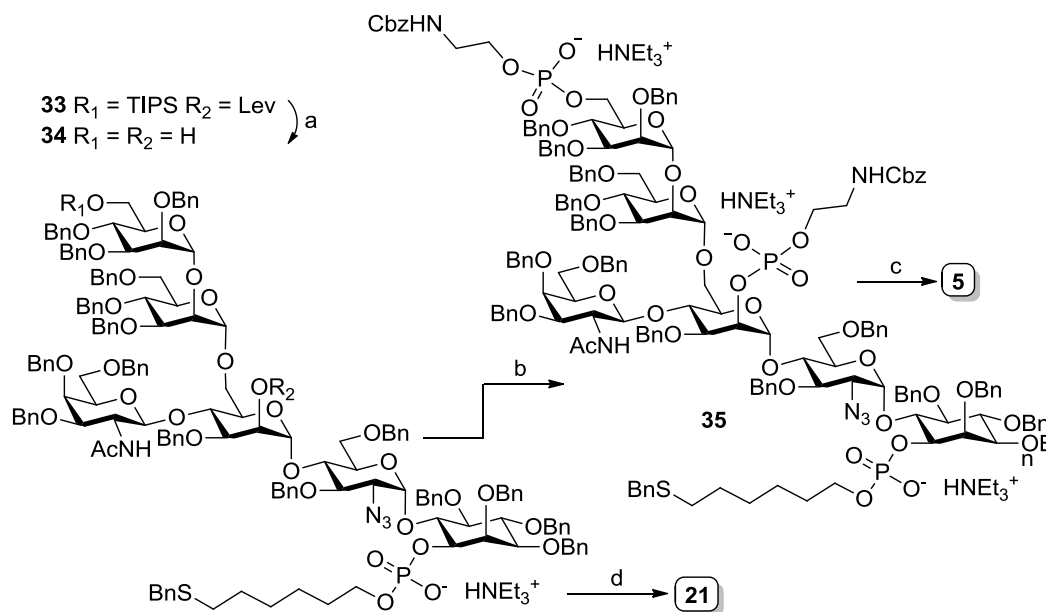


Scheme 2.5: Synthesis of the orthogonal protected phosphate **33**. *Reagents and conditions:* (a) DDQ, water, DCM, 85%; (b) **24**, TMSOTf, DCM, 4Å MS, -40 °C, 82%; (c) HF·Py, THF, 80%; (d) **8**, TBSOTf, Et₂O, MS 4Å, 0 °C, 74%; (e) Zn, AcOH, 55 °C, 74% (f) i. [Ir(COD)(PPh₂Me)₂]PF₆, H₂, THF; ii. HgCl₂, HgO, H₂O, acetone 69% (two steps); iii. Cl₃CCN, DBU, DCM, 89%; (g) **7**, TBSOTf, Et₂O, MS 4Å, 0 °C, 81%; (h) i. [Ir(COD)(PPh₂Me)₂]PF₆, H₂, THF; ii. HgCl₂, HgO, H₂O, acetone, 82% (two steps); (i) i. **9**, PivCl, Py; ii. I₂, H₂O, 82% (two steps).

Removal of the silyl group from the O6 position of ManIII required specific reaction conditions due to the presence of the acid labile phosphodiester in the molecule. Hence a non-acidic hydrofluoric acid complex was employed to cleave the TIPS ether (Scheme 2.6, page 33).¹⁰⁷ The reaction was very slow, but generated the anticipated product without cleaving the phosphodiester. Consequent treatment with hydrazine monohydrate yielded diol **34** in 62% yield over two steps. Subsequently diol **34** was either directly submitted to Birch reduction¹⁰⁸ to prepare GPI derivative **21**, which does not contain additional phosphoethanolamines, or first double phosphorylated with H-phosphonate **10** using the aforementioned standard conditions to form trisphosphate **35**. For global deprotection **35** was also subjected to metal dissolving conditions to give access to the mammalian carbohydrate moiety **5** in 59% yield. It is not possible to use hydrogenolysis over Pd/C as a method to cleave the remaining Bn ethers, because the liberated thiol functionality can poison the catalyst and attach itself *via* chemisorption to the noble metal rendering isolation of the product impossible.

¹⁰⁷ B. M. Swarts, Z. W. Guo, *Chem. Sci.* **2011**, 2, 2342-2352.

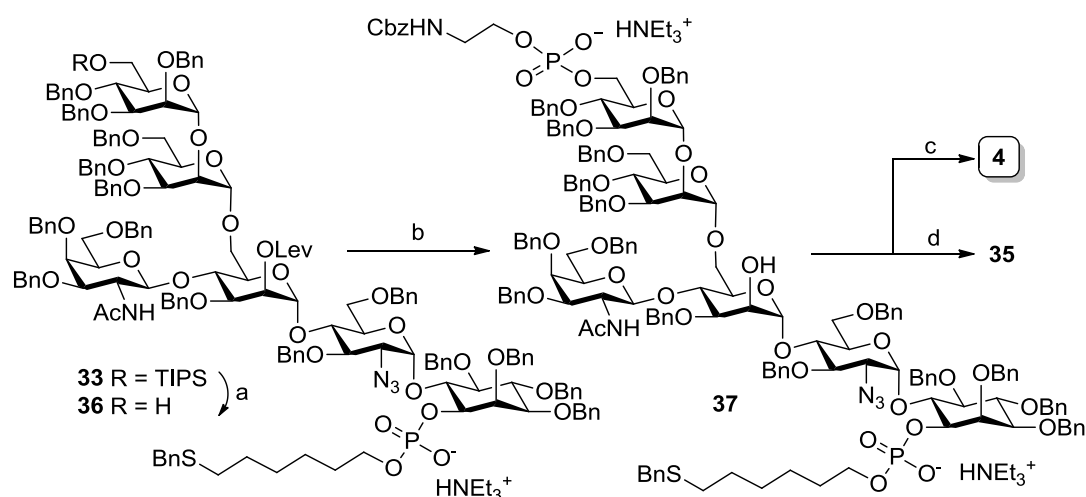
¹⁰⁸ A. J. Birch, *J. Chem. Soc.* **1944**, 430-436.



Scheme 2.6: Synthesis of the GPI derivatives **5** and **21**. *Reagents and conditions:* (a) i. $3\text{HF}\cdot\text{Et}_3\text{N}$, THF, **3d**; ii. $\text{N}_2\text{H}_4\cdot\text{H}_2\text{O}$, MeCN, 2 h, 62% (two steps) (b) i. **10**, PivCl, Py; ii. I_2 , H_2O , 64% (two steps); (c) $\text{Na}_{(s)}$, $\text{NH}_3(l)$, -78°C , *tert*-BuOH, THF, 30 min, 59%; (d) $\text{Na}_{(s)}$, $\text{NH}_3(l)$, -78°C , *tert*-BuOH, THF, 30 min, 78%.

The synthesis of **4** also started from the precursor **33** (Scheme 2.7, page 34). In order to shorten the reaction time and improve the yield of the selective hydrolysis of the TIPS ether a mild Lewis acid, namely $\text{Sc}(\text{OTf})_3$, was used at elevated temperatures to remove the orthogonal protection group in excellent yield of 93% leaving the phosphodiester untouched.¹⁰³ Formation of the H-phosphonate diester of **10** and **36** followed by oxidation gave access to the corresponding bisphosphate, which was treated with hydrazine monohydrate in a one-pot procedure to afford **37** in 88% over three steps. Global deprotection using Birch reduction conditions concluded the synthesis of the phosphoglycan **4**.

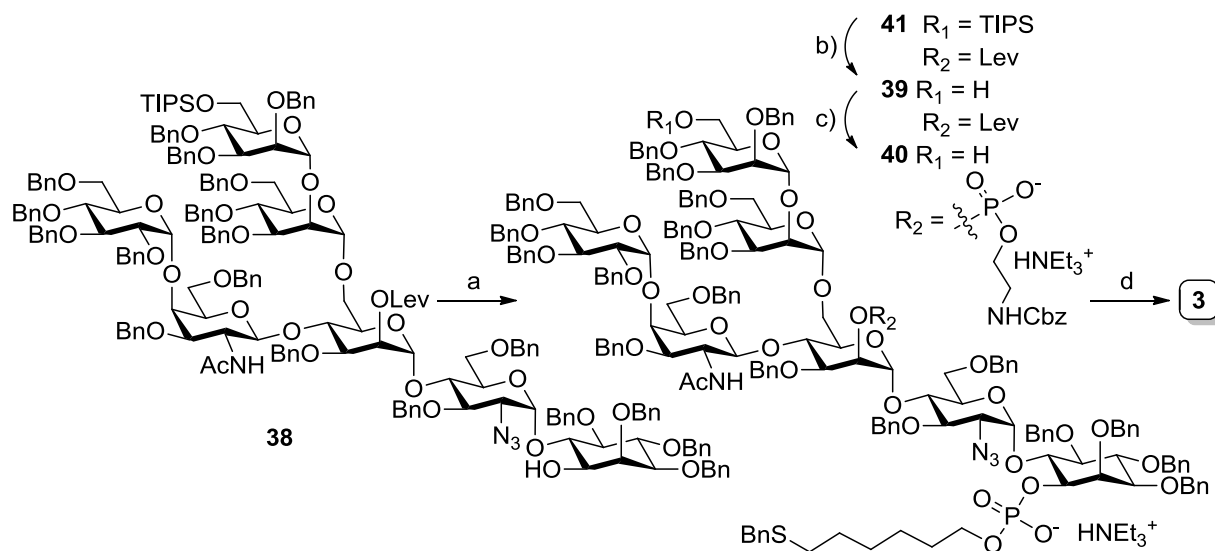
In addition precursor **37** could also be phosphorylated for a second time to generate trisphosphate **35** in 62% yield over 4 steps from **33**, which is a significant improvement over the double-phosphorylation strategy employed in the synthesis of the mammalian structure **5** (40% over three steps starting from **33**; see Scheme 2.6).



Scheme 2.7: Synthesis of the GPI derivative **4**. This route also offers an alternative for preparation of the trisphosphorylated precursor **35**. *Reagents and conditions:* (a) $\text{Sc}(\text{OTf})_3$, H_2O , MeCN , 93%; (b) i. **10**, PivCl , Py ; ii. I_2 , H_2O ; iii. N_2H_4 in THF ; 88% (three steps); (c) $\text{Na}_{(s)}$, $\text{NH}_3(l)$, -78°C , tert-BuOH , THF , 30 min, 58%; (d) **10**, PivCl , Py ; ii. I_2 , H_2O ; 76% (two steps).

Success with the late stage phosphorylation in the synthesis of **4**, **5** and **21** instilled the confidence that the original bond disconnections are also well suited for the preparation of more complex molecules such as the pseudoheptasaccharide **3** (see Scheme 2.2, page 25).

The synthesis of **3** started with alcohol **38** that was phosphorylated with thioether **9** in 87% yield over two steps (Scheme 2.8, page 35). Acidic hydrolysis of the silyl ether utilizing the previously established $\text{Sc}(\text{OTf})_3$ protocol gave access to primary alcohol **39**. A one-pot procedure yielded bisphosphate **40** via phosphorylation of **39** using H-phosphonate **10** followed by oxidation and final hydrazinolysis of the levulinic ester in 76% yield. For global deprotection of the remaining benzyl ethers, **40** was submitted to Birch reduction conditions to furnish carbohydrate antigen derivative **3** in a moderate yield of 55%.



Scheme 2.8: Synthesis of phosphoglycan **3**. *Reagents and conditions:* (a) i. **9**, PivCl, Py; ii. I_2 , H_2O , 87%; (b) $\text{Sc}(\text{OTf})_3$, MeCN, H_2O , 78%; (c) **10**, PivCl, Py; ii. I_2 , H_2O ; iii. hydrazine (1 M in THF), 76%; (d) $\text{NH}_3(\text{s})$, THF, $\text{Na}_{(\text{s})}$, -78°C , *tert*-BuOH, 35 min; 55%.

2.5 Synthesis of GPI Substructures

In order to investigate the immune response against GPIs either in the context of vaccination or upon infection with *T. gondii* in great detail, substructures of GPIs **1** and **2** (Scheme 2.1, page 22) were prepared using the orthogonal protection group strategy and retrosynthetic analysis introduced in chapter 2.2. The phosphoglycan substructures reflect the side chains **42-43**, branched mannose moieties with diverse phosphorylation patterns **44-47** and the pseudodisaccharide unit **48**⁹⁰ of the antigens **3** and **4** (Figure 2.5). In addition, mammalian substructure **49**, which contains the characteristic extra phosphoethanolamine covalently linked to the O2 position of ManI, was also synthesized.

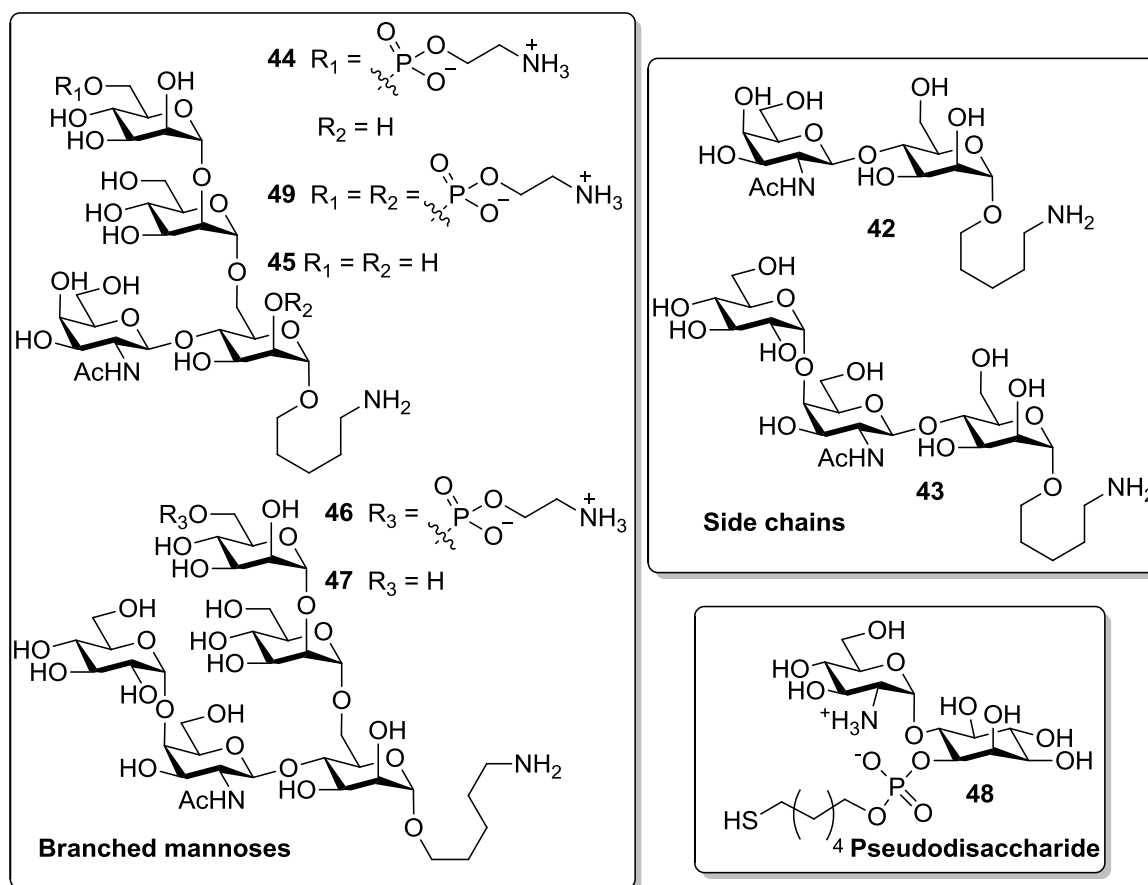
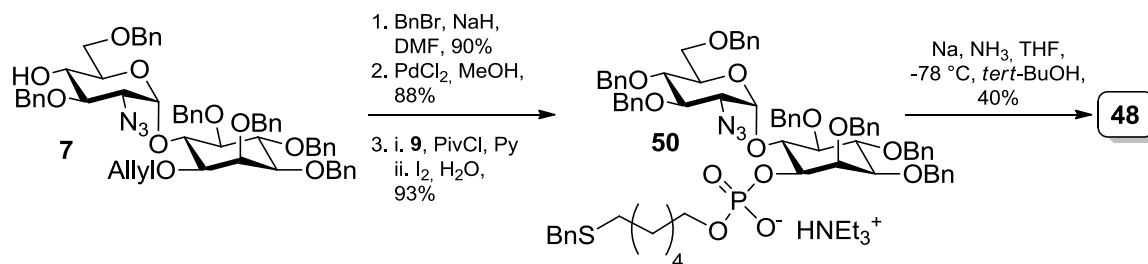


Figure 2.5: Amino linker equipped sugars **44-49**, which represent substructural motifs of GPIs **1** and **2**.

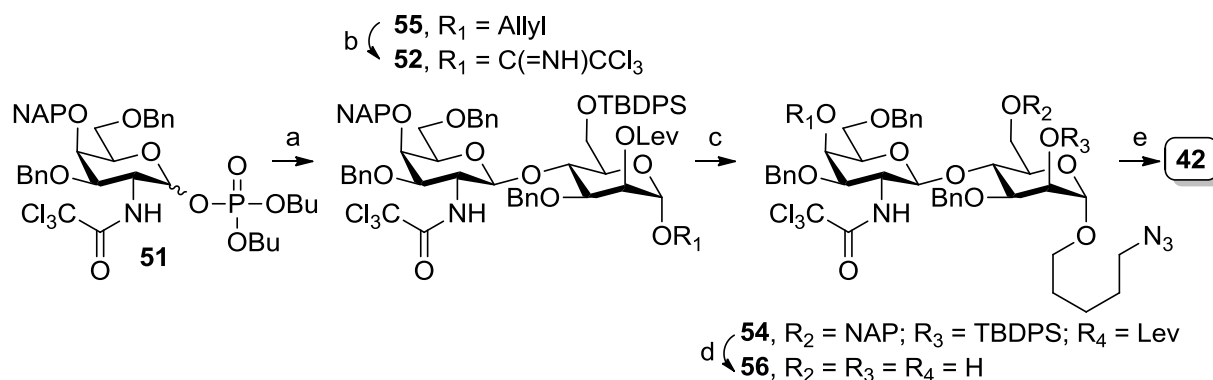
Pseudodisaccharide **48** was synthesized from the previously prepared building block **7** utilizing established synthetic protocols.⁹⁰ Benzoylation of the free hydroxyl group followed by Pd-catalyzed deallylation set the stage for phosphorylation of the O1 position of the *myo*-Ino (Scheme 2.9, page 37). Phosphorylation with thioether **9** produced precursor **50** in 74% yield

over three steps. Removal of the benzyl ethers and simultaneous reduction of the azide finally yielded substructure **48** in a reasonable yield of 40%.



Scheme 2.9: Synthesis of pseudodisaccharide derivative **48**.

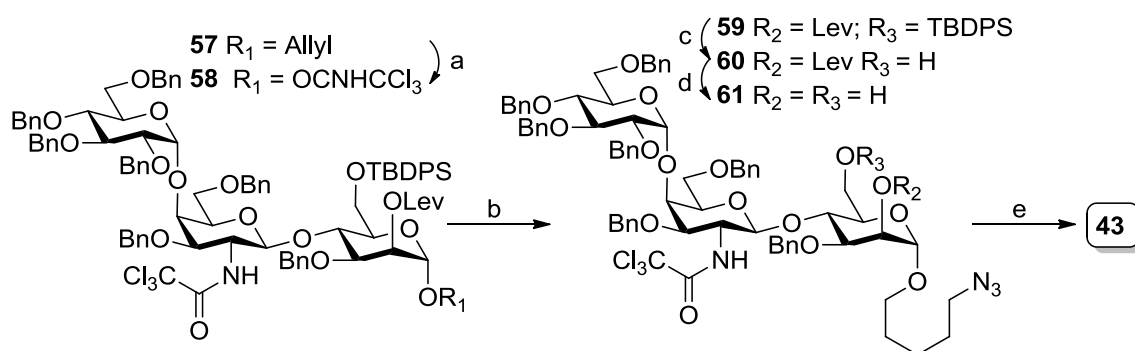
The synthesis of sugar **42** representing the side branch of GPI **2** started with the glycosylation of ManI building block **27** (Scheme 2.5, page 32) with phosphate **51** (Scheme 2.10) and subsequent conversion of the allyl moiety into an imidate to yield disaccharide **52** in 62% yield over 2 steps. Glycosylation with 5-azidopentan-1-ol¹⁰⁹ (**53**) under TBSOTf catalysis yielded fully protected azide **54**, which was submitted to a three step procedure to cleave the orthogonal protecting groups. Final hydrogenolysis liberated the remaining hydroxyl groups that were still protected as benzyl ethers and reduced the trichloroacetamide to yield **42** in 31% over 4 steps starting from **54**.



Scheme 2.10: Synthesis of side branch **42**. (a) **27**, TMSOTf, DCM, -40 °C, MS 4Å, 90%; (b) i. PdCl₂, MeOH; ii. Cl₃CCN, DBU, DCM, 62% over two steps; (c) **53**, TBSOTf, Et₂O, MS 4Å, 0 °C, 91%; (d) i. TBAF, THF; ii. hydrazine monohydrate, THF; DDQ, DCM, PBS, 48% over three steps; (e) Pd/C, H₂, MeOH, 65%.

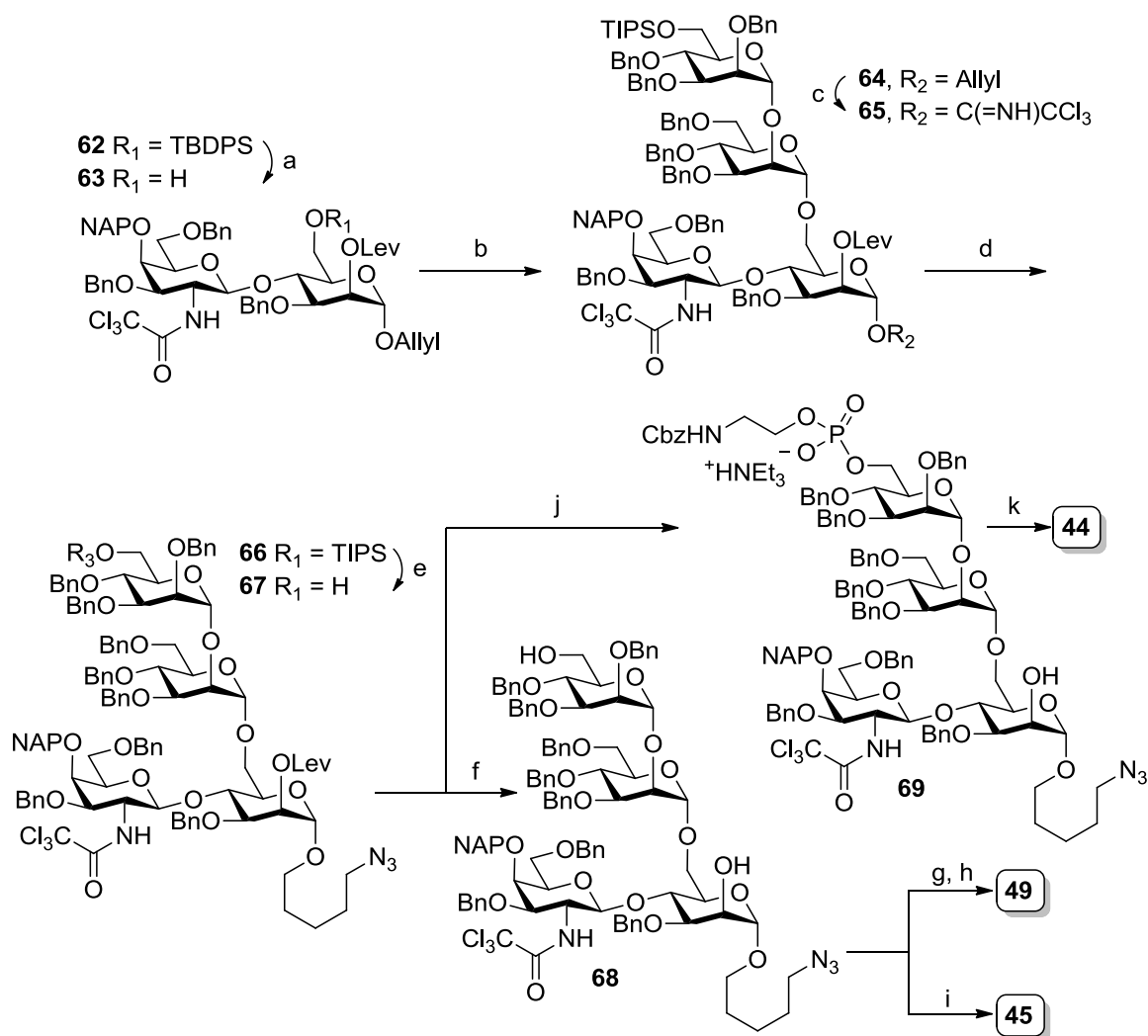
Formation of the corresponding trisaccharide **43** was achieved in a similar fashion (Scheme 2.11, page 38). The protected sugar **57** was converted into glycosylation agent **58** using already established protocols. Introduction of the linker proceeded smoothly with an excellent yield of 89% giving the α -anomer of the fully protected trisaccharide **59** as the exclusive product. A final deprotection cascade provided carbohydrate **43** in 55% yield over three steps.

¹⁰⁹ V. Gracias, K. E. Frank, G. L. Milligan, J. Aubé, *Tetrahedron* **1997**, *53*, 16241-16252.



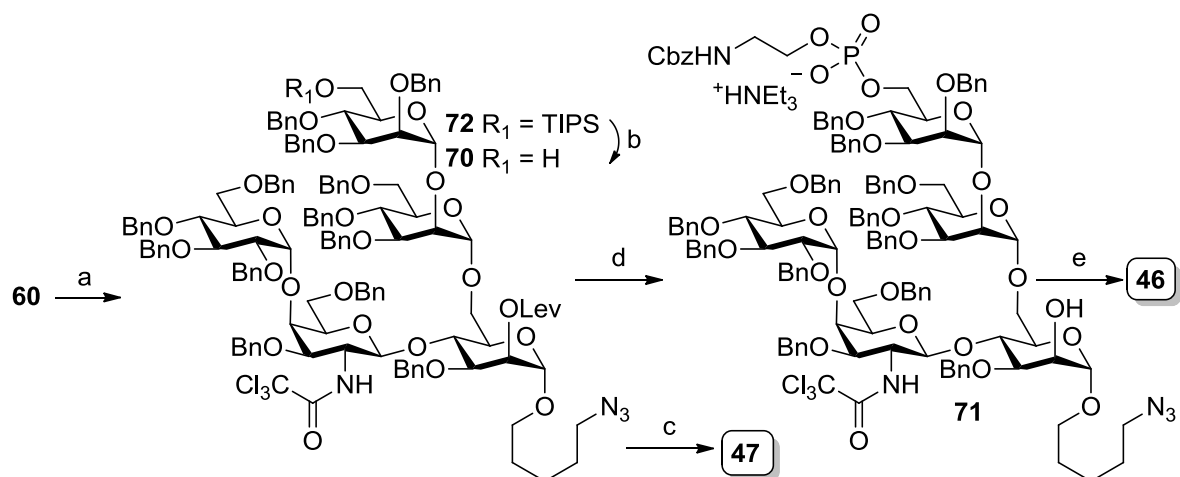
Scheme 2.11: Synthesis of trisaccharide **43** representing the branch of GPI **1**. *Reagents and conditions:* (a) i. $[\text{Ir}(\text{COD})(\text{PPh}_2\text{Me})_2]\text{PF}_6$, H_2 , THF; ii. HgCl_2 , HgO , H_2O , acetone; iii. Cl_3CCN , DBU, CH_2Cl_2 , 36% over three steps; (b) **53**, TBSOTf, Et_2O , MS 4\AA , $0\text{ }^\circ\text{C}$, 89%; (c) $\text{HF}\cdot\text{Py}$, THF, 74%; (d) hydrazine, THF, 84%; (e) Pd/C, H_2 , MeOH, 88%.

For the construction of branched mannoses **44**, **45** and **49** intermediate **62** served as a starting point (Scheme 2.12, page 39). Selective removal of the TBDPS ether yielded disaccharide acceptor **63**, which was elongated with dimannoside **8** (see Scheme 2.3, page 25) to yield branched tetrasaccharide **64** in 74% yield over two steps. Isomerization of the allyl ether followed by mild acidic hydrolysis employing mercury salts yielded an anomeric mixture of lactols that was subsequently converted into glycosylation agent **65**. Glycosylation of linker **53** with **65** yielded tetrasaccharide **66**, which was subsequently transformed into key intermediate **67** *via* deprotection of the TIPS ether. Hydrazinolysis of the Lev ester gave access to diol **68**, which was either directly hydrogenated resulting in the formation of substructure **45** or double phosphorylated before global deprotection yielded tetrasaccharide **49**. For preparation of **44** the previously established one-pot protocol (see Scheme 2.7, page 34) for the phosphorylation of the O6 position of ManIII and removal of the Lev ester produced precursor **69** in 95% yield over three steps starting from **67**. Final Pd-catalyzed hydrogenation was able to cleave all remaining protecting groups and reduced the trichloroacetamide moiety to the desired acetamide functionality, which completed the synthesis of tetrasaccharide **44**.



Scheme 2.12: Synthesis of branched mannoses **44**, **45** and **49**. *Reagents and conditions:* (a) HF•Py, THF, 86%; (b) **8**, TBSOTf, Et₂O, MS 4 Å, 0 °C, 86%; (c) i. [IrCOD(PPh₂Me)₂]PF₆, THF; ii. HgCl₂, HgO, water, acetone; iii. Cl₃CCN, DBU, DCM, 63% over three steps; (d) **53**, TBSOTf, Et₂O, MS 4 Å, 0 °C, 87%; (e) HF•Py, THF, 63%; (f) hydrazine, MeCN, 92%; (g) i. **10**, PivCl, Py; ii. water, I₂, 78%; (h) Pd/C, H₂, MeOH, 52%. (i) Pd/C, H₂, MeOH, 75%; (j) i. **10**, PivCl, Py; ii. water, I₂; iii. hydrazine monohydrate, 95%; (k) Pd/C, H₂, MeOH, 91%;

The last substructures **46** and **47** representing the branched mannose moieties of GPI **1** were build up in accordance with the general retrosynthetic analysis. Sugar acceptor intermediate **60** (see Scheme 2.11, page 38) was glycosylated with imidate **8**, before the TIPS ether was hydrolyzed giving pentasaccharide **70** in 66% yield over two steps (Scheme 2.13, page 40). Two-stage global deprotection of **70** yielded the unphosphorylated substructure **47**. In addition one-pot functionalization of **70** formed the monophosphorylated sugar **71** in 80% yield, which underwent hydrogenolysis efficiently to generate the final carbohydrate probe **46**.



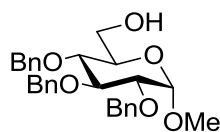
Scheme 2.13: Synthesis of pentasaccharides **46** and **47** representing substructures of GPI **1**. *Reagents and conditions:* (a) **8**, TBSOTf, Et₂O, MS 4Å, 0 °C, 69%; (b) Sc(OTf)₃, MeCN, H₂O, 95%; (c) i. hydrazine, THF, 54% ii. Pd/C, H₂, MeOH, 74%; (d) i. **10**, PivCl, Py; ii. I₂, H₂O; iii. hydrazine, 80% over three steps (one pot); (e) Pd/C, H₂, MeOH, 73%.

2.6 Conclusions and Perspectives

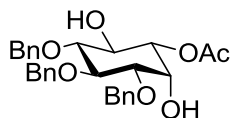
In this chapter, the synthesis of GPI-based chemical probes, which can be used for conjugation to carrier proteins or immobilization on surfaces, was described. The orthogonal Allyl/Lev/TIPS protecting group set in connection with the general retrosynthetic analysis for GPI derivatives and their substructures proved feasible and successful in generating a variety of different carbohydrates. This strategy is envisaged to be applicable for the synthesis of substructures that are lacking either the top mannose part (ManIII and ManII) or the side branch. In addition, a high yielding one-pot reaction sequence for the introduction of late stage modification was developed, which allows the preparation of GPI derivatives containing different phosphorylation patterns.

2.7 Experimental Part

All chemicals were reagent grade and used as supplied except where noted. Unless otherwise noted, all reactions were performed in dried glassware under an argon atmosphere. Pyridine and triethylamine (NEt₃) were distilled over CaH₂ prior to use. Dichloromethane (CH₂Cl₂), toluene, diethyl ether (Et₂O), tetrahydrofuran (THF) and *N,N*-dimethylformamide (DMF) were purchased from *JT Baker* or *VWR International* and purified by a Cycle-Tainer Solvent Delivery System. Molecular sieves 4 Å were purchased from *Roth*. Analytical thin-layer chromatography was performed on *Macherey-Nagel* silica gel SIL G-25 UV₂₅₄ plates (0.25 mm). Compounds were visualized by UV-light at 254 nm and by dipping the plates in a cerium sulfate ammonium molybdate (CAM) solution or 1 M ethanolic sulfuric acid solution containing 0.1wt% *m*-methoxyphenol followed by heating. Liquid chromatography was performed using forced flow of the indicated solvent on *Fluka* silica gel 60 (230-400 mesh). TEA/CO₂ buffer was prepared by filling TEA (7 mL) in a measuring cylinder and adding water until the total volume reached 500 mL. The solution was transferred to a flask and CO₂ was bubbled through the solution for 1 h at 0 °C. The buffer was stored at 4 °C. ¹H NMR spectra were obtained on a *Varian* MR-400 (400 MHz) and on a *Varian* PremiumCOMPACT 600 (600 MHz) spectrometer and are reported in parts per million (δ) relative to the resonance of the solvent (CDCl₃ 7.26 ppm ¹H; D₂O 4.79 ppm ¹H). Splitting patterns are indicated as s, singlet; d, doublet; t, triplet; q, quartet; br broad singlet; m, multiplett. Coupling constants (*J*) are reported in Hertz (Hz). ¹³C NMR spectra were obtained on a *Varian* MR-400 (100 MHz) and on a *Varian* PremiumCOMPACT 600 (125 MHz) spectrometer and are reported in parts per million (δ) relative to the resonance of the solvent (CDCl₃ 77.1 ppm ¹³C). ³¹P NMR spectra were obtained on a *Varian* MR-400 (162 MHz) and on a *Varian* PremiumCOMPACT 600 (243 MHz) spectrometer and are reported in parts per million (δ). IR Spectra were measured neat on a *Perkin-Elmer*-100 FT-IR spectrometer. Specific [α]_D²⁰ values were determined on a *Schmidt+Haensch* Unipol L1000. High-resolution mass spectra were measured by the MS service at the Institute of Organic Chemistry at the Free University Berlin using an *Agilent* 6210 ESI-TOF and are given in *m/z*. This general information is valid for all synthetic procedures in this PhD thesis including the appendix.

1-O-Methyl-2,3,4-tri-O-benzyl- α -D-glucopyranose (14)

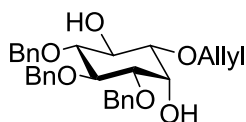
Triol **12**^{*} (7.0 g, 20.0 mmol) and BnBr (11.9 mL, 100 mmol) were dissolved in dry DMF (100 mL). The solution was cooled down to 0 °C and NaH (2.4 g, 100 mmol) was added. After 30 min the reaction was allowed to warm to r. t. and was stirred for 12 h. The reaction was quenched with MeOH (2 mL) and water (100 mL) was added. The reaction mixture was extracted with Et₂O (3x 100 mL). The organic layers were washed with brine (2x 150 mL), dried over Na₂SO₄ and solvents were removed in vacuo to yield yellow syrup. The crude product was dissolved in THF (25 mL) and TBAF·3H₂O (12.6 g, 40 mmol) was added to this solution. The reaction mixture was stirred 12 h, diluted with water (75 mL) and extracted with EtOAc (3x 100 mL). The organic layers were washed with brine (2x 150 mL), dried over Na₂SO₄ and solvents were removed in vacuo. The crude product was purified using column chromatography (cyclohexane/EtOAc 3:1) to yield **14** as yellow syrup (7.1 g, 15.4 mmol, 77%): R_f (SiO₂, EtOAc/Hexane 1:2) = 0.30; ¹H NMR (400 MHz, CDCl₃) δ 7.62 – 6.47 (m, 15H, 3x Bn), 4.91 (d, *J* = 10.9 Hz, 1H), 4.85 – 4.66 (m, 3H), 4.66 – 4.52 (m, 2H), 4.49 (d, *J* = 3.6 Hz, 1H), 3.99 – 3.86 (t, *J* = 9.2, 1H), 3.74 – 3.52 (m, 3H), 3.50 – 3.37 (m, 2H), 3.29 (s, 3H, Me), 1.60 (s, 1H, OH); ¹³C-NMR (75 MHz, CDCl₃) δ 138.58, 137.97, 128.37, 128.30, 128.02, 127.93, 127.86, 127.77, 127.52, 98.11 (Glc-1), 81.93, 79.92, 77.46, 77.34, 77.03, 76.61, 75.76, 75.03, 73.43, 70.65, 61.85, 55.22; ESI-MS: *m/z* [M+Na]⁺ calcd for C₃₉H₇₂N₃O₂₉P 487.2, obsd 487.2. Spectral data were in good agreement with Ref. [95].

1-O-Acetyl-3,4,5-tri-O-benzyl-D-myoinositol (17)

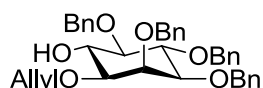
Alcohol **14** (7.1 g, 15.4 mmol) was dissolved in dry DCM (180 mL) and cooled down to 0 °C. SO₃·Py complex (10.1 g, 63.5 mmol) was added to this solution immediately followed by DIPEA (14.5 mL, 147.5 mmol). After 10 min DMSO (1.7 mL, 23.9 mmol) was added and the reaction mixture was stirred for 1.5 h at 0 °C (R_f of aldehyde (SiO₂, EtOAc/Hexane 1:2) =

* Compound **12** was provided by Y.-H. Tsai and prepared according to Ref. [95].

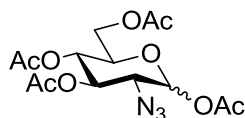
0.16). Afterwards sat. NaHCO_3 solution (150 mL) was added and the water phase was extracted with Et_2O (3x 100 mL). The combined organic layers were washed with brine (2x 100 mL), dried over Na_2SO_4 and the solvents were removed in vacuo. The crude aldehyde was placed under HV for 4 h and was afterwards dissolved in dry MeCN (200 mL). Ac_2O (9.0 mL, 95.0 mmol) and K_2CO_3 (8.8 g, 63.3 mmol) were added to the solution and the slurry was heated to reflux while stirring for 12 h (R_f of major enol acetate (SiO_2 , EtOAc/Hexane 1:2) = 0.67). The solution was cooled down to r.t. and sat. NaHCO_3 solution (200 mL) was added. The reaction mixture was extracted with Et_2O (3x 150 mL), the combined organic layers were washed with brine (100 mL) and dried over Na_2SO_4 . Solvents were removed in vacuo and the residue was placed under HV for 4 h. Crude enol ether was dissolved in water (50 mL) and acetone (200 mL) before $\text{Hg}(\text{CF}_3\text{COO})_2$ (8.1 g, 19.0 mmol) was added. After 1 h the solution was cooled down to 0 °C and 3 M $\text{NaOAc}_{(\text{aqu.})}$ (6.3 mL) was added immediately followed by the addition of brine (22 mL). The solution was stirred for 12 h at r.t., before sat. NaHCO_3 solution (200 mL) was added. The reaction mixture was extracted with Et_2O (3x 150 mL), organic layers were dried over Na_2SO_4 and solvents were removed in vacuo. The crude ketone was placed under HV for 4 h before it was dissolved in MeCN (70 mL) and added dropwise to a solution of $\text{NaBH}(\text{OAc})_3$ (16.8 g, 79.0 mmol) in HOAc (75 mL) and MeCN (75 mL) cooled down to 0 °C. After complete addition the reaction mixture was allowed to warm to r.t. and stirred for 12 h. Then sat. NaHCO_3 solution (200 mL) was added and the solution was extracted with Et_2O (3x 150 mL). The organic layers were dried over Na_2SO_4 and solvents were removed in vacuo. The residue was purified using column chromatography (cyclohexane/ethyl acetate starting from 7:3 to 1:1) to yield **17** as white solid (3.7 g, 7.5 mmol, 49 % over 4 steps): R_f (SiO_2 , EtOAc/Hexane 1:1) = 0.52; ^1H NMR (400 MHz, CDCl_3) δ 7.37 – 7.27 (m, 15H, 3xBn), 4.99 – 4.88 (m, 2H), 4.84 (d, J = 10.8 Hz, 1H), 4.78 – 4.71 (m, 2H), 4.69 (d, J = 0.9 Hz, 2H), 4.29 (t, J = 2.7 Hz, 1H), 4.11 (t, J = 9.8 Hz, 1H), 3.93 (t, J = 9.5 Hz, 1H), 3.56 (dd, J = 9.5, 2.7 Hz, 1H), 3.38 (t, J = 9.4 Hz, 1H), 2.44 (bs, 1H, OH), 2.25 (bs, 1H, OH), 2.17 (s, 3H, CH_3); ^{13}C NMR (101 MHz, CDCl_3) δ 170.86 (COCH_3), 138.58, 138.49, 137.55, 128.74, 128.57, 128.26, 128.08, 128.06, 127.86, 83.02, 81.04, 80.26, 76.00, 75.83, 73.14, 73.02, 70.48, 67.93, 21.24 (COCH_3); ESI-MS: m/z $[\text{M}+\text{Na}]^+$ calcd for $\text{C}_{39}\text{H}_{72}\text{N}_3\text{O}_{29}\text{P}$ 515.2, obsd 515.2. Spectral data were in good agreement with Ref. [97].

1-*O*-Allyl-3,4,5-tri-*O*-benzyl-D-*myo*-inositol (18)

Diol **17** (5.2 g, 10.5 mmol) was dissolved in DCM (65 mL). Ethyl vinyl ether (20.4 mL) and *p*-TsOH (0.4 g, 1.6 mmol) were added. The reaction mixture was stirred for 12 h and quenched with TEA (5 mL) (R_f of acetals (SiO₂, EtOAc/Hexane 1:2) = 0.61). Solvents were removed in vacuo, the residue was dissolved in MeOH (50 mL) and NaH (120 mg, 5.0 mmol) was added. The reaction mixture was heated to 50 °C and stirred for 12 h (R_f of the diastereomeric alcohols (SiO₂, EtOAc/Hexane 1:2) = 0.57; 0.52; 0.39). Afterwards solvents were removed in vacuo, the residue was filtered through a pad of silica gel (200 mL, DCM/MeOH 20:1) and the filtrate was evaporated to dryness. The crude residue at this stage was dissolved in DMF (100 mL) and cooled to 0 °C before allyl bromide (4.6 mL, 53.0 mmol) and TBAI (400 mg, 1.1 mmol) were added. Then NaH (1.4 g, 53.2 mmol) was added and the mixture was stirred for 12 h at r.t. (R_f of allyl ether (SiO₂, EtOAc/Hexane 1:2) = 0.81). Afterwards MeOH (6 mL) was added to quench the reaction, before the solution was diluted with THF (50 mL) and 2 N HCl (50 mL). The reaction mixture was heated to 50 °C for 2 h. Afterwards the reaction was quenched with sat. NaHCO₃ solution (300 mL) and extracted with Et₂O (3x 200 mL). The combined organic layers were washed with brine (200 mL), dried over Na₂SO₄ and evaporated to dryness. The residue was purified by silica gel column chromatography (*n*-hexane/ethyl acetate 3:1) to yield **18** as white solid (4.21 g, 8.6 mmol, 82%): R_f (SiO₂, EtOAc/Hexane 1:2) = 0.18; ¹H NMR (400 MHz, CDCl₃) δ 7.41 – 7.24 (m, 15H, 3xBn), 5.94 (ddt, J = 16.2, 10.4, 5.8 Hz, 1H, CH₂=CH), 5.29 (dq, J = 17.2, 1.5 Hz, 1H, CH₂=CH), 5.25 – 5.16 (m, 1H, CH₂=CH), 4.91 (dd, J = 11.0, 1.7 Hz, 2H), 4.87 – 4.79 (m, 2H), 4.74 (d, J = 1.8 Hz, 2H), 4.26 – 4.17 (m, 2H), 4.12 (ddt, J = 12.7, 5.9, 1.3 Hz, 1H), 4.03 (td, J = 9.5, 2.0 Hz, 1H), 3.97 (t, J = 9.5 Hz, 1H), 3.44 (dd, J = 9.6, 2.8 Hz, 1H), 3.35 (t, J = 9.4 Hz, 1H), 3.16 (dd, J = 9.6, 2.7 Hz, 1H), 2.45 (d, J = 2.0 Hz, 1H, OH), 2.41 (s, 1H, OH); ESI-MS: m/z [M+Na]⁺ calcd for C₃₉H₇₂N₃O₂₉P 513.2, obsd 512.9. Spectral data were in good agreement with Ref. [94].

1-O-Allyl-2,3,4,5-tetra-O-benzyl-D-myoinositol (12)

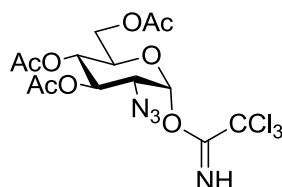
Allyl ether **18** (300 mg, 0.61 mmol) was dissolved in DMF (15 mL). TBAI (226 mg, 0.61 mmol) and BnBr (73 μ L, 0.61 mmol) were added and the solution was cooled down to 0 °C before NaH (59 mg, 2.5 mmol) was added. The solution was stirred for 14 h at r.t. and quenched with MeOH (1 mL). Sat. NaHCO₃ (30 mL) was added and the solution was extracted with Et₂O (3x 30 mL). The organic layers were dried over Na₂SO₄ and evaporated to dryness. The residue was purified using column chromatography (*n*-hexane/ethyl acetate starting from 4:1 to 2:1) to yield **12** as yellow oil that solidified upon standing (248 mg, 0.43 mmol, 70%): R_f (SiO₂, EtOAc/Hexane 1:2) = 0.58; ¹H NMR (400 MHz, CDCl₃) δ 7.42 – 7.24 (m, 20H, 4xBn), 5.95 – 5.79 (m, 1H, CH₂=CH), 5.27 (dq, J = 17.2, 1.6 Hz, 1H, CH₂=CH), 5.22 – 5.13 (m, 1H, CH₂=CH), 4.98 – 4.78 (m, 6H), 4.67 (q, J = 11.8 Hz, 2H), 4.21 – 3.91 (m, 5H), 3.44 – 3.34 (m, 2H), 3.11 (dd, J = 9.9, 2.2 Hz, 1H), 2.49 (d, J = 1.9 Hz, 1H, OH); ¹³C NMR (101 MHz, CDCl₃) δ 139.01, 138.96, 138.95, 138.50, 134.64 (CH₂=CH), 128.54, 128.45, 128.30, 128.21, 127.99, 127.93, 127.78, 127.74, 127.72, 127.66, 127.53, 117.49 (CH₂=CH), 83.59, 81.56, 81.29, 79.95, 75.97, 75.48, 74.16, 73.55, 73.06, 72.90, 71.25. Spectral data were in good agreement with Ref. [93].

1,3,4,6-Tetra-O-acetyl-2-azido-2deoxy- α/β -D-glucopyranose (20)

NaN₃ (4.4 g, 67.1 mmol) was suspended in dry MeCN (80 mL) and cooled down to 0 °C. To this slurry Tf₂O (9.4 mL, 55.6 mmol) was added drop wise in 5 min. The reaction mixture was stirred for 2 h at 0 °C before it was added drop wise at 0 °C to a solution of D-glucosamine hydrochloride (10.0 g, 46.4 mmol) in water (50 mL) containing CuSO₄·5H₂O (116 mg, 0.5 mmol) and TEA (12.9 mL, 92.8 mmol). The dark brown reaction mixture was stirred for 22 h slowly rising to r.t., before glycine (12 g, 160 mmol) was added to quench the reaction. The suspension was stirred for additional 24 h and subsequently filtered. The filter cake was washed with DCM/MeOH (1:1; 3x 40 mL) and the solvents were evaporated in vacuo. The

residue was coevaporated with toluene (40 mL) and dissolved in pyridine (200 mL). The solution was cooled down to 0 °C and acetic anhydride (200 mL) was added. The solution was stirred for 12 h at r.t., before all solvents were removed in vacuo. The residue was co evaporated with toluene (3x 40 mL) and further purified using column chromatography (cyclohexane/ethyl acetate 3:1) to yield **20** as yellow oil (11.8 g, 31.6 mmol, 68%, α/β -mixture 3:7): R_f (SiO₂, EtOAc/Hexane 2:3) = 0.52; ¹H-NMR (400MHz, CDCl₃) δ 6.29 (d, J = 3.7Hz, 1H, Glc-1 α), 5.55 (d, 1H, J = 8.6Hz, Glc-1 β), 5.44 (dd, J = 10.5, 9.4 Hz, 1H, Glc-3 α), 5.07-4.95 (m, 3H, Glc-3 β , Glc-4 α/β), 4.26-4.20 (m, 2H, Glc-6 α/β), 4.08-3.97 (m, 3H, Glc-5 α , Glc-6 α/β), 3.80 (ddd, J = 9.7, 4.5, 2.2 Hz, 2H, Glc-3 α/β), 3.63-3.36 (m, 2H, Glc-2 α/β), 2.18, 2.09, 2.08, 2.06, 2.03, 2.01 (6x s, 24H, CH₃ of OAc); ¹³C-NMR (101MHz, CDCl₃) δ 170.50, 170.00, 169.74, 169.56, 169.49, 168.51, 168.46 (7xCOCH₃), 92.53 (C1 beta), 89.91 (C1 alpha), 72.69, 72.67, 70.71, 69.71, 67.85, 67.74, 62.53, 61.39, 61.36, 60.26, 21.00, 20.88, 20.83, 20.64, 20.62, 20.60, 20.58, 20.51 (8x COCH₃); ESI-MS: m/z [M+Na]⁺ calcd for C₃₉H₇₂N₃O₂₉P 396.1, obsd 396.1.

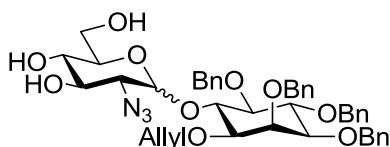
3,4,6-Tri-*O*-acetyl-2-azido-2deoxy- α -D-glucopyranosyl trichloroacetimidate (**11**)



Ethylenediamine (2.5 mL, 37.9 mmol) was added to a stirred solution of acetic acid (2.5 mL, 44.2 mmol) in dry THF (500 mL). To this slurry azide **20** (11.8 g, 31.6 mmol) in dry THF (50 mL) was added and the reaction mixture was stirred for 16 h before it was filtered. The filtrate was washed with sat. NaHCO₃ solution (300 mL), 1N HCl (300 mL) and brine (300 mL), dried over Na₂SO₄ and evaporated to dryness to yield the lactol (R_f (SiO₂, EtOAc/Hexane 1:1) = 0.44) as white foam (9.5 g, 28.6 mmol, 91%), which was pure enough for the next step. The lactol (4.0 g, 12.1 mmol) was dissolved in dry DCM (50 mL) and the resulting solution was cooled to 0 °C. Trichloroacetonitrile (12.1 mL, 121 mmol) and DBU (182 μ L, 1.2 mmol) were added and the black reaction mixture was stirred at 0 °C for 1 h and 12 h at r.t., before all solvents were removed in vacuo. The black residue was purified by column chromatography (cyclohexane/ethyl acetate 3:1) to yield **11** as yellow solid (5.1 g, 10.7 mmol, 80% over two steps): R_f (SiO₂, EtOAc/Hexane 2:3) = 0.52; ¹H NMR (400 MHz, CDCl₃) δ

8.83 (s, 1H, NH), 6.49 (d, $J = 3.6$ Hz, 1H, Glc-1), 5.52 (dd, $J = 10.3, 9.5$ Hz, 1H, Glc-3), 5.15 (t, $J = 9.8$, 1H, Glc-4), 4.27 (dd, $J = 12.3, 4.3$ Hz, 1H, Glc-6), 4.21 (ddd, $J = 10.3, 4.2, 2.0$ Hz, 1H, Glc-5), 4.13 – 4.07 (m, 1H, Glc-6), 3.77 (dd, $J = 10.5, 3.6$ Hz, 1H, Glc-2), 2.11 (s, 3H, CH₃), 2.06 (s, 3H, CH₃), 2.05 (s, 3H, CH₃); ¹³C NMR (101 MHz, CDCl₃) δ 170.58, 169.94, 169.76 (3xCOCH₃), 160.66 (CNHCCl₃), 94.15 (Glc-1), 90.65 (CNHCCl₃), 70.80, 70.25, 68.06, 61.53, 60.78, 20.81, 20.78, 20.72 (3x CH₃). Spectral data were in good agreement with Ref. [92].

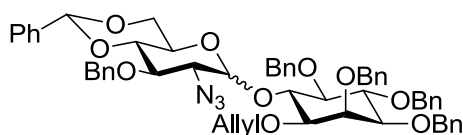
2-azido-2-deoxy- α/β -D-glucopyranosyl-(1 \rightarrow 6)-1-O-allyl-2,3,4,5-tetra-O-benzyl-D-myoinositol (21)



Trichloroacetimidate **11** (618 mg, 1.30 mmol) and alcohol **12** (377 mg, 0.65 mmol) were co evaporated with dry toluene (3x2 mL) and placed under HV for 30 min. The residue was dissolved in dry DCM (18 mL) and dry thiophene (1.0 mL, 13.0 mmol) was added. TMSOTf (23.5 μ L, 0.13 mmol) was added at r.t. and the resulting reaction mixture was stirred for 1 h. The reaction was quenched with TEA (100 μ L) and solvents were evaporated in vacuo (R_f of protected pseudodisaccharide (SiO₂, EtOAc/Hexane 1:3) = 0.51). The crude residue was dissolved in MeOH (10 mL) and NaOMe (50 mg, 0.9 mmol) was added before the solution was heated to 40 °C for 3 h. The reaction was quenched using Amberlite resin (IR 120 H⁺ form), filtered and evaporated to dryness. The residue was purified using column chromatography (DCM/MeOH 30:1) to yield pseudodisaccharide **21** as an inseparable mixture of anomers as white solid (428 mg, 0.6 mmol, 86%, $\alpha/\beta >11:2$, over two steps): Analytical data for α -anomer: R_f (SiO₂, DCM/MeOH 20:1) = 0.67; ¹H NMR (400 MHz, CDCl₃) δ 7.48 – 7.28 (m, 20H), 6.06 – 5.90 (m, 1H, CH₂=CH-CH₂), 5.66 (d, $J = 3.7$ Hz, 1H, GlcNH₂-1), 5.31 (dq, $J = 17.2, 1.5$ Hz, 1H, CH₂=CH-CH₂), 5.23 (dd, $J = 10.4, 1.4$ Hz, 1H, CH₂=CH-CH₂), 5.15 (d, $J = 11.4$ Hz, 1H), 5.01 (d, $J = 10.6$ Hz, 1H), 4.90 – 4.83 (m, 3H), 4.73 – 4.63 (m, 3H), 4.20 (dt, $J = 15.9, 9.6$ Hz, 2H), 4.07 – 4.02 (m, 3H), 3.97 – 3.90 (m, 1H), 3.84 – 3.78 (m, 1H), 3.49 – 3.33 (m, 5H), 2.73 (d, $J = 2.7$ Hz, 1H), 2.29 (d, $J = 4.5$ Hz, 1H), 1.80 (bs, 3H, 3xOH); ¹³C NMR (101 MHz, CDCl₃) δ 138.92, 138.89, 138.62, 138.33, 134.39, 128.57, 128.55, 128.48, 128.38, 128.14, 128.04, 127.87, 127.79, 127.68, 127.42, 117.45

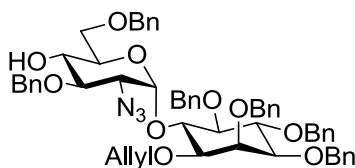
(CH₂=CH-CH₂), 97.65 (C-1), 82.08, 81.82, 81.65, 81.01, 75.95, 75.54, 75.29, 74.27, 73.08, 73.02, 72.56, 71.67, 71.08, 69.61, 62.92, 62.58.

4,6-*O*-Benzyliden-3-*O*-benzyl-2-azido-2-deoxy- α/β -D-glucopyranosyl-(1 \rightarrow 6)-1-*O*-allyl-2,3,4,5-tetra-*O*-benzyl-D-*myo*-inositol (7a**)**



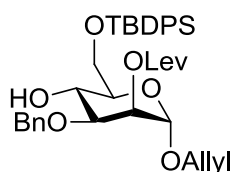
Triol **21** (251 mg, 0.33 mmol) was dissolved in dry MeCN (4 mL) and benzaldehyde dimethyl acetal (196 μ L, 1.31 mmol) and CSA (7.6 mg, 0.03 mmol) were added. The solution was stirred for 3 h before the reaction was quenched with TEA (100 μ L) and solvents were removed in vacuo. The residue was purified with column chromatography (*n*-hexane/ethyl acetate 5:1) to yield colorless oil (220 mg, 0.23 mmol, 70% yield) that was dissolved in dry DMF (5 mL). TBAI (241 mg, 0.66 mmol) and BnBr (78 μ L, 0.66 mol) were added and the solution was cooled down to 0 °C. NaH (30 mg, 1.30 mmol) was added to this solution and the reaction mixture was stirred for 3 h at r.t., before it was quenched with MeOH (100 μ L) and diluted with Et₂O (30 mL). The organic layer was washed with water (1x30 mL) and sat. brine (2x30 mL), dried over Na₂SO₄ and solvents were removed in vacuo. The residue was purified with column chromatography (*n*-hexane/ethyl acetate 8:1) to yield an inseparable mixture of anomers of **7a** as white solid (218 mg, 0.23 mmol, 71%): Analytical data for α -anomer: ¹H NMR (400 MHz, CDCl₃) δ 7.44 – 7.27 (m, 20H), 7.25 – 7.14 (m, 10H), 6.01 – 5.88 (m, 1H, CH₂=CH-CH₂), 5.75 (d, *J* = 3.8 Hz, 1H, GlcNH₂-1), 5.42 (s, 1H, benzyliden O₂CH), 5.28 (dq, *J* = 17.4, 1.5 Hz, 1H, CH₂=CH-CH₂), 5.20 (ddd, *J* = 10.4, 2.8, 1.2 Hz, 1H, CH₂=CH-CH₂), 4.98 (d, *J* = 11.7 Hz, 1H), 4.93 (d, *J* = 10.5 Hz, 1H), 4.88 (d, *J* = 11.6 Hz, 1H), 4.85 (s, 2H), 4.75 (d, *J* = 10.6 Hz, 1H), 4.68 (d, *J* = 11.7 Hz, 1H), 4.62 (d, *J* = 11.7 Hz, 1H), 4.27 (t, *J* = 9.5 Hz, 1H), 4.19 – 4.07 (m, 5H), 4.05 – 3.98 (m, 3H), 3.56 (t, *J* = 9.8 Hz, 1H), 3.50 – 3.34 (m, 4H), 3.19 (dd, *J* = 10.1, 3.8 Hz, 1H), 2.56 (d, *J* = 2.4 Hz, 1H).

3,6-di-*O*-benzyl-2-azido--2-deoxy- α -D-glucopyranosyl-(1 \rightarrow 6)-1-*O*-allyl-2,3,4,5-tetra-*O*-benzyl-D-*myo*-inositol (7)



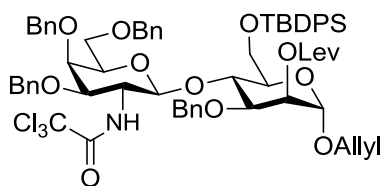
Pseudodisaccharide **7a** (500 mg, 0.53 mmol) was dissolved in dry DCM (25 mL) and powdered MS4Å (700 mg) and Et₃SiH (253 μ L, 1.59 mmol) were added. The slurry was stirred 10 min at r.t. before it was cooled down to -78 °C and stirred for another 10 min. TfOH (160 μ L, 1.80 mmol) was added and the reaction was stirred at -78 °C for 30 min before it was quenched with sat. NaHCO₃ solution (1 mL). The solution was filtered over Celite® and diluted with Et₂O (40 mL). The organic layer was washed with sat. NaHCO₃ solution (3x20 mL), dried over Na₂SO₄ and solvents were removed in vacuo. The residue was purified with column chromatography (*n*-hexane/ethyl acetate 6:1) to yield **7** as colorless oil (338 mg, 0.36 mmol, 68%): ¹H NMR (400 MHz, CDCl₃) δ 7.44 – 7.27 (m, 20H), 7.24 – 7.18 (m, 10H), 5.93 (ddt, *J* = 17.2, 10.7, 5.5 Hz, 1H, CH₂=CH-CH₂), 5.70 (d, *J* = 3.7 Hz, 1H, GlcNH₂-1), 5.27 (dq, *J* = 17.2, 1.5 Hz, 1H, CH₂=CH-CH₂), 5.18 (dd, *J* = 10.4, 1.5 Hz, 1H, CH₂=CH-CH₂), 5.03 (d, *J* = 11.1 Hz, 1H), 4.96 (d, *J* = 10.6 Hz, 1H), 4.88 (d, *J* = 1.4 Hz, 2H), 4.84 (s, 2H), 4.79 (d, *J* = 10.6 Hz, 1H), 4.69 – 4.59 (m, 3H), 4.41 (d, *J* = 12.0 Hz, 1H), 4.29 – 4.20 (m, 2H), 4.12 (t, *J* = 9.5 Hz, 1H), 4.04 – 3.95 (m, 4H), 3.81 – 3.66 (m, 2H), 3.46 – 3.34 (m, 3H), 3.29 (dd, *J* = 10.5, 4.0 Hz, 1H), 3.24 – 3.18 (m, 2H), 2.02 (d, *J* = 3.7 Hz, 1H, OH); ¹³C NMR (101 MHz, CDCl₃) δ 138.95, 138.74, 138.56, 138.41, 138.38, 138.14, 134.42, 128.66, 128.56, 128.45, 128.43, 128.37, 128.35, 128.27, 128.09, 128.02, 127.84, 127.82, 127.81, 127.67, 127.65, 127.61, 127.53, 117.23 (CH₂=CH-CH₂), 97.69 (GlcNH₂-1), 82.09, 82.03, 81.64, 81.01, 79.56, 75.88, 75.67, 75.19, 74.95, 74.23, 73.54, 73.11, 72.95, 72.37, 71.04, 69.53, 69.21, 63.02. Spectral data were in good agreement with Ref. [85].

Allyl 3-*O*-benzyl-2-*O*-levulinyl-6-*O*-tertbutyldiphenylsilyl- α -D-mannopyranoside (27)



Mannoside **6**¹¹⁰ (2.50 g, 3.18 mmol) was dissolved in PBS buffer (1.0 M, 1 mL, pH 7.4) and dichloromethane (19 mL). DDQ (0.87 g, 3.81 mmol) was added at 0 °C. After 5 h the reaction mixture was washed with sat. NaHCO₃ solution, dried over Na₂SO₄, filtered and concentrated. The crude product was purified by silica gel column chromatography to give mannoside **27** (1.83 g, 2.83 mmol, 89% yield) as colorless oil: R_f (SiO₂, EtOAc/cyclohexane 1:2) = 0.20; [α]_D²⁰: + 4.42 (c = 1.09, CHCl₃); ATR-FTIR (cm⁻¹): 3486, 3071, 2930, 2857, 1741, 1720, 1428, 1362, 1138, 1105, 1082, 1044, 741, 702; ¹H NMR (400 MHz, CDCl₃) δ 7.71-7.69 (m, 4H), 7.42-7.26 (m, 11H), 5.86 (m, 1H, =CH-), 5.35 (dd, *J* = 3.2, 1.7 Hz, 1H, Man-2), 5.24 (m, 1H, =CH₂), 5.17 (m, 1H, =CH₂), 4.84 (d, *J* = 1.7 Hz, 1H, Man-1), 4.69 (d, *J* = 11.2 Hz, 1H, CH₂ of Bn), 4.45 (d, *J* = 11.2 Hz, 1H, CH₂ of Bn), 4.14 (ddt, *J* = 13.0, 5.6, 1.5 Hz, 1H, CH₂ of allyl), 3.99 – 3.88 (m, 4H, CH₂ of allyl, Man-4, Man-6), 3.80 (dd, *J* = 9.4, 3.2 Hz, 1H, Man-3), 3.69 (dt, *J* = 9.4, 4.0 Hz, 1H, Man-5), 2.77 – 2.53 (m, 4H, CH₂ of Lev), 2.10 (s, 3H, Me of Lev), 1.05 (s, 9H, *t*Bu); ¹³C NMR (101 MHz, CDCl₃) δ 206.15 (ketone), 172.00 (ester), 137.77, 135.70, 135.59, 133.50, 133.45, 133.26, 129.67, 129.66, 128.45, 128.14, 127.88, 127.65, 127.62, 117.67 (CH₂=), 96.83 (C1), 77.64 (C3), 72.35 (C5), 71.52 (-OCH₂-), 68.22 (C2), 67.93 (-OCH₂- of allyl), 67.26 (C4), 63.87 (C6), 37.94 (-CH₂CH₂- of Lev), 29.77 (Me), 28.07 (-CH₂CH₂- of Lev), 26.80 (Me of *t*Bu), 19.31 (CMe₃); ESI-MS: *m/z* [M+Na]⁺ calcd for C₃₇H₄₆O₈Si 669.2854, obsd 669.2858.

Allyl 3,4,6-tri-*O*-benzyl-2-deoxy-2-trichloroacetamido-β-D-galactopyranosyl-(1→4)-3-*O*-benzyl-2-*O*-levulinyl-6-*O*-tertbutyldiphenylsilyl-α-D-mannopyranoside (28)



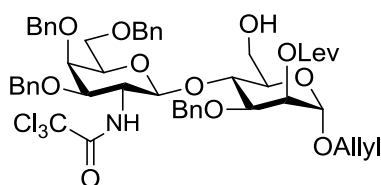
Phosphate **24**^{*} (63 mg, 0.080 mmol) and alcohol **27** (40 mg, 0.062 mmol) were coevaporated with toluene (3x2 mL) and placed under high vacuum for 30 min. The residue was dissolved in anhydrous DCM (3 mL) and molecular sieves (4Å, 150 mg) were added. The slurry was

¹¹⁰ The fully protected building block **6** was provided by M. Kozakowski and prepared according to Y.-H. Tsai, S. Götz, N. Azzouz, H. S. Hahm, P. H. Seeberger, D. Varón Silva, *Angew. Chem. Int. Edit.* **2011**, *50*, 9961-9964.

* The glycosylation agent **24** was provided by Y.-H. Tsai and was prepared according to Ref. [103]. A precursor of this building block was synthesized by H. S. Hahm.

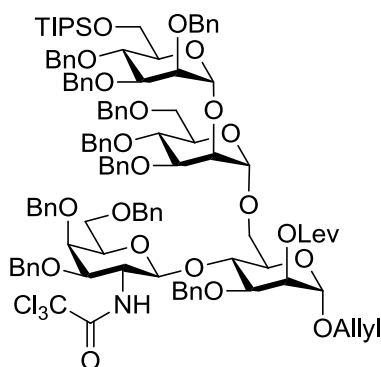
stirred for 15 min at r.t. and afterwards cooled down to $-40\text{ }^{\circ}\text{C}$. TMSOTf ($14.5\text{ }\mu\text{L}$, 0.080 mmol) was added dropwise and the yellow solution was stirred at $-40\text{ }^{\circ}\text{C}$ for 1 h, before it was quenched with TEA ($100\text{ }\mu\text{L}$) and diluted with CHCl_3 (10 mL). The reaction mixture was filtered over Celite® and solvents were removed under reduced pressure. The residue was purified using flash column chromatography (*n*-hexane/ethyl acetate 5:1) to yield **28** (62 mg , 0.051 mmol , 82% yield) as white foam: R_f (SiO_2 , *n*-hexane/ethyl acetate 3:1) = 0.55; $[\alpha]_{\text{D}}^{20}$: +30.2 ($c = 1.00$, CHCl_3); ATR-FTIR (cm^{-1}): 3409, 3066, 3032, 2929, 2858, 1737, 1717, 1520, 1362, 1140, 1105, 1065cm^{-1} ; $^1\text{H NMR}$ (600 MHz , CDCl_3) δ 7.77 – 7.71 (m, 4H), 7.43 – 7.24 (m, 21H), 7.23 – 7.16 (m, 5H), 6.32 (d, $J = 7.4\text{ Hz}$, 1H, NH), 5.93 – 5.84 (m, 1H, CH of allyl), 5.34 (dd, $J = 3.3, 1.5\text{ Hz}$, 1H, Man-2), 5.26 (dd, $J = 17.2, 1.5\text{ Hz}$, 1H, CH_2 of allyl), 5.20 (dd, $J = 10.4, 1.2\text{ Hz}$, 1H, CH_2 of allyl), 5.16 (d, $J = 8.3\text{ Hz}$, 1H, Gal-1), 4.89 (d, $J = 11.2\text{ Hz}$, 1H), 4.84 (d, $J = 1.5\text{ Hz}$, 1H, Man-1), 4.69 – 4.62 (m, 3H), 4.57 (d, $J = 11.2\text{ Hz}$, 1H), 4.47 (d, $J = 11.3\text{ Hz}$, 1H), 4.35 (d, $J = 11.8\text{ Hz}$, 1H), 4.27 (d, $J = 11.8\text{ Hz}$, 1H), 4.18 (dd, $J = 12.8, 5.3\text{ Hz}$, 1H), 4.09 – 4.03 (m, 2H), 4.01 – 3.94 (m, 4H), 3.86 (dd, $J = 11.2, 5.4\text{ Hz}$, 1H), 3.77 (dd, $J = 9.8, 4.9\text{ Hz}$, 1H), 3.70 (dt, $J = 10.9, 7.9\text{ Hz}$, 1H), 3.63 (t, $J = 8.6\text{ Hz}$, 1H), 3.45 (dd, $J = 8.0, 5.4\text{ Hz}$, 1H), 3.33 (dd, $J = 9.0, 5.2\text{ Hz}$, 1H), 2.65 – 2.53 (m, 2H, CH_2 of Lev), 2.53 – 2.46 (m, 1H, CH_2 of Lev), 2.46 – 2.40 (m, 1H, CH_2 of Lev), 2.05 (s, 3H, Me of Lev), 1.08 (s, 9H, *t*Bu); $^{13}\text{C NMR}$ (151 MHz , CDCl_3) δ 206.33 (ketone), 172.10 (ester), 161.89 (CCl_3CONH), 138.76, 138.70, 138.05, 137.80, 136.10, 135.73, 133.85, 133.62, 133.34, 129.98, 129.88, 128.57, 128.49, 128.32, 128.24, 128.13, 128.01, 127.97, 127.87, 127.84, 127.83, 127.72, 127.69, 127.20, 127.05, 117.96 (CH_2 of Allyl), 98.55 (Gal-1), 96.49 (Man-1), 92.39 (CCl_3CONH), 77.20, 76.52, 74.92, 73.56, 73.24, 72.91, 72.67, 72.21, 72.07, 71.66, 69.22, 68.16, 68.09, 63.70, 56.76, 38.06, 29.81 (Me of Lev), 28.20, 26.81 (Me of *t*Bu), 19.43 (C_{quart} of *t*Bu); ESI-MS: m/z $[\text{M}+\text{Na}]^+$ calcd for $\text{C}_{66}\text{H}_{74}\text{Cl}_3\text{NO}_{13}\text{Si}$ 1244.3893, obsd 1244.3875.

Allyl 3,4,6-tri-*O*-benzyl-2-deoxy-2-trichloroacetamido- β -D-galactopyranosyl-(1 \rightarrow 4)-3-*O*-benzyl-2-*O*-levulinyl- α -D-mannopyranoside (29)



Disaccharide **28** (62 mg, 0.051 mmol) was dissolved in THF (400 μ L) in a 15 mL Falcon™ tube and HF·Py (100 μ L) was added. The solution was stirred for 24 h at room temperature before it was quenched with sat. NaHCO₃ solution and extracted with ethyl acetate (2 x 15 mL). Solvents were removed under reduced pressure and the residue was purified using flash column chromatography (*n*-hexane/ethyl acetate 1:2→1:3) to yield **29** as yellow oil (40 mg, 0.041 mmol, 80% yield): R_f (SiO₂, *n*-hexane/ethyl acetate 1:3) = 0.24; $[\alpha]_D^{20}$: + 26.2 ($c = 1.00$, CHCl₃); ATR-FTIR (cm⁻¹): 3506, 3332, 3062, 2923, 2870, 1740, 1718, 1530, 1455, 1364, 1139, 1100, 1070, 1027; ¹H NMR (600 MHz, CDCl₃) δ 7.27 – 7.08 (m, 20H), 6.84 (d, $J = 7.3$ Hz, 1H, NH), 5.82 – 5.73 (m, 1H, CH of allyl), 5.24 (dd, $J = 3.2, 1.4$ Hz, 1H, Man-2), 5.18 (dd, $J = 17.2, 1.5$ Hz, 1H, CH₂= of allyl), 5.14 – 5.10 (m, 2H, CH₂= of allyl and Gal-1), 4.81 (d, $J = 11.4$ Hz, 1H), 4.74 (d, $J = 1.4$ Hz, 1H, Man-1), 4.61 (d, $J = 11.6$ Hz, 1H), 4.55 (d, $J = 11.2$ Hz, 1H), 4.48 (d, $J = 11.5$ Hz, 2H), 4.40 (d, $J = 11.2$ Hz, 1H), 4.31 (d, $J = 11.7$ Hz, 1H), 4.22 (d, $J = 11.7$ Hz, 1H), 4.11 (dd, $J = 10.9, 2.4$ Hz, 1H), 4.08 – 4.02 (m, 2H), 3.93 – 3.84 (m, 4H), 3.75 (dd, $J = 12.1, 3.4$ Hz, 1H), 3.72 – 3.68 (m, 1H), 3.62 – 3.57 (m, 1H), 3.55 – 3.49 (m, 2H), 3.41 – 3.35 (m, 1H), 2.52 – 2.38 (m, 3H, CH₂ of Lev), 2.33 (dt, $J = 16.7, 6.2$ Hz, 1H, CH₂ of Lev), 1.99 (s, 3H, Me of Lev).; ¹³C NMR (151 MHz, CDCl₃) δ 206.47 (ketone), 172.00 (ester), 162.17 (amide), 138.63, 138.27, 137.88, 137.66, 133.42, 128.58, 128.54, 128.46, 128.35, 128.10, 128.06, 128.03, 127.94, 127.70, 127.45, 126.86, 118.05 (CH₂= of Allyl), 98.63 (Gal-1), 96.80 (Man-1), 92.73 (CCl₃CONH), 77.24, 76.45, 74.87, 73.61, 73.50, 72.24, 71.97, 71.71, 71.07, 68.87, 68.43, 68.40, 61.76, 56.29, 38.00, 29.82, 29.80 (Me of Lev), 28.11.; ESI-MS: m/z [M+Na]⁺ calcd for C₅₀H₅₆Cl₃NO₁₃ 1006.2715, obsd 1006.2714.

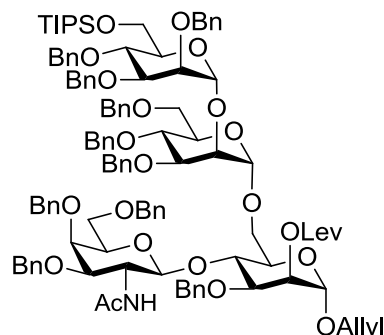
Allyl 2,3,4-tri-*O*-benzyl-6-*O*-triisopropylsilyl- α -D-mannopyranosyl-(1→2)-3,4,6-tri-*O*-benzyl- α -D-mannopyranosyl-(1→6)-3-*O*-benzyl-4-*O*-(3,4,6-tri-*O*-benzyl-2-deoxy-2-trichloroacetamido- β -D-galactopyranosyl)-2-*O*-levulinyl- α -D-mannopyranoside (30)



Disaccharide **29** (40 mg, 0.041 mmol) and dimannoside **8**^{*} (63 mg, 0.054 mmol) were coevaporated with toluene (3 x 2 mL) and placed under high vacuum for 30 min. The residue was dissolved in anhydrous diethyl ether (3 mL) and molecular sieves (4Å, 150 mg) were added. The slurry was stirred for 10 min at room temperature before it was cooled down to 0 °C and TBSOTf (9.3 µL, 0.041 mmol) was added. The reaction mixture was stirred for 1 h at 0 °C before it was quenched with TEA (100 µL) and filtered over Celite®. Solvents were evaporated under reduced pressure and the crude product was purified using flash column chromatography (*n*-hexane/ethyl acetate 4:1) to yield tetrasaccharide **30** (60 mg, 0.030 mmol, 74% yield) as yellow oil: R_f (SiO₂, *n*-hexane/ethyl acetate 4:1) = 0.24; $[\alpha]_D^{20}$: + 19.8 (*c* = 1.00, CHCl₃); ATR-FTIR (cm⁻¹): 3350, 2925, 2866, 1719, 1524, 1454, 1363, 1137, 1100, 1071, 1028; ¹H NMR (400 MHz, CDCl₃) δ 7.26 – 7.04 (m, 50H), 6.43 (s, 1H, NH {rotamer}), 6.08 (s, 1H, NH {rotamer}), 5.73 (m, 1H, =CH of allyl), 5.26 – 5.21 (m, 2H, ManI-2{5.24ppm}), 5.15 (d, *J* = 17.2 Hz, 1H, CH₂= of allyl), 5.08 (d, *J* = 8.3 Hz, 1H, Gal-1), 5.05 (d, *J* = 10.5 Hz, 1H, CH₂= of allyl), 4.83 (d, *J* = 10.9 Hz, 1H), 4.77 – 4.69 (m, 3H), 4.68 (d, *J* = 1.3 Hz, 1H, ManI-1), 4.64 – 4.22 (m, 16H), 4.15 (d, *J* = 11.7 Hz, 1H), 4.10 – 3.93 (m, 5H), 3.91 – 3.53 (m, 17H), 3.53 – 3.40 (m, 2H), 3.29 (dd, *J* = 8.2, 4.7 Hz, 1H), 2.51 – 2.29 (m, 4H, CH₂ of Lev), 1.96 (s, 3H, Me of Lev), 1.04 – 0.98 (m, 21H, TIPS); ¹³C NMR (101 MHz, CDCl₃) δ 206.33 (ketone), 172.02 (ester), 163.47 (amide {rotamer}), 162.19 (amide {rotamer}), 139.10, 138.89, 138.65, 138.58, 138.55, 138.34, 138.17, 137.99, 137.71, 133.33, 128.54, 128.48, 128.46, 128.44, 128.38, 128.34, 128.28, 128.19, 128.14, 128.08, 128.07, 128.05, 127.93, 127.88, 127.84, 127.79, 127.75, 127.73, 127.62, 127.57, 127.54, 127.45, 127.40, 127.36, 127.26, 118.43 (CH₂= of Allyl), 98.68 (Gal-1), 98.55, 98.36, 96.33 (ManI-1), 92.71 (CCl₃CO), 80.90, 79.67, 77.36, 76.38, 75.26, 75.18, 74.98, 74.95, 74.72, 74.53, 73.85, 73.60, 73.47, 73.37, 72.43, 72.27, 72.19, 72.13, 71.70, 71.39, 69.99, 68.87 (ManI-2), 68.43, 67.99, 66.41, 63.03, 56.45, 37.99 (CH₂ of Lev), 29.82 (Me of Lev), 28.13 (CH₂ of Lev), 18.22 (TIPS), 18.17 (TIPS), 12.19 (TIPS); ESI-MS: *m/z* [M+Na]⁺ calcd for C₁₁₃H₁₃₂Cl₃NO₂₃Si 2026.7917, obsd 2026.7891.

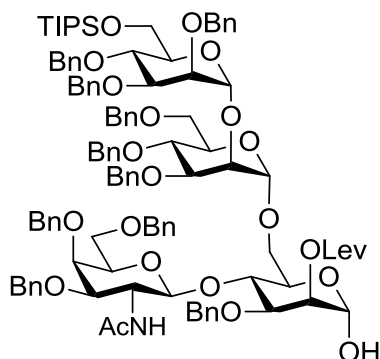
* The imidate **8** was provided by Y.-H. Tsai and was prepared according to Ref. [110].

Allyl 2,3,4-tri-*O*-benzyl-6-*O*-triisopropylsilyl- α -D-mannopyranosyl-(1 \rightarrow 2)-3,4,6-tri-*O*-benzyl- α -D-mannopyranosyl-(1 \rightarrow 6)-4-*O*-(3,4,6-tri-*O*-benzyl-2-deoxy-2-acetamido- β -D-galactopyranosyl)-3-*O*-benzyl-2-*O*-levulinyl- α -D-mannopyranoside (31**)**



Tetrasaccharide **30** (60 mg, 0.030 mmol) was dissolved in acetic acid (1 mL) and heated to 55°C to give a colorless solution. Zinc (0.2 g, 3.0 mmol) was added to this solution in three portions over 30 min. Afterwards the slurry was stirred for 2 h at 55°C before it was filtered, diluted with toluene (10 mL) and evaporated to dryness. The residue was purified using column chromatography (*n*-hexane/ethyl acetate 2:1) to yield tetrasaccharide **31** (42 mg, 0.022 mmol, 74% yield) as yellow oil: R_f (SiO₂, *n*-hexane/ethyl acetate 2:1) = 0.22; $[\alpha]_D^{20}$: +22.6 (*c* = 1.00, CHCl₃); ATR-FTIR (cm⁻¹): 3349, 2924, 2865, 1741, 1721, 1675, 1454, 1364, 1136, 1064, 1028cm⁻¹; ¹H NMR (400 MHz, CDCl₃) δ 7.30 – 7.03 (m, 50H), 6.21 (d, *J* = 7.4 Hz, 1H, NH), 5.74 (m, 1H, CH of allyl), 5.28 – 5.11 (m, 3H), 5.06 (t, *J* = 8.6 Hz, 2H), 4.85 (d, *J* = 10.8 Hz, 1H), 4.79 – 4.67 (m, 4H), 4.64 – 4.28 (m, 14H), 4.23 – 4.15 (m, 2H), 4.13 – 3.36 (m, 25H), 3.16 (dd, *J* = 8.2, 4.7 Hz, 1H), 2.51 – 2.31 (m, 4H, CH₂ of Lev), 1.96 (s, 3H, Me of Lev), 1.69 (s, 3H, Me of NHAc), 1.08 – 0.93 (m, 21H, TIPS); ¹³C NMR (101 MHz, CDCl₃) δ 206.26 (ketone), 172.12 (ester), 170.95 (amide), 139.08, 138.93, 138.70, 138.57, 138.39, 138.30, 138.08, 137.80, 133.28 (CH of Allyl), 128.59, 128.54, 128.43, 128.41, 128.36, 128.32, 128.30, 128.21, 128.15, 128.14, 128.09, 128.00, 127.94, 127.89, 127.78, 127.74, 127.61, 127.59, 127.47, 127.37, 127.29, 127.18, 118.38 (CH₂= of allyl), 100.33, 98.43, 98.11, 96.50 (4x anomeric carbon), 80.78, 79.55, 78.31, 76.49, 75.51, 75.23, 75.04, 74.57, 74.50, 74.09, 73.98, 73.50, 73.36, 73.31, 72.40, 72.35, 72.28, 72.14, 71.81, 71.76, 71.47, 70.19, 69.48, 68.95, 68.59, 68.03, 65.83, 64.68, 63.03, 55.03, 37.98 (CH₂ of Lev), 29.82 (CH₃ of Lev), 28.14 (CH₂ of Lev), 23.55 (CH₃CONH), 18.22 (TIPS), 18.17 (TIPS), 12.20 (TIPS); ESI-MS: *m/z* [M+Na]⁺ calcd for C₁₁₃H₁₃₅NO₂₃Si 1925.9125, obsd 1925.9080.

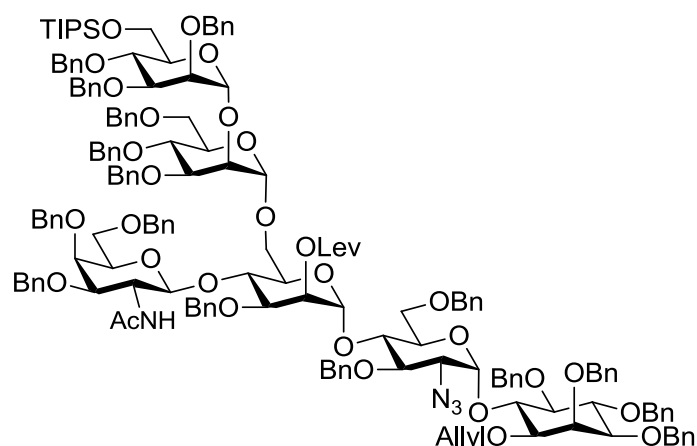
2,3,4-tri-*O*-benzyl-6-*O*-triisopropylsilyl- α -D-mannopyranosyl-(1 \rightarrow 2)-3,4,6-tri-*O*-benzyl- α -D-mannopyranosyl-(1 \rightarrow 6)-4-*O*-(3,4,6-tri-*O*-benzyl-2-deoxy-2-acetamido- β -D-galactopyranosyl)-3-*O*-benzyl-2-*O*-levulinyl- α -D-mannopyranose (32a**)**



Hydrogen was bubbled for 20 min through a solution of $[\text{IrCOD}(\text{PPh}_2\text{Me})_2]\text{PF}_6$ (10 mg, 0.012 mmol) in anhydrous THF (3 mL) to yield a pale yellow solution. The atmosphere was exchanged to nitrogen and the solution was added to tetrasaccharide **31** (40 mg, 0.021 mmol). The resulting reaction mixture was stirred for 12 h at room temperature before removal of solvents. The residue was dissolved in acetone (2.8 mL) and water (0.2 mL). HgCl_2 (34.2 mg, 0.126 mmol) and HgO (0.5 mg, 0.002 mmol) were added and the solution was stirred for 2 h at room temperature before it was diluted with ethyl acetate (15 mL) and washed with sat. NaHCO_3 solution (15 mL). The organic layer was dried over Na_2SO_4 , filtered and concentrated. The residue was purified using column chromatography (*n*-hexane/ethyl acetate 2:1) to yield lactol **32a** (27 mg, 0.014 mmol, 69% yield) as colorless oil: R_f (SiO_2 , *n*-hexane/ethyl acetate 3:2) = 0.20; $[\alpha]_D^{20}$: + 15.3 ($c = 1.00$, CHCl_3); ATR-FTIR (cm^{-1}): 3349, 2925, 2865, 1739, 1720, 1673, 1455, 1364, 1105, 1067, 1028; ^1H NMR (600 MHz, CDCl_3) δ 7.29 (d, $J = 7.3$ Hz, 2H), 7.26 – 7.10 (m, 44H), 7.07 – 7.02 (m, 4H), 6.28 (d, $J = 7.1$ Hz, 1H, NH), 5.12 (d, $J = 8.3$ Hz, 1H, GalNAc-1), 5.04 (s, 1H), 4.92 (s, 1H), 4.83 (d, $J = 10.3$ Hz, 1H), 4.76 (d, $J = 3.8$ Hz, 1H), 4.71 (d, $J = 11.6$ Hz, 1H), 4.63 – 4.40 (m, 12H), 4.35 (dd, $J = 24.0, 11.8$ Hz, 3H), 4.26 (dd, $J = 11.4, 1.6$ Hz, 2H), 4.14 – 3.93 (m, 8H), 3.87 – 3.74 (m, 5H), 3.67 (d, $J = 6.5$ Hz, 2H), 3.58 – 3.50 (m, 3H), 3.48 – 3.41 (m, 4H), 3.37 (dd, $J = 8.1, 5.3$ Hz, 1H), 3.30 (dd, $J = 8.4, 6.6$ Hz, 1H), 3.04 (dd, $J = 8.7, 5.0$ Hz, 1H), 2.53 – 2.35 (m, 4H, CH_2 of Lev), 1.99 (s, 3H, CH_3 of Lev), 1.73 (s, 3H, CH_3CONH), 1.05 – 0.99 (m, 21H, TIPS); ^{13}C NMR (151 MHz, CDCl_3) δ 206.39 (ketone), 171.90 (ester), 171.24 (amide), 139.01, 138.94, 138.89, 138.67, 138.42, 138.20, 138.17, 138.13, 137.60, 128.71, 128.59, 128.57, 128.45, 128.43, 128.30, 128.24, 128.21, 128.11, 128.10, 128.03, 127.98, 127.97, 127.95, 127.90, 127.74, 127.70, 127.69, 127.63, 127.45, 127.45, 127.16, 126.70, 100.46 (GalNAc-1; $J_{\text{CH}} =$

167Hz; β), 97.88 ($J_{CH} = 173\text{Hz}$; α), 96.81 ($J_{CH} = 172\text{Hz}$; α), 91.86 ($J_{CH} = 176\text{Hz}$, α), 79.82, 77.78, 77.37, 77.16, 76.95, 76.65, 75.99, 75.79, 75.41, 75.15, 74.89, 74.64, 73.39, 73.36, 73.12, 72.71, 72.59, 72.51, 72.33, 72.26, 72.07, 72.01, 70.96, 70.07, 69.75, 69.01, 68.32, 67.58, 62.90, 55.93, 38.11 (CH_2 of Lev), 29.89 (CH_3 of Lev), 28.22 (CH_2 of Lev), 23.54 (CH_3CONH), 18.25 (TIPS), 18.19 (TIPS), 12.26 (TIPS); ESI-MS: m/z $[\text{M}+\text{Na}]^+$ calcd for $\text{C}_{110}\text{H}_{131}\text{NO}_{23}\text{Si}$ 1885.8806, obsd 1885.8787.

2,3,4-Tri-*O*-benzyl-6-*O*-triisopropylsilyl- α -D-mannopyranosyl-(1 \rightarrow 2)-3,4,6-tri-*O*-benzyl- α -D-mannopyranosyl-(1 \rightarrow 6)-4-*O*-(3,4,6-tri-*O*-benzyl-2-deoxy-2-acetamido- β -D-galactopyranosyl)-3-*O*-benzyl-2-*O*-levulinyl- α -D-mannopyranosyl-(1 \rightarrow 4)-2-azido-3,6-di-*O*-benzyl-2-deoxy- α -D-glucopyranosyl-(1 \rightarrow 6)-1-*O*-allyl-2,3,4,5-tetra-*O*-benzyl-D-*myo*-inositol (23)

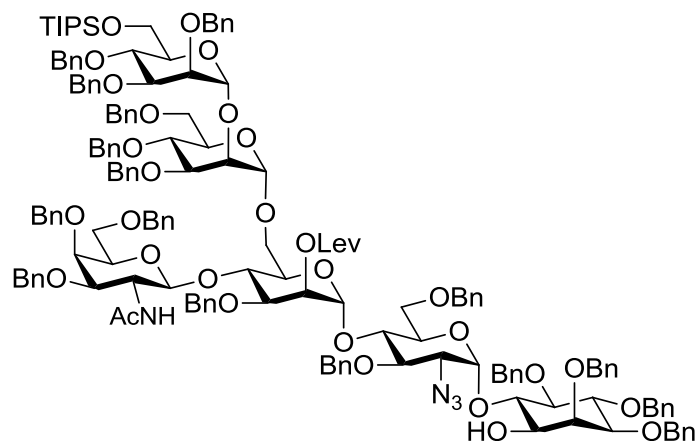


Lactol **32a** (27 mg, 0.014 mmol) was dissolved in anhydrous DCM (1 mL) and trichloroacetonitrile (145 μL , 1.45 mmol) was added. Afterwards DBU (1.1 μL , 7 μmol) was added and the reaction mixture was stirred for 1 h at room temperature before removal of solvents. The residue was purified using column chromatography (*n*-hexane/ethyl acetate 2:1 containing 0.1% TEA) to yield imidate **32** (26 mg, 0.013 mmol, 89% yield) as an inseparable mixture of anomers.

Imidate **32** (26 mg, 0.013 mmol) and pseudodisaccharide **7** (10 mg, 0.011 mmol) were evaporated with toluene (3 x 2 mL) and the residue was placed under high vacuum for 30 min. The residue was dissolved in anhydrous diethyl ether (1 mL) and molecular sieves (4 \AA , 50 mg) were added. The slurry was stirred for 10 min at room temperature before it was cooled down to 0 $^{\circ}\text{C}$ and TBSOTf (2.4 μL , 11 μmol) was added. The reaction mixture was

stirred for 1 h at 0 °C before it was quenched with TEA (50 μ L) and filtered over Celite®. Solvents were removed under reduced pressure and the crude product was purified using flash column chromatography (*n*-hexane/ethyl acetate 3:1) to yield pseudoexasaccharide **23** (24 mg, 9 μ mol, 81% yield) as yellow oil: R_f (SiO₂, *n*-hexane/ethyl acetate 2:1) = 0.51; $[\alpha]_D^{20}$: +25.3 (*c* = 1.00, CHCl₃); ATR-FTIR (cm⁻¹): 3353, 3088, 3064, 3031, 2924, 2864, 2106, 1741, 1721, 1676, 1454, 1362, 1095, 1055, 1028, 913; ¹H NMR (400 MHz, CDCl₃) δ 7.34-7.02 (m, 80H), 5.94 (d, *J* = 8.8 Hz, 1H, NH), 5.84 (m, 1H, =CH of allyl), 5.62 (d, *J* = 3.6 Hz, 1H, Glc-1), 5.29-5.28 (m, 2H, ManI-1, ManI-2), 5.18 (dd, *J* = 1.5, 17.2 Hz, 1H), 5.09-5.07 (m, 2H), 4.92 (d, *J* = 11.2 Hz, 1H), 4.84 (d, *J* = 10.6 Hz, 1H), 4.83 (d, *J* = 10.6 Hz, 1H), 4.79-3.13 (m, 68H), 2.21-2.12 (m, 4H, -CH₂- of Lev), 1.82 (s, Me of Lev, 3H), 1.57 (s, Me of -NHAc, 3H), 0.97 (br, 21H, TIPS); ¹³C NMR (101 MHz, CDCl₃) δ 205.84 (ketone of Lev), 171.75 (ester of Lev), 170.30 (amide), 138.97, 138.90, 138.86, 138.78, 138.61, 138.51, 138.48, 138.43, 138.30, 138.26, 138.20, 138.13, 137.97, 137.85, 137.63, 134.34 (=CH of allyl), 128.57, 128.54, 128.52, 128.50, 128.46, 128.40, 128.37, 128.34, 128.28, 128.25, 128.23, 128.21, 128.15, 128.06, 128.03, 127.98, 127.91, 127.79, 127.74, 127.71, 127.67, 127.63, 127.59, 127.58, 127.54, 127.52, 127.43, 127.39, 127.31, 127.23, 127.13, 126.88, 117.18 (=CH₂ of allyl), 100.80 (GalNHAc-1), 99.39 (ManII-1), 98.55 (ManIII-1), 98.38 (ManI-1), 97.51 (Glc-1), 82.03, 81.86, 81.23, 80.94, 80.58, 79.79, 79.17, 75.79, 75.65, 75.52, 75.34, 75.28, 75.05, 74.51, 74.32, 74.26, 74.09, 73.88, 73.80, 73.57, 73.50, 73.21, 72.90, 72.82, 72.64, 72.36, 72.25, 72.18, 72.04, 71.51, 71.42, 71.11, 70.90, 70.71, 69.90, 69.76, 68.98, 68.39, 66.64, 63.74, 62.87, 53.09, 37.82 (-CH₂- of Lev), 29.64 (-CH₃), 28.00 (-CH₂- of Lev), 23.19 (-CH₃), 18.17 (-CH₃ of TIPS), 18.12 (-CH₃ of TIPS), 12.11 (-CHMe₂ of TIPS); ESI-MS: *m/z* [M+Na]⁺ calcd for C₁₆₇H₁₉₀N₄O₃₂Si 2814.3025, obsd 2814.3069.

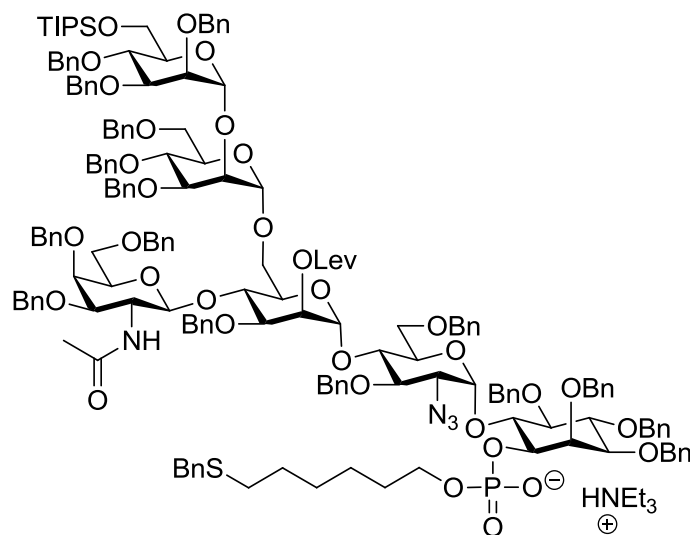
2,3,4-Tri-*O*-benzyl-6-*O*-triisopropylsilyl- α -D-mannopyranosyl-(1 \rightarrow 2)-3,4,6-tri-*O*-benzyl- α -D-mannopyranosyl-(1 \rightarrow 6)-4-*O*-(3,4,6-tri-*O*-benzyl-2-deoxy-2-acetamido- β -D-galactopyranosyl)-3-*O*-benzyl-2-*O*-levulinyl- α -D-mannopyranosyl-(1 \rightarrow 4)-2-azido-3,6-di-*O*-benzyl-2-deoxy- α -D-glucopyranosyl-(1 \rightarrow 6)-1-*O*-allyl-2,3,4,5-tetra-*O*-benzyl-D-*myo*-inositol (33a**)**



A solution of $[\text{IrCOD}(\text{PPh}_2\text{Me})_2]\text{PF}_6$ (25 mg, 0.030 mmol) in THF (2 mL) was stirred under hydrogen atmosphere until the color turned from red to colorless to pale yellow (ca. 10 min). The hydrogen atmosphere was exchanged with argon, pseudohexasaccharide **23** (0.87 g, 0.31 mmol) in THF (5 mL) was added. After 40 h, the solvent was removed and the residue was dissolved in acetone (6.5 mL). Water (0.5 mL), mercury(II) chloride (0.42 g, 1.56 mmol) and mercury(II) oxide (7.0 mg, 0.03 mmol) were added. After 20 min, $\text{NaHCO}_3(\text{aq})$ (15 mL) was added and the reaction mixture was extracted with DCM (3 x 10 mL). The combined organic layers were dried over Na_2SO_4 , filtered and concentrated. The crude product was purified by silica gel column chromatography to give alcohol **33a** (0.70 g, 0.25 mmol, 82% yield) as colorless oil: R_f (SiO_2 , *n*-hexane/ethyl acetate 2:1) = 0.21 $[\alpha]_{\text{D}}^{20}$: + 24.6 ($c = 0.71$, CHCl_3); ATR-FTIR (cm^{-1}): 3349, 3089, 3064, 3031, 2924, 2865, 2107, 1739, 1720, 1675, 1454, 1362, 1094, 1053, 1028; ^1H NMR (400 MHz, CDCl_3) δ 7.30-7.02 (m, 80H), 5.94 (d, $J = 8.6$ Hz, 1H, NH), 5.28 (d, $J = 3.5$ Hz, 1H, Glc-1), 5.27-5.26 (m, 2H, ManI-1, ManI-2), 5.10 (br, 1H, ManIII-1), 4.90 (d, $J = 11.6$ Hz, 1H), 4.88 (d, $J = 10.8$ Hz, 1H), 4.83 (d, $J = 10.7$ Hz, 1H), 4.83 (d, $J = 10.7$ Hz, 1H), 4.75-4.35 (m, 20H), 4.27-4.19 (m, 7H), 4.10-3.76 (m, 17H), 3.74-3.68 (m, 2H), 3.63-3.26 (m, 17H), 2.19-3.11 (m, 2H), 2.23-2.15 (m, 4H, CH_2 of Lev), 1.82 (s, Me of Lev, 3H), 1.57 (s, Me of -NHAc, 3H), 0.99-0.96 (m, 21H, TIPS); ^{13}C NMR (101 MHz, CDCl_3) δ 205.91 (ketone of Lev), 171.74 (ester of Lev), 170.52 (amide), 138.96, 138.91, 138.88, 138.72, 138.64, 138.49, 138.47, 138.42, 138.30, 138.26, 138.20, 137.98, 137.71, 137.61, 128.56, 128.55, 128.53, 128.50, 128.49, 128.44, 128.39, 128.37, 128.32, 128.27,

128.25, 128.19, 128.17, 128.08, 128.03, 127.98, 127.95, 127.84, 127.79, 127.77, 127.74, 127.70, 127.67, 127.64, 127.57, 127.51, 127.43, 127.31, 127.03, 100.76 (GalNHAc-1), 99.43 (ManII-1), 98.58 (ManIII-1), 98.22 (ManI-1), 98.04 (Glc-1), 82.00, 81.38, 81.00, 80.97, 80.92, 80.57, 79.53, 79.26, 77.23, 75.86, 75.79, 75.73, 75.31, 75.04, 74.91, 74.57, 74.38, 74.21, 73.89, 73.84, 73.58, 73.51, 73.30, 73.00, 72.79, 72.59, 72.39, 72.28, 72.22, 72.08, 71.58, 71.54, 70.73, 70.58, 69.85, 69.00, 68.57, 66.54, 64.61, 62.97, 53.33, 37.81 (-CH₂- of Lev), 29.69 (-CH₃), 28.01 (-CH₂- of Lev), 23.25 (-CH₃), 18.22 (-CH₃ of TIPS), 18.17 (-CH₃ of TIPS), 12.15 (-CHMe₂ of TIPS); ESI-MS: *m/z* [M+Na]⁺ calcd for C₁₆₄H₁₈₆N₄O₃₂Si 2775.2751, obsd 2775.2783.

Triethylammonium (2,3,4-tri-*O*-benzyl-6-*O*-triisopropylsilyl- α -D-mannopyranosyl-(1 \rightarrow 2)-3,4,6-tri-*O*-benzyl- α -D-mannopyranosyl-(1 \rightarrow 6)-3-*O*-benzyl-4-*O*-(3,4,6-tri-*O*-benzyl-2-deoxy-2-acetamido- β -D-galactopyranosyl)-2-*O*-levulinyl- α -D-mannopyranosyl-(1 \rightarrow 4)-2-azido-3,6-di-*O*-benzyl-2-deoxy- α -D-glucopyranosyl-(1 \rightarrow 6)-2,3,4,5-tetra-*O*-benzyl-1-*O*-(6-(benzylthio)hexyl-phosphonato)-D-*myo*-inositol (**33**)

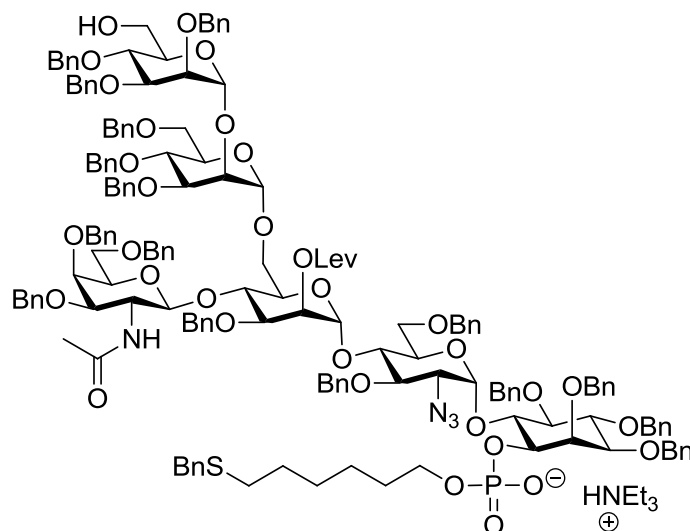


Alcohol **33a** (20 mg, 7.3 μ mol) and H-phosphonate **9*** (12.7 mg, 33 μ mol) were coevaporated (3x 2 mL) with pyridine. The residue was dissolved in pyridine (2 mL) and PivCl (6.7 μ L, 54 μ mol) was added. The solution was stirred for 2 h at r.t. before water (10 μ L, 0.56 mmol) and iodine (10.1 mg, 40 μ mol) were added. The red solution was stirred for 1 h and quenched with sat. Na₂S₃O₃. The reaction mixture was diluted with chloroform and dried over Na₂SO₄. The

* The H-phosphonate **9** was provided by Y.-H. Tsai and was prepared according to Ref. [90].

solvents were removed under reduced pressure and the residue coevaporated with toluene (3x 3 mL). The crude product was purified through flash column chromatography (starting from CHCl₃/MeOH 0% → 5% MeOH using TEA deactivated SiO₂) to yield phosphate **33** as yellow oil (18 mg, 5.9 μmol, 82%): $[\alpha]_D^{20} = +32.6$ (c = 1.00 in CHCl₃); ATR-FTIR (cm⁻¹): 2926, 2864, 2107, 1742, 1720, 1677, 1454, 1098, 1059, 1028; ¹H NMR (600 MHz, CDCl₃) δ 7.35 (d, *J* = 7.4 Hz, 2H), 7.31 – 7.04 (m, 81H), 6.99 (dd, *J* = 6.6, 2.8 Hz, 2H), 5.94 (d, *J* = 8.8 Hz, 1H, NH), 5.86 (d, *J* = 3.7 Hz, 1H, GlcNH₂-1), 5.27 – 5.24 (m, 2H, ManI-2), 5.09 (d, *J* = 1.2 Hz, 1H), 4.96 (d, *J* = 12.0 Hz, 1H, CH₂ of Bn), 4.92 – 4.81 (m, 3H, CH₂ of Bn), 4.81 – 4.57 (m, 11H), 4.57 – 4.48 (m, 4H), 4.48 – 4.38 (m, 4H), 4.38 – 4.19 (m, 12H), 4.11 – 3.72 (m, 17H), 3.69 (dd, *J* = 9.7, 7.0 Hz, 1H), 3.63 – 3.54 (m, 8H), 3.52 (t, *J* = 6.4 Hz, 1H), 3.50 – 3.30 (m, 8H), 3.25 (dd, *J* = 7.8, 3.9 Hz, 2H), 3.05 (dd, *J* = 10.2, 3.7 Hz, 1H, GlcNH₂-2), 2.86 (q, *J* = 7.3 Hz, 6H, NCH₂CH₃), 2.28 (t, 2H, -S-CH₂-CH₂-CH₂-CH₂-CH₂-O), 2.23 – 2.08 (m, 4H, CH₂ of Lev), 1.83 (s, 3H, NHAc), 1.56 – 1.48 (m, 5H, CH₃ of Lev, -S-CH₂-CH₂-CH₂-CH₂-CH₂-O), 1.42 (m_{centered}, 2H, -S-CH₂-CH₂-CH₂-CH₂-CH₂-O), 1.26 – 1.14 (m, 13H, NCH₂CH₃, -S-CH₂-CH₂-CH₂-CH₂-CH₂-O), 1.00 – 0.93 (m, 21H, TIPS); ¹³C NMR (151 MHz, CDCl₃) δ 205.92 (ketone of Lev), 171.77 (CO of Lev), 170.35 (CONH), 140.05, 139.05, 138.95, 138.88, 138.83, 138.75, 138.68, 138.58, 138.57, 138.40, 138.33, 138.24, 138.05, 137.99, 137.71, 128.92, 128.64, 128.62, 128.59, 128.57, 128.54, 128.46, 128.42, 128.40, 128.36, 128.32, 128.28, 128.26, 128.21, 128.14, 128.11, 128.09, 128.08, 128.00, 127.96, 127.84, 127.77, 127.72, 127.68, 127.67, 127.61, 127.56, 127.51, 127.49, 127.44, 127.28, 127.14, 126.97, 126.94, 100.58, 99.48, 98.79, 98.66, 96.51 (GlcNH₂-1), 81.99, 81.75, 81.23, 80.89, 80.52, 79.77, 79.24, 76.01, 75.76, 75.73, 75.57, 75.44, 75.34, 75.13, 74.76, 74.57, 74.40, 74.37, 74.26, 74.24, 74.20, 73.93, 73.85, 73.62, 73.27, 73.15, 72.96, 72.68, 72.40, 72.37, 72.32, 72.28, 72.09, 71.57, 71.49, 71.07, 70.77, 69.95 (ManI-2), 69.76, 68.98, 68.74, 66.74, 65.73, 65.69, 63.71 (GlcNH₂-2), 62.94, 53.25, 45.58, 37.90, 36.38, 31.46, 31.07, 31.02, 29.69, 29.30, 28.82, 28.06, 25.55, 23.22, 18.24, 18.18, 12.17, 8.74; ³¹P NMR (162 MHz, CDCl₃) δ -0.30; ESI-MS: *m/z* [M+Na]⁺ calcd for C₁₇₇H₂₀₅N₄O₃₅PSSi 3062.3577, obsd 3062.3573.

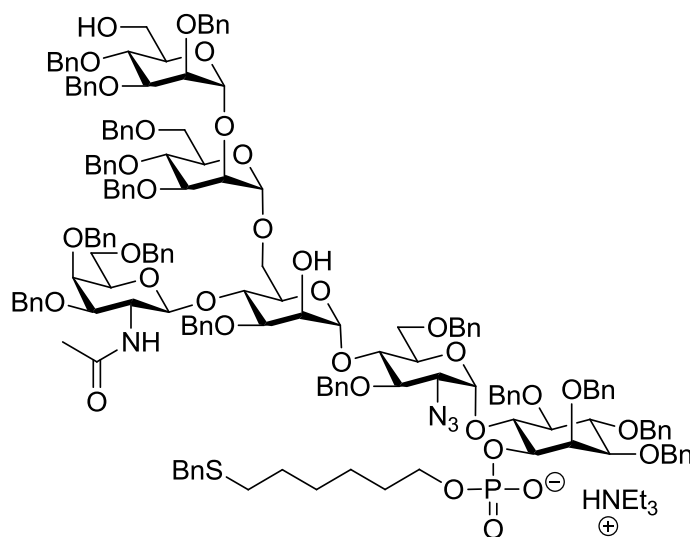
Triethylammonium (2,3,4-tri-*O*-benzyl- α -D-mannopyranosyl-(1 \rightarrow 2)-3,4,6-tri-*O*-benzyl- α -D-mannopyranosyl-(1 \rightarrow 6)-3-*O*-benzyl-4-*O*-(3,4,6-tri-*O*-benzyl-2-deoxy-2-acetamido- β -D-galactopyranosyl)-2-*O*-levuliny- α -D-mannopyranosyl-(1 \rightarrow 4)-2-azido-3,6-di-*O*-benzyl-2-deoxy- α -D-glucopyranosyl-(1 \rightarrow 6)-2,3,4,5-tetra-*O*-benzyl-1-*O*-(6-(benzylthio)hexyl-phosphonato)-D-*myo*-inositol (36)



Monophosphate **33** (59 mg, 19 μ mol) was dissolved in MeCN (2 mL). Water (13.5 μ L, 0.75 mmol) and Sc(TfO)₃ (18.5 mg, 38 μ mol) were added and the solution was heated up to 50 °C for 5 h. The reaction was quenched with pyridine (7.6 μ L, 94 μ mol) and the solvents were removed in vacuo. The residue was purified through flash column chromatography (starting from CHCl₃/MeOH 0% \rightarrow 5% MeOH using TEA deactivated SiO₂) to yield alcohol **36** as colorless oil (52 mg, 18 μ mol, 93%): [α]_D²⁰ = +31.30 (c = 1.10 in CHCl₃); ATR-FTIR (cm⁻¹): 3346, 2925, 2107, 1742, 1719, 1669, 1497, 1454, 1362, 1048, 912; ¹H NMR (600 MHz, CDCl₃) δ 7.43 – 6.88 (m, 85H), 6.01 (d, *J* = 8.2 Hz, 1H, NH), 5.88 (d, *J* = 3.7 Hz, 1H, GlcNH₂-1), 5.27 – 5.14 (m, 2H, ManI-2), 4.94 (m, 1H), 4.90 – 4.63 (m, 13H), 4.59 (d, *J* = 10.7 Hz, 1H), 4.55 – 4.28 (m, 18H), 4.25 – 4.20 (m, 1H), 4.17 (dd, *J* = 11.8, 5.3 Hz, 2H), 4.13 – 3.97 (m, 3H), 3.95 (t, *J* = 2.2 Hz, 1H), 3.90 (t, *J* = 9.6 Hz, 1H), 3.87 – 3.50 (m, 23H), 3.49 – 3.38 (m, 7H), 3.16 (dd, *J* = 6.9, 3.1 Hz, 1H), 3.06 (dd, *J* = 10.2, 3.7 Hz, 1H, GlcNH₂-2), 2.76 (q, *J* = 7.2 Hz, 6H, NCH₂CH₃), 2.34 – 2.08 (m, 6H, CH₂ of Lev, -S-CH₂-CH₂-CH₂-CH₂-CH₂-CH₂-O), 1.85 (s, 3H, CH₃ of Lev), 1.64 (s, 3H, NHAc), 1.54 – 1.47 (m, 2H, -S-CH₂-CH₂-CH₂-CH₂-CH₂-O), 1.45 – 1.37 (m, 2H, -S-CH₂-CH₂-CH₂-CH₂-CH₂-O), 1.25 – 1.16 (m, 4H, -S-CH₂-CH₂-CH₂-CH₂-CH₂-O), 1.13 (t, *J* = 7.3 Hz, 9H, NCH₂CH₃); ¹³C NMR (151 MHz, CDCl₃) δ 206.17 (ketone of Lev), 171.72, 170.70, 140.03, 139.03, 138.87, 138.74, 138.69, 138.65, 138.62, 138.52, 138.48, 138.44, 138.41, 138.35, 138.19, 138.10, 138.00,

128.91, 128.63, 128.54, 128.53, 128.47, 128.45, 128.39, 128.36, 128.34, 128.33, 128.30, 128.28, 128.25, 128.11, 128.09, 128.08, 128.02, 128.00, 127.96, 127.81, 127.81, 127.77, 127.73, 127.67, 127.60, 127.56, 127.52, 127.47, 127.45, 127.43, 127.34, 127.24, 127.12, 126.93, 100.75, 99.86, 99.32, 98.90, 96.39 (GlcNH₂-1), 81.92, 81.79, 81.18, 80.09, 80.05, 79.55, 79.07, 76.08, 75.92, 75.72, 75.41, 75.26, 75.14, 75.10, 75.05, 74.94, 74.73, 74.55, 74.10, 73.95, 73.52, 73.48, 73.43, 73.09, 73.03, 72.42, 72.36, 72.29, 72.23, 72.18, 71.72, 71.28, 69.97, 69.67, 69.46 (ManI-2), 68.90, 68.67, 67.15, 65.71, 65.67, 63.39 (Glc-NH₂-2), 62.37, 54.27, 45.89 (NCH₂CH₃), 37.88, 36.36, 31.45 (-S-CH₂-CH₂-CH₂-CH₂-CH₂-CH₂-O), 31.06, 31.01, 29.70, 29.29, 28.81, 28.01, 25.54, 23.44, 9.62 (NCH₂CH₃); ³¹P NMR (243 MHz, CDCl₃) δ -1.08; ESI-MS: *m/z* [M+Na]⁺ calcd for C₁₆₈H₁₈₅N₄O₃₅PSSi 2922.1969, obsd 2922.2032.

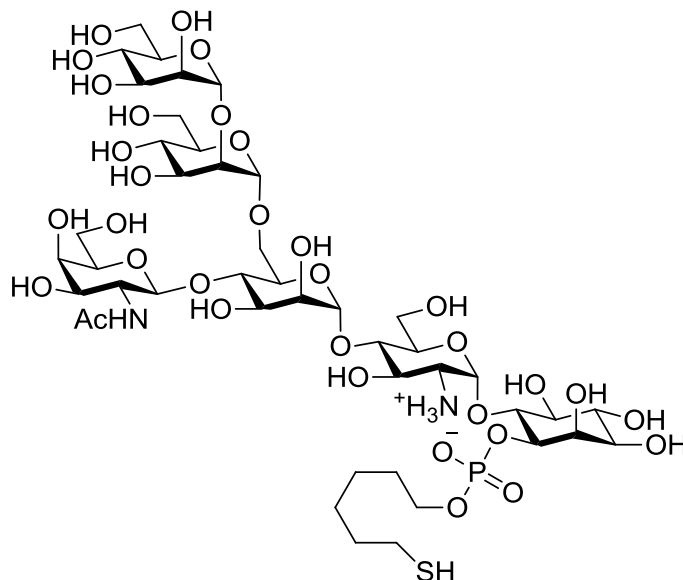
Triethylammonium (2,3,4-tri-*O*-benzyl- α -D-mannopyranosyl-(1→2)-3,4,6-tri-*O*-benzyl- α -D-mannopyranosyl-(1→6)-3-*O*-benzyl-4-*O*-(3,4,6-tri-*O*-benzyl-2-deoxy-2-acetamido- β -D-galactopyranosyl)- α -D-mannopyranosyl-(1→4)-2-azido-3,6-di-*O*-benzyl-2-deoxy- α -D-glucopyranosyl-(1→6)-2,3,4,5-tetra-*O*-benzyl-1-*O*-(6-(benzylthio)hexyl-phosphonato)-D-*myo*-inositol (34)



Phosphate **33** (44 mg, 14 μ mol) was dissolved in a BD Falcon Tube™ (15 mL) using MeCN (1 mL) and triethylamine trihydrofluoride (200 μ L) was added. The solution was stirred for 3 days before it was diluted with CHCl₃ (15 mL) and washed with triethylamine buffer (2x 15 mL). The organic layer was dried over sodium sulfate, filtered and evaporated to dryness. The residue was dissolved in MeCN (1 mL) and hydrazine monohydrate (2 drops, 64wt%) was

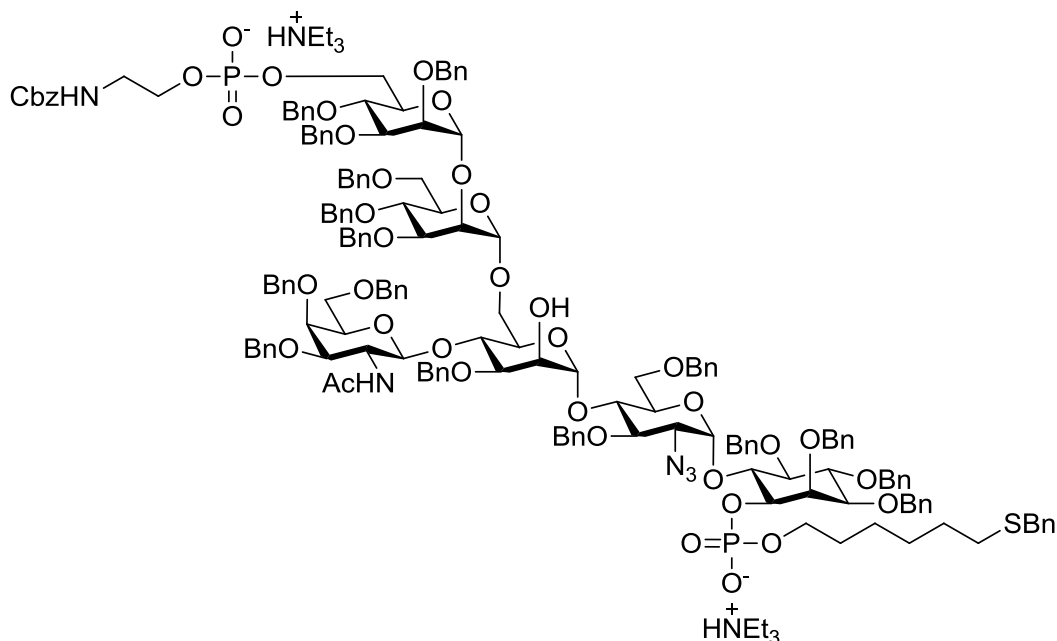
added to the solution. The reaction was stirred for 2 h, evaporated to dryness and purified using flash column chromatography (from 0% to 4% MeOH in CHCl₃ using triethylamine deactivated silica gel) to yield **34** as colorless foam (25 mg, 8.7 μmol, 62% over 2 steps): $[\alpha]_D^{20} = +36.1$ (c = 1.50 in CHCl₃); ATR-FTIR (cm⁻¹): 3321, 2926, 2864, 2106, 1675, 1096, 1053, 1028; ¹H NMR (400 MHz, CDCl₃) δ 7.43 – 7.07 (m, 85H), 5.96 – 5.90 (m, 2H), 5.24 (s, 1H), 5.05 – 4.51 (m, 21H), 4.49 – 4.24 (m, 16H), 4.21 – 4.12 (m, 3H), 4.10 – 3.98 (m, 4H), 3.96 – 3.86 (m, 3H), 3.86 – 3.44 (m, 27H), 3.39 (dd, J = 9.0, 5.7 Hz, 1H), 3.13 (dd, J = 10.2, 3.6 Hz, 1H), 2.87 (q, J = 7.2 Hz, 6H, CH₂ of TEA), 2.47 (bs, 1H, OH), 2.43 (s, 1H, OH), 2.35 (t, J = 7.4 Hz, 2H, BnS-CH₂), 1.72 (s, 3H, Me of NHAc), 1.62 – 1.53 (m, 2H), 1.53 – 1.44 (m, 2H), 1.34 – 1.22 (m, 4H), 1.18 (t, J = 7.3 Hz, 9H, Me of TEA); ¹³C NMR (101 MHz, CDCl₃) δ 170.55 (amide), 140.06, 138.98, 138.90, 138.80, 138.77, 138.72, 138.68, 138.62, 138.59, 138.53, 138.44, 138.40, 138.32, 138.15, 138.02, 137.71, 128.94, 128.62, 128.56, 128.53, 128.50, 128.48, 128.44, 128.40, 128.38, 128.35, 128.32, 128.31, 128.27, 128.14, 128.11, 128.08, 128.05, 128.00, 127.93, 127.88, 127.79, 127.76, 127.67, 127.59, 127.57, 127.47, 127.29, 127.11, 126.96, 101.25, 101.12, 99.65, 99.57, 96.34 (5x C-1), 81.95, 81.90, 81.17, 80.14, 80.08, 79.50, 76.42, 76.14, 75.77, 75.50, 75.24, 75.19, 74.72, 74.62, 74.53, 74.23, 74.16, 73.73, 73.70, 73.60, 73.17, 73.03, 72.89, 72.56, 72.39, 72.35, 72.21, 71.72, 71.57, 70.70, 70.24, 69.82, 69.66, 69.13, 69.00, 66.69, 65.78, 65.72, 63.50, 62.40, 53.80, 45.53 (CH₂ of TEA), 36.40, 31.48, 31.11, 31.03, 29.83, 29.33, 28.85, 25.57, 23.45, 8.76 (Me of TEA); ³¹P NMR (162 MHz, CDCl₃) δ -1.17; ESI-MS: *m/z* [M-H+3Na]²⁺ calcd for C₁₆₃H₁₇₉N₄O₃₃PS 1426.0774, obsd 1426.0767.

α -D-Mannopyranosyl-(1 \rightarrow 2)- α -D-mannopyranosyl-(1 \rightarrow 6)-4-O-(2-deoxy-2-acetamido- β -D-galactopyranosyl)- α -D-mannopyranosyl-(1 \rightarrow 4)-2-amino-2-deoxy- α -D-glucopyranosyl-(1 \rightarrow 6)-1-O-(thiohexyl-phosphonato)-D-myoinositol (21**)**



Approximately 10 mL ammonia were condensed in a flask and *tert*-BuOH (2 drops) was added. Afterwards small pieces of sodium were added till a dark blue colour was established. Phosphate **34** (10 mg, 3.5 μ mol) was dissolved in dry THF (1.5 mL) and added to the ammonium solution at -78 °C. The reaction was stirred for 30 min at this temperature. The reaction was quenched with dry MeOH (2 mL) and the ammonia was blown off using a stream of nitrogen. The pH of the resulting solution was adjusted with concentrated acetic acid to 7-8. Solvents were removed in vacuo and the residue was purified using a small G10 column (GE Healthcare) to yield **21** as white solid (3.3 mg, 2.7 μ mol, 78%): ^1H NMR (400 MHz, D_2O) δ 5.56 (d, J = 3.5 Hz, 1H, GlcNH₂-1), 5.22 (s, 1H), 5.19 (s, 1H), 5.05 (s, 1H), 4.51 (d, J = 8.4 Hz, 1H, GalNAc-1), 4.30 – 3.62 (m, 35H), 3.57 (dd, J = 10.0, 2.3 Hz, 1H), 3.49 – 3.33 (m, 2H), 2.79 (t, J = 7.2 Hz, 2H, HS-CH₂), 2.10 (s, 3H, Me of NHAc), 1.80 – 1.57 (m, 4H), 1.52 – 1.35 (m, 4H); ^{13}C NMR (151 MHz, D_2O) δ 177.27 (amide), 104.80, 104.21 (GalNAc-1), 101.52, 97.98 (GlcNH₂-1, gHSQC), 81.07, 78.93, 78.74, 78.04, 75.83, 75.48, 74.82, 74.04, 73.80, 73.64, 73.15, 72.94, 72.72, 72.57, 72.13, 71.57, 70.31, 69.60, 69.37, 69.17, 68.85, 65.09, 63.78, 63.70, 63.64, 62.74, 56.73 (Glc-NH₂-2), 55.25, 40.72, 32.33, 30.89, 29.80, 27.20, 24.98 (Me of NHAc); ^{31}P NMR (162 MHz, D_2O) δ 0.18; ESI-MS: m/z $[\text{M}+2\text{Na}]^{2+}$ calcd for $\text{C}_{88}\text{H}_{156}\text{N}_4\text{O}_{66}\text{P}_2\text{S}_2$ 1248.8854, obsd 1248.8805.

Bistriethylammonium (2,3,4-tri-*O*-benzyl-6-*O*-(2-(*N*-benzyloxycarbonyl)aminoethyl-phosphonato)- α -D-mannopyranosyl-(1 \rightarrow 2)-3,4,6-tri-*O*-benzyl- α -D-mannopyranosyl-(1 \rightarrow 6)-3-*O*-benzyl-4-*O*-(3,4,6-tri-*O*-benzyl-2-deoxy-2-acetamido- β -D-galactopyranosyl)- α -D-mannopyranosyl-(1 \rightarrow 4)-2-azido-3,6-di-*O*-benzyl-2-deoxy- α -D-glucopyranosyl-(1 \rightarrow 6)-2,3,4,5-tetra-*O*-benzyl-1-*O*-(6-(benzylthio)hexyl-phosphonato)-D-*myo*-inositol (37)

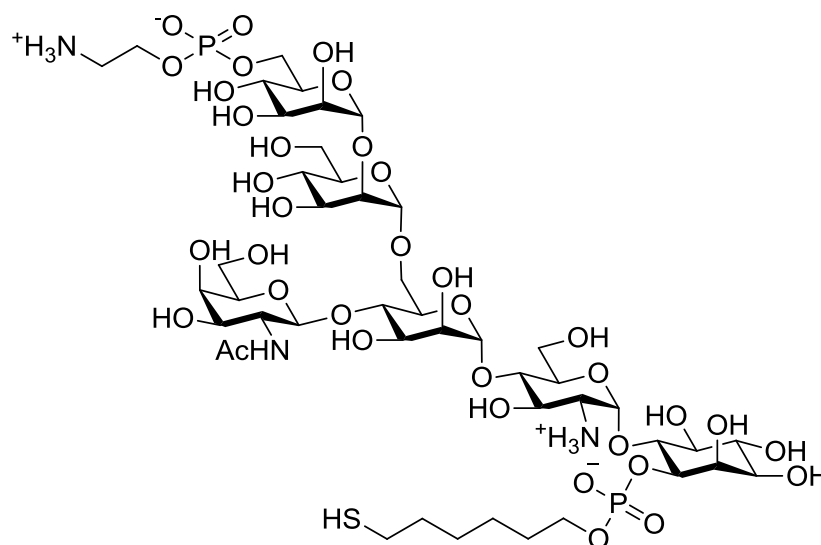


Alcohol **36** (52 mg, 17 μ mol) and H-phosphonate **10*** (28 mg, 78 μ mol) were coevaporated with pyridine (3x2 mL). The residue was dissolved in pyridine (2 mL) and PivCl (16.1 μ L, 131 μ mol) was added. The solution was stirred for 2 h at r.t. before water (15.6 μ L, 0.87 mmol) and iodine (24 mg, 96 μ mol) were added. The red solution was stirred for 1 h and afterwards quenched with hydrazine (1M in THF; 300 μ L, 0.3 mmol). The reaction mixture was stirred for 18 h before the solvents were removed in vacuo and the residue was purified through flash column chromatography (starting from CHCl₃/MeOH 3% \rightarrow 10% MeOH using TEA deactivated SiO₂) to yield bisphosphate **37** as yellow oil (50 mg, 15 μ mol, 88%): $[\alpha]_D^{20} = +32.46$ (c = 1.00 in CHCl₃); ATR-FTIR (cm⁻¹): 3387, 3063, 2929, 2108, 1672, 1497, 1057, 1029, 839; ¹H NMR (400 MHz, CDCl₃) δ 7.37 – 6.90 (m, 90H), 6.28 (s, 1H, NHAc), 5.89 (d, *J* = 3.5 Hz, 1H, GlcNH₂-1), 5.19 (d, *J* = 1.6 Hz, 1H), 5.05 – 4.15 (m, 40H), 4.14 – 4.02 (m, 3H), 3.98 – 3.35 (m, 36H), 3.28 – 3.20 (m, 1H), 3.14 (dd, *J* = 9.2, 4.5 Hz, 1H), 3.05 (dd, *J* = 10.2, 3.5 Hz, 1H, GlcNH₂-2), 2.61 (q, *J* = 7.3 Hz, 12H, NCH₂CH₃), 2.28 (t, *J* = 7.4 Hz, 2H, -S-CH₂-CH₂-CH₂-CH₂-CH₂-CH₂-O), 1.92 – 1.76 (m, 3H, COCH₃), 1.58 – 1.37 (m, 4H, -S-CH₂-CH₂-CH₂-CH₂-CH₂-CH₂-O), 1.26 – 1.13 (m, 4H, -S-CH₂-CH₂-CH₂-CH₂-CH₂-O),

* The H-phosphonate **10** was provided by Y.-H. Tsai and was prepared according to Ref. [104].

0.97 (t, $J = 7.3$ Hz, 18H, NCH_2CH_3); ^{13}C NMR (151 MHz, CDCl_3) δ 170.84 (COCH_3), 156.58 ($\text{O}(\text{CO})\text{NH}$), 138.71, 128.87, 128.50, 128.44, 128.36, 128.30, 128.21, 128.03, 127.94, 127.86, 127.76, 127.50, 126.91, 102.05, 101.15, 100.26, 98.71, 96.19, 82.02, 81.79, 81.06, 80.17, 80.03, 79.66, 77.37, 77.16, 76.95, 76.36, 75.93, 75.58, 75.19, 74.84, 74.80, 74.65, 74.03, 73.49, 72.79, 72.29, 71.62, 71.56, 71.49, 71.41, 70.08, 69.75, 69.64, 68.97, 66.34, 65.70, 65.04, 64.09, 63.49, 58.17, 45.70, 38.76, 36.34, 32.00, 31.44, 29.78, 29.59, 29.44, 29.27, 28.80, 27.54, 25.50, 22.77, 14.21, 8.71; ^{31}P NMR (243 MHz, CDCl_3) δ -0.03, -1.67; ESI-MS: m/z $[\text{M}-\text{H}]^-$ calcd for $\text{C}_{173}\text{H}_{191}\text{N}_5\text{O}_{38}\text{P}_2\text{S}$ 3041.2353, obsd 3041.2393.

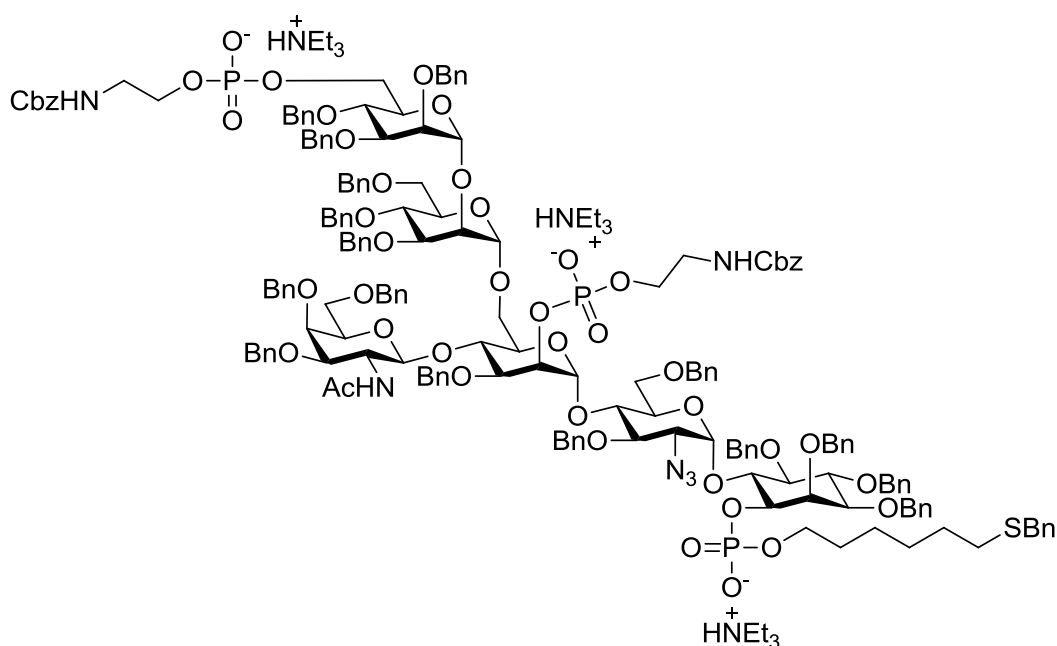
6-*O*-Aminoethylphosphonato- α -D-mannopyranosyl-(1 \rightarrow 2)- α -D-mannopyranosyl-(1 \rightarrow 6)-4-*O*-(2-deoxy-2-acetamido- β -D-galactopyranosyl)- α -D-mannopyranosyl-(1 \rightarrow 4)-2-amino-2-deoxy- α -D-glucopyranosyl-(1 \rightarrow 6)-1-*O*-(thiohexyl-phosphonato)-D-*myo*-inositol (4)



Approximately 10 mL ammonia were condensed in a flask and *tert*-BuOH (2 drops) was added. Afterwards small pieces of sodium were added till a dark blue colour was established. Bisphosphate **37** (28 mg, 8.6 μmol) was dissolved in dry THF (1.5 mL) and added to the ammonium solution at -78 $^\circ\text{C}$. The reaction was stirred for 30 min at this temperature. The reaction was quenched with dry MeOH (2 mL) and the ammonia was blown off using a stream of nitrogen. The pH of the resulting solution was adjusted with concentrated acetic acid to 7-8. Solvents were removed in vacuo and the residue was purified using a small G10 column (GE Healthcare) to yield **4** as white solid (6.7 mg, 4.9 μmol , 58%): ^1H NMR (600

MHz, D₂O) δ 5.54 (d, $J = 3.9$ Hz, 1H, GlcNH₂), 5.23 (s, 1H), 5.19 (s, 1H), 5.03 (s, 1H), 4.51 (d, $J = 8.3$ Hz, 1H, GalNAc-1), 4.29 – 3.66 (m, 36H), 3.63 – 3.53 (m, 2H), 3.45 (td, $J = 9.3, 4.3$ Hz, 1H), 3.38 (dd, $J = 10.9, 4.3$ Hz, 1H, GlcNH₂-2), 3.34 – 3.29 (m, 2H), 2.80 (t, $J = 7.1$ Hz, 1H), 2.58 (t, $J = 7.1$ Hz, 1H), 2.12 (s, 3H, Me of NHAc), 1.80 – 1.59 (m, 4H, linker), 1.51 – 1.36 (m, 4H, linker); ¹³C NMR (151 MHz, D₂O) δ 177.30 (amide), 105.02, 104.34 (GalNAc-1), 104.09, 101.16, 98.15 (Glc-NH₂-1), 81.69, 79.37, 78.78, 78.01, 75.69, 75.40, 74.84, 74.60, 74.05, 73.92, 73.62, 73.15, 73.08, 72.82, 72.64, 72.49, 72.03, 71.56, 70.32, 69.61, 69.21, 68.85, 67.28, 64.53, 64.50, 63.76, 63.70, 62.81, 56.64 (GlcNH₂-2), 55.19, 42.66, 40.73, 35.53, 32.31, 30.88, 29.67, 27.20, 27.00, 26.29, 24.96 (Me of NHAc); ³¹P NMR (243 MHz, D₂O) δ -2.62, -2.83; ESI-MS: m/z [M-2H]²⁻ calcd for C₄₆H₈₅N₃O₃₆P₂S 673.6981, obsd 673.7104.

Tristriethylammonium (2,3,4-tri-*O*-benzyl-6-*O*-(2-(*N*-benzyloxycarbonyl)aminoethyl-phosphonato)- α -D-mannopyranosyl-(1 \rightarrow 2))-3,4,6-tri-*O*-benzyl- α -D-mannopyranosyl-(1 \rightarrow 6)-4-*O*-(3,4,6-tri-*O*-benzyl-2-deoxy-2-acetamido- β -D-galactopyranosyl)-3-*O*-benzyl-2-*O*-(2-(*N*-benzyloxycarbonyl)aminoethyl-phosphonato)- α -D-mannopyranosyl-(1 \rightarrow 4)-2-azido-3,6-di-*O*-benzyl-2-deoxy- α -D-glucopyranosyl-(1 \rightarrow 6)-2,3,4,5-tetra-*O*-benzyl-1-*O*-(6-(benzylthio)hexyl-phosphonato)-D-*myo*-inositol (35)



Procedure A:

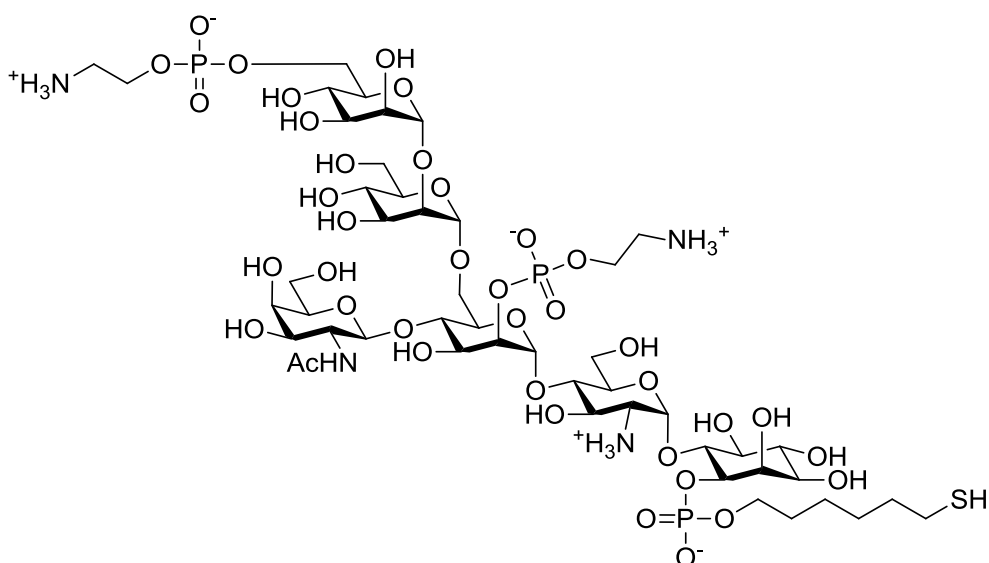
Alcohol **36** (16 mg, 4.9 μmol) and H-phosphonate **10** (8.1 mg, 22.5 μmol) were coevaporated with pyridine (3x2 mL). The residue was dissolved in pyridine (2 mL) and PivCl (4.6 μL , 36.8 μmol) was added. The solution was stirred for 2 h at r.t. before water (10 μL , 0.56 mmol) and iodine (6.8 mg, 27 μmol) were added. The red solution was stirred for 1 h and afterwards quenched with sat. $\text{Na}_2\text{S}_2\text{O}_3$ solution. The solvents were removed in vacuo and the residue was purified through flash column chromatography (starting from $\text{CHCl}_3/\text{MeOH}$ 3% \rightarrow 10% MeOH using TEA deactivated SiO_2) to yield trisphosphate **35** as yellow oil (13.5 mg, 3.8 μmol , 76%).

Procedure B:

Diol **34** (15 mg, 5.2 μmol) and H-phosphonate **10** (16 mg, 44 μmol) were coevaporated with pyridine (3x2 mL). The residue was dissolved in pyridine (1.5 mL) and PivCl (5.4 μL , 44 μmol) was added. The solution was stirred for 2 h at r.t. before water (10 μL , 0.56 mmol) and iodine (11.9 mg, 47 μmol) were added. The red solution was stirred for 1 h and afterwards quenched with hydrazine monohydrate (1 drop, 64wt%). The solvents were removed in vacuo and the residue was coevaporated with toluene (4x 2 mL). The crude product was purified through flash column chromatography (starting from $\text{CHCl}_3/\text{MeOH}$ 3% \rightarrow 10% MeOH using TEA deactivated SiO_2) to yield trisphosphate **35** as yellow oil (12 mg, 3.3 μmol , 64%): $[\alpha]^{20}_{\text{D}} = +22.00$ ($c = 1.00$ in CHCl_3); ATR-FTIR (cm^{-1}): 3358, 2927, 2108, 1641, 1454, 1398, 1054, 7028, 838, 804; ^1H NMR (600 MHz, cdCl_3) δ 7.56 – 6.77 (m, 90H), 6.44 (s, 2H, CbzNH), 6.22 (s, 1H, NHC(=O)CH₃), 5.87 (s, 1H, GlcNH₂-1), 5.49 (s, 1H), 5.09 – 3.35 (m, 83H), 3.30 (dd, $J = 14.2, 7.1$ Hz, 1H), 3.26 – 3.17 (m, 2H), 3.17 – 3.08 (m, 2H), 3.07 – 2.79 (m, 1H), 2.58 (q, $J = 7.2$ Hz, 18H, NCH₂CH₃), 2.27 (t, $J = 7.4$ Hz, 2H, -S-CH₂-CH₂-CH₂-CH₂-CH₂-CH₂-O), 2.05 – 1.98 (m, 2H), 1.90 – 1.83 (m, 3H, NHC(=O)CH₃), 1.59 – 1.36 (m, 4H, -S-CH₂-CH₂-CH₂-CH₂-CH₂-O), 1.27 – 1.12 (m, 4H, -S-CH₂-CH₂-CH₂-CH₂-CH₂-O), 0.99 (t, $J = 7.2$ Hz, 27H, NCH₂CH₃); ^{13}C NMR (151 MHz, CDCl_3) δ 156.57 (OCONH), 140.07, 139.03, 138.78, 138.73, 138.67, 138.32, 137.23, 128.93, 128.54, 128.49, 128.44, 128.39, 128.36, 128.31, 128.28, 128.25, 128.23, 128.18, 128.03, 128.01, 127.97, 127.93, 127.82, 127.71, 127.60, 127.57, 127.54, 127.51, 127.41, 127.38, 127.30, 127.15, 127.06, 126.94, 126.84, 100.59, 98.53, 96.54 (GlcNH₂-1), 81.89, 81.20, 75.58, 75.04, 74.83, 74.67, 73.28, 72.84, 72.30, 66.39, 66.23, 65.70, 63.97, 45.85 (NCH₂CH₃), 42.97, 42.52, 40.10, 36.39, 34.58, 33.94, 32.05, 31.56, 31.50 (S-CH₂-CH₂-CH₂-CH₂-CH₂-O), 31.08, 31.03, 30.33,

29.82, 29.79, 29.74, 29.63, 29.48, 29.32, 29.28, 29.08, 28.84, 25.55, 22.81, 21.56, 14.99, 14.30, 14.24, 13.23, 9.91 (NCH₂CH₃); ³¹P NMR (243 MHz, CDCl₃) δ 0.17, -0.02, -1.15; ESI-MS: *m/z* [M+5Na-3H]²⁺ calcd for C₁₈₃H₂₀₃N₆O₄₃P₃S 1705.6062, obsd 1705.6285.

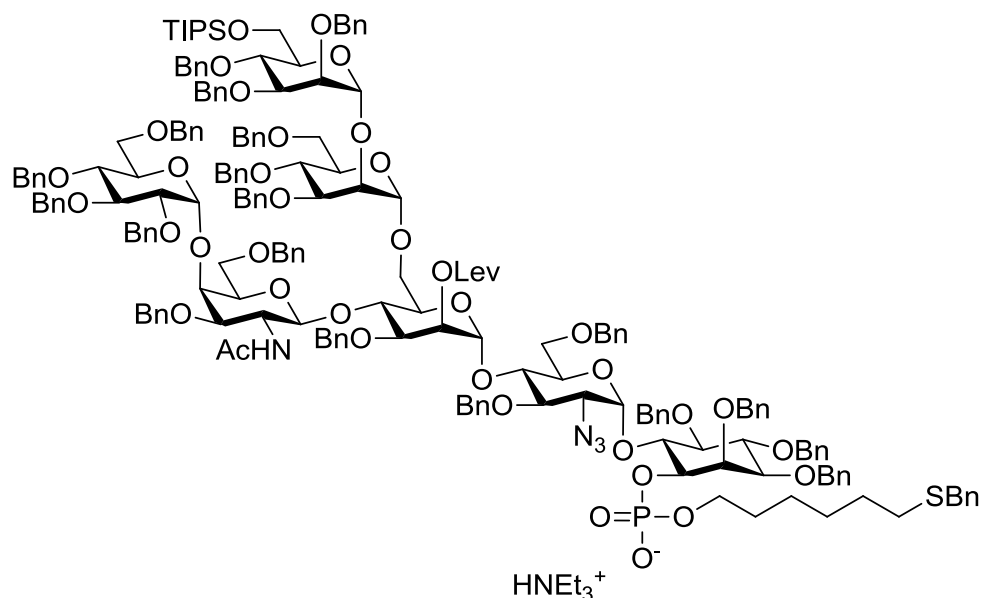
6-*O*-Aminoethylphosphonato- α -D-mannopyranosyl-(1 \rightarrow 2)- α -D-mannopyranosyl-(1 \rightarrow 6)-2-*O*-aminoethylphosphonato-4-*O*-(2-deoxy-2-acetamido- β -D-galactopyranosyl)- α -D-mannopyranosyl-(1 \rightarrow 4)-2-amino-2-deoxy- α -D-glucopyranosyl-(1 \rightarrow 6)-1-*O*-(thiohexylphosphonato)-D-*myo*-inositol (5)



Approximately 10 mL ammonia were condensed in a flask and *tert*-BuOH (2 drops) was added. Afterwards small pieces of sodium were added till a dark blue colour was established. Trisphosphate **35** (12 mg, 3.3 μ mol) was dissolved in dry THF (1.5 mL) and added to the ammonium solution at -78 °C. The reaction was stirred for 30 min at this temperature. The reaction was quenched with dry MeOH (2 mL) and the ammonia was blown off using a stream of nitrogen. The pH of the resulting solution was adjusted with concentrated acetic acid to 7-8. Solvents were removed in vacuo and the residue was purified using a small G10 column (GE Healthcare) to yield **5** as white solid (2.9 mg, 2.0 μ mol, 59%): ¹H NMR (400 MHz, D₂O) δ 5.57 – 5.52 (m, 1H, GlcNH₂-1), 5.45 (s, 1H, ManI-1), 5.19 (s, 1H), 5.04 (s, 1H), 4.53 (d, *J* = 8.4 Hz, 2H, ManI-1, GalNAc-1), 4.29 – 3.52 (m, 39H), 3.44 (t, *J* = 9.3 Hz, 1H), 3.41 – 3.34 (m, 1H, GlcNH₂-2), 3.34 – 3.26 (m, 4H), 2.79 (t, *J* = 7.3 Hz, 2H, HS-CH₂), 2.11 (s, 3H, Me of NHAc), 1.81 – 1.57 (m, 4H), 1.53 – 1.36 (m, 4H); ¹³C NMR (151 MHz, D₂O) δ 174.66 (amide), 102.43, 101.62, 99.55, 99.01, 95.45 (Glc-NH₂-1, gHSQC), 79.26, 76.16,

75.40, 74.13, 73.24, 72.24, 71.99, 71.43, 70.56, 70.21, 69.96, 69.89, 68.04, 67.75, 66.97, 66.58, 66.26, 64.72, 62.49, 61.98, 61.19, 61.13, 60.15, 52.65, 40.13, 40.08, 38.11, 29.76, 28.31, 27.22, 24.62, 22.37 (Me of NHAc); ^{31}P NMR (162 MHz, D_2O) δ 0.36, 0.14, -0.81; ESI-MS: m/z $[\text{M-H}+3\text{Na}]^{2+}$ calcd for $\text{C}_{96}\text{H}_{178}\text{N}_6\text{O}_{78}\text{P}_6\text{S}_2$ 1505.8935, obsd 1505.8834.

Triethylammonium (2,3,4-tri-*O*-benzyl-6-*O*-triisopropylsilyl- α -D-mannopyranosyl-(1 \rightarrow 2)-3,4,6-tri-*O*-benzyl- α -D-mannopyranosyl-(1 \rightarrow 6)-3-*O*-benzyl-4-*O*-(2,3,4,6-tetra-*O*-benzyl- α -D-glucopyranosyl-(1 \rightarrow 4)-3,6-di-*O*-benzyl-2-deoxy-2-acetamido- β -D-galactopyranosyl)-2-*O*-levulinyl- α -D-mannopyranosyl-(1 \rightarrow 4)-2-azido-3,6-di-*O*-benzyl-2-deoxy- α -D-glucopyranosyl-(1 \rightarrow 6)-2,3,4,5-tetra-*O*-benzyl-1-*O*-(6-(benzylthio)hexylphosphonato)-D-*myo*-inositol (**41**)

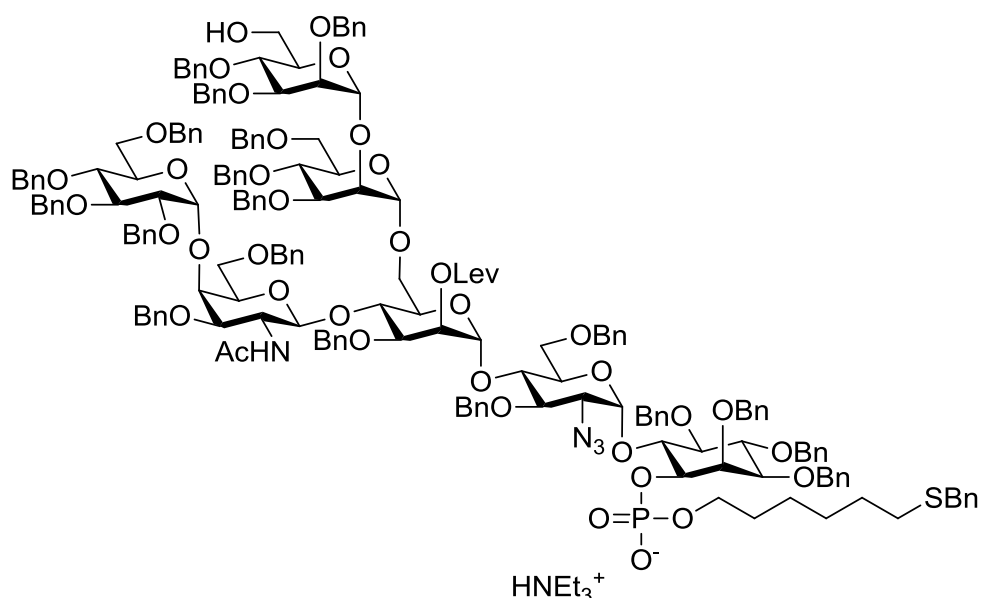


Alcohol **38*** (50 mg, 16 μmol) and H-phosphonate **10** (39 mg, 100 μmol) were co evaporated with dry pyridine (3x2 mL). The residue was dissolved in dry pyridine (2 mL) and PivCl (14.5 μL , 118 μmol) was added. The solution was stirred for 2h at r.t. before water (14 μL , 0.79 mmol) and iodine (29.9 mg, 118 μmol) were added. The red solution was stirred for 1h and quenched with sat. $\text{Na}_2\text{S}_3\text{O}_3$. The reaction mixture was diluted with chloroform (10 mL) and dried over Na_2SO_4 . The solvents were removed in vacuo and the residue was purified through flash column chromatography on deactivated (1 % TEA in CHCl_3) silica gel (starting from $\text{CHCl}_3/\text{MeOH}$ 0% \rightarrow 5% MeOH) to yield phosphate **41** as yellow oil (49 mg, 14 μmol , 87%); R_f (SiO_2 , $\text{MeOH}/\text{CHCl}_3$ 1:20) = 0.43; $[\alpha]_D^{20} = +42.33$ ($c = 1.00$ in CHCl_3); ATR-FTIR

* Pseudoheptasaccharide **38** was provided by Y.-H. Tsai and synthesized according to Ref. [110].

(cm^{-1}): 3064, 3032, 2926, 2865, 2107, 1742, 1720, 1678, 1497, 1454, 1362, 1054, 1028, 913; ^1H NMR (600 MHz, CDCl_3) δ 7.49 – 6.87 (m, 100H), 6.07 (d, $J = 9.0$ Hz, 1H, NH), 5.78 (s, 1H), 5.25 (s, 2H, ManI-2), 5.07 (s, 1H), 4.94 (d, $J = 11.9$ Hz, 1H, CH_2 of Bn), 4.89 – 3.89 (m, 49H), 3.86 – 3.74 (m, 11H), 3.73 – 3.66 (m, 2H), 3.63 (dd, $J = 8.9, 2.9$ Hz, 1H), 3.60 – 3.45 (m, 11H), 3.44 – 3.36 (m, 4H), 3.34 – 3.22 (m, 5H), 3.03 (dd, $J = 10.1, 3.6$ Hz, 1H), 2.85 (q, $J = 7.3$ Hz, 6H, NCH_2CH_3), 2.78 (d, $J = 9.4$ Hz, 1H), 2.27 (t, $J = 7.4$ Hz, 2H, BnS-CH_2), 2.24 – 2.04 (m, 4H, CH_2 of Lev), 1.80 (s, 3H, CH_3 of Lev), 1.70 (s, 3H, NHCOCH_3), 1.55 – 1.34 (m, 4H, $-\text{S-CH}_2\text{-CH}_2\text{-CH}_2\text{-CH}_2\text{-CH}_2\text{-O}$), 1.23 – 1.16 (m, 4H, $-\text{S-CH}_2\text{-CH}_2\text{-CH}_2\text{-CH}_2\text{-CH}_2\text{-O}$), 1.12 (t, $J = 7.6$ Hz, 9H, NCH_2CH_3), 1.00 – 0.94 (m, 21H, TIPS); ^{13}C NMR (151 MHz, CDCl_3) δ 205.92 (ketone of Lev), 171.76 (CO of Lev), 170.21 (NHCOCH_3), 140.02, 139.09, 139.03, 138.94, 138.91, 138.84, 138.76, 138.74, 138.69, 138.60, 138.57, 138.30, 138.15, 138.10, 138.01, 137.54, 128.92, 128.77, 128.72, 128.65, 128.62, 128.57, 128.54, 128.46, 128.44, 128.39, 128.36, 128.33, 128.31, 128.28, 128.27, 128.25, 128.24, 128.22, 128.16, 128.12, 128.10, 128.07, 127.98, 127.87, 127.84, 127.82, 127.77, 127.71, 127.67, 127.65, 127.63, 127.57, 127.55, 127.52, 127.48, 127.44, 127.29, 127.27, 127.18, 127.14, 126.94, 126.45, 101.71, 100.84, 99.65, 98.84, 98.65, 96.71, 82.20, 81.99, 81.51, 81.19, 81.03, 80.51, 80.12, 79.80, 79.13, 77.95, 77.53, 76.81, 75.93, 75.74, 75.43, 75.35, 75.26, 75.15, 74.75, 74.69, 74.54, 74.43, 74.03, 73.86, 73.63, 73.48, 73.23, 73.20, 73.00, 72.85, 72.39, 72.36, 72.07, 71.53, 71.37, 70.88, 70.79, 70.06 (ManI-2), 69.67, 68.77, 68.59, 67.74, 66.87, 65.80, 63.72, 62.90, 52.87, 45.42 (NCH_2CH_3), 38.57, 37.83, 36.38, 31.46, 31.00, 30.95, 29.82, 29.66, 29.30 (CH_3 of Lev), 28.81, 28.04, 27.69, 27.41, 25.52, 23.31 (NHCOCH_3), 18.24, 18.18, 14.25, 12.18, 8.55 (NCH_2CH_3); ^{31}P NMR (243 MHz, CDCl_3) δ -1.45; ESI-MS: m/z $[\text{M-2H}]^{2-}$ calcd for $\text{C}_{204}\text{H}_{233}\text{N}_4\text{O}_{40}\text{PSSi}$ 1734.7730, obsd 1734.7564.

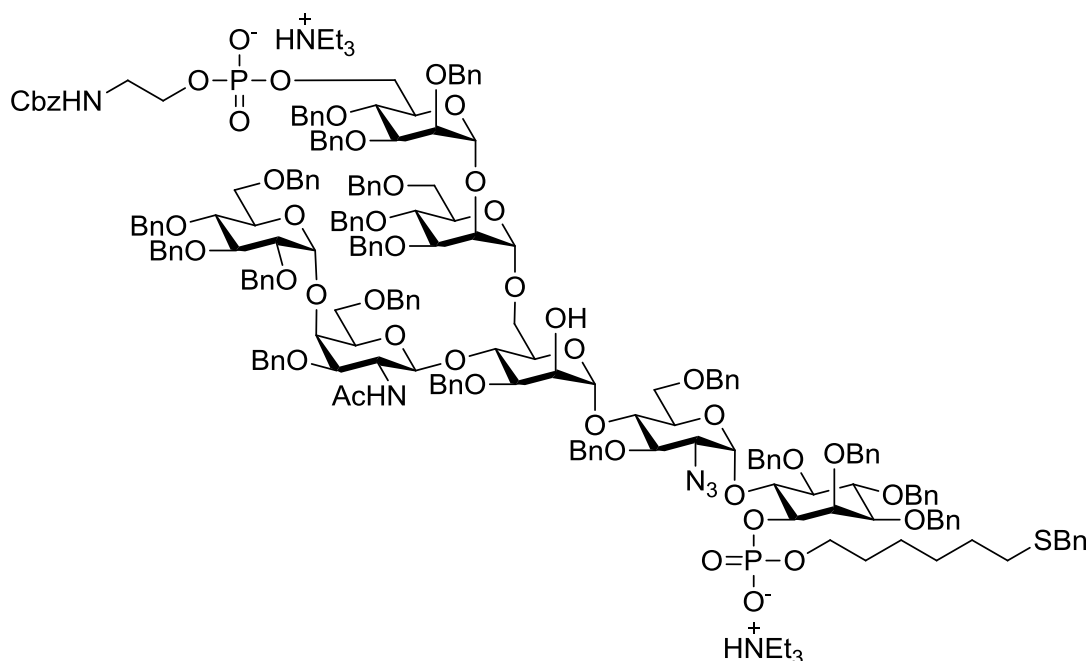
Triethylammonium (2,3,4-tri-*O*-benzyl- α -D-mannopyranosyl-(1 \rightarrow 2)-3,4,6-tri-*O*-benzyl- α -D-mannopyranosyl-(1 \rightarrow 6)-3-*O*-benzyl-4-*O*-(2,3,4,6-tetra-*O*-benzyl- α -D-glucopyranosyl-(1 \rightarrow 4)-3,6-di-*O*-benzyl-2-deoxy-2-acetamido- β -D-galactopyranosyl)-2-*O*-levulinyl- α -D-mannopyranosyl-(1 \rightarrow 4)-2-azido-3,6-di-*O*-benzyl-2-deoxy- α -D-glucopyranosyl-(1 \rightarrow 6)-2,3,4,5-tetra-*O*-benzyl-1-*O*-(6-(benzylthio)hexyl-phosphonato)-D-*myo*-inositol (39)



Phosphate **41** (43 mg, 12 μ mol) was dissolved in MeCN (2 mL). Water (8.7 μ L, 0.48 mmol) and Sc(TfO)₃ (11.8 mg, 24 μ mol) were added and the solution was heated up to 50 °C for 5 h. The reaction was quenched with pyridine (4.8 μ L, 60 μ mol) and the solvents were removed *in vacuo*. The residue was co evaporated with toluene (3x 2 mL) and purified through flash column chromatography on deactivated (1 % TEA in CHCl₃) silica gel (starting from CHCl₃/MeOH 0% \rightarrow 5% MeOH) to yield alcohol **39** as colorless oil (32 mg, 9.4 μ mol, 78%): $[\alpha]_D^{20} = +47.37$ (c = 1.00 in CHCl₃); ATR-FTIR (cm⁻¹): 3363, 3031, 2926, 2862, 2107, 1742, 1719, 1671, 1497, 1454, 1362, 1068, 1049, 1028, 697; ¹H NMR (600 MHz, CDCl₃) δ 7.55 – 6.71 (m, 100H), 6.19 (s, 1H, NH), 5.87 (s, 1H), 5.20 (s, 1H), 5.17 (s, 1H), 5.03 – 4.16 (m, 40H), 4.15 – 3.33 (m, 43H), 3.28 (d, *J* = 10.6 Hz, 1H), 3.21 – 3.11 (m, 1H), 3.02 (d, *J* = 7.7 Hz, 1H), 2.87 (d, *J* = 10.1 Hz, 1H), 2.80 (q, *J* = 7.0 Hz, 6H, NCH₂CH₃), 2.35 – 2.13 (m, 6H, BnS-CH₂, CH₂ of Lev), 1.85 (s, 3H, CH₃ of Lev), 1.75 (s, 3H, NHCOCH₃), 1.59 – 1.35 (m, 4H, -S-CH₂-CH₂-CH₂-CH₂-CH₂-CH₂-O), 1.28 – 1.13 (m, 4H, -S-CH₂-CH₂-CH₂-CH₂-CH₂-CH₂-O), 1.10 (t, *J* = 7.3 Hz, 1H, NCH₂CH₃); ¹³C NMR (151 MHz, CDCl₃) δ 206.20 (ketone of Lev), 171.68 (CO of Lev), 170.78 (NHCO), 149.97, 140.04, 139.04, 138.99, 138.87, 138.78, 138.68, 138.64, 138.54, 138.49, 138.30, 138.20, 138.10, 128.93, 128.82,

128.55, 128.49, 128.48, 128.43, 128.39, 128.37, 128.33, 128.30, 128.17, 128.08, 128.03, 127.96, 127.90, 127.80, 127.75, 127.66, 127.62, 127.59, 127.55, 127.53, 127.45, 127.35, 127.12, 126.95, 126.82, 101.45, 100.42, 100.04, 99.52, 99.19, 96.41, 82.15, 81.91, 81.21, 80.37, 79.99, 79.65, 77.96, 76.20, 75.86, 75.70, 75.36, 75.29, 75.13, 75.04, 74.93, 74.74, 74.10, 73.60, 73.53, 73.36, 73.29, 73.00, 72.56, 72.37, 72.31, 72.26, 72.17, 71.69, 71.20, 70.79, 69.84, 69.48, 69.26 (ManI-2), 69.00 67.98, 67.79, 65.75, 65.71, 63.32, 62.50, 54.82, 45.44 (NCH₂CH₃), 37.88, 36.39, 32.06, 31.47, 31.06, 29.91, 29.83, 29.72, 29.45, 29.39, 29.31, 28.84, 28.03, 27.71, 27.36, 25.55, 23.59, 22.83, 17.85, 14.26, 12.43, 8.60 (NCH₂CH₃); ³¹P NMR (162 MHz, CDCl₃) δ -1.14; ESI-MS: *m/z* [M+Cl-H]²⁻ calcd for C₁₉₅H₂₁₃N₄O₄₀PS 1673.6918, obsd 1673.6842.

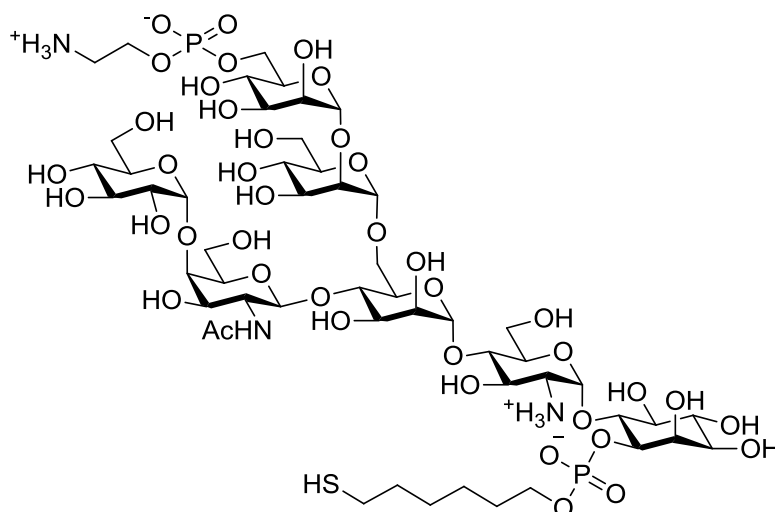
Bistriethylammonium (2,3,4-tri-*O*-benzyl-6-*O*-(2-(*N*-benzyloxycarbonyl)aminoethyl-phosphonato)- α -D-mannopyranosyl-(1 \rightarrow 2)-3,4,6-tri-*O*-benzyl- α -D-mannopyranosyl-(1 \rightarrow 6)-3-*O*-benzyl-4-*O*-(2,3,4,6-tetra-*O*-benzyl- α -D-glucopyranosyl-(1 \rightarrow 4)-3,6-di-*O*-benzyl-2-deoxy-2-acetamido- β -D-galactopyranosyl)- α -D-mannopyranosyl-(1 \rightarrow 4)-2-azido-3,6-di-*O*-benzyl-2-deoxy- α -D-glucopyranosyl-(1 \rightarrow 6)-2,3,4,5-tetra-*O*-benzyl-1-*O*-(6-(benzylthio)hexyl-phosphonato)-D-*myo*-inositol (40)



Alcohol **39** (31 mg, 9.1 μ mol) and H-phosphonate **10** (14.7 mg, 41 μ mol) were co evaporated with dry pyridine (3x2 mL). The residue was dissolved in dry pyridine (2 mL) and PivCl (8.4 μ L, 68 μ mol) was added. The solution was stirred for 2 h at r.t. before water (8.2 μ L, 0.45

mmol) and iodine (12.7 mg, 50 μmol) were added. The red solution was stirred for 1h and quenched with hydrazine (1M in THF; 227 μL , 0.28 mmol). The reaction mixture is stirred for 18 h. The solvents are removed *in vacuo* and the residue was purified through flash column chromatography on deactivated (1 % TEA in CHCl_3) silica gel (starting from $\text{CHCl}_3/\text{MeOH}$ 0% \rightarrow 10% MeOH) to yield bisphosphate **40** as yellow oil (25.3mg, 6.9 μmol , 76%): $[\alpha]_D^{20} = +46.01$ (c = 1.00 in CHCl_3); ATR-FTIR (cm^{-1}): 3344, 2926, 2864, 2108, 1683, 1497, 1454, 1363, 1093, 1071, 1028, 863; ^1H NMR (600 MHz, CDCl_3) δ 7.38 – 6.79 (m, 105H), 6.23 (s, 1H, NHCOCH_3), 5.87 (d, $J = 3.4$ Hz, 1H), 5.15 (s, 1H), 5.00 – 3.30 (m, 90H), 3.24 (d, $J = 10.3$ Hz, 1H), 3.11 (d, $J = 4.6$ Hz, 1H), 3.03 (d, $J = 8.0$ Hz, 1H), 2.80 (d, $J = 10.2$ Hz, 1H), 2.69 (q, $J = 7.2$ Hz, 12H, NCH_2CH_3), 2.28 (t, $J = 7.4$ Hz, 2H, BnS-CH_2), 1.86 (s, 1H, NHCOCH_3), 1.59 – 1.36 (m, 4H, $-\text{S-CH}_2\text{-CH}_2\text{-CH}_2\text{-CH}_2\text{-CH}_2\text{-CH}_2\text{-O}$), 1.26 – 1.11 (m, 4H, $-\text{S-CH}_2\text{-CH}_2\text{-CH}_2\text{-CH}_2\text{-CH}_2\text{-CH}_2\text{-O}$), 1.02 (t, $J = 7.3$ Hz, 18H, NCH_2CH_3); ^{31}P NMR (243 MHz, CDCl_3) δ 0.00, -1.32; ESI-MS: m/z $[\text{M}-2\text{H}]^{2-}$ calcd for $\text{C}_{200}\text{H}_{219}\text{N}_5\text{O}_{43}\text{P}_2\text{S}$ 1735.2077, obsd 1735.2054.

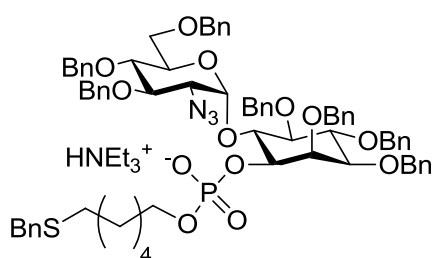
6-O-Aminoethylphosphonato- α -D-mannopyranosyl-(1 \rightarrow 2)- α -D-mannopyranosyl-(1 \rightarrow 6)-4-O-(α -D-glucopyranosyl-(1 \rightarrow 4)-2-deoxy-2-acetamido- β -D-galactopyranosyl)- α -D-mannopyranosyl-(1 \rightarrow 4)-2-amino-2-deoxy- α -D-glucopyranosyl-(1 \rightarrow 6)-1-O-(thiohexylphosphonato)-D-myoinositol (3)



Bisphosphate **40** (20 mg, 5.4 μmol) was dissolved in dry THF (2 mL) and *tert*-butanol (2 drops). The solution was cooled down to -78 $^{\circ}\text{C}$ and approximately 10 mL ammonia was condensed in the flask. Afterwards small fresh cut pieces of sodium were added till a dark

blue color was established. The reaction was stirred for 35 min at $-78\text{ }^{\circ}\text{C}$. The reaction was quenched with MeOH (2 mL) and ammonia was blown off using a stream of nitrogen. The solution was adjusted with concentrated acetic acid to pH 7. Water was removed by freeze drying and the residue was purified using a Sephadex super fine G-25 (GE Healthcare) column (1 cmx20 cm) to yield sulfide **3** as white solid (4.5 mg, 3.0 μmol , 55%): ^1H NMR (400 MHz, D_2O) δ 5.59 (d, $J = 3.6$ Hz, 1H, GlcNH₂-1), 5.27 (s, 1H), 5.23 (s, 1H), 5.07 (s, 1H), 4.99 (d, $J = 3.8$ Hz, 1H, Glc-1), 4.60 (d, $J = 8.2$ Hz, 1H, GalNAc-1), 4.31 – 3.67 (m, 42H), 3.60 (dd, $J = 10.1, 3.6$ Hz, 2H), 3.55 – 3.39 (m, 3H), 3.35 (t, $J = 5.0$, 1H), 2.83 (t, $J = 7.2$ Hz, 1H), 2.61 (t, $J = 7.1$ Hz, 1H), 2.14 (s, 3H, Me of NHAc), 1.82 – 1.58 (m, 4H, linker), 1.54 – 1.38 (m, 4H, linker); ^{13}C NMR (151 MHz, D_2O) δ 177.28 (amide), 105.01, 104.76 (GalNAc-1), 103.91, 102.82 (Glc-1), 101.11, 99.97 (GlcNH₂-1), 81.64, 79.91, 79.30, 79.25, 79.15, 78.84, 78.04, 75.70, 75.69, 75.39, 75.36, 75.29, 74.84, 74.61, 74.55, 74.40, 74.32, 74.08, 73.94, 73.62, 73.16, 72.86, 72.83, 72.66, 72.58, 72.55, 72.50, 72.27, 72.18, 72.12, 72.06, 71.82, 71.62, 69.60, 69.22, 68.87, 67.29, 64.51, 64.48, 63.77, 62.98, 62.82, 62.52, 56.58, 55.08, 42.72, 42.67, 40.75, 35.52, 32.28, 30.88, 29.80, 29.67, 27.30, 27.18, 26.99, 26.52, 26.29, 25.84, 24.96; ^{31}P NMR (162 MHz, D_2O) δ 0.40, 0.22; ESI-MS: m/z $[\text{M}-2\text{H}]^{2-}$ calcd for $\text{C}_{52}\text{H}_{95}\text{N}_3\text{O}_{41}\text{P}_2\text{S}$ 754.7245, obsd 754.7304.

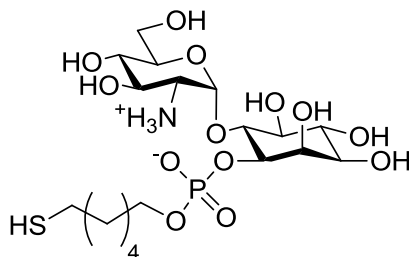
Triethylammonium 2-azido-3,4,6-tri-*O*-benzyl-2-deoxy- α -D-glucopyranosyl-(1 \rightarrow 6)-2,3,4,5-tetra-*O*-benzyl-1-*O*-(6-(*S*-benzyl)thiohexyl phosphono)-D-myo-inositol (50)



Alcohol **7** (60 mg, 0.063 mmol) was dissolved in DMF (2 mL) and BnBr (15 μL , 0.127 mmol) was added. The solution was cooled down to $0\text{ }^{\circ}\text{C}$ and NaH (7.6 mg, 0.316 mmol) was added. The solution was stirred for 3 h at r.t. before it was quenched with MeOH (1 mL), diluted with EtOAc (20 mL) and washed with sat. sodium bicarbonate solution (3x 20 mL). The organic layer was dried over sodium sulfate and evaporated to dryness. The residue was purified with column chromatography (*n*-hexane/ethyl acetate 10:1 \rightarrow 7:1) to yield fully protected sugar (R_f (SiO_2 , *n*-hexane/ethyl acetate 10:1) = 0.25) as colorless oil (59 mg, 0.057

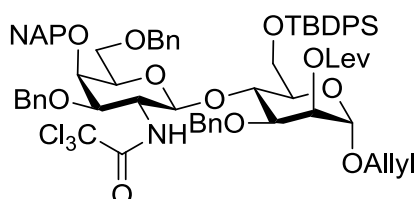
mmol, 90%). The fully protected sugar (59 mg, 0.057 mmol) was dissolved in MeOH (5 mL) and DCM (3 mL) and PdCl₂ (2 mg, 0.011 mmol) was added. The brown solution was stirred for 12 h at r.t. (turned black) before it was filtered over Celite® and evaporated to dryness. The residue was purified with column chromatography (*n*-hexane/ethyl acetate 5:1) to yield the free alcohol (R_f (SiO₂, *n*-hexane/ethyl acetate 5:1) = 0.21) as colorless oil (50 mg, 0.050 mmol, 88%). The free alcohol was phosphorylated *via* the following procedure. The alcohol (50 mg, 0.050 mmol) and H-phosphonate **9** (28 mg, 0.075 mmol) were coevaporated with pyridine (3x 2 mL) and placed under HV for 30 min. The residue was dissolved in pyridine (2 mL) and PivCl (15.4 μL, 0.125 mmol) was added. The solution was stirred for 1 h before water (2 drops) and iodine (25 mg, 0.100 mmol) were added. The solution was stirred for 3 h, before it was quenched with sat. sodium thiosulfate solution and evaporated to dryness. The residue was coevaporated with toluene (4x2 mL) and purified with column chromatography (CHCl₃/MeOH 95:5, on TEA deactivated SiO₂) to yield **50** as colorless oil (64 mg, 0.050 mmol, 88%): R_f (SiO₂, CHCl₃/MeOH 10:1) = 0.43; ¹H NMR (400 MHz, CDCl₃) δ 12.35 (s, 1H, HNEt₃⁺), 7.43 (d, *J* = 7.0 Hz, 2H), 7.37 – 7.18 (m, 33H), 7.12 (t, *J* = 7.4 Hz, 1H), 7.09 – 7.04 (m, 2H), 7.01 (t, *J* = 7.5 Hz, 2H), 5.83 (d, *J* = 3.7 Hz, 1H, GlcNH₂-1), 5.01 (d, *J* = 11.8 Hz, 1H), 4.94 (d, *J* = 12.2 Hz, 2H), 4.86 (s, 2H), 4.78 – 4.70 (m, 5H), 4.62 (d, *J* = 11.6 Hz, 1H), 4.53 (d, *J* = 12.0 Hz, 1H), 4.44 (d, *J* = 11.1 Hz, 1H), 4.38 – 4.31 (m, 2H), 4.28 (d, *J* = 12.0 Hz, 1H), 4.11 (dd, *J* = 18.6, 9.2 Hz, 2H), 4.06 – 3.90 (m, 3H), 3.76 – 3.69 (m, 1H), 3.67 (s, 2H, Ph-CH₂-S), 3.55 (dd, *J* = 9.9, 2.1 Hz, 1H), 3.47 (t, *J* = 9.1 Hz, 1H), 3.40 – 3.30 (m, 2H), 3.23 (dd, *J* = 10.3, 3.7 Hz, 1H), 2.97 (q, *J* = 6.5 Hz, 6H, CH₂ of TEA), 2.42 – 2.23 (m, 2H), 1.64 – 1.54 (m, 2H), 1.54 – 1.44 (m, 2H), 1.34 – 1.22 (m, 13H, Me of TEA and 4H of Linker); ¹³C NMR (101 MHz, CDCl₃) δ 139.79, 138.84, 138.71, 138.54, 138.50, 138.22, 138.18, 138.11, 128.89, 128.51, 128.46, 128.36, 128.32, 128.30, 128.25, 128.22, 128.14, 128.12, 127.98, 127.97, 127.92, 127.81, 127.72, 127.61, 127.58, 127.48, 127.45, 127.31, 127.08, 126.91, 96.89 (GlcNH₂-1), 81.94, 81.55, 81.00, 79.93, 78.45, 77.98, 77.92, 76.68, 76.11, 75.70, 75.24, 74.85, 74.82, 74.41, 74.33, 73.35, 72.32, 70.08, 68.08, 66.30, 63.37, 45.53 (CH₂ of TEA), 36.33 (Ph-CH₂-S), 31.41, 30.86, 30.79, 29.24, 28.75, 25.43, 8.56 (Me of TEA). Spectral data were in good agreement with Ref. [90].

2-Amino-2-deoxy- α -D-glucopyranosyl-(1 \rightarrow 6)-1-O-(6-thiohexyl phosphono)-D-myoinositol (48)



Phosphate **50** (10 mg, 7.3 μ mol) was dissolved in dry THF (2 mL) and *tert*-butanol (2 drops). The solution was cooled down to -78 $^{\circ}$ C and approximately 10 mL ammonia was condensed in the flask. Afterwards small fresh cut pieces of sodium were added till a dark blue color was established. The reaction was stirred for 35 min at -78 $^{\circ}$ C, before it was quenched with MeOH (2 mL) and the ammonia was blown off using a stream of nitrogen. The solution was adjusted with concentrated acetic acid to pH 7. Water was removed by freeze drying and the residue was purified using a Sephadex super fine G-25 (GE Healthcare) column (1 cmx20 cm) to yield a mixture of sulfide and disulfide of **48** as white solid (1.6 mg, 3.0 μ mol, 40%): 1 H NMR (600 MHz, D₂O) δ 5.58 (d, J = 3.9 Hz, 1H, GlcNH₂-1), 4.27 – 4.17 (m, 2H), 4.13 (dt, J = 10.1, 3.2 Hz, 1H), 3.99 – 3.90 (m, 4H), 3.86 – 3.81 (m, 2H), 3.72 (t, J = 9.7 Hz, 1H), 3.59 – 3.54 (m, 2H), 3.44 (t, J = 9.4 Hz, 1H), 3.37 (dd, J = 10.5, 4.0 Hz, 1H), 2.79 (t, J = 7.2 Hz, 1H), 2.57 (t, J = 7.1 Hz, 1H), 1.78 – 1.59 (m, 4H), 1.50 – 1.36 (m, 4H); 31 P NMR (243 MHz, D₂O) δ 0.23; ESI-MS: m/z [M+H]⁺ calcd for C₁₈H₃₆NO₁₃S 538.1718, obsd 538.1726. Spectral data were in good agreement with Ref. [90].

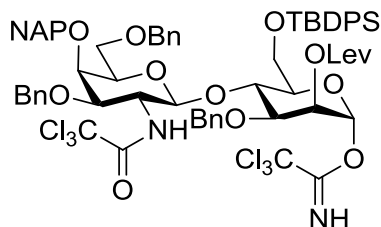
Allyl 3,6-Di-O-benzyl-2-deoxy-2-trichlor-acetamido-4-O-2-naphthylmethyl- β -D-galactopyranosyl-(1 \rightarrow 4)-3-O-benzyl-6-O-*tert*butyldiphenylsilyl-2-O-levulinyl- α -D-mannopyranoside (55)



Mannopyranoside **27** (160 mg, 0.247 mmol) and phosphate **51**^{*} (269 mg, 0.322 mmol) were coevaporated with toluene (3x 2 mL) and placed under high vacuum for 30 min. The residue was dissolved in DCM (4 mL) and molecular sieves (500 mg, MS 4Å) was added. The slurry was stirred 10 min before it was cooled down to -40 °C. TMSOTf (58 µL, 0.322 mmol) was added and the reaction mixture was stirred for 45 min at -40 °C before it was quenched with TEA (0.3 mL), filtered, evaporated to dryness and purified using flash column chromatography to give disaccharide **55** (284 mg, 0.223 mmol, 90% yield) as white foam: R_f (SiO₂, *n*-hexane/ethyl acetate 3:1) = 0.49; $[\alpha]_D^{20}$: + 30.2 (*c* = 0.67, CHCl₃); ATR-FTIR (cm⁻¹): 3406, 3062, 2929, 2858, 1736, 1716, 1362, 1139, 1103, 1062; ¹H NMR (400 MHz, CDCl₃) δ 7.85 – 7.79 (m, 1H), 7.79 – 7.70 (m, 7H), 7.52 – 7.27 (m, 19H), 7.22 – 7.10 (m, 5H), 6.37 (d, *J* = 7.3 Hz, 1H, NH), 5.96 – 5.84 (m, 1H, CH=), 5.36 (dd, *J* = 3.2, 1.8 Hz, 1H, Man-2), 5.28 (dd, *J* = 17.2, 1.4 Hz, 1H, CH₂=), 5.24 – 5.18 (m, 2H, CH₂= and GalNAc-1 *J*_{H,H} = 8.2), 5.03 (d, *J* = 11.4 Hz, 1H), 4.86 (d, *J* = 1.5 Hz, 1H, Man-1), 4.79 – 4.61 (m, 4H), 4.48 (d, *J* = 11.3 Hz, 1H), 4.33 (d, *J* = 11.7 Hz, 1H), 4.27 – 4.16 (m, 2H), 4.12 – 3.96 (m, 6H), 3.87 (dd, *J* = 11.1, 5.5 Hz, 1H), 3.83 – 3.64 (m, 3H), 3.48 (dd, *J* = 8.1, 5.3 Hz, 1H), 3.34 (dd, *J* = 8.9, 5.1 Hz, 1H), 2.64 – 2.36 (m, 4H, CH₂ of Lev), 2.05 (s, 3H, Me of Lev), 1.09 (s, 9H, *t*Bu); ¹³C NMR (101 MHz, CDCl₃) δ 206.38 (ketone), 172.09 (ester), 161.91 (amide), 138.67, 137.92, 137.77, 136.07, 135.70, 133.78, 133.57, 133.29, 133.24, 133.05, 129.97, 129.86, 128.55, 128.47, 128.23, 128.06, 128.00, 127.98, 127.95, 127.85, 127.83, 127.79, 127.76, 127.71, 127.18, 126.91, 126.79, 126.44, 126.09, 125.92, 117.99, 98.48 (GalNAc-1), 96.42 (Man-1), 92.33 (CCl₃), 77.36, 77.12, 76.55, 74.92, 73.50, 73.17, 72.84, 72.64, 72.10, 71.95, 71.51, 69.05 (Man-2), 68.05, 63.73, 56.76, 37.97, 29.79, 28.10, 26.76 (*t*Bu), 19.40 (C_{qu} of *t*Bu); ESI-MS: *m/z* [M+Na]⁺ calcd for C₇₀H₇₆Cl₃NO₁₃Si 1294.4049, obsd 1294.4103.

^{*} Phosphate **51** was provided by Y.-H. Tsai and prepared according to Ref. [110]. A precursor of this compound was provided by H. S. Hahm.

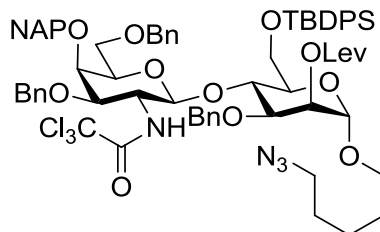
3,6-Di-*O*-benzyl-2-deoxy-2-trichloroacetamido-4-*O*-2-naphthylmethyl- β -D-galactopyranosyl-(1 \rightarrow 4)-3-*O*-benzyl-6-*O*-*tert*butyldiphenylsilyl-2-*O*-levulinyl- α -D-mannopyranosyl trichloroacetimidate (52**)**



Disaccharide **55** (60 mg, 0.047 mmol) was dissolved in MeOH (3 mL) and DCM (0.5 mL). PdCl₂ (1.7 mg, 9.4 μ mol) were added and the reaction mixture was stirred for 4 h, before it was evaporated to dryness and purified using flash column chromatography to give lactol **52a** (41 mg, 0.033 mmol, 71% yield) as white foam and as an inseparable mixture of anomers: R_f (SiO₂, *n*-hexane/ethyl acetate 3:1) = 0.14; ESI-MS: *m/z* [M+Na]⁺ calcd for C₆₇H₇₂Cl₃NO₁₃Si 1254.3736, obsd 1254.3886.

The lactol (40 mg, 0.032 mmol) was dissolved in DCM (1 mL) and trichloroacetonitrile (98 μ L, 0.973 mmol). The solution was cooled down to 0 °C and DBU (0.5 μ L, 3.2 μ mol) was added to the reaction mixture. The reaction was stirred 3 h at r. t. before the solution was evaporated to dryness and purified using flash column chromatography to give imidate **52** (39 mg, 0.028 mmol, 87% yield) as white foam: R_f (SiO₂, *n*-hexane/ethyl acetate 3:1) = 0.43; [α]_D²⁰: + 39.4 (c = 0.1, CHCl₃); ATR-FTIR (cm⁻¹): 3055, 2929, 2857, 1719, 1151, 1105; ¹H NMR (400 MHz, CDCl₃) δ 8.66 (s, 1H, NH of imidate), 7.82 – 7.63 (m, 9H), 7.49 – 7.41 (m, 3H), 7.39 – 7.24 (m, 15H), 7.19 – 7.04 (m, 5H), 6.37 (d, J = 7.3 Hz, 1H, NH of amide), 6.26 (d, J = 1.8 Hz, 1H, Man-1), 5.44 – 5.40 (m, 1H, Man-2), 5.06 – 4.98 (m, 2H, GalNAc-1), 4.75 – 4.61 (m, 4H), 4.47 (d, J = 11.4 Hz, 1H), 4.34 (t, J = 10.7 Hz, 2H), 4.25 (d, J = 11.8 Hz, 1H), 4.05 (d, J = 1.8 Hz, 1H), 4.00 – 3.80 (m, 6H), 3.64 (t, J = 8.4 Hz, 1H), 3.49 – 3.44 (m, 1H), 3.39 (dd, J = 8.8, 5.1 Hz, 1H), 2.65 – 2.38 (m, 4H, CH₂ of Lev), 2.03 (s, 3H, Me of Lev), 1.04 (s, 9H, *t*Bu); ¹³C NMR (101 MHz, CDCl₃) δ 206.22 (ketone), 171.93 (ester), 161.86 (amide), 159.92 (imidate), 138.36, 137.72, 136.04, 135.78, 133.27, 133.08, 129.97, 128.67, 128.53, 128.26, 128.14, 128.08, 128.00, 127.90, 127.79, 127.53, 127.37, 126.80, 126.42, 126.14, 125.97, 98.76 (GalNAc-1), 95.02 (Man-1), 92.47, 91.01 (2x CCl₃), 75.44, 75.10, 74.96, 73.59, 73.42, 72.35, 72.04, 71.79, 68.28, 56.29, 37.99, 29.83, 28.07, 26.80 (Me of *t*Bu), 19.50 (C_{qu} of *t*Bu); ESI-MS: *m/z* [M+Na]⁺ calcd for C₆₉H₇₂Cl₆N₂O₁₃Si 1399.2803, obsd 1399.2888.

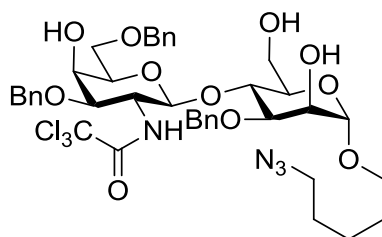
1-*O*-5-Azidopentyl 3,6-di-*O*-benzyl-2-deoxy-2-trichloroacetamido-4-*O*-2-naphthylmethyl- β -D-galactopyranosyl-(1 \rightarrow 4)-3-*O*-benzyl-6-*O*-*tert*butyldiphenylsilyl-2-*O*-levulinyl- α -D-mannopyranose (54)



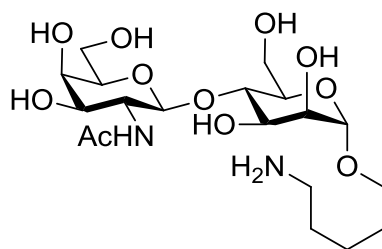
Trichloroacetimidate **52** (18 mg, 0.013 mmol) and alcohol **53**^{*} (3.4 mg, 0.026 mmol) were dissolved in Et₂O (1 mL) and molecular sieves (4Å powdered, 50 mg) was added. The slurry was stirred 10 min at r.t. before it was cooled down to 0 °C and TMSOTf (1.2 μL, 6.53 μmol) was added. The reaction mixture was stirred at 0 °C for 1 h before it was quenched with TEA (50 μL), filtered and evaporated to dryness. The residue was purified using flash column chromatography to give azide **54** (16 mg, 0.012 mmol, 91% yield) as yellow oil: R_f (SiO₂, *n*-hexane/ethyl acetate 3:1) = 0.40; [α]_D²⁰: + 19.0 (c = 1.6, CHCl₃); ATR-FTIR (cm⁻¹): 2928, 2858, 2096, 1717, 1362, 1102, 1063; ¹H NMR (400 MHz, CDCl₃) δ 7.83 – 7.63 (m, 8H), 7.50 – 7.22 (m, 19H), 7.21 – 7.07 (m, 5H), 6.32 (d, J = 7.3 Hz, 1H, NH of amide), 5.28 (s, 1H, Man-2), 5.16 (d, J = 8.3 Hz, 1H, GalNAc-1), 4.99 (d, J = 11.3 Hz, 1H), 4.78 – 4.57 (m, 5H, Man-1), 4.44 (d, J = 11.2 Hz, 1H), 4.28 (d, J = 11.7 Hz, 1H), 4.18 (d, J = 11.6 Hz, 1H), 4.08 – 3.94 (m, 4H), 3.91 (dd, J = 9.1, 3.4 Hz, 1H, Man-3), 3.82 (dd, J = 11.1, 5.7 Hz, 1H), 3.68 (ddd, J = 30.6, 15.8, 8.0 Hz, 4H), 3.47 – 3.34 (m, 2H), 3.31 – 3.22 (m, 3H), 2.62 – 2.32 (m, 4H, CH₂ of Lev), 2.03 (s, 3H, Me of Lev), 1.59 (dq, J = 14.6, 7.3 Hz, 4H), 1.44 – 1.34 (m, 2H), 1.04 (s, 9H, *t*Bu); ¹³C NMR (101 MHz, CDCl₃) δ 206.49 (ketone), 172.19 (ester), 161.97 (amide), 138.73, 137.94, 137.79, 136.09, 135.74, 133.28, 133.09, 130.03, 129.91, 128.60, 128.51, 128.28, 128.10, 128.04, 128.02, 127.89, 127.83, 127.80, 127.75, 127.21, 126.88, 126.49, 126.15, 125.98, 98.62 (GalNAc-1), 97.27 (Man-1), 92.35 (CCl₃), 77.36, 76.70, 74.98, 73.55, 73.18, 73.02, 72.64, 72.16, 71.96, 71.50, 69.12, 68.06, 67.42, 63.84, 56.83, 51.40, 38.03, 29.85, 29.05, 28.81, 28.15, 26.79, 23.56, 19.43 (C_{qu} of *t*Bu); ESI-MS: *m/z* [M+Na]⁺ calcd for C₇₂H₈₁Cl₃N₄O₁₃Si 1367.4503, obsd 1367.4615.

^{*} The linker **53** was provided by Dr. D. C. K. Rathwell and was synthesized according to Ref. [109].

1-*O*-5-Azidopentyl 3,6-di-*O*-benzyl-2-deoxy-2-trichloroacetamido- β -D-galactopyranosyl-(1 \rightarrow 4)-3-*O*-benzyl- α -D-mannopyranose (56)

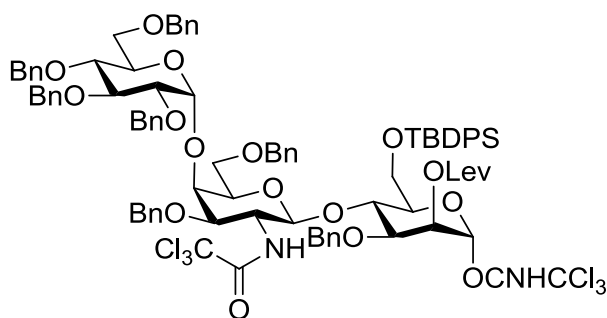


Azide **54** (16 mg, 12.0 μ mol) was dissolved in 1 M TBAF solution in THF (200 μ L, 0.20 mmol) and THF (1 mL) and stirred for 1 h. Afterwards hydrazine monohydrate (58 μ L, 1.19 mmol) was added and the reaction mixture was stirred for 1 h at r.t. before it was diluted with ethyl acetate (25 mL) and washed with sat. NaHCO₃ solution (3x 15 mL). The organic layer was dried over Na₂SO₄, filtered and evaporated to dryness. The residue was dissolved in DCM/PBS (1 mL; 10:1) and DDQ (4 mg, 18 μ mol) was added. The reaction mixture was stirred for 1 h before it was diluted with ethyl acetate (25 mL) and washed with sat. NaHCO₃ solution (3x 15 mL). The organic layer was dried over Na₂SO₄, filtered and evaporated to dryness. The residue was purified using flash column chromatography to give triol **56** (5 mg, 5.8 μ mol, 48% yield) as yellow oil: R_f (SiO₂, *n*-hexane/ethyl acetate 1:3) = 0.20; $[\alpha]_D^{20}$: +30.5 (c = 0.50, CHCl₃); ATR-FTIR (cm⁻¹): 3323, 2925, 2856, 2100, 1695, 1455, 1101, 1067; ¹H NMR (400 MHz, CDCl₃) δ 7.39 – 7.20 (m, 15H), 7.06 (d, J = 5.3 Hz, 1H, NH), 5.05 (d, J = 7.6 Hz, 1H, GalNAc-1), 4.83 – 4.74 (m, 2H, Man-1), 4.69 (d, J = 11.7 Hz, 1H), 4.56 – 4.34 (m, 4H), 4.21 (t, J = 9.5 Hz, 1H), 4.02 – 3.92 (m, 3H), 3.87 – 3.79 (m, 2H), 3.78 – 3.71 (m, 1H), 3.70 – 3.53 (m, 6H), 3.42 – 3.33 (m, 1H), 3.28 (t, J = 6.8 Hz, 2H), 3.05 – 2.91 (m, 2H, OH), 2.76 (s, 1H, OH), 1.67 – 1.53 (m, 4H), 1.45 – 1.36 (m, 2H); ¹³C NMR (101 MHz, CDCl₃) δ 162.24 (amide), 138.33, 137.84, 137.33, 128.70, 128.66, 128.57, 128.26, 128.11, 127.99, 127.80, 127.22, 99.36 (Man-1), 99.09 (GalNAc-1), 92.76 (CCl₃), 79.15, 78.34, 76.49, 73.79, 73.18, 72.10, 71.97, 71.54, 71.47, 69.36, 68.88, 67.60, 65.20, 61.38, 55.15, 52.33, 51.42, 47.38, 37.24, 32.08, 29.05, 28.78, 23.56; ESI-MS: m/z [M+Na]⁺ calcd for C₄₀H₄₉Cl₃N₄O₁₁ 889.2361, obsd 889.2327.

1-O-5-Aminopentyl **α -D-glucopyranosyl-(1 \rightarrow 4)-2-deoxy-2-acetamido- β -D-galactopyranosyl--(1 \rightarrow 4)- α -D-mannopyranose (**42**)**

Triol **56** (5 mg, 5.8 μ mol) was dissolved in MeOH (1.5 mL) and HOAc (2 drops). Pd/C (21.5 mg, 20 μ mol, 10 wt%) was added and hydrogen was bubbled through the slurry for 10 min. Afterwards the slurry was stirred for 12 h under hydrogen atmosphere before it was filtered through a syringe filter and evaporated to dryness. The residue was submitted to SEC chromatography (Sephadex-G25, 5% EtOH in water) to yield disaccharide **42** (1.8 mg, 3.8 μ mol, 65%) as white solid: ^1H NMR (400 MHz, D_2O) δ 4.82 (s, 1H, Man-1), 4.45 (d, $J = 8.0$ Hz, 1H, GalNAc-1), 3.98 – 3.85 (m, 4H), 3.83 – 3.59 (m, 9H), 3.57 – 3.47 (m, 1H, $\text{CH}_2\text{-O}$), 2.96 (t, $J = 7.4$ Hz, 2H, $\text{CH}_2\text{-NH}_2$), 2.04 (s, 3H, NHAc), 1.70 – 1.54 (m, 4H, $\text{CH}_2\text{-CH}_2\text{-CH}_2$), 1.48 – 1.34 (m, 2H, $\text{CH}_2\text{-CH}_2\text{-CH}_2$); ^{13}C NMR (101 MHz, D_2O) δ 101.77 (GalNAc-1), 99.19 (Man-1), 77.34, 75.22, 70.88, 70.52, 69.31, 67.45, 67.35, 60.89, 60.30, 52.36, 39.23 ($\text{CH}_2\text{-NH}_2$), 27.85, 26.47, 22.35 ($\text{CH}_2\text{-CH}_2\text{-CH}_2$), 22.04 (Me); ESI-MS: m/z $[\text{M}+\text{H}]^+$ calcd for $\text{C}_{19}\text{H}_{36}\text{Cl}_3\text{N}_2\text{O}_{11}$ 469.2392, obsd 469.2397.

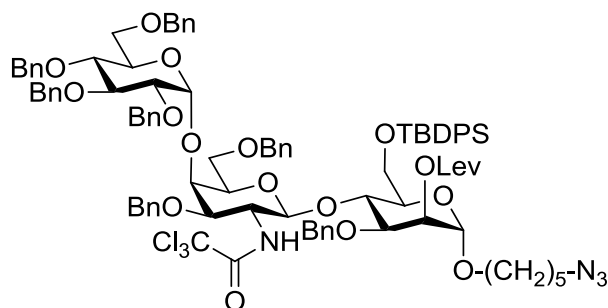
2,3,4,6-tetra-*O*-benzyl- α -D-glucopyranosyl-(1 \rightarrow 4)-3,6-di-*O*-benzyl-2-deoxy-2-trichloroacetamido- β -D-galactopyranosyl-3-*O*-benzyl-6-*O*-tertbutyldiphenylsilyl-2-*O*-levulinyl- α -D-mannopyranosyl trichloroacetimidate (58**)**



A solution of $[\text{IrCOD}(\text{PPh}_2\text{Me})_2]\text{PF}_6$ (4.9 mg, 5.8 μmol) in THF (3 mL) was stirred under hydrogen at 20 °C until the colour turned from red to colourless to pale yellow. The hydrogen atmosphere was exchanged with nitrogen. This solution was then added into a flask with mannopyranoside **57*** (300 mg, 0.181 mmol). After overnight stirring, the solvent was removed and the residue was dissolved in a mixture of acetone (3.6 mL) and water (0.4 mL). Mercury(II) chloride (295 mg, 1.09 mmol) and mercury(II) oxide (3.9 mg, 0.018 mmol) were added. After 1 h, the reaction mixture was diluted with chloroform and washed with saturated $\text{NaHCO}_3(\text{aq})$, dried over Na_2SO_4 , filtered and concentrated to give the crude lactol **58a**: R_f (SiO_2 , EtOAc/Hexane 1:4 = 0.09), which was purified by flash column chromatography to yield an inseparable mixture of anomers. The lactol **58a** was dissolved in DCM (1mL) and 2,2,2-trichloroacetonitrile (0.23 mL, 2.32 mmol) and DBU (1 drop) was added. After 1 h, the solvent was removed to give a brown oil that was purified by flash column chromatography to give imidate **58** (115 mg, 0.065 mmol, 36% yield over three steps) as a white foam: R_f (SiO_2 , EtOAc/Hexane 1:3) = 0.33; $[\alpha]_D^{20}$: + 48.9 ($c = 0.35$, CHCl_3); ATR-FTIR (cm^{-1}): 3031, 2929, 1719, 1454, 1428, 1361, 1150, 1103, 1028; ^1H NMR (400 MHz, CHCl_3) δ 8.65 (s, 1H, NH of imidate), 7.77 – 7.68 (m, 4H), 7.45 – 7.14 (m, 35H), 7.12 (dd, $J = 6.9, 2.7$ Hz, 2H), 7.09 – 7.04 (m, 2H), 6.49 (d, $J = 7.5$ Hz, 1H, NH), 6.28 (d, $J = 2.0$ Hz, 1H, Man-1), 5.35 (dd, $J = 3.3, 2.2$ Hz, 1H, Man-2), 5.13 (d, $J = 3.4$ Hz, 1H, Glc-1), 5.07 (d, $J = 8.1$ Hz, 1H, GalNAc-1), 4.86 – 4.72 (m, 6H), 4.69 (d, $J = 11.2$ Hz, 1H), 4.61 (d, $J = 11.0$ Hz, 1H), 4.49 (m, 3H), 4.41 – 4.33 (m, 2H), 4.29 (d, $J = 12.0$ Hz, 1H), 4.24 – 4.14 (m, 3H), 4.11 (d, $J = 12.2$ Hz, 1H), 4.06 (d, $J = 9.4$ Hz, 1H), 3.95 (m, 5H), 3.85 – 3.78 (m, 1H), 3.78 – 3.71 (m, 1H), 3.59 (dd, $J = 9.9, 3.4$ Hz, 1H), 3.56 – 3.50 (m, 2H), 3.42 (dd, $J = 10.7, 2.0$ Hz, 1H), 3.05 (dd, $J = 10.6, 1.6$ Hz, 1H), 2.73 – 2.46 (m, 4H, CH_2 of Lev), 2.08 (s, 3H, Me of Lev), 1.10 (s, 9H, *tert*Bu); ^{13}C NMR (101 MHz, CHCl_3) δ 206.09 (ketone of Lev), 171.90, 161.61, 159.83, 138.80, 138.49, 138.39, 138.34, 138.31, 138.00, 137.96, 136.02, 135.78, 133.77, 133.03, 129.91, 128.51, 128.47, 128.43, 128.32, 128.29, 128.28, 128.18, 128.15, 128.00, 127.87, 127.82, 127.74, 127.69, 127.65, 127.59, 127.57, 127.38, 127.32, 100.21 (Glc-1, $J_{\text{C,H}} = 172$ Hz), 98.66 (GalNAc-1, $J_{\text{C,H}} = 164$ Hz), 95.00 (Man-1, $J_{\text{C,H}} = 181$ Hz), 92.45, 90.92 ($2 \times \text{CCl}_3$), 82.20, 80.10, 77.81, 76.51, 75.31, 75.03, 74.97, 73.88, 73.73, 73.66, 73.53, 73.32, 73.16, 72.41, 71.92, 71.60, 70.88, 68.80, 67.70, 67.45, 62.70, 56.32, 37.96, 29.80, 28.10, 26.81, 19.50; ESI-MS: m/z $[\text{M}+\text{Na}]^+$ calcd for $\text{C}_{92}\text{H}_{98}\text{Cl}_6\text{N}_2\text{O}_{18}\text{Si}$ 1783.4590, obsd 1783.4538.

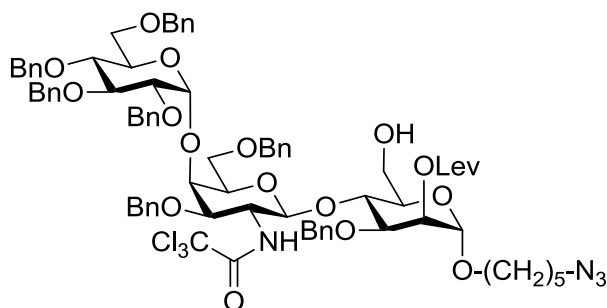
* Trisaccharide **58** was provided by Y.-H. Tsai and prepared according to Ref. [110].

1-*O*-5-Azidopentyl 2,3,4,6-tetra-*O*-benzyl- α -D-glucopyranosyl-(1 \rightarrow 4)-3,6-di-*O*-benzyl-2-deoxy-2-trichloroacetamido- β -D-galactopyranosyl-3-*O*-benzyl-6-*O*-*tert*butyldiphenylsilyl-2-*O*-levulinyl- α -D-mannopyranose (59)

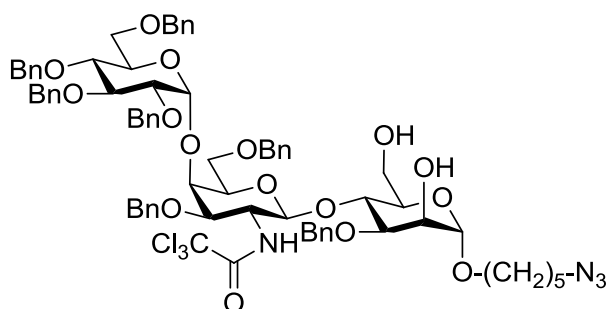


Imidate **58** (115 mg, 0.065mmol) and linker **53** (12.7 mg, 0.098mmol) were co evaporated with toluene (3x2 mL) and placed under high vacuum for 30 min. The residue was dissolved in diethylether (2 mL) and powdered molecular sieves (100 mg, 4Å) was added. The slurry was stirred for 10 min at r.t. before it was cooled down to 0 °C and TBSOTf (15.0 μ L, 0.065 mmol) was added. After 1 h at 0 °C the reaction was quenched with TEA (50 μ L), filtered and evaporated to dryness. The residue was purified by flash column chromatography to give trisaccharide **59** (100 mg, 0.058 mmol, 89%) as a white foam: R_f (SiO₂, EtOAc/Hexane 1:2) = 0.58; $[\alpha]_D^{20}$: + 58.2 (c = 1.11, THF); ATR-FTIR (cm⁻¹): 3036, 2926, 2864, 2108, 1683, 1454, 1362, 1093, 1071, 1028; ¹H NMR (400 MHz, CDCl₃) δ 7.80 – 7.71 (m, 4H), 7.47 – 7.14 (m, 39H), 7.09 – 7.05 (m, 2H), 6.46 (d, J = 7.2 Hz, 1H, NH), 5.29 – 5.25 (m, 2H, GalNAc-1, Man-2), 5.12 (d, J = 3.3 Hz, 1H, Glc-1), 4.86 – 4.67 (m, 9H), 4.50 – 4.35 (m, 3H), 4.22 – 3.99 (m, 10H), 3.97 (dd, J = 9.0, 3.4 Hz, 1H), 3.91 (dd, J = 11.1, 5.6 Hz, 1H), 3.82 – 3.69 (m, 3H), 3.66 – 3.56 (m, 2H), 3.47 (dd, J = 8.4, 5.5 Hz, 1H), 3.41 (dt, J = 9.6, 6.6 Hz, 1H), 3.38 – 3.32 (m, 2H), 3.27 (t, J = 6.9 Hz, 2H), 2.98 (d, J = 9.2 Hz, 1H), 2.69 – 2.42 (m, 4H, CH₂ of Lev), 2.07 (s, 3H, Me of Lev), 1.67 – 1.56 (m, 4H), 1.47 – 1.37 (m, 2H), 1.09 (s, 9H, *tert*Bu); ¹³C NMR (101 MHz, CHCl₃) δ ¹³C NMR (101 MHz, CDCl₃) δ 206.46 (ketone), 172.15 (ester), 163.52, 161.82, 138.78, 138.76, 138.44, 138.33, 138.21, 137.97, 137.87, 136.09, 135.71, 133.72, 133.25, 130.01, 129.84, 128.44, 128.43, 128.35, 128.32, 128.28, 128.19, 128.04, 127.98, 127.92, 127.82, 127.74, 127.71, 127.69, 127.66, 127.63, 127.59, 127.54, 127.49, 127.29, 127.14, 126.93, 100.03 (Glc-1), 98.86 (GalNAc-1), 97.19 (Man-1), 92.17 (CCl₃), 82.11, 80.02, 77.82, 77.36, 76.16, 76.00, 75.39, 75.03, 73.82, 73.63, 73.43, 73.29, 73.04, 72.56, 71.85, 71.34, 70.74, 69.35, 67.60, 67.45, 67.29, 63.86, 56.86, 51.33, 37.99, 29.78, 28.92, 28.72, 28.17, 26.75, 23.47, 19.39; ESI-MS: m/z [M+Na]⁺ calcd for C₉₅H₁₀₇Cl₃N₄O₁₈Si 1749.6314, obsd 1749.6305.

1-*O*-5-Azidopentyl 2,3,4,6-tetra-*O*-benzyl- α -D-glucopyranosyl-(1 \rightarrow 4)-3,6-di-*O*-benzyl-2-deoxy-2-trichlor-acetamido- β -D-galactopyranosyl-3-*O*-benzyl-2-*O*-levulinyl- α -D-mannopyranose (60**)**

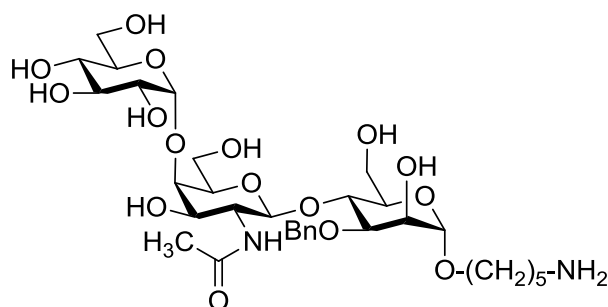


Trisaccharide **59** (100mg, 0.058 mmol) was transferred to a 15 mL Falcon™ tube and dissolved in THF (2 mL). HF·pyridine (200 μ L) was added and the solution was stirred for 18 h at r.t. before it was quenched with saturated NaHCO₃(aq), diluted with CHCl₃ (10 mL) dried over Na₂SO₄, filtered and concentrated. The residue was purified by flash column chromatography to give alcohol **60** (66 mg, 0.044 mmol, 77% yield) as a white foam: R_f (SiO₂, EtOAc/Hexane 2:1) = 0.20; $[\alpha]_D^{20}$: + 49.2 (c = 0.98, CHCl₃); ATR-FTIR (cm⁻¹): 2927, 2096, 1716, 1522, 1454, 1361, 1070, 1027; ¹H NMR (400 MHz, CHCl₃) δ 7.40 – 7.13 (m, 32H), 7.10 – 7.01 (m, 3H), 5.30 (d, J = 7.9 Hz, 1H, GalNAc-1), 5.24 (dd, J = 3.2, 1.6 Hz, 1H, Man-2), 5.08 (d, J = 3.3 Hz, 1H, Glc-1), 4.87 – 4.61 (m, 9H), 4.44 (dd, J = 16.0, 10.2 Hz, 2H), 4.36 (d, J = 10.6 Hz, 1H), 4.24 – 4.01 (m, 9H), 3.95 (dd, J = 9.0, 3.3 Hz, 1H), 3.88 – 3.78 (m, 3H), 3.76 – 3.54 (m, 6H), 3.48 – 3.33 (m, 3H), 3.27 (t, J = 6.9 Hz, 2H), 2.98 (d, J = 9.5 Hz, 1H), 2.59 – 2.40 (m, 4H, CH₂ of Lev), 2.20 (bs, 1H, OH), 2.05 (s, 3H, Me of Lev), 1.65 – 1.53 (m, 4H), 1.47 – 1.35 (m, 2H); ¹³C NMR (101 MHz, CHCl₃) δ 206.50 (ketone of Lev), 172.10, 162.03, 138.88, 138.48, 138.43, 138.40, 138.16, 137.93, 128.51, 128.48, 128.46, 128.39, 128.37, 128.32, 128.20, 128.06, 127.82, 127.74, 127.70, 127.65, 127.60, 127.51, 127.42, 127.34, 126.99, 100.15 (Glc-1), 99.00 (GalNAc-1), 97.52 (Man-1), 92.64, 82.10, 80.20, 77.84, 76.22, 76.02, 75.41, 75.07, 73.90, 73.72, 73.63, 73.33, 73.09, 71.84, 71.48, 71.20, 70.83, 69.31 (Man-2), 67.75, 67.59, 61.99, 56.56, 51.34, 37.94, 29.72, 28.95, 28.70, 28.16, 23.45; ESI-MS: m/z [M+Na]⁺ calcd for C₇₉H₈₉Cl₃N₄O₁₈ 1511.5128, obsd 1511.5059.

1-O-5-Azidopentyl 2,3,4,6-tetra-O-benzyl- α -D-glucopyranosyl-(1 \rightarrow 4)-3,6-di-O-benzyl-2-deoxy-2-trichloroacetamido- β -D-galactopyranosyl-3-O-benzyl- α -D-mannopyranose (61)

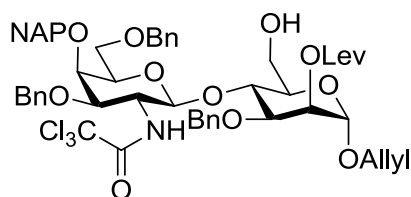
Alcohol **60** (9.6 mg, 6.45 μ mol) was dissolved in CHCl_3 (1 mL) and hydrazine monohydrate (2 drops, 64 wt%) was added. The solution was stirred for 1 h before the reaction mixture was evaporated to dryness. The residue was purified by flash column chromatography to give azide **61** (7.5 mg, 5.4 μ mol, 84% yield) as colorless oil: R_f (SiO_2 , EtOAc/Hexane 3:1) = 0.68; $[\alpha]_D^{20}$: + 46.2 ($c = 0.75$, CHCl_3); ATR-FTIR (cm^{-1}): 2927, 1095, 1716, 1497, 1454, 1060; ^1H NMR (600 MHz, CHCl_3) δ 7.40 – 7.14 (m, 28H), 7.13 – 7.09 (m, 2H), 7.07 (t, $J = 7.8$ Hz, 1H), 6.93 (t, $J = 7.5$ Hz, 2H), 6.84 (d, $J = 6.2$ Hz, 1H), 6.78 (d, $J = 7.4$ Hz, 2H), 5.29 (d, $J = 8.0$ Hz, 1H, GalNAc-1), 5.05 (dd, $J = 12.6, 6.9$ Hz, 2H), 4.97 (d, $J = 10.8$ Hz, 1H), 4.85 (d, $J = 12.0$ Hz, 1H), 4.80 – 4.71 (m, 4H), 4.49 (d, $J = 12.1$ Hz, 1H), 4.46 – 4.38 (m, 3H), 4.34 (dd, $J = 17.9, 10.7$ Hz, 2H), 4.24 – 4.14 (m, 6H), 4.05 (t, $J = 8.6$ Hz, 1H), 4.00 – 3.89 (m, 3H), 3.85 (s, 1H), 3.81 – 3.74 (m, 3H), 3.73 (dd, $J = 9.3, 2.4$ Hz, 1H), 3.68 – 3.55 (m, 4H), 3.46 (dd, $J = 10.4, 1.5$ Hz, 1H), 3.40 – 3.34 (m, 1H), 3.27 (t, $J = 6.9$ Hz, 2H), 2.96 (dd, $J = 10.4, 1.7$ Hz, 1H), 1.66 – 1.53 (m, 4H), 1.45 – 1.36 (m, 2H); ^{13}C NMR (151 MHz, CHCl_3) δ 162.11 (C=O of amide), 139.51, 138.39, 138.21, 138.14, 137.91, 137.80, 137.58, 128.99, 128.64, 128.59, 128.54, 128.50, 128.43, 128.41, 128.19, 127.98, 127.88, 127.77, 127.66, 127.57, 127.53, 126.05, 100.61, 99.31, 96.71 (GalNAc-1), 92.48 (CCl_3), 82.06, 80.82, 78.96, 77.74, 75.67, 75.43, 75.37, 74.56, 73.61, 73.47, 73.35, 73.05, 72.16, 71.93, 71.29, 69.99, 68.63, 67.42, 67.22, 66.82, 62.16, 55.53, 51.44, 29.12, 28.81, 23.60; ESI-MS: m/z $[\text{M}+\text{Na}]^+$ calcd for $\text{C}_{74}\text{H}_{83}\text{Cl}_3\text{N}_4\text{O}_{16}$ 1413.4733, obsd 1413.4678.

1-O-5-Aminopentyl α -D-glucopyranosyl-(1→4)-2-deoxy-2-acetamido- β -D-galactopyranosyl--(1→4)- α -D-mannopyranose (**43**)



Azide **61** (7.5 mg, 5.4 μ mol) was dissolved in MeOH (2 mL) before Pd/C (28.7 mg, 10 wt%) and HOAc (2 drops) were added. Hydrogen was bubbled through this slurry for 10 min before the slurry was stirred for 24 h under the same atmosphere. The slurry was filtered through a syringe filter and concentrated. The residue was purified using a G-25 size exclusion column (running buffer 5% EtOH in water) to yield trisaccharide **43** (3 mg, 4.8 μ mol, 88% yield) as white solid. $[\alpha]_D^{20}$: + 37.9 ($c = 0.33$, H₂O); ATR-FTIR (cm^{-1}): 3312, 1625, 1316, 1045; ¹H NMR (400 MHz, D₂O) δ 4.96 (d, $J = 3.8$ Hz, 1H), 4.88 (s, 1H), 4.58 (d, $J = 8.3$ Hz, 1H), 4.13 (dt, $J = 10.3, 2.8$ Hz, 1H), 4.08 – 3.96 (m, 4H), 3.94 – 3.64 (m, 13H), 3.62 – 3.55 (m, 2H), 3.53 – 3.46 (m, 1H), 3.03 (t, $J = 7.6$ Hz, 2H), 2.10 (s, 3H), 1.77 – 1.58 (m, 4H), 1.53 – 1.37 (m, 2H); ¹³C NMR (101 MHz, D₂O) δ 174.65 (amide), 102.14, 100.14, 99.24, 77.80, 76.54, 75.35, 72.63, 71.89, 71.72, 70.96, 70.10, 69.51, 69.48, 69.12, 67.43, 60.42, 60.26, 59.84, 52.36, 39.36, 27.93, 26.59, 22.44 (Me); ESI-MS: m/z $[M+H]^+$ calcd for C₂₅H₄₆N₂O₁₆ 631.2920, obsd 631.2854.

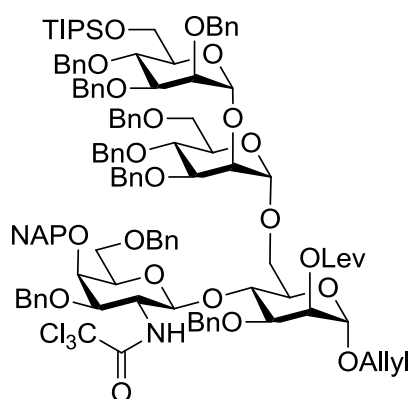
Allyl **3,6-Di-O-benzyl-2-deoxy-2-trichloroacetamido-4-O-2-naphthylmethyl- β -D-galactopyranosyl-(1→4)-3-O-benzyl-2-O-levulinyl- α -D-mannopyranoside (63)**



Disaccharide **62** (73 mg, 0.057 mmol) was dissolved in THF (0.8 mL) and HF·Py (200 μ L) was added. The solution was stirred for 18 h, quenched with sat. NaHCO₃ solution and diluted

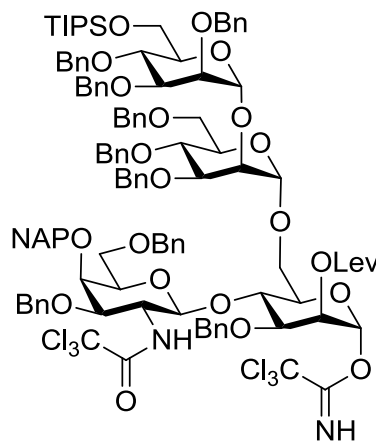
with Et₂O (20 mL). The organic layer was washed with sat. NaHCO₃ solution (3x 20 mL), dried over sodium sulfate, filtered and evaporated to dryness. The residue was purified using flash column chromatography to give alcohol **63** (51 mg, 0.049 mmol, 86% yield) as white foam: R_f (SiO₂, *n*-hexane/ethyl acetate 1:1) = 0.07; [α]²⁰_D: + 36.3 (c = 0.14, CHCl₃); ATR-FTIR (cm⁻¹): 3339, 2921, 2874, 1739, 1702, 1363, 1137, 1098, 1064; ¹H NMR (400 MHz, CDCl₃) δ 7.80 – 7.65 (m, 4H), 7.45 (ddd, J = 9.5, 7.4, 2.4 Hz, 3H), 7.36 – 7.11 (m, 15H), 6.94 (d, J = 7.2 Hz, 1H, NH), 5.83 (ddd, J = 22.4, 10.8, 5.7 Hz, 1H, CH=), 5.30 (dd, J = 2.9, 1.8 Hz, 1H, Man-2), 5.27 – 5.15 (m, 3H, GalNAc-1, CH₂=), 5.01 (d, J = 11.5 Hz, 1H), 4.80 (d, J = 1.3 Hz, 1H, Man-1), 4.74 – 4.67 (m, 2H), 4.61 (d, J = 11.2 Hz, 1H), 4.52 (d, J = 11.7 Hz, 1H), 4.46 (d, J = 11.2 Hz, 1H), 4.36 (d, J = 11.6 Hz, 1H), 4.27 – 4.18 (m, 2H), 4.16 – 4.07 (m, 2H), 4.05 – 3.89 (m, 4H), 3.84 (dd, J = 12.2, 3.4 Hz, 1H), 3.76 (dd, J = 12.1, 2.2 Hz, 1H), 3.69 – 3.57 (m, 3H), 3.48 (dd, J = 7.3, 4.0 Hz, 1H), 2.41 – 2.13 (m, 4H, CH₂ of Lev), 2.00 (s, 3H, Me of Lev); ¹³C NMR (101 MHz, CDCl₃) δ 206.47 (ketone), 172.00 (ester), 162.18 (amide), 138.16, 137.74, 137.65, 136.04, 133.38, 133.24, 133.05, 128.57, 128.52, 128.48, 128.11, 128.03, 127.94, 127.76, 127.46, 126.77, 126.73, 126.43, 126.14, 125.97, 118.06, 98.48 (GalNAc-1), 96.74 (Man-1), 92.68 (CCl₃), 76.45, 74.90, 73.58, 73.45, 72.28, 72.02, 71.69, 71.64, 70.87, 68.66, 68.40, 68.31, 61.74, 56.20, 37.77, 29.72, 27.87; ESI-MS: *m/z* [M+Na]⁺ calcd for C₅₄H₅₈Cl₃NO₁₃ 1056.2866, obsd 1056.2962.

Allyl 2,3,4-tri-*O*-benzyl-6-*O*-triisopropylsilyl- α -D-mannopyranosyl-(1 \rightarrow 2)-3,4,6-tri-*O*-benzyl- α -D-mannopyranosyl-(1 \rightarrow 6)-3-*O*-benzyl-4-*O*-(3,6-di-*O*-benzyl-4-*O*-2-naphthylmethyl-2-deoxy-2-trichloroacetamido- β -D-galactopyranosyl)-2-*O*-levulinyl- α -D-mannopyranoside (64)



Disaccharide **63** (49 mg, 0.047 mmol) and imidate **8** (73 mg, 0.062 mmol) were coevaporated with toluene (3x2 mL) and placed under high vacuum for 30 min. The residue was dissolved in diethylether (2 mL) and powdered molecular sieves (150 mg, 4Å) was added. The slurry was stirred for 10 min at r.t. before it was cooled down to 0 °C and TBSOTf (1.6 µL, 7.1 µmol) was added. The reaction mixture was stirred at 0 °C for 1 h before it was quenched with TEA (10 µL), diluted with CHCl₃, filtered and concentrated. The residue was purified by flash column chromatography to give tetrasaccharide **64** (84 mg, 0.041 mmol, 86% yield) as a white foam: R_f (SiO₂, *n*-hexane/ethyl acetate 3:1) = 0.32; [α]²⁰_D: + 19.1 (c = 0.40, CHCl₃); ATR-FTIR (cm⁻¹): 3063, 3031, 2924, 2865, 1719, 1363, 1072, 1028; ¹H NMR (400 MHz, CDCl₃) δ 7.79 – 7.74 (m, 1H), 7.71 – 7.57 (m, 3H), 7.49 – 7.07 (m, 48H), 5.81 (ddd, J = 22.1, 10.9, 6.3 Hz, 1H, CH=), 5.36 – 5.28 (m, 2H, ManI-2), 5.22 (dd, J = 17.3, 1.1 Hz, 1H, CH₂=), 5.18 (d, J = 8.3 Hz, 1H, GalNAc-1), 5.13 (d, J = 10.4 Hz, 1H, CH₂=), 4.91 (d, J = 11.1 Hz, 2H), 4.81 (d, J = 10.8 Hz, 2H), 4.75 (s, 1H), 4.71 – 4.54 (m, 7H), 4.52 – 4.27 (m, 9H), 4.23 – 3.49 (m, 25H), 3.39 (dd, J = 8.6, 5.0 Hz, 1H), 2.53 – 2.28 (m, 4H, CH₂ of Lev), 2.02 (s, 3H, Me of Lev), 1.13 – 1.00 (m, 21H, TIPS); ¹³C NMR (101 MHz, CDCl₃) δ 206.41 (ketone), 172.05 (ester), 162.23 (amide), 139.05, 138.85, 138.50, 138.26, 138.13, 137.88, 137.73, 136.08, 133.29, 133.22, 133.03, 128.55, 128.47, 128.43, 128.39, 128.37, 128.30, 128.19, 128.15, 128.07, 128.06, 127.98, 127.89, 127.82, 127.75, 127.73, 127.59, 127.46, 127.38, 127.19, 126.76, 126.43, 126.11, 125.93, 118.49, 98.61, 98.48, 98.26, 96.29, 92.68 (CCl₃), 80.89, 79.63, 77.40, 76.38, 75.28, 75.20, 74.91, 74.86, 74.68, 74.50, 73.84, 73.58, 73.43, 73.36, 73.18, 72.42, 72.26, 72.17, 72.13, 72.06, 71.88, 71.65, 71.29, 69.94, 69.65, 68.76, 68.39, 67.97, 66.39, 63.02, 56.41, 37.90 (CH₂ of Lev), 29.81 (Me of Lev), 28.03 (CH₂ of Lev), 18.21 (TIPS), 18.16 (TIPS), 12.16 (TIPS); ESI-MS: *m/z* [M+Na]⁺ 2078.8090 calcd for C₁₁₇H₁₃₄Cl₃NO₂₃Si, obsd 2078.8095.

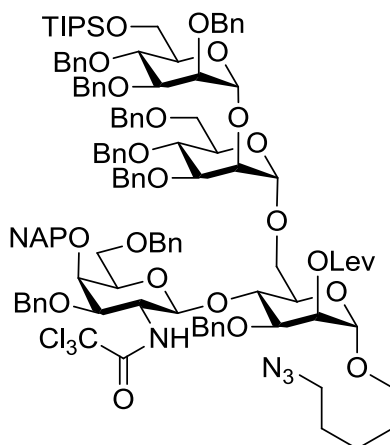
2,3,4-Tri-*O*-benzyl-6-*O*-triisopropylsilyl- α -D-mannopyranosyl-(1 \rightarrow 2)-3,4,6-tri-*O*-benzyl- α -D-mannopyranosyl-(1 \rightarrow 6)-3-*O*-benzyl-4-*O*-(3,6-di-*O*-benzyl-4-*O*-2-naphthylmethyl-2-deoxy-2-trichloroacetamido- β -D-galactopyranosyl)-2-*O*-levulinyl- α -D-mannopyranoside trichloroacetimidate (65**)**



A solution of $[\text{IrCOD}(\text{PPh}_2\text{Me})_2]\text{PF}_6$ (6 mg, 7.1 μmol) in THF (3 mL) was stirred under hydrogen at 20 $^\circ\text{C}$ until the colour turned from red to colourless to pale yellow. The hydrogen atmosphere was ex-changed with nitrogen. This solution was then added into a flask with tetrasaccharide **64** (82 mg, 0.040 mmol). After stirring for 12 h, the solvent was removed [analytical data for enol ether: $^1\text{H NMR}$ (400 MHz, CDCl_3) δ 6.09 (dd, $J = 12.3, 1.5$ Hz, 1H, -O-CH=); ESI-MS: m/z $[\text{M}+\text{Na}]^+$ 2078.8090 calcd for $\text{C}_{117}\text{H}_{134}\text{Cl}_3\text{NO}_{23}\text{Si}$, obsd 2078.8121) and the residue was dissolved in a mixture of acetone (2 mL) and water (0.2 mL). Mercury(II) chloride (65 mg, 0.239 mmol) and mercury(II) oxide (0.9 mg, 0.004 mmol) were added. After 20 min, the reaction mixture was diluted with chloroform (20 mL) and washed with saturated $\text{NaHCO}_3(\text{aq})$, dried over Na_2SO_4 , filtered and concentrated to give the crude lactol **65a**: R_f (SiO_2 , EtOAc/Hexane 1:3 = 0.40). The lactol was dissolved in DCM (1.5 mL) and 2,2,2-trichloroacetonitrile (0.12 mL, 1.196 mmol) and cooled down to 0 $^\circ\text{C}$ before DBU (1 drop) was added. After 2.5 h at 0 $^\circ\text{C}$, the solvent was removed to give a brown oil that was purified by flash column chromatography to yield imidate **65** (54 mg, 0.025 mmol, 63% yield) as yellow foam: R_f (SiO_2 , EtOAc/Hexane 1:2) = 0.63; $[\alpha]_D^{20}$: + 20.7 ($c = 0.25$, THF); ATR-FTIR (cm^{-1}): 2927, 2865, 1748, 1719, 1364, 1065, 1028; $^1\text{H NMR}$ (400 MHz, CDCl_3) δ 8.68 (s, 1H, NH of imidate), 7.79 – 7.74 (m, 1H), 7.69 (d, $J = 8.1$ Hz, 2H), 7.61 (s, 1H), 7.46 – 7.37 (m, 3H), 7.34 – 7.10 (m, 43H), 6.16 (d, $J = 1.9$ Hz, 1H, ManI-1), 5.43 (t, $J = 2.5$, 1H, ManI-2), 5.27 (s, 1H), 5.15 (d, $J = 8.2$ Hz, 1H, GalNAc-1), 4.91 (dd, $J = 11.3, 5.0$ Hz, 2H), 4.80 – 4.75 (m, 2H), 4.72 – 4.54 (m, 7H), 4.51 – 4.42 (m, 4H), 4.42 – 4.39 (m, 1H), 4.38 – 4.31 (m, 4H), 4.21 (d, $J = 11.6$ Hz, 1H), 4.15 – 3.92 (m, 8H), 3.90 – 3.76 (m, 6H), 3.74 – 3.53 (m, 7H), 3.49

– 3.38 (m, 2H), 2.53 – 2.31 (m, 4H, CH₂ of Lev), 2.03 (s, 3H, Me of Lev), 1.13 – 1.03 (m, 21H, TIPS); ¹³C NMR (101 MHz, CDCl₃) δ 206.09 (ketone), 171.79 (ester), 162.20 (amide), 159.37 (imine), 139.10, 138.91, 138.64, 138.56, 138.38, 138.27, 137.88, 137.67, 136.05, 133.23, 133.05, 128.56, 128.50, 128.45, 128.42, 128.40, 128.34, 128.27, 128.11, 128.09, 128.05, 127.99, 127.93, 127.88, 127.86, 127.78, 127.75, 127.73, 127.62, 127.56, 127.42, 127.32, 126.76, 126.38, 126.14, 125.96, 98.76 (GalNAc-1), 98.38, 98.29, 94.74, 92.64 (CCl₃), 90.86 (CCl₃), 81.07, 79.63, 77.36, 77.31, 75.75, 75.31, 75.20, 74.94, 74.72, 74.52, 73.83, 73.62, 73.26, 72.95, 72.48, 72.24, 72.19, 72.02, 71.88, 71.74, 71.62, 69.69, 68.39, 67.90, 65.90, 63.04, 56.34, 37.85, 29.83, 29.80, 27.94, 18.23 (TIPS), 18.18 (TIPS), 12.16 (TIPS); ESI-MS: *m/z* [M+Na]⁺ calcd for C₁₁₆H₁₃₀Cl₆N₂O₂₃Si 2183.6854, obsd 2183.6850.

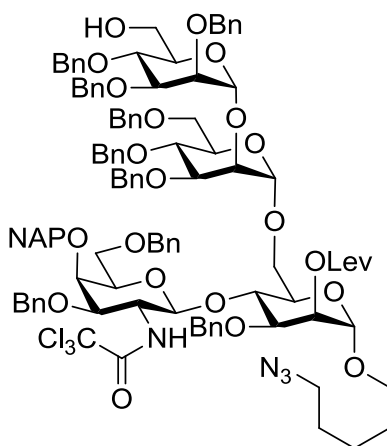
1-*O*-5-Azidopentyl 2,3,4-tri-*O*-benzyl-6-*O*-triisopropylsilyl- α -D-mannopyranosyl-(1 \rightarrow 2)-3,4,6-tri-*O*-benzyl- α -D-mannopyranosyl-(1 \rightarrow 6)-3-*O*-benzyl-4-*O*-(3,6-di-*O*-benzyl-4-*O*-2-naphthylmethyl-2-deoxy-2-trichloroacetamido- β -D-galactopyranosyl)-2-*O*-levulinyl- α -D-mannopyranoside (66)



Trichloroacetimidate **65** (50 mg, 0.023 mmol) and linker **53** (6 mg, 0.046 mmol) were coevaporated with toluene (3x 2 mL) and the residue was placed under HV for 30 min. The residue was dissolved in toluene (1 mL) and molecular sieves (4Å powdered, 100 mg) was added. The slurry was stirred 10 min at r.t. before it was cooled down to 0 °C and TBSOTf (1.1 μL, 4.6 μmol) was added. The reaction mixture was stirred at 0 °C for 1 h before it was quenched with TEA (50 μL), filtered and evaporated to dryness. The residue was purified using flash column chromatography to give azide **66** (43 mg, 0.020 mmol, 87% yield) as yellow amorphous solid: R_f (SiO₂, *n*-hexane/ethyl acetate 3:1) = 0.49 (same R_f value as the

imidate); $[\alpha]_D^{20}$: + 15.1 ($c = 0.32$, THF); ATR-FTIR (cm^{-1}): 3063, 3031, 2925, 2864, 2096, 1718, 1363, 1058, 1027; ^1H NMR (400 MHz, CDCl_3) δ 7.79 – 7.73 (m, 1H), 7.71 – 7.63 (m, 2H), 7.59 (s, 1H), 7.46 – 7.36 (m, 3H), 7.34 – 7.07 (m, 45H), 5.27 (s, 2H, ManI-2), 5.14 (d, $J = 8.2$ Hz, 1H, GalNAc-1), 4.90 (dd, $J = 11.3, 2.7$ Hz, 2H), 4.84 – 4.77 (m, 2H), 4.69 – 4.55 (m, 7H), 4.51 – 4.29 (m, 9H), 4.21 – 4.13 (m, 2H), 4.11 – 3.50 (m, 23H), 3.39 (dd, $J = 8.1, 4.4$ Hz, 1H), 3.31 (dt, $J = 9.6, 6.2$ Hz, 1H), 3.18 (t, $J = 6.9$ Hz, 2H, $\text{CH}_2\text{-N}_3$), 2.51 – 2.26 (m, 4H, CH_2 of Lev), 2.00 (s, 3H, Me of Lev), 1.57 – 1.43 (m, 4H), 1.41 – 1.28 (m, 2H), 1.11 – 1.01 (m, 21H, TIPS); ^{13}C NMR (101 MHz, CDCl_3) δ 206.38 (ketone), 172.11 (ester), 162.20 (amide), 139.03, 138.85, 138.56, 138.52, 138.36, 138.30, 138.17, 137.93, 137.73, 136.07, 133.23, 133.05, 128.58, 128.48, 128.45, 128.42, 128.35, 128.31, 128.23, 128.15, 128.12, 128.06, 127.99, 127.88, 127.85, 127.80, 127.74, 127.70, 127.60, 127.47, 127.37, 127.21, 126.80, 126.44, 126.13, 125.96, 98.74 (GalNAc-1), 98.69, 98.38, 97.30, 92.72 (CCl_3), 81.01, 79.65, 76.34, 75.32, 75.24, 74.96, 74.90, 74.70, 74.57, 73.90, 73.61, 73.53, 73.41, 73.13, 72.40, 72.25, 72.13, 71.88, 71.69, 71.40, 69.99, 69.70, 68.94, 68.46, 67.35, 66.55, 63.10, 56.34, 51.33, 37.90, 29.84, 28.92, 28.73, 28.05, 23.55, 18.23 (TIPS), 18.18 (TIPS), 12.17 (TIPS); ESI-MS: m/z $[\text{M}+\text{Na}]^+$ calcd for $\text{C}_{119}\text{H}_{139}\text{Cl}_3\text{N}_4\text{O}_{23}\text{Si}$ 2149.8574, obsd 2149.8583.

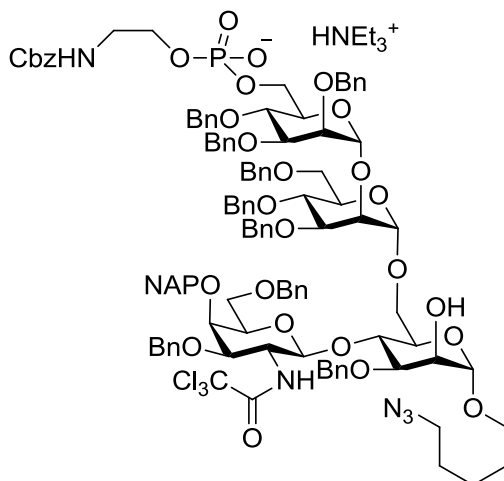
1-O-5-Azidopentyl 2,3,4-tri-O-benzyl- α -D-mannopyranosyl-(1 \rightarrow 2)-3,4,6-tri-O-benzyl- α -D-mannopyranosyl-(1 \rightarrow 6)-3-O-benzyl-4-O-(3,6-di-O-benzyl-4-O-2-naphthylmethyl-2-deoxy-2-trichloroacetamido- β -D-galactopyranosyl)-2-O-levulinyl- α -D-mannopyranoside (67)



In a 15 mL Falcon tube azide **66** (42 mg, 0.020 mmol) was dissolved in THF (0.4 mL) and HF \cdot Py (100 μL) was added. The solution was stirred for 3 h before it was quenched with

saturated $\text{NaHCO}_3(\text{aq})$, diluted with EtOAc (20 mL), washed with saturated $\text{NaHCO}_3(\text{aq})$ (3x 20 mL), dried over Na_2SO_4 , filtered and evaporated to dryness. The residue was purified by flash column chromatography to give alcohol **67** (54 mg, 0.025 mmol, 63% yield) as white foam: R_f (SiO_2 , EtOAc/Hexane 1:2) = 0.25; $[\alpha]_D^{20}$: + 18.7 ($c = 1.60$, CHCl_3); ATR-FTIR (cm^{-1}): 2923, 2869, 2096, 1717, 1363, 1065, 1027; ^1H NMR (400 MHz, CDCl_3) δ 7.82 – 7.77 (m, 1H), 7.74 – 7.68 (m, 2H), 7.64 (s, 1H), 7.54 (d, $J = 7.2$ Hz, 1H), 7.48 – 7.41 (m, 3H), 7.37 – 7.14 (m, 42H), 7.14 – 7.08 (m, 2H), 5.29 (dd, $J = 3.3, 1.9$ Hz, 1H, ManI-2), 5.26 (d, $J = 8.3$ Hz, 1H, GalNAc-1), 5.09 (d, $J = 1.6$ Hz, 1H), 5.02 (d, $J = 1.3$ Hz, 1H), 4.98 – 4.89 (m, 2H, 2x CH-Ar), 4.85 (d, $J = 10.7$ Hz, 1H, CH-Ar), 4.74 – 4.40 (m, 16H), 4.27 (d, $J = 11.7$ Hz, 1H), 4.20 – 4.12 (m, 2H), 4.03 (t, $J = 2.1$ Hz, 1H), 3.98 – 3.47 (m, 22H), 3.41 – 3.30 (m, 2H), 3.24 (t, $J = 6.9$ Hz, 2H, $\text{CH}_2\text{-N}_3$), 2.61 – 2.35 (m, 4H, CH_2 of Lev), 2.06 (s, 3H, Me of Lev), 1.65 – 1.48 (m, 4H), 1.47 – 1.33 (m, 2H); ^{13}C NMR (101 MHz, CDCl_3) δ 206.47 (ketone), 172.11 (ester), 162.40 (amide), 138.67, 138.62, 138.58, 138.53, 138.46, 138.43, 137.95, 137.78, 136.08, 133.27, 133.08, 128.60, 128.50, 128.46, 128.42, 128.38, 128.37, 128.32, 128.16, 128.08, 128.02, 128.00, 127.98, 127.92, 127.85, 127.80, 127.76, 127.72, 127.65, 127.57, 127.51, 127.30, 126.95, 126.86, 126.48, 126.12, 125.94, 99.97, 99.08, 99.01, 97.34 (ManI-1), 92.75 (CCl_3), 80.14, 79.81, 77.36, 76.65, 75.43, 75.33, 75.28, 75.11, 75.02, 74.93, 74.79, 73.95, 73.53, 73.44, 73.39, 72.84, 72.60, 72.46, 72.40, 72.24, 72.12, 72.00, 71.30, 70.48, 69.43, 68.76, 68.38, 67.72, 67.54, 62.87, 56.82, 51.38, 37.97, 29.83, 28.97, 28.75, 28.12, 23.54; ESI-MS: m/z $[\text{M}+\text{Na}]^+$ calcd for $\text{C}_{110}\text{H}_{119}\text{Cl}_3\text{N}_4\text{O}_{23}$ 1993.7236, obsd 1993.7257.

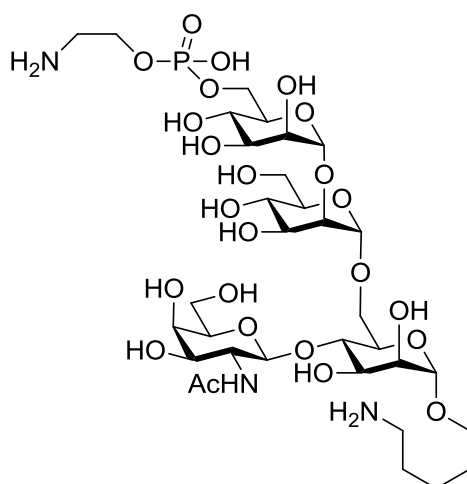
Triethylammonium 1-*O*-5-azidopentyl 2,3,4-tri-*O*-benzyl-6-*O*-(2-(*N*-benzyloxycarbonyl)aminoethyl-phosphonato)- α -D-mannopyranosyl-(1 \rightarrow 2)-3,4,6-tri-*O*-benzyl- α -D-mannopyranosyl-(1 \rightarrow 6)-3-*O*-benzyl-4-*O*-(3,6-di-*O*-benzyl-4-*O*-2-naphthylmethyl-2-deoxy-2-trichloroacetamido- β -D-galactopyranosyl)- α -D-mannopyranoside (69)



Alcohol **67** (14 mg, 7.1 μ mol) and H-phosphonate **10** (12.8 mg, 0.036 mmol) were co evaporated with dry pyridine (3x2 mL) and placed under high vacuum for 30 min. The residue was dissolved in pyridine (1 mL) and PivCl (4.4 μ L, 0.036 mmol) was added. The solution was stirred for 2 h at r.t. before water (1 drop) and iodine (10.8 mg, 0.043 mmol) were added. The solution was stirred for 1 h before hydrazine monohydrate (3 drops, 64 wt%) was added. The reaction mixture was stirred for 12 h before it was concentrated and purified by flash column chromatography (TEA deactivated SiO₂, from 0 to 5% of MeOH in CHCl₃) to give phosphate **69** (15 mg, 6.7 μ mol, 95% yield) as yellow amorphous solid: R_f (SiO₂, 5% of MeOH in CHCl₃) = 0.16; $[\alpha]_D^{20}$: + 22.1 (c = 1.5, CHCl₃); ATR-FTIR (cm⁻¹): 2963, 2928, 2865, 2096, 1711, 1363, 1259, 1052, 1026; ¹H NMR (400 MHz, CDCl₃) δ 7.79 – 7.74 (m, 1H), 7.73 – 7.63 (m, 3H), 7.46 – 7.39 (m, 3H), 7.38 – 7.03 (m, 45H), 5.83 (s, 1H, NH), 5.18 (s, 1H), 5.12 – 4.78 (m, 7H), 4.75 (s, 1H), 4.71 – 4.38 (m, 14H), 4.34 – 4.24 (m, 2H), 4.19 – 4.09 (m, 2H), 4.08 – 3.51 (m, 23H), 3.46 – 3.34 (m, 2H), 3.34 – 3.10 (m, 6H), 2.63 (dd, J = 14.0, 6.8 Hz, 6H, CH₂ of TEA), 1.52 – 1.39 (m, 4H), 1.35 – 1.28 (m, 2H), 1.05 (t, J = 7.2 Hz, 9H, CH₃ of TEA); ¹³C NMR (101 MHz, CDCl₃) δ 163.09 (amide), 156.51 (Cbz), 139.13, 139.02, 138.84, 138.72, 138.66, 138.58, 138.54, 138.47, 138.34, 136.94, 136.54, 133.30, 133.02, 128.61, 128.55, 128.42, 128.41, 128.33, 128.14, 128.07, 128.03, 127.96, 127.88, 127.84, 127.78, 127.73, 127.66, 127.64, 127.59, 127.53, 127.42, 127.27, 126.64, 126.50, 125.98, 125.77, 101.35, 100.70, 98.54, 97.42, 93.21 (CCl₃), 80.16, 79.65, 79.56, 78.16, 77.36,

76.42, 75.72, 75.53, 75.04, 74.86, 74.67, 74.57, 73.75, 73.57, 73.48, 73.04, 72.94, 72.86, 72.39, 72.21, 71.87, 71.74, 71.67, 71.06, 70.44, 70.15, 69.97, 69.24, 66.77, 66.56, 66.23, 65.53, 65.48, 64.06, 55.14, 51.36, 45.89 (CH₂ of TEA), 29.83, 29.78, 28.84, 28.78, 23.61, 10.02 (CH₃ of TEA); ³¹P NMR (162 MHz, CDCl₃) δ -1.96; ESI-MS: *m/z* [M-H]⁻ calcd for C₁₁₅H₁₂₄Cl₃N₅O₂₆P 2127.7376, obsd 2127.7903.

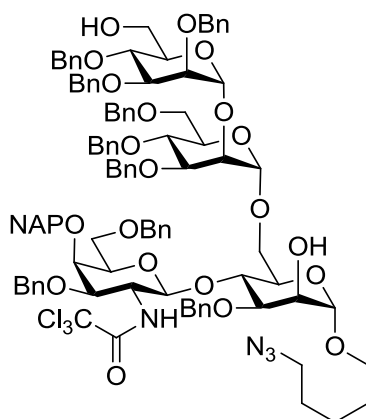
1-*O*-5-aminopentyl 6-*O*-(aminoethyl-phosphonato)- α -D-mannopyranosyl-(1 \rightarrow 2)- α -D-mannopyranosyl-(1 \rightarrow 6)-4-*O*-(2-deoxy-2-acetamido- β -D-galactopyranosyl)- α -D-mannopyranoside (44)



Phosphate **69** (15 mg, 6.7 μ mol) was dissolved CHCl₃ (2 mL) and washed Amberlite IR120 H resin (200 mg) was added. The slurry was stirred for 30 min before it was filtered and concentrated. The residue was dissolved in MeOH (2 mL) and HOAc (2 drops). Pd/C (35.8 mg, 0.034 mmol, 10 wt%) was added and hydrogen was bubbled through the slurry for 10 min. Afterwards the slurry was stirred for 18 h under hydrogen atmosphere before it was filtered through a syringe filter and evaporated to dryness. The residue was submitted to SEC chromatography (Sephadex-G25, 5% EtOH in water) to yield phosphate **44** (5.6 mg, 6.1 μ mol, 91%) as white solid: ¹H NMR (400 MHz, D₂O) δ 5.18 (s, 1H), 5.03 (s, 1H), 4.87 (s, 1H), 4.50 (d, *J* = 8.4 Hz, 1H, GalNAc-1), 4.20 – 4.12 (m, 3H, P-O-CH₂-CH₂-NH₂), 4.10 (dd, *J* = 2.6, 1.9 Hz, 1H), 4.03 – 3.67 (m, 23H), 3.63 – 3.55 (m, 1H), 3.32 (t, 2H, P-O-CH₂-CH₂-NH₂), 3.06 – 3.00 (m, 2H, O-CH₂-CH₂-CH₂-CH₂-CH₂-NH₂), 2.12 (s, 3H, Me of NHAc), 1.75 – 1.64 (m, 4H, O-CH₂-CH₂-CH₂-CH₂-CH₂-NH₂), 1.54 – 1.39 (m, 2H, O-CH₂-CH₂-CH₂-CH₂-NH₂); ¹³C NMR (101 MHz, D₂O) δ 174.56 (amide), 102.44 (ManI-1), 101.74 (GalNAc-

1), 99.34, 98.14, 79.14, 76.95, 75.31, 73.02, 71.92, 71.84, 70.40, 70.14, 70.06, 69.79, 69.35, 69.20, 67.60, 66.82, 66.13, 66.04, 64.59, 64.53, 61.79 (d, $J = 5.1$ Hz, P-O-CH₂), 61.01, 52.46, 40.03, 39.95, 39.31, 27.96 (O-CH₂-CH₂-CH₂-CH₂-CH₂-NH₂), 26.46 (O-CH₂-CH₂-CH₂-CH₂-CH₂-NH₂), 22.50 (O-CH₂-CH₂-CH₂-CH₂-CH₂-NH₂), 22.29 (Me of NHAc); ³¹P NMR (162 MHz, D₂O) δ 0.31; ESI-MS: m/z [M+H]⁺ calcd for C₃₃H₆₂N₃O₂₄P 916.3534, obsd 916.3544.

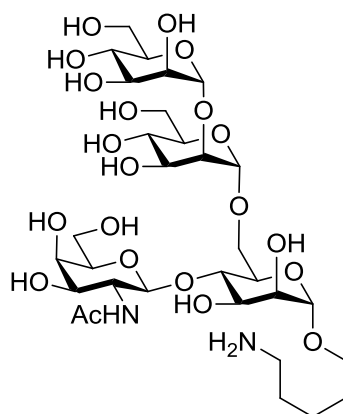
1-*O*-5-Azidopentyl 2,3,4-tri-*O*-benzyl- α -D-mannopyranosyl-(1 \rightarrow 2)-3,4,6-tri-*O*-benzyl- α -D-mannopyranosyl-(1 \rightarrow 6)-3-*O*-benzyl-4-*O*-(3,6-di-*O*-benzyl-4-*O*-2-naphthylmethyl-2-deoxy-2-trichloroacetamido- β -D-galactopyranosyl)- α -D-mannopyranoside (68)



Alcohol **67** (16 mg, 8.1 μ mol) was dissolved in MeCN (0.5 mL) and hydrazine monohydrate (4 μ L, 0.081 mmol, 64wt%) was added. The solution was stirred for 6 h, diluted with EtOAc (20 mL), washed with 1 M HCl (3x 20 mL) and saturated NaHCO₃(aq) (1x 20 mL), dried over Na₂SO₄, filtered and evaporated to dryness to yield diol **68** (14 mg, 7.5 μ mol, 92%) as yellow syrup: R_f (SiO₂, *n*-hexane/EtOAc 1:1) = 0.67; $[\alpha]_D^{20}$: + 23.9 ($c = 1.4$, CHCl₃); ATR-FTIR (cm⁻¹): 3030, 2924, 2858, 2096, 1720, 1364, 1056, 1028; ¹H NMR (400 MHz, CDCl₃) δ 7.81 – 7.76 (m, 1H), 7.69 (dd, $J = 12.1, 6.5$ Hz, 2H), 7.62 (s, 1H), 7.47 – 7.38 (m, 4H), 7.36 – 7.14 (m, 42H), 7.11 – 7.06 (m, 2H), 5.10 – 5.04 (m, 3H, GalNAc-1, 2xMan-1), 4.97 (d, $J = 11.6$ Hz, 1H), 4.91 – 4.81 (m, 3H), 4.78 (d, $J = 1.5$ Hz, 1H, Man-1), 4.71 – 4.46 (m, 12H), 4.44 (d, $J = 2.7$ Hz, 2H), 4.38 (d, $J = 11.4$ Hz, 1H), 4.29 (d, $J = 11.6$ Hz, 1H), 4.16 (d, $J = 11.6$ Hz, 1H), 4.08 – 3.97 (m, 4H), 3.95 (dd, $J = 3.2, 1.8$ Hz, 1H), 3.92 – 3.57 (m, 19H), 3.45 (dd, $J = 8.1, 4.7$ Hz, 1H), 3.36 (dt, $J = 9.9, 6.3$ Hz, 1H), 3.23 (t, $J = 6.9$ Hz, 2H), 1.62 – 1.50 (m, 4H), 1.44 – 1.33 (m, 2H); ¹³C NMR (101 MHz, CDCl₃) δ 162.23 (amide), 138.69, 138.66, 138.61, 138.57, 138.55, 138.43, 137.95, 137.75, 136.03, 133.28, 133.11, 128.60, 128.57, 128.49, 128.43, 128.41, 128.38, 128.35, 128.23, 128.14, 128.05, 128.03, 128.00, 127.94, 127.88,

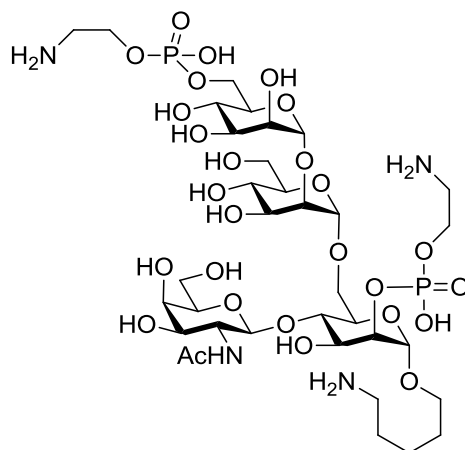
127.85, 127.82, 127.76, 127.72, 127.65, 127.63, 127.56, 127.53, 127.49, 126.90, 126.46, 126.14, 125.97, 99.69, 99.39, 99.30, 98.82, 92.80 (CCl₃), 80.29, 79.75, 78.27, 77.80, 77.36, 75.54, 75.32, 75.24, 75.11, 75.02, 74.78, 74.53, 73.71, 73.66, 73.50, 73.38, 72.92, 72.54, 72.50, 72.48, 72.34, 72.30, 72.19, 72.06, 70.67, 69.57, 68.77, 67.44, 66.69, 62.97, 56.40, 51.42, 29.03, 28.79, 23.59, 22.84; ESI-MS: m/z [M+Na]⁺ calcd for C₁₀₅H₁₁₃Cl₃N₄O₂₁ 1805.6841, obsd 1805.6866.

α -D-mannopyranosyl-(1→2)- α -D-mannopyranosyl-(1→6)-4-O-(2-deoxy-2-acetamido- β -D-galactopyranosyl)- α -D-mannopyranoside (45)



Diol **68** was dissolved in MeOH (1 mL) and HOAc (2 drops). Pd/C (17 mg, 0.016 mmol, 10 wt%) was added and hydrogen was bubbled through the slurry for 10 min. Afterwards the slurry was stirred for 18 h under hydrogen atmosphere before it was filtered through a syringe filter and evaporated to dryness. The residue was submitted to SEC chromatography (Sephadex-G25, 5% EtOH in water) to yield tetrasaccharide **45** (1.9 mg, 2.4 μ mol, 75%) as white solid: ¹H NMR (400 MHz, D₂O) δ 5.19 (d, J = 1.6 Hz, 1H), 5.04 (d, J = 1.6 Hz, 1H), 4.86 (d, J = 1.6 Hz, 1H), 4.50 (d, J = 8.4 Hz, 1H, GalNAc-1), 4.09 (dd, J = 3.3, 1.7 Hz, 1H), 4.05 – 3.99 (m, 2H), 3.99 – 3.63 (m, 22H), 3.61 – 3.54 (m, 1H), 3.03 (t, 2H, CH₂-NH₂), 2.10 (s, 3H, Me of NHAc), 1.74 – 1.64 (m, 4H), 1.54 – 1.40 (m, 2H); ¹³C NMR (101 MHz, D₂O) δ 174.59 (amide), 102.19, 101.63 (GalNAc-1), 99.35, 98.48, 78.54, 76.64, 75.34, 73.17, 73.14, 70.48, 70.23, 70.07, 69.85, 69.35, 69.26, 67.57, 66.85, 66.67, 65.91, 61.07, 61.00, 60.96, 60.90, 52.51, 39.29 (CH₂-NH₂), 27.93, 26.48 (2x CH₂ of Linker), 22.44 (Me of NHAc), 22.28 (CH₂ of Linker); ESI-MS: m/z [M+H]⁺ calcd for C₃₁H₅₆N₂O₂₁ 793.3448, obsd 793.3437.

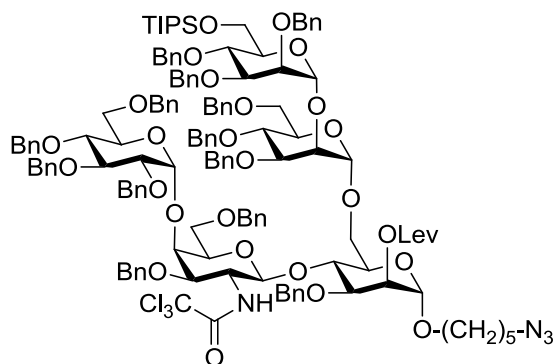
1-O-5-aminopentyl 6-O-(aminoethyl-phosphonato)- α -D-mannopyranosyl-(1 \rightarrow 2)- α -D-mannopyranosyl-(1 \rightarrow 6)-4-O-(2-deoxy-2-acetamido- β -D-galactopyranosyl)-2-O-(aminoethyl-phosphonato)- α -D-mannopyranoside (49**)**



Diol **68** (8 mg, 4.3 μ mol) and H-phosphonate **10** (15.4 mg, 0.043 mmol) were coevaporated with pyridine (3x 2 mL) and placed under HV for 30 min. The residue was dissolved in pyridine (1 mL) and PivCl (5.3 μ L, 0.043 mmol) was added. The reaction mixture was stirred for 1 h before water (1 drop) and iodine (11.9 mg, 0.047 mmol) was added. The reaction mixture was stirred for 12 h, before hydrazine monohydrate (3 drops, 64wt%) was added to quench excess of iodine. The solution was evaporated to dryness and coevaporated with toluene (4x 2 mL). The residue was purified by flash column chromatography (TEA deactivated SiO₂, from 0 to 10% of MeOH in CHCl₃). The fractions, which contained the desired product were pooled and evaporated to dryness. The residue was dissolved in CHCl₃ (2 mL) and Amberlite IR120 H resin (100 mg) was added. The slurry was stirred for 30 min before it was filtered and concentrated to give protected bisphosphate **49a** (8 mg, 6.7 μ mol, 78% yield) as yellow amorphous solid [selected analytical data: R_f (SiO₂, 10% MeOH in CHCl₃) = 0.58; ATR-FTIR (cm⁻¹): 2924, 2855, 2095, 1717, 1363, 1259, 1055, 1027; ¹H NMR (400 MHz, CDCl₃) δ 7.79 – 7.74 (m, 1H), 5.27 (s, 1H), 3.25 (t, J = 6.9 Hz, 2H); ³¹P NMR (162 MHz, CDCl₃) δ -0.17, -0.55; ESI-MS: m/z [M-2H]²⁻ 1191.8878 calcd for C₁₂₅H₁₃₅Cl₃N₆O₃₁P₂, obsd 1191.8860]. Protected bisphosphate **49a** (8 mg, 6.7 μ mol) was dissolved in MeOH (1 mL) and HOAc (2 drops). Pd/C (17.8 mg, 0.017 mmol, 10 wt%) was added and hydrogen was bubbled through the slurry for 10 min. Afterwards the slurry was stirred for 18 h under hydrogen atmosphere before it was filtered through a syringe filter and evaporated to dryness. The residue was submitted to SEC chromatography (Sephadex-G25, 5% EtOH in water) to yield tetrasaccharide **49** (1.8 mg, 2.4 μ mol, 52%) as white solid: ¹H

NMR (600 MHz, D₂O) δ 5.20 (s, 1H), 5.05 (s, 2H), 4.53 (d, J = 8.4 Hz, 1H, GalNAc-1), 4.42 – 4.38 (m, 1H), 4.25 – 4.12 (m, 6H, 2x P-O-CH₂-CH₂-NH₂), 4.12 – 4.09 (m, 1H), 4.05 – 4.00 (m, 2H), 4.00 – 3.70 (m, 20H), 3.66 – 3.61 (m, 1H), 3.32 (dt, J = 16.0, 4.5 Hz, 4H, 2x P-O-CH₂-CH₂-NH₂), 3.07 – 3.02 (m, 2H, CH₂-NH₂ of linker), 2.13 (s, 3H, Me of NHAc), 1.76 – 1.67 (m, 4H, linker), 1.54 – 1.44 (m, 2H, linker); ¹³C NMR (151 MHz, D₂O) δ 177.29 (amide), 105.10, 104.37 (GalNAc-1), 101.34, 100.60, 81.93, 79.22, 78.02, 76.61, 76.57, 75.91, 74.63, 74.58, 73.11, 73.04, 72.85, 72.68, 72.50, 71.13, 71.10, 70.34, 70.24, 69.51, 69.32, 68.89, 67.35, 64.59 (d, J = 5.1 Hz, P-O-CH₂-CH₂-NH₂), 64.59, 64.49 (d, J = 5.2 Hz, P-O-CH₂-CH₂-NH₂), 63.78, 55.20, 42.71 (d, J = 7.9 Hz, P-O-CH₂-CH₂-NH₂), 42.63 (d, J = 8.2 Hz, P-O-CH₂-CH₂-NH₂), 42.02 (CH₂-NH₂ of linker), 30.62, 29.13, 25.14 (middle CH₂ of linker), 24.98 (Me of NHAc); ³¹P NMR (162 MHz, D₂O) δ 0.28, -0.82; ESI-MS: m/z [M-2H+3Na]⁺ calcd for C₃₅H₆₈N₄O₂₇P₂ 1105.3078, obsd 1105.3060.

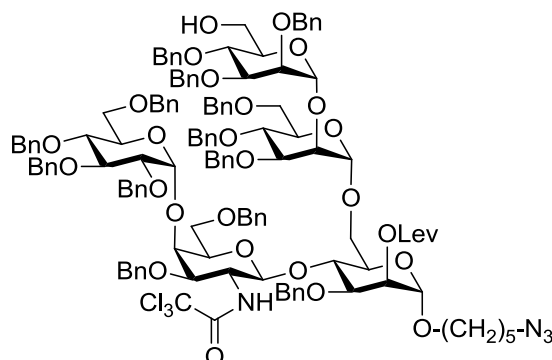
1-O-5-Azidopentyl 2,3,4-tri-O-benzyl-6-O-triisopropylsilyl- α -D-mannopyranosyl-(1 \rightarrow 2)-3,4,6-tri-O-benzyl- α -D-mannopyranosyl-(1 \rightarrow 6)-3-O-benzyl-4-O-(2,3,4,6-tetra-O-benzyl- α -D-glucopyranosyl-(1 \rightarrow 4))-3,6-di-O-benzyl-2-deoxy-2-trichloroacetamido- β -D-galactopyranosyl)-2-O-levulinyl- α -D-mannopyranoside (72)



Alcohol **60** (56 mg, 0.038 mmol) and imidate **8** (53mg, 0.045mmol) were coevaporated with toluene (3x2 mL) and placed under high vacuum for 30 min. The residue was dissolved in diethylether (2 mL) and powdered molecular sieves (100 mg, 4Å) was added. The slurry was stirred for 10 min at r.t. before it was cooled down to 0 °C and TBSOTf (10.4 μ L, 0.045 mmol) was added. The reaction mixture was stirred at 0 °C for 1 h before it was wuenched with TEA (50 μ L), diluted with CHCl₃, filtered and concentrated. The residue was purified by flash column chromatography to give pentasaccharide **72** (65 mg, 0.026 mmol, 69% yield) as a white foam: R_f (SiO₂, EtOAc/Hexane 1:3) = 0.21; $[\alpha]_D^{20}$: + 38.4 (c = 1.00, CHCl₃); ATR-

FTIR (cm^{-1}): 2865, 2097, 1717, 1497, 1454, 1362, 1070; ^1H NMR (400 MHz, CHCl_3) δ 7.37 (d, $J = 7.2$ Hz, 2H), 7.33 – 7.10 (m, 60H), 7.06 (d, $J = 7.4$ Hz, 1H), 7.01 (dd, $J = 6.6, 2.9$ Hz, 2H), 5.28 (d, $J = 1.4$ Hz, 1H), 5.23 (dd, $J = 3.4, 1.9$ Hz, 1H, ManI-2), 5.09 (d, $J = 8.1$ Hz, 1H, GalNAc-1), 4.96 (d, $J = 3.5$ Hz, 1H, Glc-1), 4.91 (d, $J = 10.9$ Hz, 1H), 4.88 (d, $J = 1.6$ Hz, 1H), 4.83 (d, $J = 10.6$ Hz, 1H), 4.74 – 4.56 (m, 13H), 4.54 – 4.29 (m, 8H), 4.28 – 4.21 (m, 2H), 4.20 – 4.15 (m, 2H), 4.10 – 3.82 (m, 16H), 3.79 – 3.48 (m, 13H), 3.33 (dt, $J = 9.8, 6.3$ Hz, 1H), 3.24 (dd, $J = 10.7, 1.6$ Hz, 1H), 3.18 (t, $J = 6.9$ Hz, 2H), 2.87 (dd, $J = 10.5, 1.4$ Hz, 1H), 2.50 – 2.31 (m, 4H, CH_2 of Lev), 1.98 (s, 3H, Me), 1.57 – 1.45 (m, 4H), 1.38 – 1.26 (m, 2H), 1.17 – 1.01 (m, 21H, TIPS); ^{13}C NMR (151 MHz, CHCl_3) δ 206.13 (ketone of Lev), 172.17 (ester of Lev), 161.93 (C=O of amide), 139.12, 138.92, 138.88, 138.73, 138.64, 138.63, 138.58, 138.49, 138.36, 138.35, 138.28, 138.07, 138.00, 128.56, 128.52, 128.46, 128.43, 128.38, 128.34, 128.31, 128.29, 128.27, 128.26, 128.24, 128.22, 128.17, 128.14, 128.06, 128.00, 127.96, 127.91, 127.89, 127.85, 127.83, 127.79, 127.77, 127.75, 127.73, 127.71, 127.70, 127.66, 127.59, 127.55, 127.49, 127.44, 127.38, 127.33, 127.08, 100.14 (Glc-1, $J_{C,H} = 170$ Hz), 99.11 (GalNAc-1, $J_{C,H} = 164$ Hz), 99.00 ($J_{C,H} = 174$ Hz), 98.62 ($J_{C,H} = 172$ Hz), 97.30 ($J_{C,H} = 172$ Hz), 92.72 (CCl_3), 82.16, 81.10, 80.09, 79.77, 77.84, 76.79, 75.45, 75.38, 75.31, 75.18, 75.10, 75.03, 74.98, 74.62, 74.13, 74.07, 73.96, 73.62, 73.49, 73.31, 73.29, 72.56, 72.43, 72.36, 72.23, 71.78, 71.76, 71.63, 70.79, 70.17, 69.78, 69.63, 68.00, 67.60, 67.49, 66.49, 63.16, 56.23, 51.34, 37.89, 29.74, 28.90, 28.73, 28.13, 26.16, 23.53, 18.25, 18.23, 18.20, 18.16, 12.25, 12.21; ESI-MS: m/z $[\text{M}+\text{Na}]^+$ calcd for $\text{C}_{142}\text{H}_{165}\text{Cl}_3\text{N}_4\text{O}_{28}\text{Si}$ 2533.0342, obsd 2533.0302.

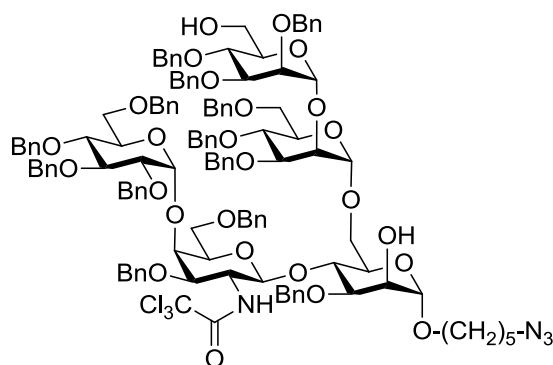
1-*O*-5-Azidopentyl 2,3,4-tri-*O*-benzyl- α -D-mannopyranosyl-(1 \rightarrow 2)-3,4,6-tri-*O*-benzyl- α -D-mannopyranosyl-(1 \rightarrow 6)-3-*O*-benzyl-4-*O*-(2,3,4,6-tetra-*O*-benzyl- α -D-glucopyranosyl-(1 \rightarrow 4)-3,6-di-*O*-benzyl-2-deoxy-2-trichloroacetamido- β -D-galactopyranosyl)-2-*O*-levulinyl- α -D-mannopyranoside (70**)**



Pentasaccharide **72** (37 mg, 0.015 mmol) was dissolved in MeCN (1.5 mL) and water (2 drops). Sc(OTf)₃ (10.9 mg, 0.022 mmol) was added and the reaction mixture was heated to 50 °C for 6 h. The reaction mixture was quenched with TEA (50 μ L) and evaporated to dryness. The residue was purified by flash column chromatography to give alcohol **70** (33 mg, 0.014 mmol, 95% yield) as white foam: R_f (SiO₂, EtOAc/Hexane 1:2) = 0.24; $[\alpha]_D^{20}$: + 43.0 ($c = 1.00$, CHCl₃); ATR-FTIR (cm⁻¹): 3030, 2920, 2097, 1717, 1454, 1362, 1072, 1028; ¹H NMR (400 MHz, CHCl₃) δ 7.61 (d, $J = 7.1$ Hz, 1H), 7.35 – 7.11 (m, 60H), 7.09 (dd, $J = 7.6, 1.8$ Hz, 2H), 7.02 – 6.98 (m, 2H), 5.29 (d, $J = 8.2$ Hz, 1H, GalNAc-1), 5.23 (dd, $J = 3.4, 1.9$ Hz, 1H, ManI-2), 5.04 – 5.00 (m, 3H, ManII-1, ManIII-1, Glc-1), 4.91 – 4.78 (m, 3H), 4.76 – 4.60 (m, 10H), 4.59 – 4.48 (m, 6H), 4.43 (s, 2H), 4.40 – 4.30 (m, 3H), 4.13 – 3.96 (m, 9H), 3.92 (dd, $J = 8.4, 3.5$ Hz, 1H, ManI-3), 3.89 – 3.56 (m, 18H), 3.55 – 3.49 (m, 2H), 3.38 – 3.25 (m, 3H), 3.18 (t, $J = 6.9$ Hz, 2H), 2.92 (dd, $J = 10.8, 1.6$ Hz, 1H), 2.66 (t, $J = 6.3$ Hz, 1H), 2.60 – 2.36 (m, 4H, CH₂ of Lev), 2.03 (s, 3H, Me of Lev), 1.60 – 1.47 (m, 4H), 1.41 – 1.31 (m, 2H); ¹³C NMR (101 MHz, CHCl₃) δ 206.43 (ketone of Lev), 172.13 (ester of Lev), 162.33 (C=O of amide), 138.94, 138.75, 138.74, 138.70, 138.68, 138.66, 138.53, 138.50, 138.47, 138.32, 138.13, 138.02, 128.59, 128.47, 128.45, 128.44, 128.43, 128.40, 128.37, 128.34, 128.18, 128.14, 128.02, 127.87, 127.85, 127.84, 127.83, 127.80, 127.70, 127.65, 127.57, 127.45, 127.33, 127.22, 126.89, 100.05, 99.94, 99.35, 99.32, 97.24 (ManI-1), 92.64, 82.01, 80.33, 80.05, 79.97, 77.85, 77.36, 76.29, 75.51, 75.47, 75.38, 75.27, 75.16, 75.05, 75.01, 74.88, 74.45, 74.15, 73.59, 73.50, 73.14, 73.11, 72.97, 72.70, 72.39, 72.36, 72.14, 71.88, 71.20, 70.77, 70.59, 69.36, 68.91 (ManI-2), 68.16, 67.77, 67.62, 67.49, 62.94, 56.91, 51.37, 37.97,

29.82, 28.91, 28.70, 28.17, 23.50; ESI-MS: m/z $[M+Na]^+$ calcd for $C_{133}H_{145}Cl_3N_4O_{28}$ 2375.9025, obsd 2375.9018.

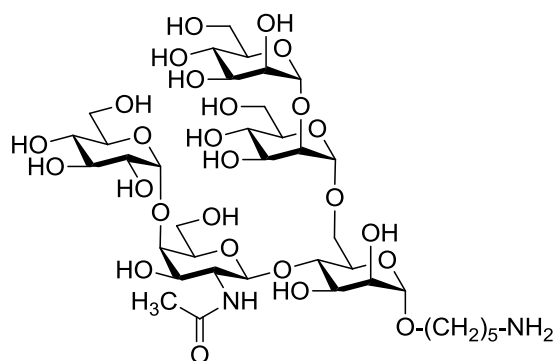
1-*O*-5-Azidopentyl 2,3,4-tri-*O*-benzyl- α -D-mannopyranosyl-(1 \rightarrow 2)-3,4,6-tri-*O*-benzyl- α -D-mannopyranosyl-(1 \rightarrow 6)-3-*O*-benzyl-4-*O*-(2,3,4,6-tetra-*O*-benzyl- α -D-glucopyranosyl-(1 \rightarrow 4)-3,6-di-*O*-benzyl-2-deoxy-2-trichloroacetamido- β -D-galactopyranosyl)- α -D-mannopyranoside (47a)



Pentasaccharide **70** (15 mg, 6.37 μ mol) was dissolved in MeCN (1 mL) and hydrazine monohydrate (31 μ L, 64 wt%) was added. The solution was stirred for 1 h before the reaction mixture was evaporated to dryness. The residue was purified by flash column chromatography to give diol **47a** (8 mg, 3.55 μ mol, 56% yield) as colorless oil: R_f (SiO₂, EtOAc/Hexane 3:1) = 0.68; $[\alpha]_D^{20}$: + 42.3 (c = 0.80, CHCl₃); ATR-FTIR (cm⁻¹): 3411, 3030, 2924, 2096, 1713, 1454, 1041, 1027; ¹H NMR (400 MHz, CHCl₃) δ 7.34 – 7.07 (m, 63H), 6.94 – 6.89 (m, 2H), 5.13 (d, J = 8.2 Hz, 1H, GalNAc-1), 5.08 (d, J = 1.7 Hz, 1H), 5.03 (d, J = 1.6 Hz, 1H), 5.01 (d, J = 3.3 Hz, 1H, Glc-1), 4.88 (d, J = 11.0 Hz, 1H), 4.82 (d, J = 10.7 Hz, 1H), 4.78 – 4.73 (m, 3H), 4.69 (dd, J = 12.4, 6.4 Hz, 5H), 4.63 (d, J = 1.7 Hz, 1H), 4.61 – 4.47 (m, 6H), 4.42 (t, J = 12.1 Hz, 4H), 4.32 (d, J = 11.6 Hz, 1H), 4.27 (d, J = 10.6 Hz, 1H), 4.22 – 4.11 (m, 3H), 4.10 – 3.95 (m, 6H), 3.90 – 3.51 (m, 23H), 3.39 – 3.29 (m, 2H), 3.18 (t, J = 6.9 Hz, 2H), 2.93 (dd, J = 10.5, 1.6 Hz, 1H), 2.70 (d, J = 1.5 Hz, 1H), 2.44 (t, J = 6.6 Hz, 1H), 1.58 – 1.47 (m, 4H), 1.40 – 1.30 (m, 2H); ¹³C NMR (101 MHz, CHCl₃) δ 162.05 (C=O of amide), 139.11, 138.84, 138.73, 138.68, 138.66, 138.49, 138.41, 138.31, 138.27, 138.20, 137.97, 128.72, 128.59, 128.55, 128.50, 128.47, 128.40, 128.37, 128.35, 128.29, 128.28, 128.21, 128.14, 128.03, 127.99, 127.86, 127.80, 127.78, 127.77, 127.74, 127.69, 127.66, 127.64, 127.62, 127.59, 127.56, 127.54, 127.51, 127.45, 127.14, 100.24, 99.73, 99.16, 98.78, 98.54, 92.65 (CCl₃), 82.04, 80.51, 80.34, 79.94, 78.12, 77.85, 76.37, 75.46, 75.33, 75.22, 75.13, 74.94, 74.65,

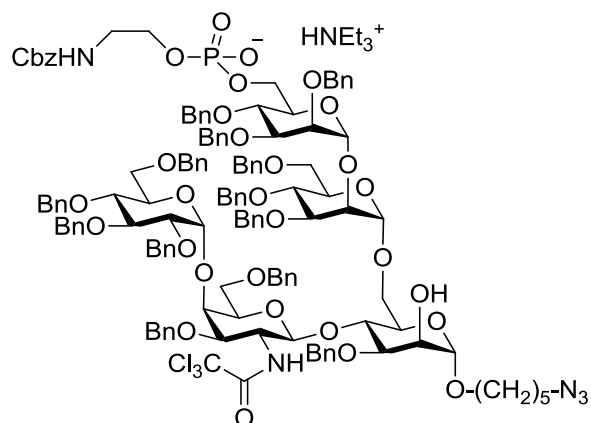
74.50, 73.61, 73.47, 73.27, 72.98, 72.52, 72.36, 72.27, 72.17, 71.81, 71.79, 70.96, 70.82, 69.39, 68.37, 68.01, 67.50, 67.28, 67.13, 62.89, 56.17, 51.40, 28.98, 28.76, 23.59; ESI-MS: m/z $[M+Na]^+$ calcd for $C_{128}H_{139}Cl_3N_4O_{26}$ 2277.8656, obsd 2277.8638.

1-O-5-Aminopentyl α -D-mannopyranosyl-(1 \rightarrow 2)- α -D-mannopyranosyl-(1 \rightarrow 6)-4-O-(α -D-glucopyranosyl-(1 \rightarrow 4)-2-deoxy-2-acetamido- β -D-galactopyranosyl)- α -D-mannopyranoside (47)



Diol **47a** (8 mg, 3.55 μ mol) was dissolved in MeOH (2 mL) and HOAc (2 drops). Pd/C (18.9 mg, 0.018mmol, 10 wt%) was added and hydrogen was bubbled through the slurry for 10 min. Afterwards the slurry was stirred for 24 h under hydrogen atmosphere before it was filtered through a syringe filter and evaporated to dryness. The residue was submitted to SEC chromatography (Sephadex-G25, 5% EtOH in water) to yield pentasaccharide **47** (2.5 mg, 2.62 μ mol, 74%) as white solid: $[\alpha]_D^{20}$: + 53.8 ($c = 0.25$, water); ATR-FTIR (cm^{-1}): 3271, 2930, 1643, 1558, 1407, 1018; 1H NMR (600 MHz, D_2O) δ 5.24 (d, $J = 1.1$ Hz, 1H), 5.09 (d, $J = 1.1$ Hz, 1H), 5.01 (d, $J = 3.8$ Hz, 1H, Glc-1), 4.92 (d, $J = 1.3$ Hz, 1H), 4.61 (d, $J = 8.3$ Hz, 1H, GalNAc-1), 4.18 – 4.15 (m, 1H), 4.14 (dd, $J = 2.9, 1.8$ Hz, 1H), 4.11 (d, $J = 2.7$ Hz, 1H), 4.09 – 3.70 (m, 26H), 3.66 – 3.61 (m, 2H), 3.54 (t, $J = 9.7$ Hz, 1H), 3.07 (t, $J = 7.6$ Hz, 2H), 2.15 (s, 3H, Me), 1.79 – 1.69 (m, 4H), 1.57 – 1.46 (m, 2H); ^{13}C NMR (151 MHz, D_2O) δ 177.31 (amide), 104.91, 104.73 (GalNAc-1), 102.86, 102.01 (Glc-1), 101.22, 81.26, 79.94, 79.31, 78.12, 75.89, 75.34, 74.60, 74.41, 72.99, 72.83, 72.72, 72.69, 72.61, 72.59, 72.15, 72.10, 71.85, 70.30, 69.60, 69.42, 68.70, 63.80, 63.71, 63.01, 62.57, 55.13, 42.05, 30.67, 29.27, 25.20, 25.02; ESI-MS: m/z $[M+Na]^+$ calcd for $C_{37}H_{66}N_2O_{26}$ 977.3796, obsd 977.3750.

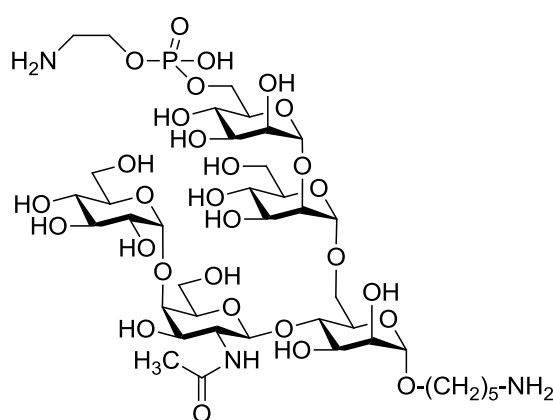
Triethylammonium **1-*O*-5-azidopentyl** **2,3,4-tri-*O*-benzyl-6-*O*-(2-(*N*-benzyloxycarbonyl)aminoethyl-phosphonato)- α -D-mannopyranosyl-(1 \rightarrow 2)-3,4,6-tri-*O*-benzyl- α -D-mannopyranosyl-(1 \rightarrow 6)-3-*O*-benzyl-4-*O*-(2,3,4,6-tetra-*O*-benzyl- α -D-glucopyranosyl-(1 \rightarrow 4)-3,6-di-*O*-benzyl-2-deoxy-2-trichloroacetamido- β -D-galactopyranosyl)- α -D-mannopyranoside (**71**)**



Alcohol **70** (18 mg, 7.65 μ mol) and H-phosphonate **10** (9.7 mg, 0.027 mmol) were coevaporated with dry pyridine (3x2 mL) and placed under high vacuum for 30 min. The residue was dissolved in pyridine (2 mL) and PivCl (4.7 μ L, 0.038 mmol) was added. This solution was stirred for 2 h at r.t. before water (1 drop) and iodine (9.7 mg, 0.038 mmol) were added. The solution was stirred for 1 h before hydrazine monohydrate (40 μ L, 64 wt%) was added. The reaction mixture was stirred for 18 h before it was concentrated and purified by flash column chromatography to give phosphate **71** (16 mg, 6.12 μ mol, 80% yield) as white foam: R_f (SiO₂, MeOH/CHCl₃ 1:9) = 0.63; $[\alpha]_D^{20}$: + 46.1 (c = 1.6, CHCl₃); ATR-FTIR (cm⁻¹): 3030, 2925, 2095, 1712, 1497, 1454, 1052, 1028; ¹H NMR (400 MHz, CDCl₃) δ 12.01 (s, 1H, HNEt₃⁺), 7.42 (d, J = 7.2 Hz, 2H), 7.35 – 7.14 (m, 60H), 7.13 – 7.09 (m, 4H), 7.08 – 7.04 (m, 4H), 5.58 (s, 1H, NH), 5.16 (s, 1H), 5.06 – 4.95 (m, 3H), 4.91 – 4.81 (m, 3H), 4.81 – 4.74 (m, 2H), 4.72 – 4.59 (m, 6H), 4.59 – 4.41 (m, 9H), 4.40 – 4.28 (m, 3H), 4.23 (dd, J = 11.9, 7.0 Hz, 2H), 4.19 – 4.00 (m, 6H), 4.00 – 3.82 (m, 6H), 3.81 – 3.49 (m, 16H), 3.33 (d, J = 9.9 Hz, 1H), 3.27 (dt, J = 10.1, 6.1 Hz, 1H), 3.16 – 3.06 (m, 3H), 2.89 (dd, J = 10.8, 1.6 Hz, 1H), 2.82 – 2.70 (m, 6H, CH₂ of TEA), 1.49 – 1.35 (m, 4H), 1.35 – 1.19 (m, 2H), 1.12 (t, J = 7.3 Hz, 9H, Me of TEA); ¹³C NMR (126 MHz, CDCl₃) δ 162.88 (amide), 156.44 (amide of Cbz), 139.27, 139.16, 139.11, 138.85, 138.75, 138.62, 138.55, 138.46, 138.30, 136.94, 128.63, 128.59, 128.45, 128.33, 128.25, 128.18, 128.12, 128.05, 127.83, 127.75, 127.69, 127.53, 127.28, 126.75, 101.45, 100.63, 98.45, 97.32, 93.16 (CCl₃), 82.23, 80.42, 80.26, 79.47, 78.90, 78.04, 75.61, 75.43, 75.24, 74.97, 74.58, 74.04, 73.82, 73.30, 73.17, 73.08,

72.74, 72.15, 71.78, 71.65, 71.06, 70.86, 70.32, 69.03, 67.74, 66.73, 66.61, 66.34, 65.39, 64.01, 54.86, 51.34, 45.59, 42.03, 29.83, 29.39, 28.74, 23.58, 22.83, 8.56; ^{31}P NMR (162 MHz, D_2O) δ - 2.26; ESI-MS: m/z $[\text{M}-\text{H}]^-$ calcd for $\text{C}_{138}\text{H}_{151}\text{Cl}_3\text{N}_5\text{O}_{31}\text{P}$ 2510.9190, obsd 2510.9392.

1-*O*-5-aminopentyl 6-*O*-(aminoethyl-phosphonato)- α -D-mannopyranosyl-(1 \rightarrow 2)- α -D-mannopyranosyl-(1 \rightarrow 6)-4-*O*-(α -D-glucopyranosyl-(1 \rightarrow 4)-2-deoxy-2-acetamido- β -D-galactopyranosyl)- α -D-mannopyranoside (46)



Phosphate **71** (16 mg, 6.12 μmol) was dissolved in CHCl_3 (2 mL) and washed Amberlite IR120 H $^+$ resin (50 mg) was added. The slurry was stirred for 45 min before it was filtered and concentrated. The residue was dissolved in MeOH (2 mL) and HOAc (2 drops). Pd/C (32.6 mg, 0.031 mmol, 10 wt%) was added and hydrogen was bubbled through the slurry for 10 min. Afterwards the slurry was stirred for 24 h under hydrogen atmosphere before it was filtered through a syringe filter and evaporated to dryness. The residue was submitted to SEC chromatography (Sephadex-G25, 5% EtOH in water) to yield phosphate **46** (4.8 mg, 4.45 μmol , 73%) as white solid: $[\alpha]_{\text{D}}^{20}$: + 64.0 ($c = 0.48$, water); ATR-FTIR (cm^{-1}): 3335, 2484, 1634, 1020; ^1H NMR (400 MHz, D_2O) δ 5.22 (d, $J = 1.4$ Hz, 1H), 5.06 (d, $J = 1.5$ Hz, 1H), 4.99 (d, $J = 3.9$ Hz, 1H, Glc-1), 4.90 (d, $J = 1.7$ Hz, 1H), 4.58 (d, $J = 8.3$ Hz, 1H, GalNAc-1), 4.23 – 4.11 (m, 5H), 4.09 (d, $J = 2.8$ Hz, 1H), 4.08 – 4.00 (m, 4H), 4.00 – 3.71 (m, 21H), 3.66 – 3.58 (m, 2H), 3.52 (dd, $J = 10.1, 9.3$ Hz, 1H), 3.34 (t, $J = 4.9$ Hz, 2H), 3.07 (t, $J = 7.5$ Hz, 2H), 2.14 (s, 3H, Me), 1.80 – 1.67 (m, 4H), 1.59 – 1.42 (m, 2H); ^{13}C NMR (101 MHz, D_2O) δ 174.59 (C=O of amide), 102.46, 102.18 (GalNAc-1), 100.16 (Glc-1), 99.32, 98.15, 79.15, 77.49, 76.62, 75.39, 73.06, 72.66, 71.99, 71.89, 71.73, 70.21, 70.14, 69.94, 69.84, 69.47, 69.37, 69.16, 67.61, 66.88, 66.21, 66.04, 64.65, 61.83, 61.10, 60.33, 59.89, 52.41, 40.09,

40.02, 39.37, 28.01, 26.51, 22.56, 22.33; ^{31}P NMR (162 MHz, D_2O) δ 0.36; ESI-MS: m/z $[\text{M}-\text{H}+2\text{Na}]^+$ calcd for $\text{C}_{39}\text{H}_{72}\text{N}_3\text{O}_{29}\text{P}$ 1122.3701, obsd 1122.3667.

Chapter 3 – Synthetic GPIs for Medical Applications

3.1 Preparation of GPI-Based Glycoconjugates

Carbohydrate-based vaccines were first reported in the first half of the 20th century.¹¹¹ It was demonstrated that injection of type-specific capsular polysaccharides isolated from pneumococci induced antibodies against these pathogens. The antibody titers elicited by polysaccharides generally last for a period of 5-8 month and generate immunity in healthy adults.¹¹² These findings lead to the development of PPV-14 in 1977 and its follower Pneumovax23 in 1983, which are capsular polysaccharide vaccines derived from 14 and 23 pneumococcal serotypes, respectively.¹¹³ However, populations that have an immature or compromised immune system, e.g. infants, children or the elderly, usually generate an insufficient immune response against these types of vaccines.⁸⁰ To overcome this hurdle, polysaccharides (Pevnar 13®, *Streptococcus pneumoniae*) or synthetic glycans (QuimiHib®, *Haemophilus influenzae*) can be conjugated to immunogenic carrier proteins to form glycoconjugates. These neoglycoproteins have the ability to raise an immune response against the conjugated carbohydrate and effectively prevent bacterial infections in all age groups. Based on the success of this class of inoculants potential antiparasitic¹¹⁴, antiviral¹¹⁵ and anticancer¹¹⁶ glycoconjugate vaccines were developed in the last decades using tools from carbohydrate chemistry and glycobiology.

The Seeberger group has a long-standing interest in the creation of immunity against apicomplexan parasites such as the causative agent of malaria, *P. falciparum*. The research conducted in this field culminated in the preparation of a GPI-based glycoconjugate antitoxin vaccine that significantly elongated the lifetime of parasite challenged mice and protected

¹¹¹ T. Francis, W. S. Tillett, *J. Exp. Med.* **1930**, *52*, 573-585.

¹¹² M. Heidelberger, M. M. Dilapi, M. Siegel, A. W. Walter, *J. Immunol.* **1950**, *65*, 535-541.

¹¹³ J. B. Robbins, R. Austrian, C.-J. Lee, S. C. Rastogi, G. Schiffman, J. Henrichsen, P. H. Mäkelä, C. V. Broome, R. R. Facklam, R. H. Tiesjema RH, J. C. Parker Jr., *J. Infect. Dis.* **1983**, *148*, 1136-1159.

¹¹⁴ M. E. Rogers, O. V. Sizova, M. A. Ferguson, A. V. Nikolaev, P. A. Bates PA, *J. Infect. Dis.* **2006**, *194*, 512-518.

¹¹⁵ I. J. Krauss, J. G. Joyce, A. C. Finnefrock, H. C. Song, V. Y. Dudkin, X. Geng, J. D. Warren, M. Chastain, J. W. Shiver, S. J. Danishefsky, *J. Am. Chem. Soc.* **2007**, *129*, 11042-11044.

¹¹⁶ N. Gaidzik, A. Kaiser, D. Kowalczyk, U. Westerlind, B. Gerlitzki, H. P. Sinn, E. Schmitt, H. Kunz, *Angew. Chem. Int. Ed.* **2011**, *50*, 9977-9981.

them against malarial acidosis, pulmonary oedema and cerebral symptoms.¹¹⁷ For this reason, it was envisioned that a glycoconjugate vaccine based on the GPIs of *T. gondii* would be a valuable approach for the development of a vaccine against this apicomplexan pathogen.

The carbohydrate antigens **1** and **2** (synthesis described in Chapter 2), which resemble the phosphoglycan of the two GPIs of *T. gondii*, were conjugated *via* maleimide chemistry¹¹⁸ to the diphtheria toxin variant CRM₁₉₇, a carrier protein that is constituent of different licensed conjugate vaccines (Scheme 3.1, page 110).^{80,119} At first free Lys and Arg groups of CRM₁₉₇ were acylated with the activated ester Sulfo-GMBS (**3**) using sodium bicarbonate as a base to introduce maleimide functionalities to the carrier protein. MALDI-TOF analysis at this stage indicated that 12-20 linker molecules were covalently attached to the carrier (for *m/z* spectra see Chapter 3.5, Figure 3.12, page 122). In addition the SDS-PAGE analysis showed a shift of CRM₁₉₇ to higher molecular masses and the formation of two broad bands (Figure 3.1). In a second step the thiol handles of **1** or **2** were reacted with the α,β -unsaturated carbonyl moieties in a Michael addition to form stable thioether bonds with the protein at a pH of 7.4. Mass spectroscopy of the resulting glycoconjugates revealed that on average five carbohydrate antigens were coupled to the protein, which was confirmed by a shift of the glycoconjugates in the SDS-PAGE to masses between 70 and 100 kDa. Remaining maleimide groups were quenched with an excess of L-cysteine, which did not significantly alter the spectrum of the MALDI-TOF analysis nor the band in the gel electrophoresis.

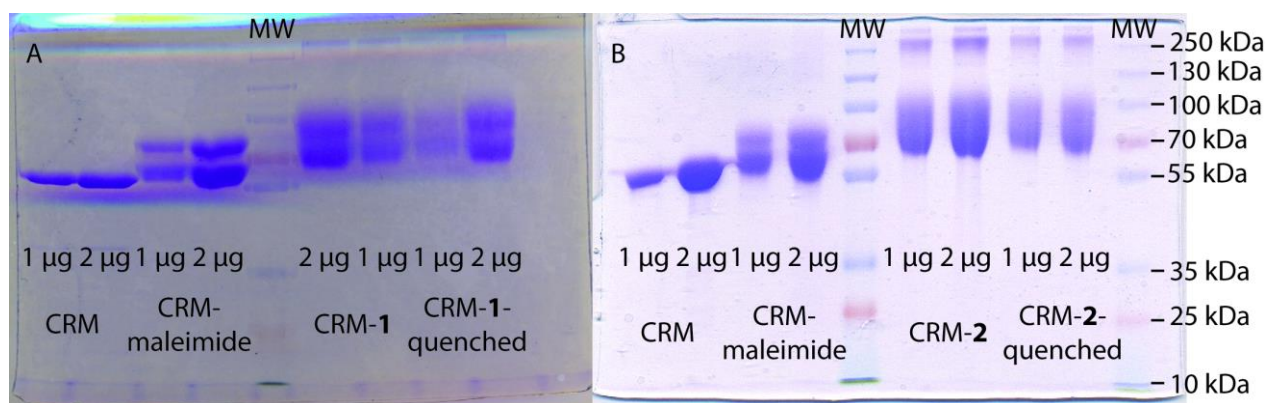
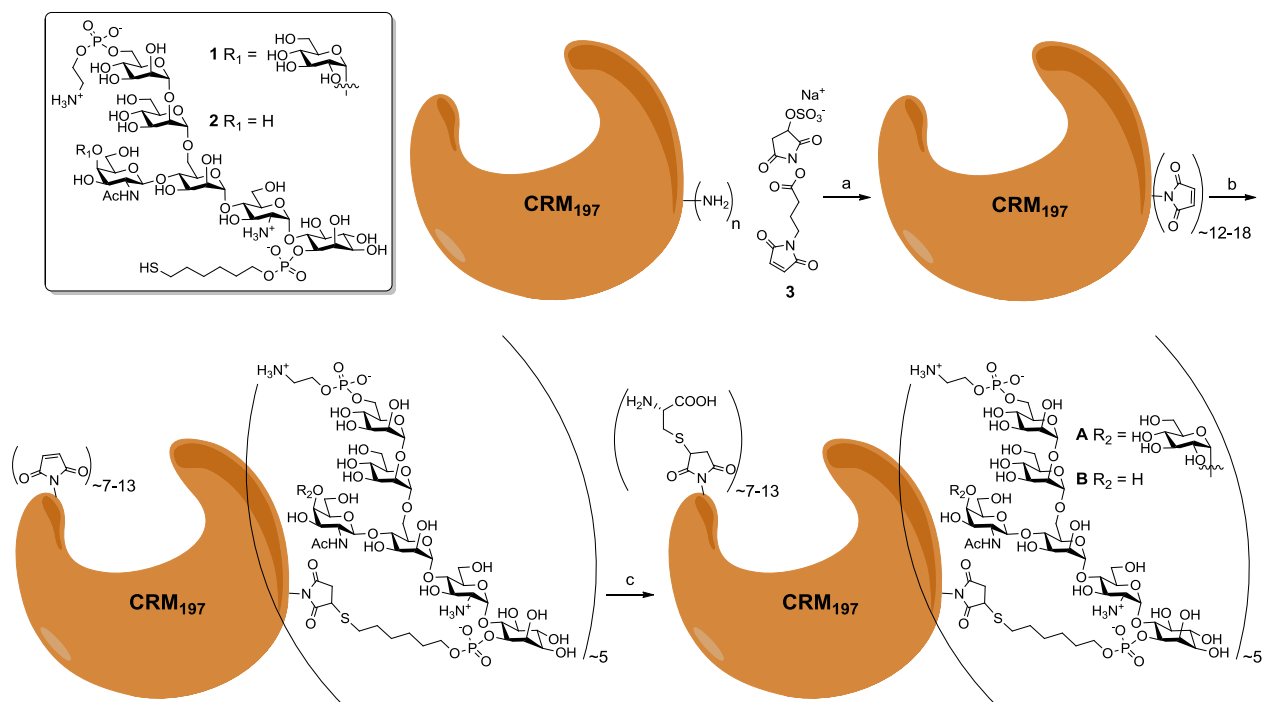


Figure 3.1: SDS-PAGE analysis of CRM₁₉₇ and the corresponding conjugates for (A) GPI **1** and (B) GPI **2**. The bands were visualized using Coomassie staining and the molecular weight marker lane is labeled with MW.

¹¹⁷ L. Schofield, M. C. Hewitt, K. Evans, M. A. Siomos, P. H. Seeberger, *Nature* **2002**, *418*, 785–789.

¹¹⁸ G. T. Hermanson, in *Bioconjugate Techniques (1st edition)*, (Ed: G. T. Hermanson), Academic Press, San Diego (CA), 1996, Chapter 5.

¹¹⁹ M. Bröker, P. M. Dull, R. Rappuoli, P. Costantino, *Vaccine* **2009**, *27*, 5574-5580.



Scheme 3.1: Reaction scheme for the preparation of GPI glycoconjugates **A** and **B** using maleimide chemistry. *Reagents and conditions:* (a) H_2O , NaHCO_3 , r.t., 2 h; (b) **1** or **2**, PBS, r.t., 3 h; (c) L-cysteine, 4 °C, 30 min, 78-95% over 3 steps.

3.2 Immunological Evaluation of GPI-Based Glycoconjugates

The mouse strain BALB/c, which is a suitable animal model for *T. gondii* vaccine studies⁷², was chosen to assess the immunogenic properties of neoglycoproteins **A** and **B**. Mice ($n = 3$ for each group) were immunized individually with either glycoconjugate **A** or **B** in a prime-boost regime (Figure 3.2).

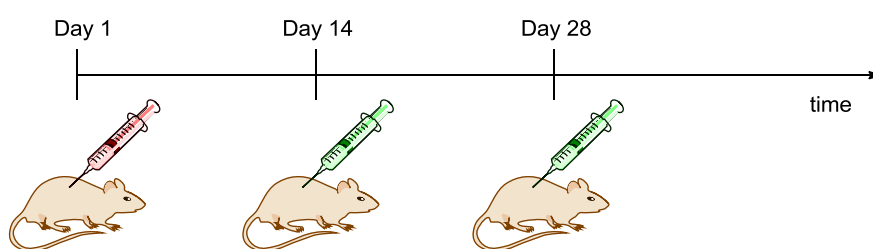


Figure 3.2: Time schedule for the prime-boost immunization studies of glycoconjugates **A** and **B**. Employed adjuvants are reflected by the color of the syringe (red = complete Freund's Adjuvant; green = incomplete Freund's Adjuvant).

The potential vaccine candidate **A** proved immunogenic in all mice. IgG directed against GPI **1** could already be detected one week after the prime immunization by carbohydrate microarray analysis and the serum antibody level increased steadily over the course of the experiment (Figure 3.3). The nature of the IgG response was further evaluated, demonstrating that the raised antibodies mainly consisted of the IgG1 and IgG2a subclasses, while IgG3 was almost undetectable (for pictures of carbohydrate microarrays see Chapter 3.5, Figure 3.12, page 124).

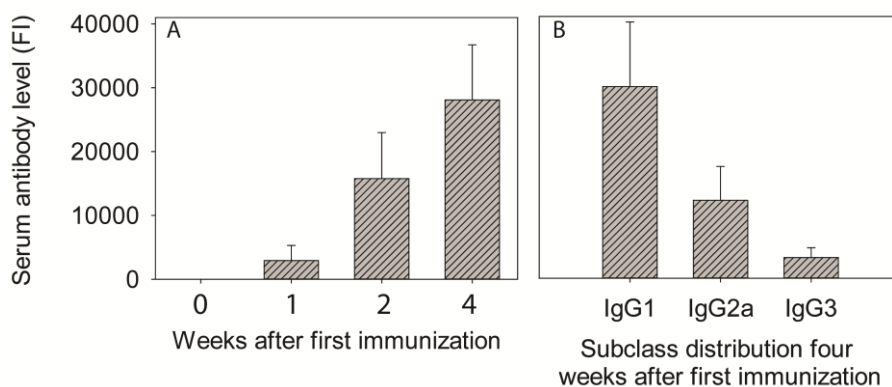


Figure 3.3: Serum antibody levels against antigen **1** in mice immunized with neoglycoprotein **A** at a dilution of 1:100. (A) Total serum IgG levels and (B) IgG subclass levels. Bars represent mean values averaged over all mice including standard error of the mean. FI = Fluorescence intensity.

In addition substructures **4-6** (synthesis described in Chapter 2), which represent the side branch and the branched mannose moieties of the GPI, were used to address the specificity and epitope recognition of the immune response (Figure 3.4). The IgG response of all animals was highly specific towards the full GPI-glycan **1**, as antibodies did not recognize any of the substructures.

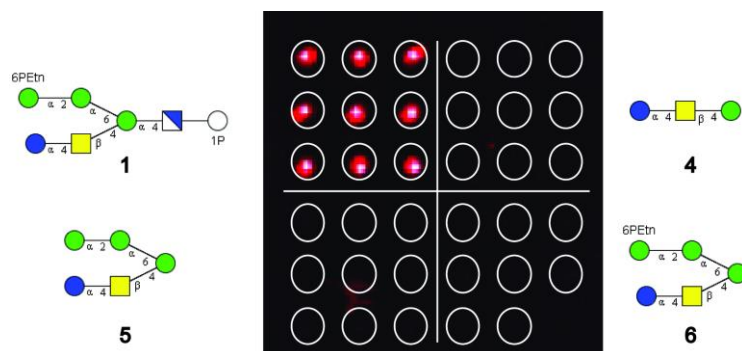


Figure 3.4: Representative scan of a carbohydrate microarray incubated with serum from one mouse six weeks after first immunization with glycoconjugate **A** at a dilution of 1:1000. The printing pattern is superimposed and the total IgG level was analyzed. Maleimide chemistry was used for the immobilization of the carbohydrates (printing concentration = 100 μ M for all compounds).

To confirm that the immune response against glycoconjugate **A** recognizes the natural GPI antigen displayed on the parasite, *T. gondii* tachyzoites were incubated with serum of immunized mice and analyzed with immunofluorescence confocal microscopy* (Figure 3.5).

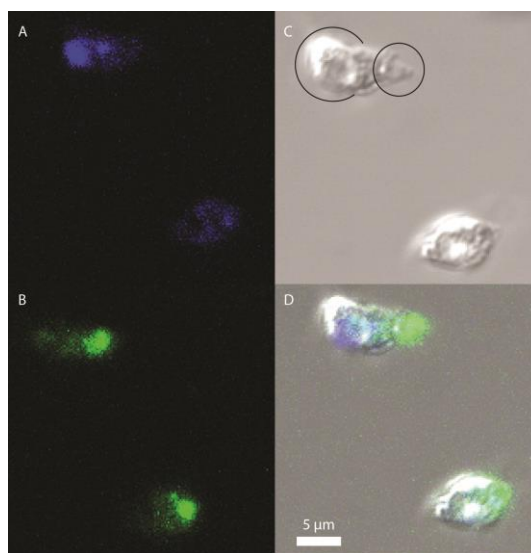


Figure 3.5: Immunofluorescence pictures of paraformaldehyde-fixed purified *T. gondii* tachyzoites grown in HFF cells stained with (A) DAPI indicating nuclear staining (B) pooled serum of mice immunized with neoglycoconjugate **A** (six weeks after first immunization) and a secondary FITC-conjugated anti-mouse-IgG antibody, (C) differential interference contrast image, and (D) merge of (A), (B) and (C). Full circle in (C) indicates the apical, and half circle the basolateral end of the parasite.

* Immunofluorescence microscopy was performed by Dr. N. Azzouz.

The antibodies bound to the surface of the parasite and showed preferential localization at the apical end of the cell. In contrast, antibodies binding to the parasite were not detectable in sera of mice before immunization (data not shown). These findings indicate that the Glc bearing GPI of *T. gondii* potentially plays a role in the formation or function of the apical complex, which is essential for invasion of host cells and replication of the parasite.¹²⁰

Gratifyingly also glycoconjugate **B** elicited a highly specific immune response against carbohydrate **2** in all immunized mice (Figure 3.6, page 114). Interestingly only little cross-reactivity against the α -Glc containing glycan **1** and the linear structure **8*** (see Scheme 3.2, page 115), which is related to GPIs found on the surface of *P. falciparum*, was observed. Most importantly, antibodies against the mammalian structure **7**, which only differs from glycan **2** by an additional phosphoethanolamine at the O2-position of ManI, were not detected. These results suggest that a glycoconjugate vaccine based on the GPI glycans of *T. gondii* will not trigger an immune response against self-antigens in mammals.

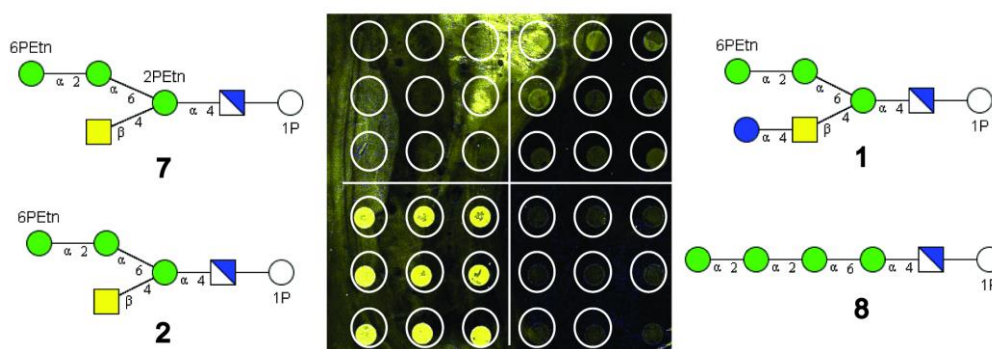


Figure 3.6: Representative scan of a carbohydrate microarray incubated with serum from one mouse six weeks after first immunization with glycoconjugate **B** at a dilution of 1:100 (right). The printing pattern is superimposed and the total IgG level was analyzed. Maleimide chemistry was used for the immobilization of the carbohydrates (printing concentration = 1 mM for all compounds).

Immunofluorescence microscopy revealed that the polyclonal antibodies in the serum of mice immunized with neoglycoconjugate **B** bound the parasite (Figure 3.7, page 114). In contrast to the immune response against conjugate **A**, GPI **2** seems to be distributed evenly over the whole membrane. These data are in accordance with the literature, because GPI **2** serves as a membrane anchor for different surface antigens such as SAG1, which is also uniformly spread on the surface of the parasite, and evidently colocalizes with this phosphoglycolipid.⁵⁵

¹²⁰ K. Hu, J. Johnson, L. Florens, M. Fraunholz, S. Suravajjala, C. DiLullo, J. Yates, D. S. Roos, J. M. Murray, *PLoS Pathog.* **2006**, *2*, e13.

* Compound **8** was provided by Dr. D. Varón Silva and prepared according to Ref. [90].

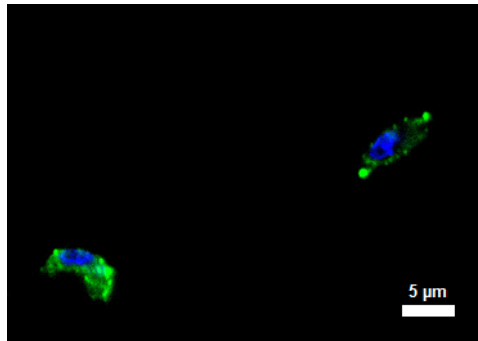
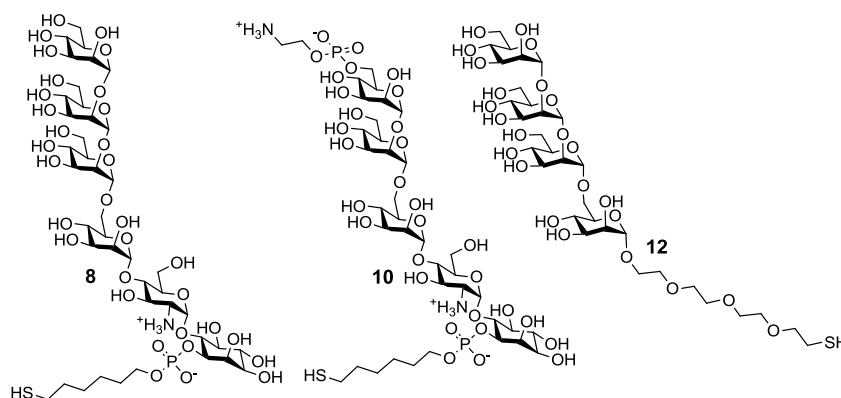


Figure 3.7: Immunofluorescence pictures of paraformaldehyde-fixed purified *T. gondii* tachyzoites grown in HFF cells stained with DAPI (indicating nuclear staining) and pooled serum of mice immunized with neoglycoconjugate **B** (six weeks after first immunization) and a secondary FITC-conjugated anti-mouse-IgG antibody.

3.3 Diagnostic Potential of Synthetic GPI Glycans

It was described in 1983 that humans elicit an early IgM response against a “low molecular weight antigen” upon infection with *T. gondii*.¹²¹ This antigen could later be identified as a mixture of closely related GPI structures.¹²² With the synthetic structures **1**, **2** and **9**, which represent the carbohydrate moieties of GPIs identified in *T. gondii*, as well as their corresponding substructures **4-6**, the mammalian phosphoglycan **7** and the *P. falciparum* related saccharide **8** and **10**^{*} in hand, a microarray was developed to investigate the immune response against GPIs during toxoplasmosis. As reference compounds pseudodisaccharide **11** (synthesis is described in Chapter 2) and oligomannoside **12**¹²³ (Scheme 3.2) were chosen for this study, in which 30 reference sera^{*} from patients with different toxoplasmosis disease states were analyzed.



Scheme 3.2: Structures of carbohydrates **8**, **10** and **12** that were used in combination with other glycans to fabricate a microarray, which enables detection of anti-GPI antibodies in serum of patients suffering from toxoplasmosis.

As can be seen in Figure 3.8B and C (see page 116) the IgG and IgM immune response against GPIs in toxoplasmosis patients is mainly directed against the full GPI structure **1** as well as the substructures **4-6** containing the α Glc motif. GPI carbohydrates **2** and **9** that only contain the simple β GalNAc branch are less recognized. Some individual sera also recognized the linear structures **8** or **10** as well as the pseudodisaccharide **12** (data not shown). Antibodies against tetramannoside **11** were also found in some patients, but did not seem to be correlated

¹²¹ S. D. Sharma, J. Mullenax, F. G. Araujo, H. A. Erlich, J. S. Remington, *J. Immunol.* **1983**, *131*, 977-983.

¹²² B. Striepen, C. F. Zinecker, J. B. Damm, P. A. Melgers, G. J. Gerwig, M. Koolen, J. F. Vliegthart, J. F. Dubremetz, R. T. Schwarz, *J. Mol. Biol.* **1997**, *266*, 797-813.

^{*} Compound **10** was provided by Dr. Y.-U. Kwon and prepared according to Ref. [90].

¹²³ Oligomannoside **12** was provided by Dr. B. L. Stocker and prepared according to A. Hölemann, B. L. Stocker, P. H. Seeberger, *J. Org. Chem.* **2006**, *71*, 8071-8088.

^{*} Reference sera were provided by Prof. Dr. Uwe Groß (Institut für Medizinische Mikrobiologie, Universitätsklinikum Göttingen)

As anticipated, high amounts of IgG antibodies against GPIs **1** and **2** as well as substructures **4-6** were only detected in acutely and latently infected toxoplasmosis patients (see Figure 3.8 for representative scans). High levels of IgM antibodies that predominantly recognized GPI **1** were exclusively found in acute toxoplasmosis samples. Interestingly, most non-infected sera contained IgM antibodies recognizing the α Glc bearing structures in low levels that are in the same range as IgM levels found in latently infected patients. Given that phosphoglycan **1** was predominantly recognized in this screening, serum antibody levels against this structure were determined in detail and statistically analyzed (Figure 3.9).

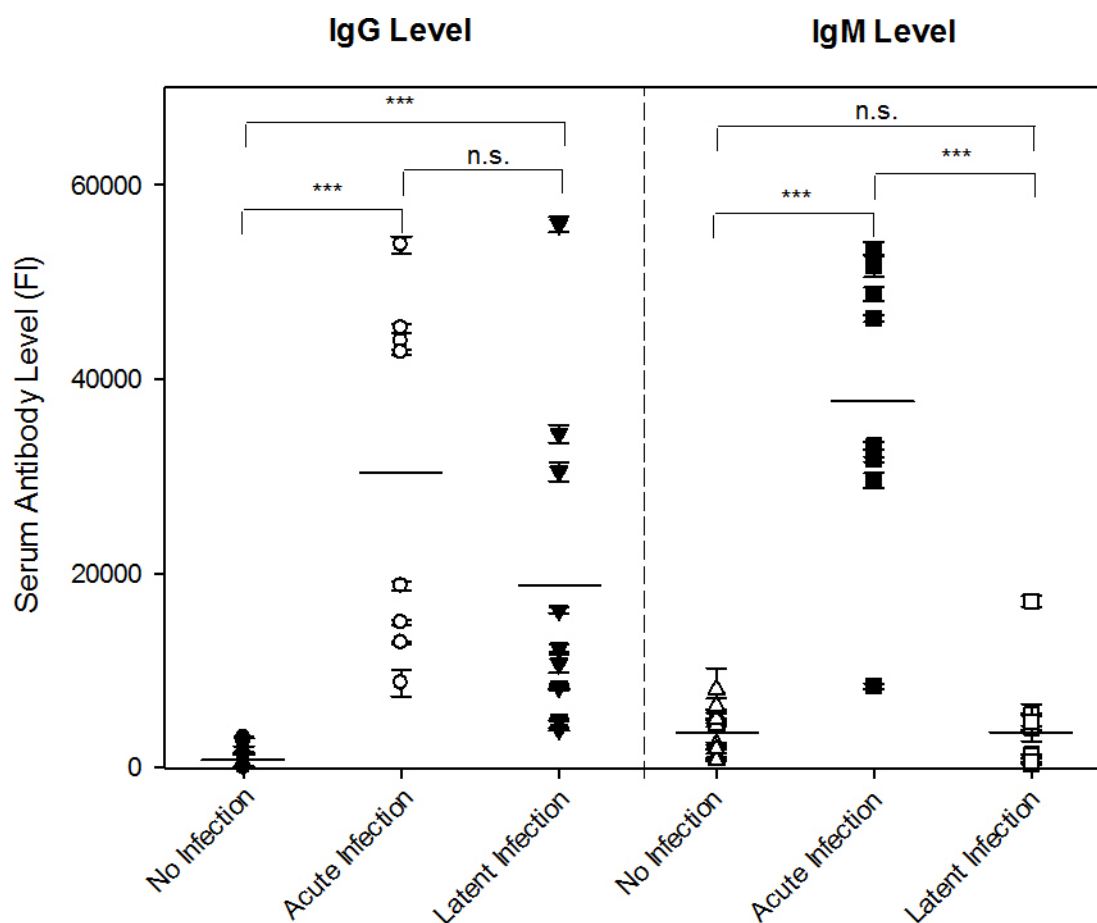


Figure 3.9: IgG and IgM level against antigen **1** in sera samples from different toxoplasmosis cohorts including standard deviation for every data point (n. s. = not significant; *** = $P < 0.005$; calculated by a Mann-Whitney Rank Sum Test using SigmaPlot 12.0). Description of cohorts: No Infection ($n = 10$); Acute Infection ($n = 8$); Latent Infection ($n = 10$). Black bars represent mean IgG/IgM levels.

This analysis clearly shows that IgG as well as IgM serum antibody levels against GPI **1** are significantly increased during the acute phase of the infection. While the concentration of IgG in the blood does not considerably decrease after the acute infection, IgM level drop to values that are similar to samples of non-infected individuals. The obtained results indicate that carbohydrate antigen **1** may be a suitable diagnostic marker to distinguish acute from latent toxoplasmosis. This is especially important because initial infection with *T. gondii* during

pregnancy can cause congenital infectious diseases leading to considerable morbidity of fetuses or even fetal death, forms of mental and physical retardation, and retinal inflammation.¹²⁴ Congenital toxoplasmosis can be prevented only by stopping transmission from mother to fetus using spiramycin (antifolate drug) as a treatment. In order to prevent fetal infections, countries like Austria and France already conduct a systematic prenatal screening for toxoplasmosis.¹²⁵ Diagnosis heavily relies on serological analysis of IgG and IgM titers against *T. gondii*. IgM antibodies rise quickly in response to infection and are therefore used as a crucial parameter for the diagnosis of an acute infection, whereas IgG titers against *T. gondii* are usually measured to differentiate between non-infected and infected individuals. Unfortunately, commercially available test kits for toxoplasmosis have high false positive rates, because IgM titers can be persistently elevated for many months after the first infection. In addition antigen preparations that are used for ELISA or agglutination essays usually consist of a mixture of isolated antigens that can have batch to batch variations and contain antigenic compounds that give false positive results.¹²⁶ Obviously there is great potential for harm when treatment is initiated based on a false positive result. Therefore, more reliable test systems are needed to accurately discriminate between acute and latent infections. This goal might be achievable by using defined synthetic antigens.

Despite the relative small sample size a ROC analysis was performed in order to estimate the discriminative power of antibody levels against glycan **1** to group patient samples into non-infected and infected individuals (Figure 3.10A) as well as acutely and latently infected patients (Figure 3.10B, page 119).¹²⁷ To distinguish between non-infected and infected individuals, glycan array fluorescence elicited by IgG or IgM antibodies was used with high values assigned to infected patients. In the same way, antibody fluorescence was employed for the discrimination of acute (high fluorescence) and latent infections (low fluorescence). The results indicate a high discriminative power for IgG fluorescence to differentiate between non-infected and infected individuals with a value of 1 for the area under the ROC curve. Likewise IgM fluorescence has a value of 0.99 for the area under the ROC curve and a high diagnostic accuracy to discriminate between acutely and latently infected patients. Thus, clear thresholds can be assigned in this small sample set to distinguish between all populations.

¹²⁴ J. G. Montoya, O. Liesenfeld, *Lancet* **2004**, 363, 1965-1976.

¹²⁵ E. Stillwaggon, C. S. Carrier, M. Sautter, R. McLeod, *PLoS Negl. Trop. Dis.* **2011**, 5, e1333.

¹²⁶ A. Dao, N. Azzouz, C. Eloundou Nga, J. F. Dubremetz, R. T. Schwarz, B. Fortier, *Eur. J. Clin. Microbiol. Infect. Dis.* **2003**, 22, 418-421.

¹²⁷ A. Linden, *J. Eval. Clin. Pract.* **2006**, 12, 132-139.

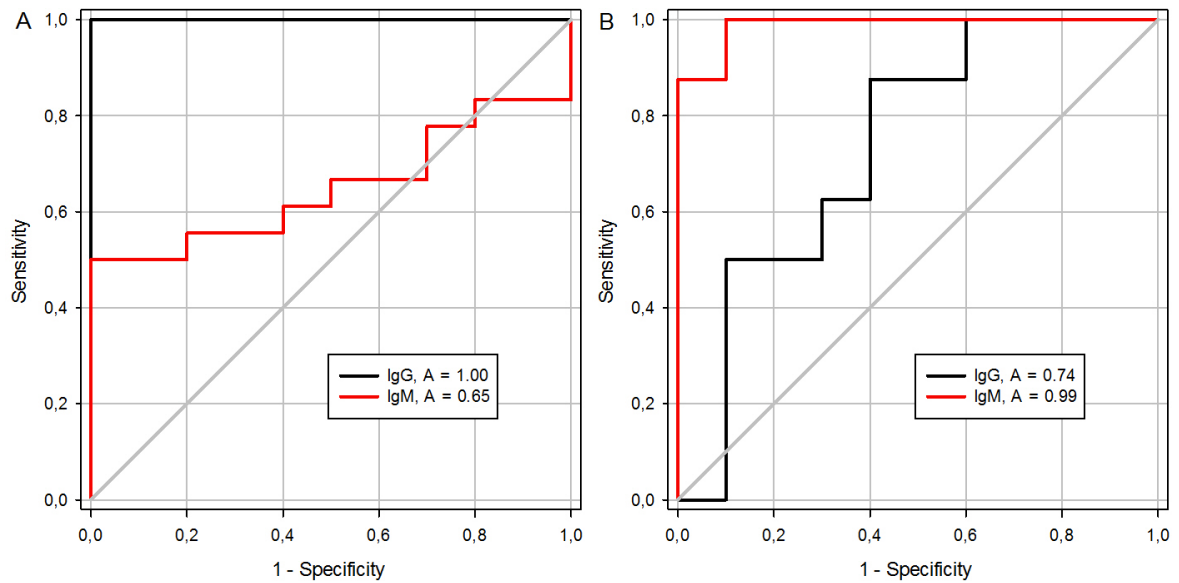


Figure 3.10: ROC analysis to assess diagnostic and predictive accuracy of the microarray test employing antigen **1** (calculated with SigmaPlot 12.0). The area under the ROC curve was determined for the capability of the diagnostic tool to distinguish between (A) non-infected and infected individuals and (B) acutely and latently infected patients. Glycan array fluorescence elicited by either IgG or IgM antibodies against carbohydrate **1** (high values) was used to discriminate between the aforementioned diseases states. The diagonal grey line indicates a test that cannot discriminate between two disease states (random guess; $A = 0.50$).

3.4 Conclusion and Outlook

In summary it was shown that the carbohydrates **1** and **2**, which resemble the phosphoglycan moiety of the GPIs found on the surface of the *T. gondii*, can be used for preparation of immunogenic neoglycoconjugates that have the ability to induce a specific parasite recognizing immune response in mice. In order to investigate the protective properties of glycoconjugates **A** and **B**, challenge experiments using a mouse model and the virulent RH strain of *T. gondii* have to be conducted. Especially antibodies against GPI **1** could induce a sterile immunity in mice or humans if they interfere with the invasion process by blocking the interaction between the apical complex of *T. gondii* and the host cell.

Furthermore GPI **1** was used as a diagnostic marker on a carbohydrate microarray and revealed promising potential in distinguishing different disease states of toxoplasmosis in human blood samples. In future studies larger cohorts have to be screened for antibodies recognizing GPIs of *T. gondii* as well as related substructures to determine reliable statistical data sets that enable the determination of threshold values not only for glycan **1** but also for other potential synthetic carbohydrate antigens such as trisaccharide **4** as well as pentasaccharides **5** and **6**.

3.5 Experimental Part

Materials and Methods:

Preparation of Glycoconjugates A and B: CRM₁₉₇ (1 mg, 0.017 μmol , Pfēnex Inc.) was dissolved in sterile filtered NaHCO₃ solution (2 mg mL⁻¹, 0.5 mL). Sulfo-GMBS (1 mg, 2.6 μmol , Thermo Scientific) dissolved in sterile filtered water (0.5 mL) was added to the solution. The solution was agitated for 2 h under the exclusion of light. To wash away unreacted linker the solution was concentrated to 250 μL volume using an Amicon® Ultra-4 Centrifugal Filter Unit (10 kDa cut off, Millipore) and washed twice with water (2x 1 mL). Thiol **1** or **2** (250 μg , 0.165 μmol ; in 250 μL water) that was already incubated for 1 h with an equimolar amount of TCEP·HCl (Thermo Scientific) was added to the solution of the linker modified CRM₁₉₇ (250 μL). To this solution 10x PBS (50 μL @ pH = 7.4) was added. The reaction mixture was agitated for 3 h under the exclusion of light, before a cysteine solution (10 mg mL⁻¹, 100 μL) was added to quench unreacted maleimide groups (incubation for 30 min at 4 °C under the exclusion of light). To wash away unreacted thiols, TCEP and cysteine the solution was concentrated again to 250 μL volume and washed twice with water (2x 1 mL) using an Amicon® Ultra-4 Centrifugal Filter Unit. The concentrated conjugate solution (**A** or **B**) was divided in aliquots and lyophilized. The white powder (0.9-1.1 mg, 0.013-0.015 μmol , 78-95% yield, for both conjugates the yield varies from batch to batch in the aforementioned range) was stored at -25°C until use. Purity and loading were assessed using SDS-PAGE (10% denaturing gel without DTT; “PageRuler Plus Prestained Protein Ladder, 10 to 250 kDa” from Thermo Scientific was used as a protein size marker) and MALDI-TOF (Matrix DHAP + 1% TFA) analysis (Figure 3.11).[†]

[†] MALDI-TOF analysis was performed by C. Martin and E. Settels.

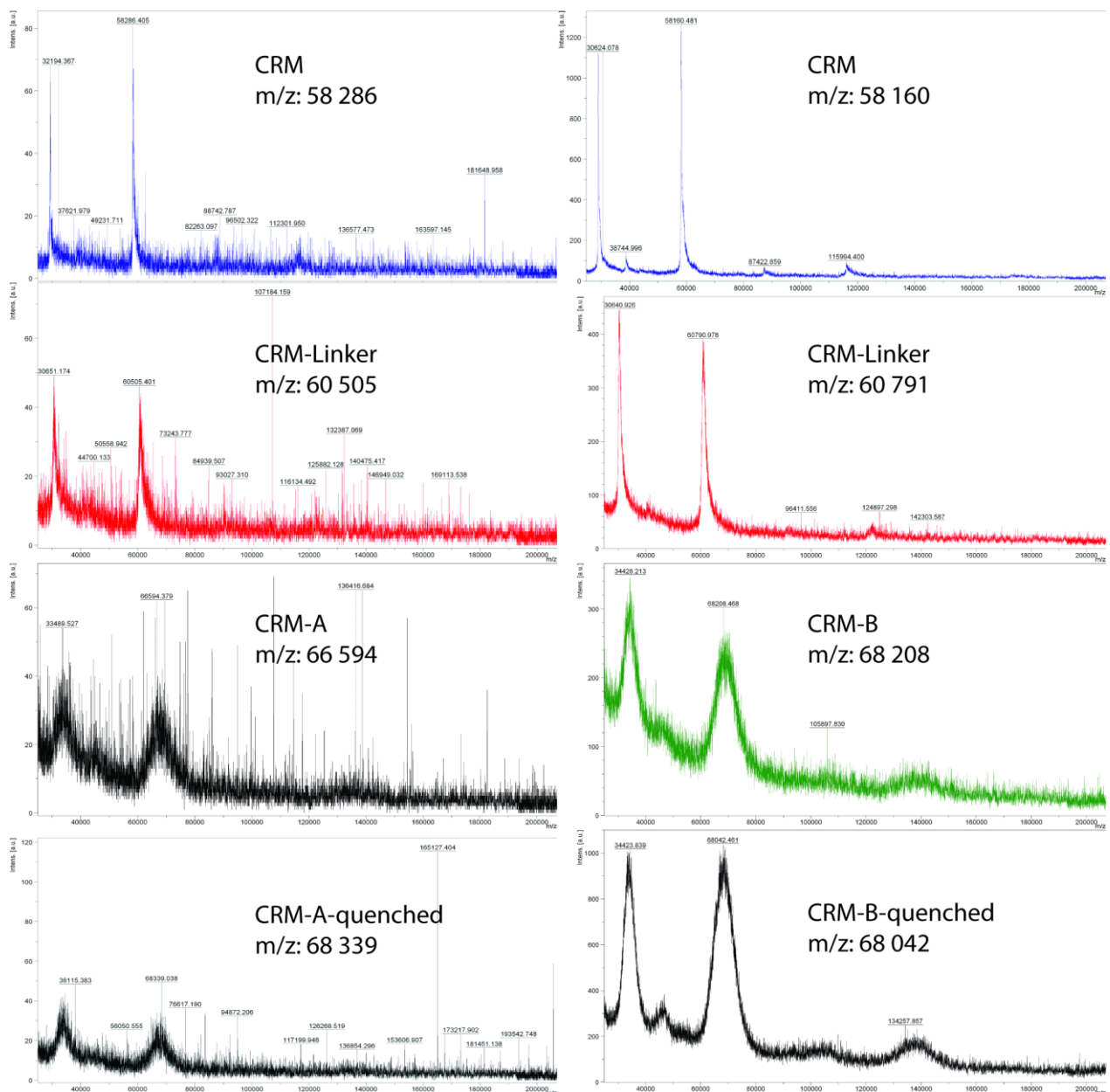


Figure 3.12: MALDI-TOF analysis of the different stages during glycoconjugate preparation.

*Immunization of BALB/c Mice with Glycoconjugates A and B:** Three 6 week's old female BALB/c mice were immunized *s.c.* with 100 μL (for each mouse) of a suspension that consisted of 35 μg of glycoconjugate (**A** or **B**), which was dissolved in 50 μL sterile PBS and 50 μL of CFA. The mice were boosted twice in a two week interval. For the boosting 100 μL of a suspension that consisted of 35 μg of glycoconjugate (**A** or **B**), which was dissolved in 50 μL sterile PBS and 50 μL of IFA was injected *s.c.* into the mice. Serum samples were drawn

* Immunizations and serum collection was performed by A. Wahlbrink, Dr. C. Anish and A. Reinhardt.

from the tail vein at different time points and centrifuged. The obtained serum was analyzed using carbohydrate microarrays.

Fabrication of Maleimide-Functionalized Slides: Maleimide-functionalized slides were produced by submerging amine-coated slides (GAPS II slides, Corning) in *N*-(γ -maleimidobutyryloxy) sulfosuccinimide ester (Thermo Scientific) in DMF (2 mM) with DIPEA (2.5% v/v) for 24 h at room temperature. Slides were washed three times with water and three times with ethanol, dried by placing the slides for 2 h in a high vacuum and stored under argon until spotting.

Fabrication of carbohydrate microarrays: Carbohydrates were dissolved in phosphate buffer (50 mM NaH₂PO₄, pH 8.5 for amine linker compounds) or PBS (pH 7.4 for thiols, including an equimolar amount of TCEP·HCl). The compounds were robotically printed using a piezoelectric spotting device (S3, Scienion) onto maleimide-functionalized slides or epoxy slides (sciCHIPEPOXY, Scienion), in 50% relative humidity at 23 °C. For completion of the immobilization reaction, printed slides were stored for 18 h in a humified chamber. Slides were stored in an anhydrous environment. Prior to the experiment, the slides were washed three times with water and the remaining maleimido or epoxy groups were quenched by incubating the slides in an aqueous 0.1% v/v β -mercaptoethanol solution for 1 h at 25 °C. The slides were then rinsed three times with water and dried by centrifugation.

*Mouse Serum Analysis:** Microarrays were blocked with BSA (2.5%, w/v) in PBS for 1 h at room temperature. Blocked slides were washed twice with PBS, centrifuged (1,200 rpm), and incubated with the indicated dilution of mouse sera in PBS for 1 h. After washing with PBS, microarrays were incubated with an ALEXA-Fluor®635-labelled goat anti-mouse IgG antibody (Invitrogen) or another appropriate secondary fluorescent antibody (ALEXA-Fluor®594-labelled goat anti-mouse IgG1; ALEXA-Fluor®635-labelled goat anti-mouse IgG2a; ALEXA-Fluor®488-labelled goat anti-mouse IgG3; ALEXA-Fluor®594-labelled goat anti-mouse IgM; all from Invitrogen) at 1:400 in PBS containing 1% BSA for 1 h. The slides were then washed with PBS again, dipped into double-distilled water for 3 s and subsequently dried by centrifugation and analyzed using a fluorescence microarray scanner (Genepix® 4300A, Molecular Devices; “mean fluorescence values-background”; Figure 3.12, page 124).

* Mouse sera were analyzed by Dr. N. Azzouz.

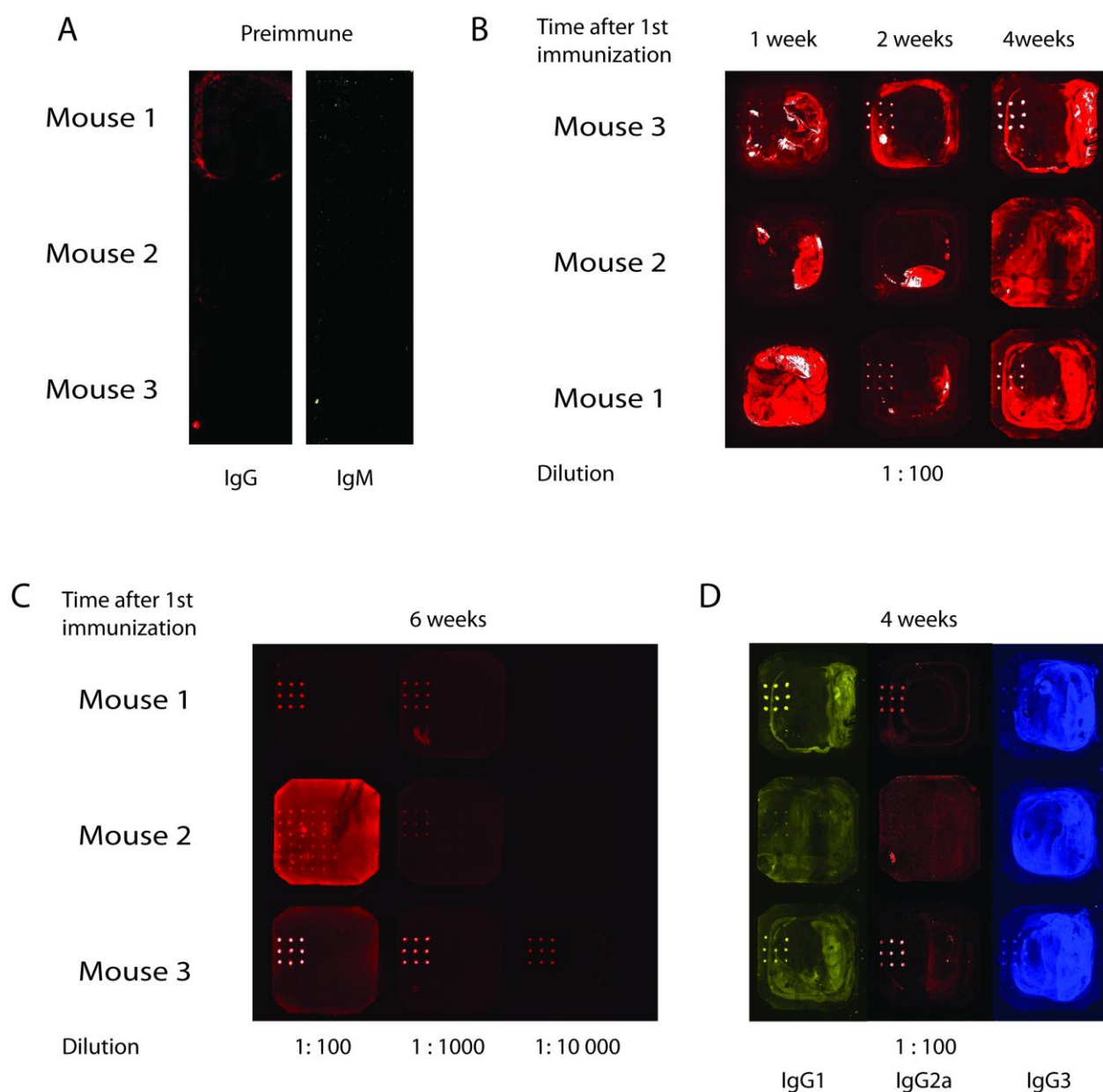


Figure 3.12: Carbohydrate microarray pictures of the sera of all 3 mice immunized with glycoconjugate A. (A) Total IgG and IgM level analysis of preimmune sera. (B) Total IgG level analysis over the course of four weeks. (C) Total IgG level analysis 6 weeks after 1st immunization. (D) Isotyping 4 weeks after the 1st immunization. The printing pattern is the same as in Figure 3.4 (see page 112).

*Staining of Tachyzoites:** *T. gondii* (RH strain) were grown in HFF cell monolayers and collected by gentle scrapping of the cell culture flask (300 cm²). The obtained cell suspension was centrifuged (1,200 rpm, 5 min), the supernatant discarded and the pellet resuspended in DMEM (10 mL, Life Technologies™). The suspension was pushed through needles (20, 23, 25, 27 G) to destroy remaining HFF cells. The resulting suspension was purified using a glass-wool column and PBS as an eluent. The tachyzoites were centrifuged (4,000 rpm, 5 min) and washed with PBS (3x 10 mL) and fixed with 4% (w/v) paraformaldehyde in PBS (1 h). After three washes with PBS, monolayers were permeabilized with PBS containing

* Cultivation and staining of tachyzoites was performed by Dr. N. Azzouz.

0.005% (w/v) saponin and 10% (w/v) bovine serum albumin for 30 min. Coverslips were incubated with pooled mouse serum (dilution 1:100) in 3% BSA in PBS for 1 h at room temperature, followed by a FITC-conjugated anti-mouse antibody (dilution 1:200, Dako). After five final washes with PBS, glass cover slides were mounted in Fluoroprep (Dako) and recorded by using a 100× Plan-NeoFluar oil objective lens with NA 1.30 using an Axiophot microscope (Zeiss). Epifluorescence images were captured by a SpotRT monochrome camera (Diagnostic Instruments Inc.).

Serological Analysis of Different Toxoplasmosis Cohorts: Collection of serum samples and their serological analysis was performed by the laboratory of Prof. Dr. Uwe Groß (Institut für Medizinische Mikrobiologie, Universitätsklinikum Göttingen). The sera were analyzed according to manufacturer instruction using an indirect immunofluorescence antibody test (IFT) (Toxo-Spot IF, bioMérieux), IgG-ELISA (VIDAS® TOXO IgG II, bioMérieux), IgM-ELISA (VIDAS® TOXO IgM, bioMérieux) and IgA-ELISA (Platelia™ Toxo IgA, Bio-Rad). The sera were characterized according to the results shown in Table 3.1 (see page 126).

Sample number	Characterization	IFT	IgG	IgM	IgA
1	N	neg	-	-	-
2	N	neg	-	-	-
3	L	1:256	194	neg	neg
4	A/L	1:256	58	0,85	13,72
5	A	1:4096	126	1,73	11,41
6	N	neg	-	-	-
7	L	1:64	53	neg	neg
8	A	1:4096	116	2,17	14,74
9	L	1:64	64	neg	neg
10	N	neg	-	-	-
11	L	1:64	138	neg	neg
12	L	1:64	61	neg	neg
13	N	neg	-	-	-
14	A/L	1:256	56	4,92	14,20
15	A	1:4096	>300	7,33	11,69
16	L	1:16	17	neg	neg
17	L	1:64	37	neg	neg
18	N	neg	-	-	-
19	N	neg	-	-	-
20	N	neg	-	-	-
21	L	1:16	11	neg	neg
22	A	1:16384	>300	9,97	35,86
23	A	1:4096	>300	1,40	14,09
24	L	1:16	11	neg	neg
25	A	1:4096	>300	1,62	18,32
26	L	1:256	189	neg	neg
27	N	neg	-	-	-
28	A	1:4096	172	2,95	25,88
29	N	neg	-	-	-
30	A	1:4096	289	4,00	23,05

Table 3.1: Serological analysis of serum samples from different toxoplasmosis cohorts and corresponding classification of the diseases state (N = no infection; A = acute infection; L = latent infection; A/L = acute or latent infection).

Human Serum Carbohydrate Microarray Analysis: Sera sample preparation was performed according to a literature protocol.¹²⁸ In brief, each serum sample was diluted 1:15 with PBS containing 0.1% v/v Tween20 and 3% w/v BSA, thoroughly vortexed for 15 s and incubated at 37 °C for 15 min to dissolve potential lipid aggregates. Insoluble residual sample components were removed by centrifugation for 30 s in a table-top centrifuge at 13,000 rpm. Samples were transferred to the microarray and gently rocked in a sealed humidified incubator for 2 h at 37 °C. Unbound sample components were removed with a series of washes with 0.1 (1 time) and 0.001% v/v Tween 20 (2 times) in PBS. Afterwards microarrays were incubated

¹²⁸ F. Jacob, D. R. Goldstein, N. V. Bovin, T. Pochechueva, M. Spengler, R. Caduff, D. Fink, M. I. Vuskovic, M. E. Huflejt, V. Heinzelmann-Schwarz, *Int. J. Cancer* **2012**, *130*, 138-146.

for 1 h at r.t. with ALEXA-Fluor®594 goat anti-human-IgM antibody (μ -chain specific, Life Technologies) and ALEXA-Fluor®488 anti-human-IgG antibody ($Fc\gamma$ specific, Dianova) diluted 1:400 in PBS containing 0.1% v/v Tween20 and 3% w/v BSA. The slides were washed as described above, dipped into double-distilled water for 3 s and subsequently dried by centrifugation. The slides were analyzed using a fluorescence microarray scanner (Genepix® 4300A, Molecular Devices, “mean fluorescence values-background”). The results were highly reproducible as can be seen in Figure 3.13 (see page 128).

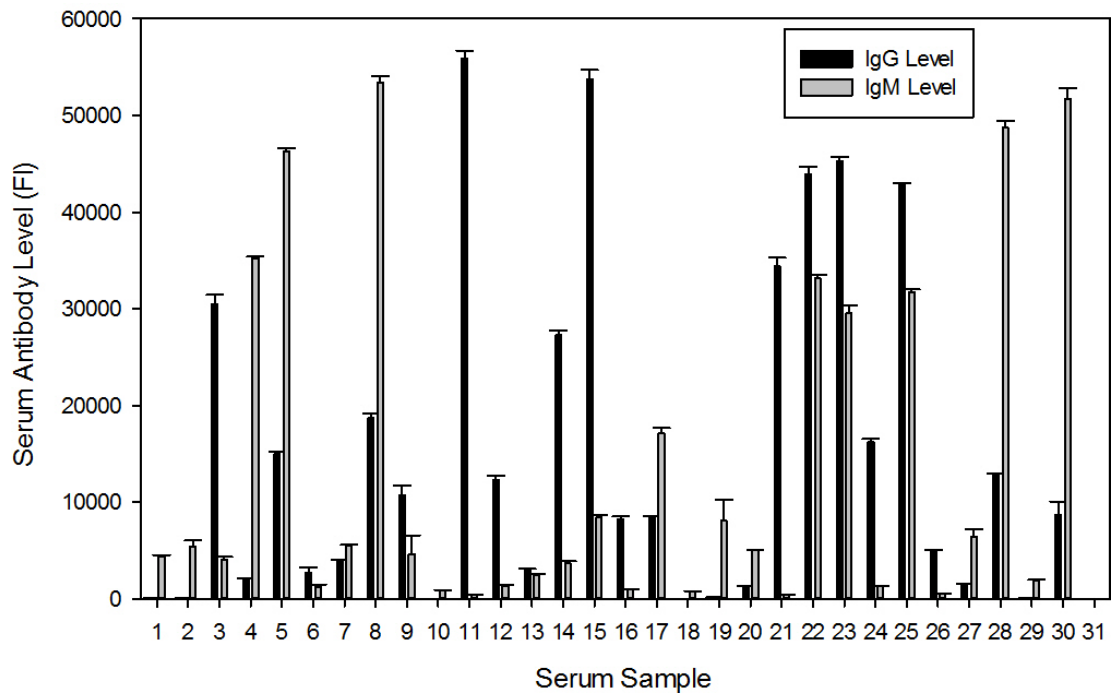
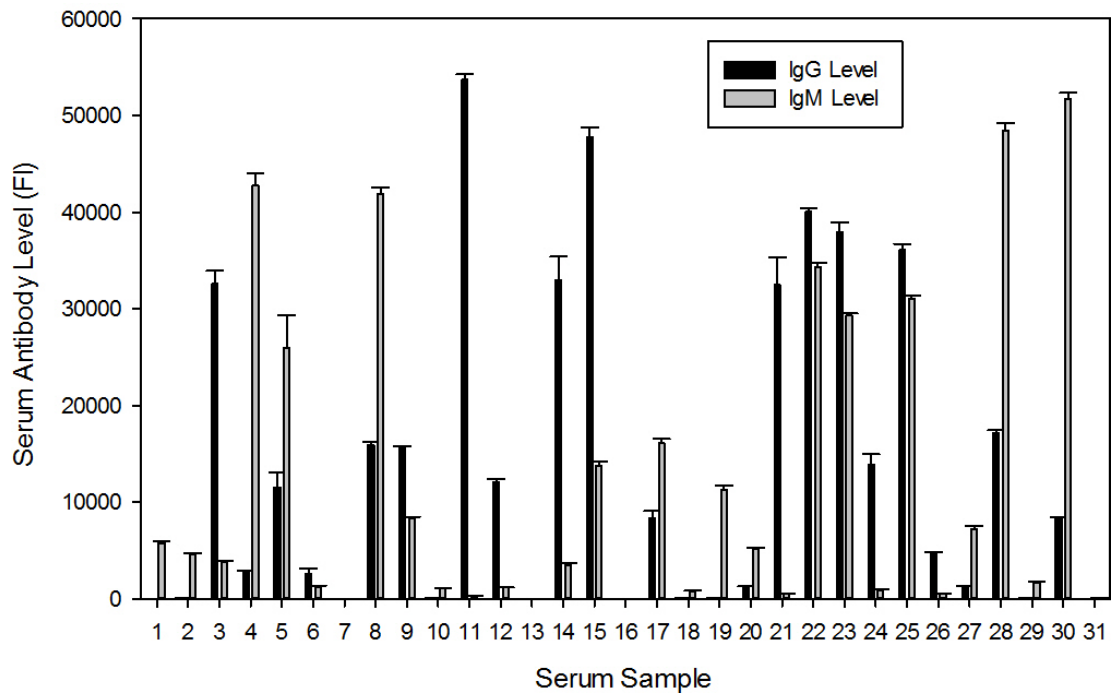
A**B**

Figure 3.13: Serum antibody levels against antigen 1 of all 30 serum samples (31 = negative control = 0.1% v/v Tween20 and 3% w/v BSA). Bar charts **A** and **B** resemble results obtained by microarray analysis on different days (samples 7, 13 and 16 were not analyzed in **B** and are therefore adjusted to zero).

Chapter 4 - Defining the Interaction of Human Lectin ZG16p and Mycobacterial PIMs

4.1 The Human Lectin ZG16p

ZG16p is a 16-kDa soluble protein initially identified in rat pancreas where it is associated with the zymogen granule membrane.¹²⁹ The protein was recently detected in the human colon, small intestine, and serum as well as in the pancreas.¹³⁰ ZG16p plays a role in packaging pancreatic enzymes into zymogen granules and separating them from constitutively secreted proteins.¹³¹ ZG16p has been considered a primary binding partner of GAGs in pancreatic granules.¹³²

ZG16p has an amino acid sequence homology with the CRD of jacalin, a jackfruit lectin.¹³³ A recent X-ray crystallographic analysis revealed that human ZG16p has a jacalin-related β -prism fold, which is closely related to BanLec, a mannose-binding lectin in bananas, and therefore categorized as a member of the L-type lectin family. Previous glycan-microarray screening studies demonstrated that ZG16p has broad specificity for glycans consisting of mannose, including mannan and Ser/Thr-linked *O*-mannose, and glucosyl oligosaccharides, such as short fragments of β 1,3-glucans.¹³⁰ Asp151 is a key mannose binding residue as evidenced by the mutation of Asp151 to Asn which abolishes glycan binding properties. In addition to its mannose binding property, ZG16p also binds GAGs, especially heparin and heparin sulfate. Thus, ZG16p interacts with both GAGs and mannose. Recent crystallographic and NMR studies indicate that the dual glycan binding property of ZG16p originates from two distinguishable binding modes. Mannosides use a shallow mannose-binding site made up of three loops, GG loop (between β 1 and β 2 strands, Gly31-Gly35), recognition loop (between β 7 and β 8 strands, Lys102-Tyr104), and binding loop (between β 11 and β 12 strands, Ser146-

¹²⁹ U. Cronshagen, P. Voland, H. F. Kern, *Eur. J. Cell Biol.* **1994**, 65, 366-377.

¹³⁰ H. Tateno, R. Yabe, T. Sato, A. Shibazaki, T. Shikanai, T. Gono, H. Narimatsu, J. Hirabayashi, *Glycobiology* **2012**, 22, 210-220.

¹³¹ R. Kleene, H. Dartsch, H. F. Kern, *Eur. J. Cell Biol.* **1999**, 78, 79-90.

¹³² K. Kumazawa-Inoue, T. Mimura, S. Hosokawa-Tamiya, Y. Nakano, N. Dohmae, A. Kinoshita-Toyoda, H. Toyoda, K. Kojima-Aikawa, *Glycobiology* **2012**, 22, 258-266.

¹³³ Kanagawa, M.; Satoh, T.; Ikeda, A.; Nakano, Y.; Yagi, H.; Kato, K.; Kojima-Aikawa, K.; Yamaguchi, Y. *Biochem. Biophys. Res. Commun.* **2011**, 404, 201-205.

Leu149), whereas sulfated oligosaccharides bind to a positively charged surface consisting of a cluster of basic amino acid residues.^{132,133}

Most of the mannose-binding animal C-type lectins, including DC-SIGN, the mannose receptor, Dectin-2, Mincle, and Langerin, are involved in host immunity through recognition of mannans of pathogenic bacteria.^{134,135,136} These lectins recognize other monosaccharides in addition. Mincle interacts with mannans of the pathogenic fungi, *Malassezia* and *Candida*, and activates the innate immune response through FcR γ and it is also known to be a receptor for mycobacterial cord factor.^{137,138,139} Langerin (also known as CD207) mediates carbohydrate-dependent internalization of pathogens on Langerhans cells, an initial stage of the adaptive immune response.¹⁴⁰ Langerin has diverse glycan-binding preferences including the pathogenic mannans of *Malassezia* and *Candida* and also 6-sulfated galactose such as in keratan sulfate.¹⁴¹

The majority of the above-mentioned mammalian lectins are signaling molecules which have trans-membrane domains that help to localize the proteins to specific membrane regions, like rafts or microdomains, and help in transmitting signals into the cell. Others are secreted mammalian lectins like MBL, a liver-derived serum protein which plays a role in the innate immune response by binding to the surface glycans of a wide range of pathogens where it can activate the complement system or act directly as an opsonin.^{6,142} The proteins of the Reg family are secreted proteins containing a C-type lectin-like domain, and they play a role in pancreatic function and associated diseases.¹⁴³ Human RegIII, which is expressed and secreted by intestinal cells, binds proteoglycans on the surface of Gram-positive bacteria, and kills it in a calcium-independent manner.¹⁴⁴ RegI α binds and aggregates several bacterial

¹³⁴ K. Drickamer, *Curr. Opin. Struct. Biol.* **1999**, *9*, 585-560.

¹³⁵ C. G. Figdor, Y. van Kooyk, G. J. Adema, *Nat. Rev. Immunol.* **2002**, *2*, 77-84.

¹³⁶ T. B. Geijtenbeek, S. I. Gringhuis, *Nat. Rev. Immunol.* **2009**, *9*, 465-479.

¹³⁷ C. A. Wells, J. A. Salvage-Jones, X. Li, K. Hitchens, S. Butcher, R. Z. Murray, A. G. Beckhouse, Y. L. Lo, S. Manzanero, C. Cobbold, K. Schroder, B. Ma, S. Orr, L. Stewart, D. Lebus, P. Sobieszczuk, D. A. Hume, J. Stow, H. Blanchard, R. B. Ashman, *J. Immunol.* **2008**, *180*, 7404-7413.

¹³⁸ S. Yamasaki, M. Matsumoto, O. Takeuchi, T. Matsuzawa, E. Ishikawa, M. Sakuma, H. Tateno, J. Uno, J. Hirabayashi, Y. Mikami, K. Takeda, S. Akira, T. Saito, *Proc. Natl. Acad. Sci. U S A* **2009**, *106*, 1897-1902.

¹³⁹ E. Ishikawa, T. Ishikawa, Y. S. Morita, K. Toyonaga, H. Yamada, O. Takeuchi, T. Kinoshita, S. Akira, Y. Yoshikai, S. Yamasaki, *J. Exp. Med.* **2009**, *206*, 2879-2888.

¹⁴⁰ L. de Witte, A. Nabatov, M. Pion, D. Fluitsma, M. A. de Jong, T. de Gruijl, V. Piguet, Y. van Kooyk, T. B. Geijtenbeek, *Nat. Med.* **2007**, *13*, 367-371.

¹⁴¹ H. Tateno, K. Ohnishi, R. Yabe, N. Hayatsu, T. Sato, M. Takeya, H. Narimatsu, J. Hirabayashi, *J. Biol. Chem.* **2010**, *285*, 6390-6400.

¹⁴² R. A. Childs, K. Drickamer, T. Kawasaki, S. Thiel, T. Mizuochi, T. Feizi, *Biochem. J.* **1989**, *262*, 131-138.

¹⁴³ E. Laurine, X. Manival, C. Montgelard, C. Bideau, J. L. Berge-LeFranc, M. Erard, J. M. Verdier, *Biochim. Biophys. Acta* **2005**, *1727*, 177-187.

¹⁴⁴ H. L. Cash, C. V. Whitham, C. L. Behrendt, L. V. Hooper, *Science* **2006**, *313*, 1126-1130.

strains, including Gram-positive and -negative as well as aerobic or anaerobic bacteria.¹⁴⁵ In addition RegIV binds mannan at two calcium ion-independent sites.¹⁴⁶

Similar to the C-type lectins, ZG16p, binds pathogenic fungi *Candida* and *Malassezia* in a mannose dependent manner.¹³⁰ Therefore it is possible that human ZG16p is involved in the gastrointestinal immune system through binding target glycans of pathogens. To investigate the binding properties of ZG16p on a molecular level a screening was performed employing a pathogen-related glycan microarray to identify novel interaction partners of this human lectin. Thereby it was revealed that PIM1 and PIM2 (Figure 4.1), which are major cell wall components of some pathogenic bacteria including *M. tuberculosis* (see Chapter 1.2), bind to ZG16p. To elucidate the binding mode of ZG16p with the PIMs in solution synthetic carbohydrates **1** and **2** were prepared and utilized as probes in STD-NMR experiments. These findings raise the possibility that human ZG16p may be involved in mucosal defense against mycobacteria through recognitions of short PIM saccharides on the cell surface of these pathogens.

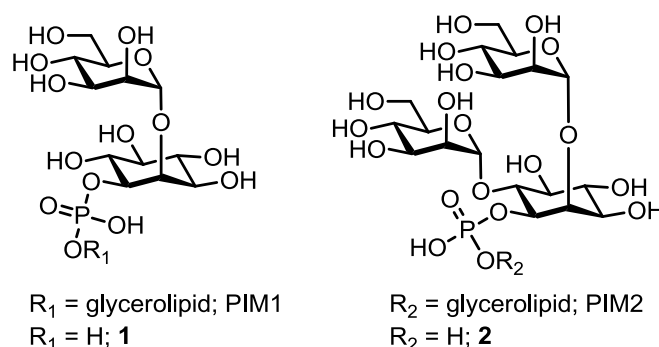


Figure 4.1: Chemical structures of PIM1 and PIM2 as well as synthetic compounds **1** and **2**.

¹⁴⁵ J. Iovanna, J. M. Frigerio, N. Dusetti, F. Ramare, P. Raibaud, J. C. Dagorn, *Pancreas* **1993**, *8*, 597-601.

¹⁴⁶ M. R. Ho, Y. C. Lou, S. Y. Wei, S. C. Luo, W. C. Lin, P. C. Lyu, C. Chen, *J. Mol. Biol.* **2010**, *402*, 682-695.

4.2 Identification of Novel Binding Partners of ZG16p Using a Carbohydrate Microarray

It was speculated that ZG16p plays a role in the host immune defense *via* binding cell-wall glycans of pathogenic bacteria. Therefore a carbohydrate microarray analysis¹⁴⁷ of ZG16p using a pathogen-related microarray was performed (Figure 4.2A, page 133).^{*} This array comprised a small set of glycoconjugates, lipid-linked glycans and polysaccharides, derived from mycobacteria and fungal pathogens. Mannose-containing neoglycolipids of the mammalian type served as controls. Wild type ZG16p bound strongly to PIM1 and PIM2 (arrayed as a mixture), exhibiting fluorescent intensities similar to the positive controls Man α -O-Thr and Man α -O-Ser. Interestingly, the intensity associated with PIM5 and PIM6 (arrayed as a mixture) was much lower. PIM2 and PIM6 are the two most abundant classes of PIMs found in *M. bovis*, *M. tuberculosis* H37Rv, and *M. smegmatis* 607.¹⁴⁸ Evidently ZG16p preferentially binds PIM1 and PIM2 rather than PIM6. DC-SIGN, through its interaction with PIMs, is considered to be a key molecule during infection with *M. tuberculosis*.¹⁴⁹ In contrast to ZG16p, DC-SIGN preferentially binds PIM5 and PIM6, rather than the shorter PIM1 and PIM2.⁹⁵ Compared to the wild type ZG16p, the D151N mutant showed little or no binding to the abovementioned probes (Figure 4.2B), which is in accord with previously published data.¹³⁰ LAM and LM, the major glycolipids found in the cell wall of all the *Mycobacterium* species, elicited little or no binding signals. LAM and LM from *M. tuberculosis* were well bound by plant lectin Con A, which was included as a positive control (Figure 4.2C). ZG16p showed no significant binding towards *M. tuberculosis* cord factor TDM, sulfolipids and arabinogalactans, or fungal derived glucan polysaccharides. The murine Dectin-1, which was analyzed in parallel for comparison, showed the predicted binding to curdlan, a β 1 \rightarrow 3 linked Glc polysaccharide (Figure 4.2D).¹⁵⁰

¹⁴⁷ Y. Liu, R. A. Childs, A. S. Palma, M. A. Campanero-Rhodes, M. S. Stoll, W. Chai, T. Feizi, *Methods Mol. Biol.* **2012**, 808, 117-136.

^{*} Microarray was fabricated and analyzed by Dr. Yan Liu (Glycosciences Laboratory, Imperial College, London). ZG16p was expressed and purified by A. Ikeda (Structural Glycobiology Team, RIKEN, Tokyo).

¹⁴⁸ M. Gilleron, V. F. Quesniaux, G. Puzo, *J. Biol. Chem.* **2003**, 278, 29880-29889.

¹⁴⁹ N. N. Driessen, R. Ummels, J. J. Maaskant, S. S. Gurcha, G. S. Besra, G. D. Ainge, D. S. Larsen, G. F. Painter, C. M. Vandenbroucke-Grauls, J. Geurtsen, B. J. Appelmelk, *Infect. Immun.* **2009**, 77, 4538-4547.

¹⁵⁰ A. S. Palma, T. Feizi, Y. Zhang, M. S. Stoll, A. M. Lawson, E. Díaz-Rodríguez, M. A. Campanero-Rhodes, J. Costa, S. Gordon, G. D. Brown, W. Chai, *J. Biol. Chem.* **2006**, 281, 5771-5779.

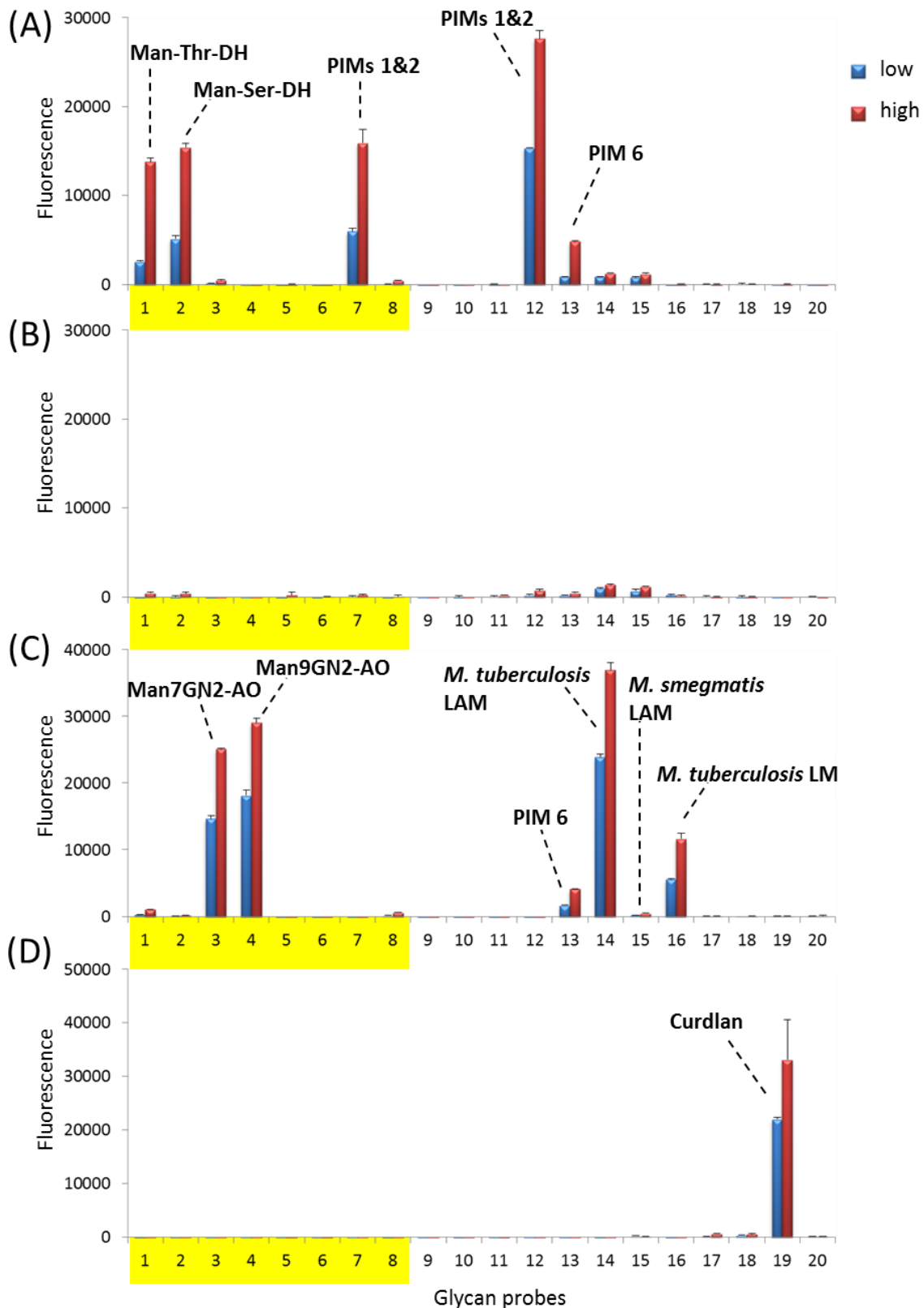


Figure 4.2: Microarray analyses using a small pathogen-related array comprising 20 glycan probes (lipid-tagged probes or polysaccharides). The fluorescence intensities for the wild-type ZG16p (A) and D151N mutant (B) are shown, together with those for the plant lectin Con A (C) and murine C-type lectin Dectin-1 (D) which were included for comparison. The list of glycan probes and their information can be found in the materials and methods section. Each probe was printed at two levels indicated with a blue bar for low level and a red bar for high level. Shaded in yellow are probes printed at 2 and 5 fmol/spot; the remaining probes were printed at 0.03 and 0.1 ng/spot.

4.3 Chemical Synthesis of PIM Glycans

Phosphoglycans **1** and **2** were prepared according to modified reported procedures (Scheme 4.1, page 135).^{151,152,153,154,155,156} The carbohydrates **1** and **2** utilized in our NMR experiments required to be soluble in water, which is why a monoester of phosphoric acid was installed at the O1-position of *myo*-Ino instead of a phosphodiester bearing a DAG moiety. The syntheses of **1** and **2**, commenced from the common *myo*-Ino building block **3**⁹⁴. To prepare **1**, a temporary PMB ether was selectively placed at the O2 position of **3** followed by benzylation and acidic cleavage to furnish glycosyl acceptor **4** in 58% yield over three steps. Glycosylation of **4** with phosphate **5**¹⁵⁷ at $-40\text{ }^{\circ}\text{C}$ in toluene exclusively formed the α -linked pseudodisaccharide **6** in 84% yield (Man-1; $^1J_{\text{C1-H1}} = 175\text{ Hz}$). Isomerization of the allyl ether using *in situ* generated iridium hydride¹⁰⁵ and hydrolysis of the corresponding enol ether unveiled an alcohol function at the O1 position of the *myo*-Ino. Phosphonylation with the mixed anhydride of pivalic acid and *H*-phosphonate **7**¹⁵⁸ followed by oxidation provided the triethylammonium salt **8** in 73% yield over three steps starting from **6**. Subjecting **8** to deacetylation and subsequent final hydrogenolysis over palladium in methanol yielded **1** in an excellent yield of 97% over two steps.

The synthesis of **2** continued with a double glycosylation of **3** with glycosylphosphate **5** under conditions similar to those used in synthesis of **6**. Pseudotrisaccharide **9** was obtained in 62% yield and the α -configuration of both anomeric linkages could be confirmed (Man-1; $^1J_{\text{C1-H1}} = 173$ and 176 Hz , respectively). Exposure of **9** to PdCl_2 in a mixture of CH_2Cl_2 and methanol selectively removed the allyl ether in 64% yield. Final phosphorylation of the corresponding alcohol **10** with phosphonate **7** formed phosphate **11**, which was deacetylated and submitted to hydrogenolysis to provide **2** in 49% yield over four steps.

¹⁵¹ P. S. Patil, S. C. Hung, *Chem. Eur. J.* **2009**, *15*, 1091-1094.

¹⁵² A. Ali, M. R. Wenk, M. J. Lear, *Tetrahedron Lett.* **2009**, *50*, 5664-5666.

¹⁵³ B. S. Dyer, J. D. Jones, G. D. Ainge, M. Denis, D. S. Larsen, G. F. Painter, *J. Org. Chem.* **2007**, *72*, 3282-3288.

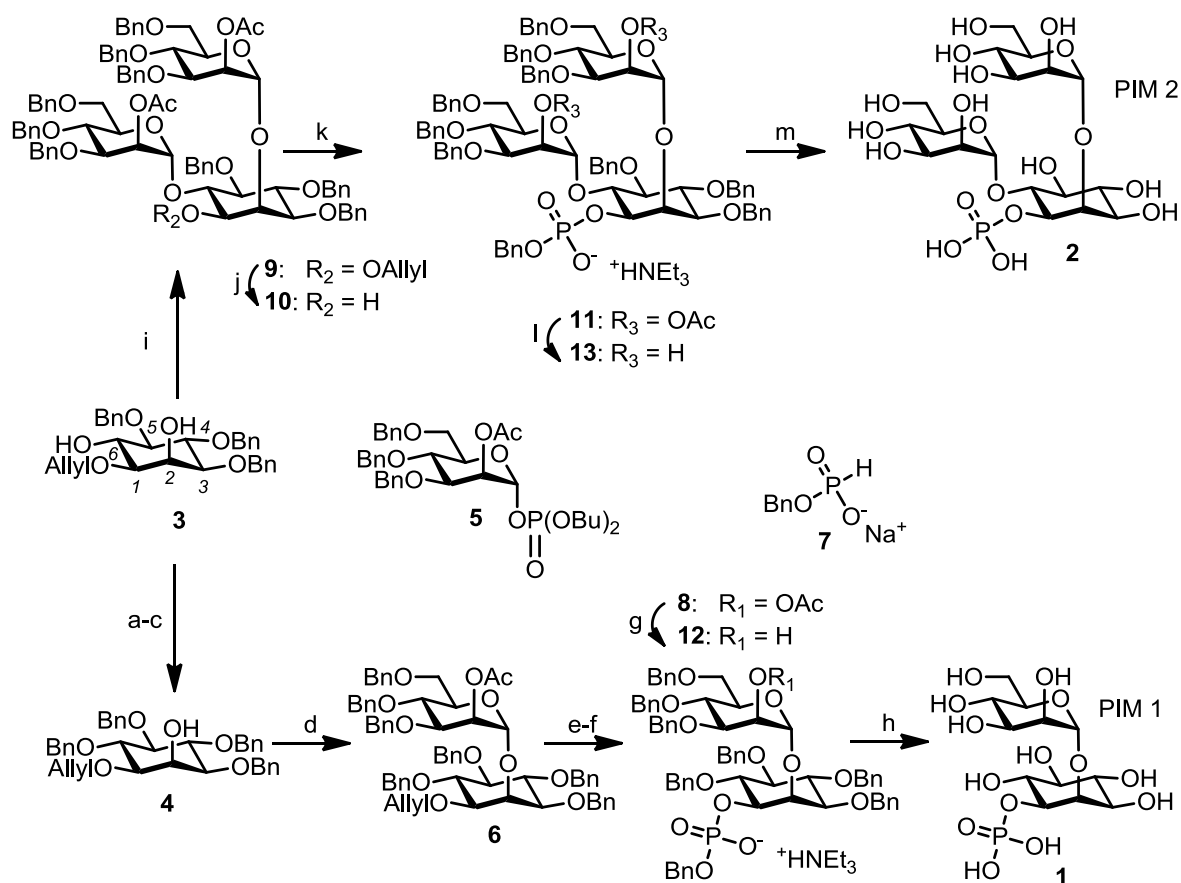
¹⁵⁴ G. D. Ainge, J. Hudson, D. S. Larsen, G. F. Painter, G. S. Gill, J. L. Harper, *Bioorg. Med. Chem.* **2006**, *14*, 5632-5642.

¹⁵⁵ A. Stadelmaier, R. R. Schmidt, *Carbohydr. Res.* **2003**, *338*, 2557-2569.

¹⁵⁶ C. J. J. Elie, C. E. Dreef, R. Verduyn, G. A. van der Marel, J. H. van Boom, *Tetrahedron* **1989**, *45*, 3477-3486.

¹⁵⁷ A. Ravidà, X. Liu, L. Kovacs, P. H. Seeberger, *Org. Lett.* **2006**, *8*, 1815-1818.

¹⁵⁸ L. Knerr, X. Pannecoucke, G. Schmitt, B. Luu, *Tetrahedron Lett.* **1996**, *37*, 5123-5126.



Scheme 4.1: Synthesis of carbohydrate NMR probes **1** and **2**. *Reagents and conditions:* (a) PMBCl (1 equiv), NaH, DMF, $-20\text{ }^{\circ}\text{C}$, 41% (69% based on recovered starting material); (b) BnBr, NaH, DMF, $0\text{ }^{\circ}\text{C}$, 90%; (c) CHCl_3/TFA (9:1), 93%; (d) **7** (1.3 equiv), TMSOTf, toluene, $-40\text{ }^{\circ}\text{C}$, 84%; (e) i. $[\text{Ir}(\text{COD})(\text{PPh}_2\text{Me})_2]\text{PF}_6$, H_2 , THF; ii. $\text{HCl}_{(\text{aq})}$, 92%; (f) i. **9**, PivCl, Py; ii. I_2 , H_2O , 79%; (g) NaH, MeOH, 99%; (h) 10% Pd/C, H_2 , MeOH, 98%; (i) **7** (2.6 equiv), TMSOTf, toluene, $-40\text{ }^{\circ}\text{C}$, 62%; (j) PdCl_2 , $\text{CH}_2\text{Cl}_2/\text{MeOH}$ (1:1), 64%; (k) i. **9**, PivCl, Py; ii. I_2 , H_2O , 68%; (l) NaH, MeOH, 78%; (h) 10% Pd/C, H_2 , MeOH, 92%.

4.4 STD-NMR Analysis of the Interaction between PIM1/2 and ZG16p

STD-NMR is now widely applied in the analysis of various types of binding events, including protein-small molecular weight ligand screenings.^{159,160,161} STD-NMR is applicable for analyses of biological interactions occurring over a wide K_D range (0.1 μM – 10 mM), and thus is eminently suitable for the study of lectin-glycan binding events.¹⁶²

The technique is based on the determination of the difference between two NMR experiments of the same sample and can identify the binding epitope of a ligand on an atomic level (Figure 4.3., page 137).¹⁶³ In the first experiment (the “*on-resonance*” spectrum) the protein of interest is selectively saturated (multiple pulses at a resonance where no ligand signals are present, e.g. 0.0 to -1.0 ppm). Saturation spreads *via* the process of spin diffusion over the whole protein. At the event of ligand binding the saturation is transferred from the protein to the small molecule by intermolecular ^1H - ^1H cross-relaxation at the protein-small molecule interface. Therefore protons of binding ligands, which are in close contact with the investigated protein, receive a more pronounced saturation effect that manifests itself in decreased signal intensities in the “*on-resonance*” spectrum. After the binding event the ligand dissociates back into the solution where the saturated state persists. The population of saturated ligands only increases over the time during the experiment when the on- and off-rates of the binding event are in a range that allows fast exchange of the ligand molecules. Hence tight binding interactions (K_D values in the nM region) cannot be studied with this method, because the population of saturated ligands would be too small to be detectable. This of course also applies to interactions that are too weak (K_D values in the M range).

The second experiment (the “*off-resonance*” spectrum) uses the same STD pulse sequence as the first one, but the sample is irradiated at a resonance (e.g. 30-40 ppm) that does not saturate any nucleus. This results essentially in a 1D- ^1H -NMR spectrum.

¹⁵⁹ M. Mayer, B. Meyer, *J. Am. Chem. Soc.* **2001**, *123*, 6108-6117.

¹⁶⁰ M. Mayer, B. Meyer, *Angew. Chem. Int. Ed.* **1999**, *38*, 1784-1788.

¹⁶¹ B. Meyer, T. Peters, *Angew. Chem. Int. Ed.* **2003**, *42*, 864-890.

¹⁶² A. Ardá, P. Blasco, D. Varón Silva, V. Schubert, S. André, M. Bruix, F. J. Cañada, H. J. Gabius, C. Unverzagt, J. Jiménez-Barbero, *J. Am. Chem. Soc.* **2013**, *135*, 2667-2675.

¹⁶³ C. A. Lepre, J. M. Moore, J. W. Peng, *Chem. Rev.* **2004**, *104*, 3641-3676.

Subtraction of the “*on-resonance*” from the “*off-resonance*”-spectrum generates the STD spectrum that reveals only binding molecules and also gives structural information about their binding epitopes.

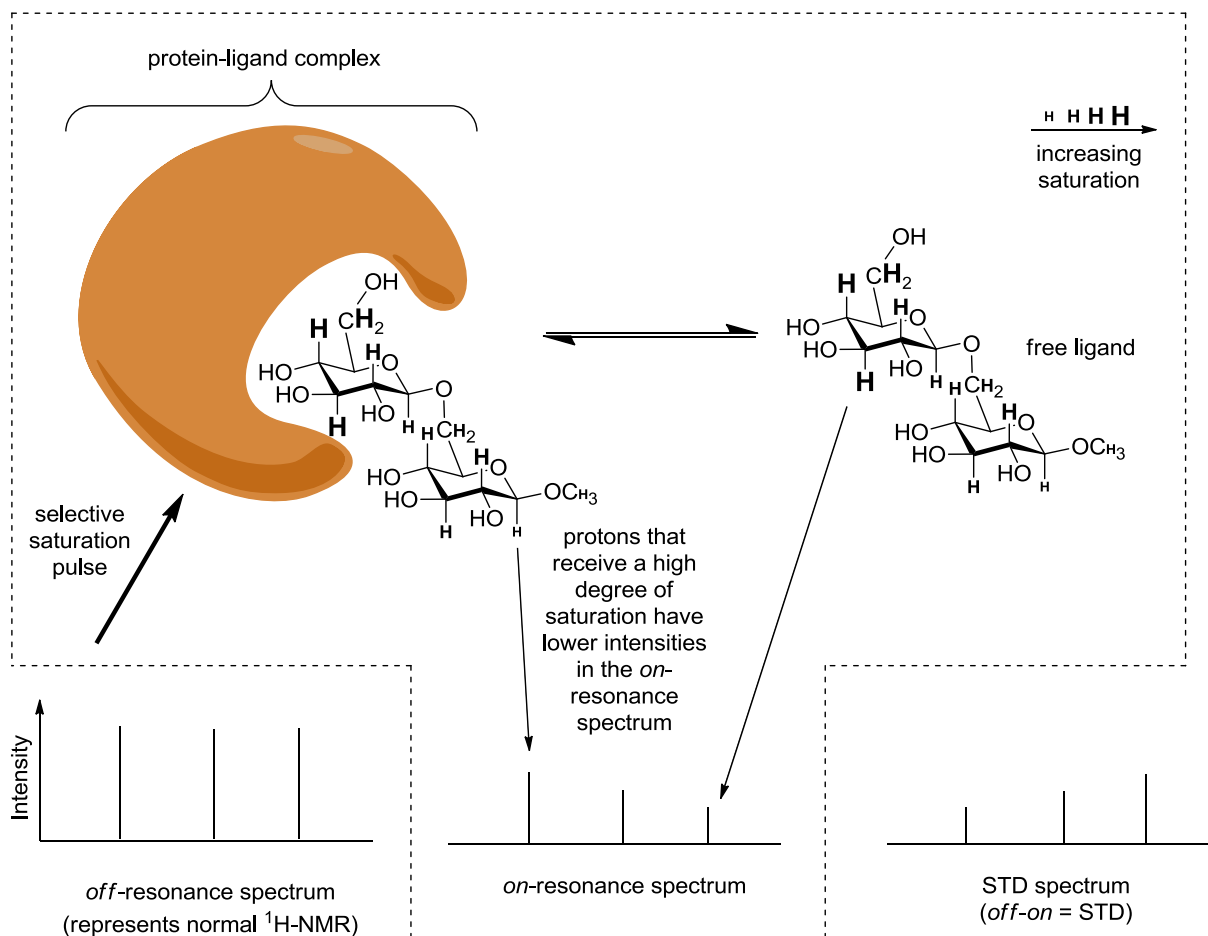


Figure 4.3: Schematic presentation of the events during the measurement of an “*on-resonance*”-spectrum that is needed for the generation of a STD spectrum (dashed polygon). Relative intensities representing the *off-* and STD spectrum are displayed as well.

To understand the interactions of ZG16p with the simple carbohydrate *O*-methyl- α -D-mannopyranoside (**14**) and the sugars **1** and **2**, in solution phase, STD-NMR spectra were collected in the presence of ZG16p (Figure 4.4, page 138). All three ligands exhibited potent STD-NMR signals. The observation clearly indicates that the main constituent of the STD-NMR spectra reflect the saturation transfer effect from ZG16p to the mannosides **1**, **2** and **14**, which confirms their binding.

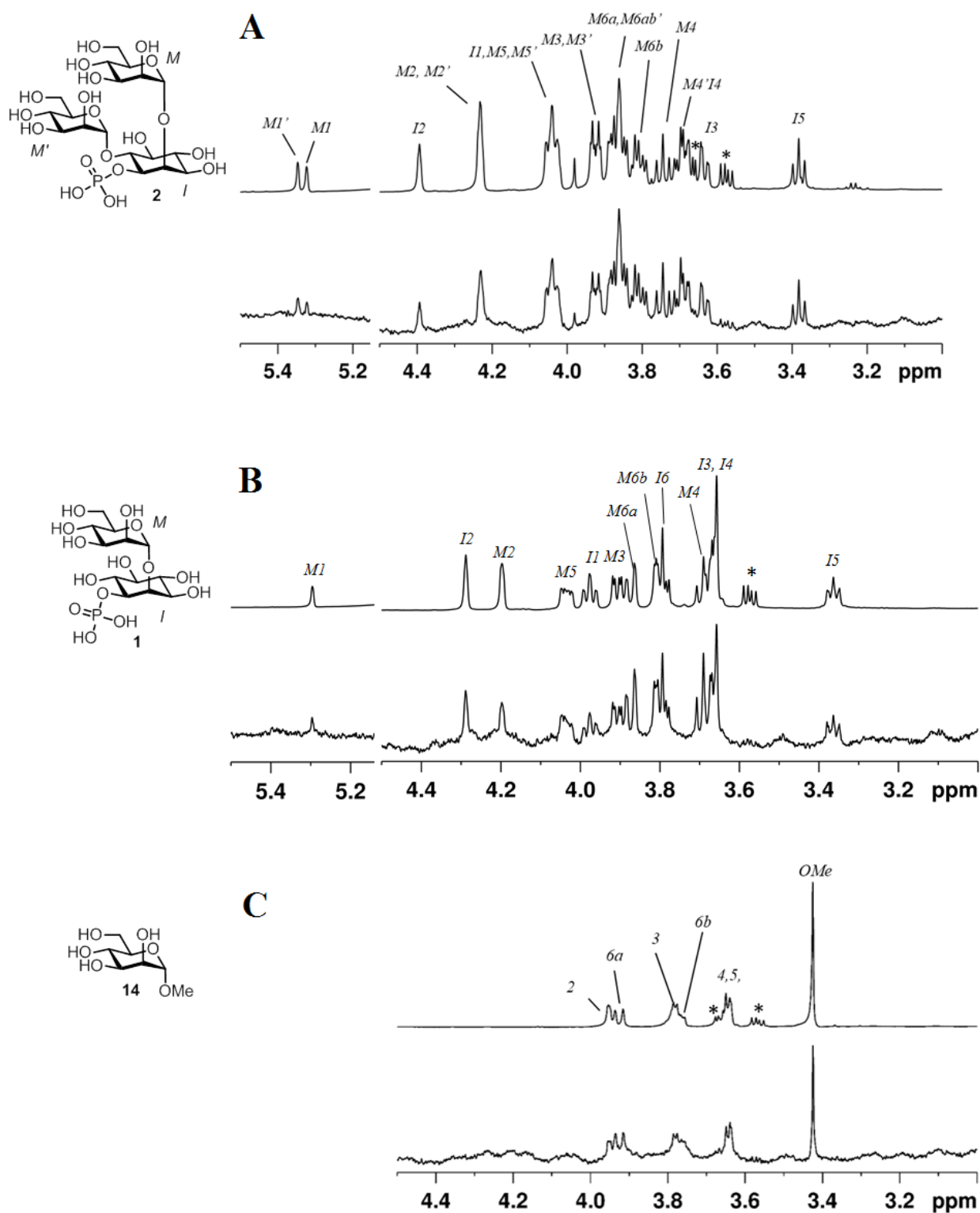


Figure 4.4: ^1H -NMR *off*-resonance spectra (straight baseline) and STD-NMR spectra of (A) **2**; (B) **1** and (C) **14** in the presence of ZG16p. In each case, there is a 100-fold excess of carbohydrate ligand over protein. Signals originating from residual glycerol are marked with an *. Signals of the ligands are indicated.

The binding epitopes determined by using the relative STD-amplification factor (%AF) revealed that the most pronounced interactions between all three ligands and ZG16p were *via*

protons H4, H5 and H6 of the mannose residue/s (Figure 4.5).^{*} In the case of the monosaccharide **14**, the binding epitope is mainly the pyranose ring (75-100%), whereas the methyl group at the anomeric position (57%) is interacting less with the protein. A similar binding epitope is apparent with glycan **1**. While the inositol moiety received a weaker saturation effect (65-70%), the H3 and H6 positions of the mannose residue showed the highest STD-NMR signal (80-100%). Therefore, the H3-H6 residue of the mannose was identified as the binding epitope of **1**. In the case of glycan **2**, STD-NMR spectra clearly indicated that ZG16p interacted almost equally with both mannose residues (H4-H6) and the H3 position of the *myo*-Ino.

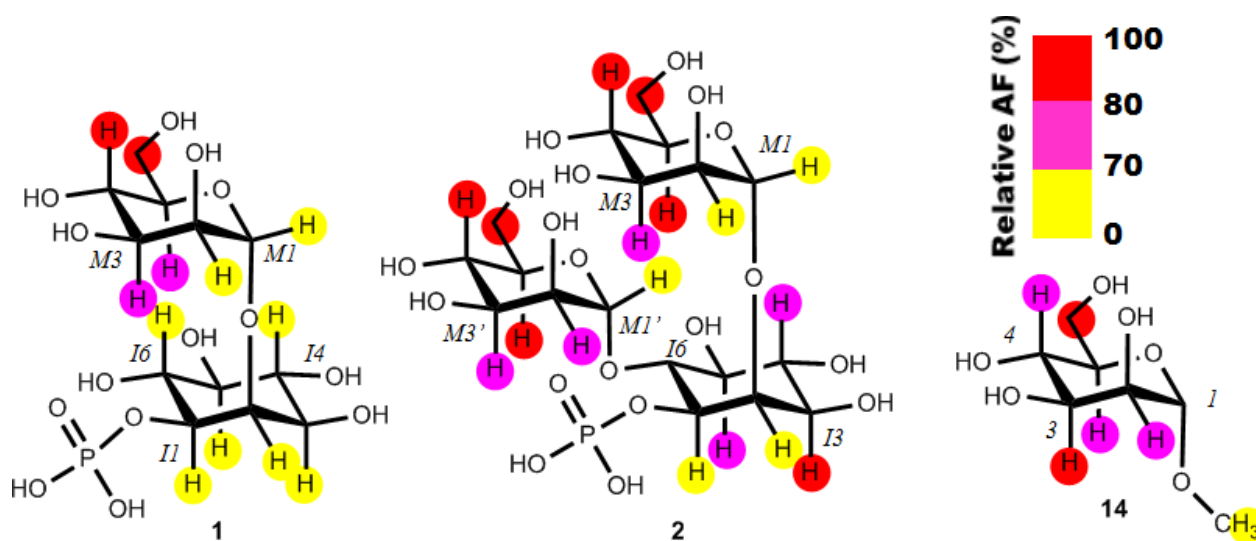


Figure 4.5: Binding epitopes determined by relative STD-AF(%) of sugar ligands **1**, **2** and **14**. An averaged AF-value was formally assigned to overlapping signals.

Intrigued by the obtained structural data our collaboration partners also performed 2D chemical shift perturbation experiments¹⁶⁴ employing ¹⁵N labeled ZG16p and the three ligands **1**, **2** and **14**. In addition a ¹³C/¹⁵N labeled ZG16p was produced that allowed full assignment of almost all peptide backbone ¹H/¹⁵N cross peaks using various 2D and 3D NMR techniques. Together with docking simulations a feasible binding model that describes the interaction between ZG16p and phosphoglycan **1** was determined. This model places most of the inositol moiety outside of the ligand-binding groove (Figure 4.6, page 140).

Natural PIMs have a hydrophobic phosphatidyl group attached to the O1-position of the Ino, which anchors it to the cell surface of mycobacteria and is crucial for interactions with different human proteins. For example, mouse CD1d, a known receptor of PIMs, has hydrophobic grooves wherein acyl chains of glycolipids are bound.¹⁶⁵ In contrast, ZG16p

^{*} STD-AF values were calculated by Dr. S. Hanashima (Structural Glycobiology Team, RIKEN, Tokyo).

¹⁶⁴ M. P. Williamson, *Prog. Nucl. Magn. Reson. Spectrosc.* **2013**, *73*, 1-16.

¹⁶⁵ D. M. Zajonc, G. D. Ainge, G. F. Painter, W. B. Severn, I. A. Wilson, *J. Immunol.* **2006**, *177*, 4577-4583.

lacks these structural motifs, and binding of this protein involves mainly the sugar moiety of PIMs.

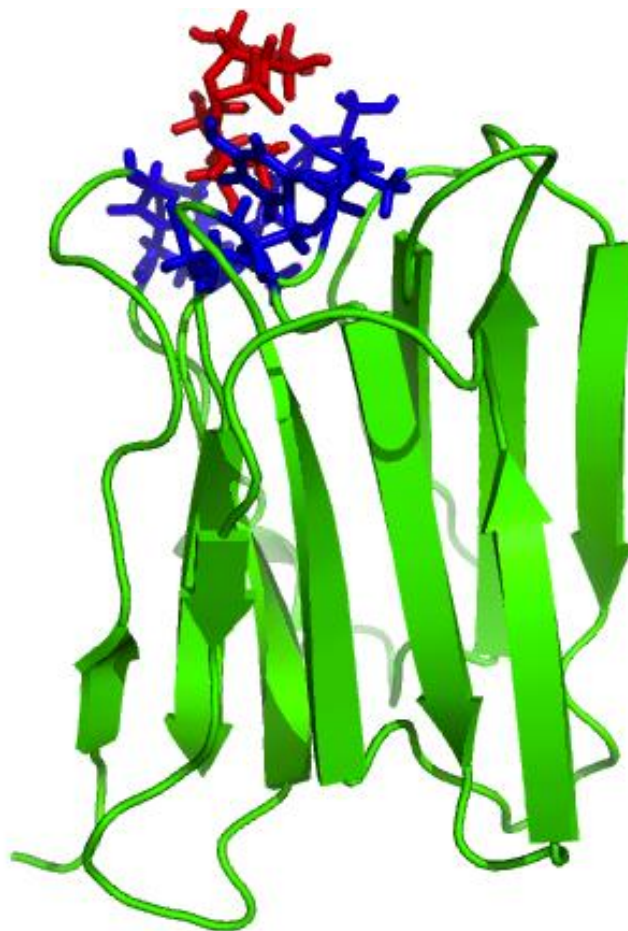


Figure 4.6: Binding model of glycan **1** to human ZG16p. Multiple binding modes of **1** are shown. The Ino moiety (colored in red) is placed outside the ligand-binding groove. The model was created with docking simulations using the crystal structure of glycerol-ZG16p (PDB ID; 3APA).¹³³

4.5 Possible Role of ZG16p in Mucosal Immune Response

The main portals of entry of tuberculosis and the nontuberculous mycobacteria are the respiratory tract and gastrointestinal tract. Gastrointestinal tuberculosis is a major health problem in many underdeveloped countries. PIMs are a class of glycolipids synthesized by all species of mycobacteria and are essential for normal growth and viability of mycobacteria. It could be likely that human ZG16p secreted into the intestine may be involved in the mucosal immune response by 'opsonizing' the bacteria through binding to short PIM structures. The fact that ZG16p also binds to endogenous GAGs using independent binding sites raises the question if ZG16p may function in the presence of 'co-factors': i.e. other macromolecules may interact with this human lectin to express the function cooperatively.

In the pancreas, ZG16p associates with the GPI-anchored protein GP-2 that has the ability to bind GAGs in the zymogene granule.¹⁶⁶ GP-2 is also expressed in epithelial M cells at Peyer's patches in the intestine, and is involved in the mucosal immune system.¹⁶⁷ ZG16p might associate with GP-2 at the M cell surface *via* GAGs and adapter molecules like annexins.¹⁶⁸ It was already hypothesized that in pancreatic acinar cells, GP-2 associates with glycosaminoglycan *via* annexin IV,¹⁶⁹ which is expressed in the intestine¹⁷⁰. In addition, GP-2 is involved in regulating endo- and exocytosis in the apical and basal plasma membrane.¹⁷¹ Binding of PIMs to ZG16p therefore could induce a specific interaction/signal cascade with GP-2 which maybe leads to endocytosis of mycobacteria or also secretion of different proteins/cytokines to kill the pathogen (Figure 4.7, page 142). These hypotheses are subjects for future investigations.

¹⁶⁶ K. Schmidt, M. Schrader, H. F. Kern, R. Kleene, *J. Biol. Chem.* **2001**, *276*, 14315-14323.

¹⁶⁷ K. Hase, K. Kawano, T. Nochi, G. S. Pontes, S. Fukuda, M. Ebisawa, K. Kadokura, T. Tobe, Y. Fujimura, S. Kawano, A. Yabashi, S. Waguri, G. Nakato, S. Kimura, T. Murakami, M. Iimura, K. Hamura, S. Fukuoka, A. W. Lowe, K. Itoh, H. Kiyono, H. Ohno, *Nature* **2009**, *462*, 226-230.

¹⁶⁸ T. Horlacher, C. Noti, J. L. de Paz, P. Bindschädler, P.; M.-L. Hecht, D. F. Smith, M. N. Fukuda, P. H. Seeberger, *Biochemistry* **2011**, *50*, 2650-2659.

¹⁶⁹ Y. Tsujii-Hayashi, M. Kitahara, T. Yamagaki, K. Kojima-Aikawa, I. Matsumoto, *J. Biol. Chem.* **2002**, *277*, 47493-47499.

¹⁷⁰ K. Kojima, H. K. Ogawa, N. Seno, K. Yamamoto, T. Irimura, T. Osawa, I. Matsumoto, *J. Biol. Chem.* **1992**, *267*, 20536-20539.

¹⁷¹ S. Fukuoka, S. D. Freedman, H. Yu, V. P. Sukhatme, G. A. Scheele, *Proc. Natl. Acad. Sci. U S A* **1992**, *89*, 1189-1193.

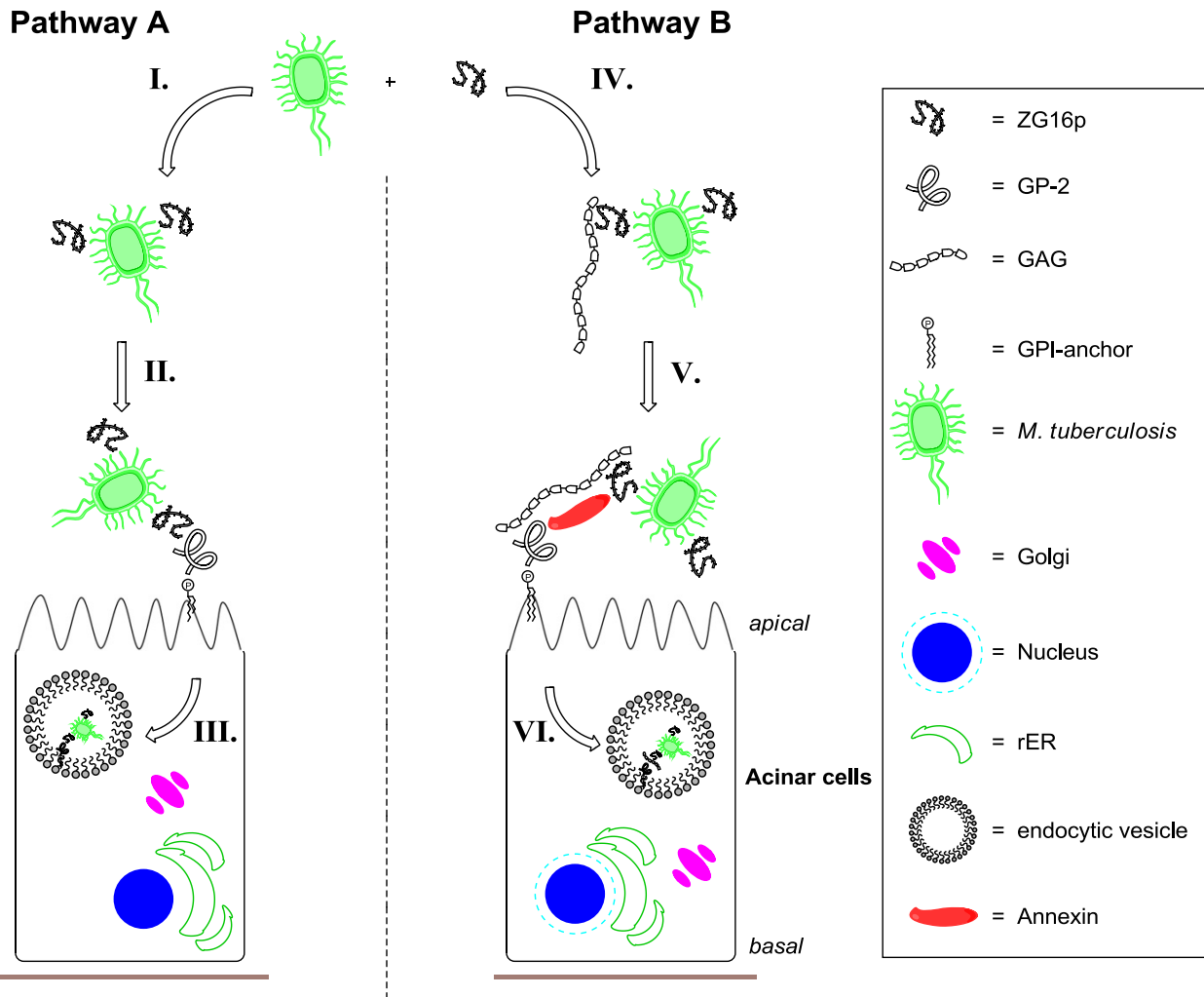


Figure 4.7: Hypotheses for the mode of action of ZG16p. *Pathway A:* **I.** ZG16p binds to PIMs on the surface of *M. tuberculosis*; **II.** After binding to the mycobacterium, ZG16p interacts with the GPI-anchored GP-2; **III.** The binding event leads to GP-2 mediated endocytosis of the pathogen/ZG16p complex and clearance of the mycobacterium from the intestines; *Pathway B:* **IV.** ZG16p binds to PIMs on the surface of *M. tuberculosis* and simultaneously to extracellular GAGs; **V.** Annexins mediate an interaction between ZG16p and the GPI-anchored GP-2 via GAGs; **VI.** The binding event leads to GP-2 mediated endocytosis of the pathogen/GAG/Annexin/ZG16p complex and clearance of the mycobacterium from the intestines.

4.6 Experimental Part

Materials and Methods:

Expression and Preparation of ZG16p: Recombinant ZG16p protein and the mutant D151N were prepared by Akemi Ikeda (Structural Glycobiology Team, RIKEN, Tokyo) using the pCold-MBP vector, according to the previously reported procedures.¹³³ For microarray analyses, (GST)-tagged ZG16p protein (21-167) and its mutant GST-ZG16p (D151N) were prepared by Akemi Ikeda (Structural Glycobiology Team, RIKEN, Tokyo) using the pCold-GST vector, according to the previously reported procedures.^{172,173}

Glycan Microarray: The microarrays comprised four mannose-containing neoglycolipids¹⁷⁴, nine compounds (antigen preparations from Mycobacteria) received from Biodefense and Emerging Infections Research Resources Repository (BEI Resources), and three fungal derived glucan polysaccharides (Table 4.1, page 144). The arrays were generated robotically by Dr. Liu Yan (Glycosciences Laboratory, Imperial College, London) using a non-contact arrayer on nitrocellulose coated microarray slides.¹⁴⁷ All the probes are arrayed with carrier lipids (phosphatidylcholine and cholesterol; Sigma Aldrich) as described, except for *M. tuberculosis* arabinogalactan and the glucan polysaccharides (positions 17-19) which were arrayed in the absence of the lipid carriers. Microarray analyses with GST-tagged ZG16p proteins GST-ZG16p and GST-ZG16p (D151N) were performed by Dr. Yan Liu (Glycosciences Laboratory, Imperial College, London) according to the previously reported procedures.¹⁵⁰ In brief, microarray slides were blocked at ambient temperature for 60 min with 3% w/v bovine serum albumin (BSA) in phosphate buffered saline (PBS). The GST-ZG16p and GST-ZG16p (D151N) were incubated at 100 μgml^{-1} in the presence of 1% BSA for 90 min, followed by rabbit anti-GST antibody Z-5 (Santa Cruz), 1:200, and then biotinylated anti-rabbit IgG (Sigma), 1:200. Biotinylated Con A (Vector) and hexa-His-tagged murine Dectin-1 (Sino Biological) were analysed at 0.5 $\mu\text{g/ml}$ and 15 $\mu\text{g/ml}$, respectively. The His-tagged Dectin-1 was overlaid tested as a protein-antibody complex that was prepared by pre-incubating with mouse monoclonal anti-poly-histidine and biotinylated anti-mouse IgG antibodies (both from Sigma) at a ratio of 1:3:3 (by weight). Binding was detected with Alexa Fluor-647-labelled streptavidin (Molecular Probes).

¹⁷² T. Satoh, Y. Chen, D. Hu, S. Hanashima, K. Yamamoto, Y. Yamaguchi, *Mol. Cell* **2010**, *40*, 905-916.

¹⁷³ K. Hayashi, C. Kojima, *J. Biomol. NMR* **2010**, *48*, 147-155.

¹⁷⁴ Y. Liu, T. Feizi, M. A. Campanero-Rhodes, R. A. Childs, Y. Zhang, B. Mulloy, P. G. Evans, H. M. Osborn, D. Otto, P. R. Crocker, W. Chai, *Chem. Biol.* **2007**, *14*, 847-859.

Glycan	Probe	Structure
1	Man-Thr-DH	Man α -Thr-DHPE
2	Man-Ser-DH	Man α -Ser-DHPE
3	Man7(D1)GN2-AO	Man α -6 Man α -3Man α -6 Man β -4GlcNAc β -4GlcNAc-AO Man α -2Man α -2Man α -3
4	Man9GN2-AO	Man α -2Man α -6 Man α -2Man α -3Man α -6 Man β -4GlcNAc β -4GlcNAc-AO Man α -2Man α -2Man α -3
5	<i>M. tuberculosis</i> TDM	Purified Trehalose Dimycolate (TDM) from <i>Mycobacterium tuberculosis</i> , Strain H37Rv (BEI Number NR-14844)
6	TDB	Trehalose-6,6-dibehenate (TDB), a synthetic analogue of TDM (SIGMA)
7	<i>M. tuberculosis</i> PIMs 1&2	Purified PIM 1 & 2 from <i>Mycobacterium tuberculosis</i> , Strain H37Rv (BEI Number NR-14846)
8	<i>M. tuberculosis</i> PIM 6	Purified PIM 6 from <i>Mycobacterium tuberculosis</i> , Strain H37Rv (BEI Number NR-14847)
9	<i>M. tuberculosis</i> MME	Purified Mycolic Acid Methyl Esters from <i>Mycobacterium tuberculosis</i> , Strain H37Rv (BEI Number NR-14854)
10	<i>M. tuberculosis</i> TDM	Purified Trehalose Dimycolate from <i>Mycobacterium tuberculosis</i> , Strain H37Rv (BEI Number NR-14844)
11	<i>M. tuberculosis</i> Sulfolipid-1	Purified Sulfolipid-1 from <i>Mycobacterium tuberculosis</i> , Strain H37Rv (BEI Number NR-14845)
12	<i>M. tuberculosis</i> PIMs 1&2	Purified PIM 1 & 2 from <i>Mycobacterium tuberculosis</i> , Strain H37Rv (BEI Number NR-14846)
13	<i>M. tuberculosis</i> PIM 6	Purified PIM 6 from <i>Mycobacterium tuberculosis</i> , Strain H37Rv (BEI Number NR-14847)
14	<i>M. tuberculosis</i> LAM	Purified Lipoarabinomannan (LAM) from <i>Mycobacterium tuberculosis</i> , Strain H37Rv (BEI Number NR-14848)
15	<i>M. smegmatis</i> LAM	Purified LAM from <i>Mycobacterium smegmatis</i> (BEI Number NR-14849)
16	<i>M. tuberculosis</i> LM	Purified Lipomannan (LM) from <i>Mycobacterium tuberculosis</i> , Strain H37Rv (BEI Number NR-14850)
17	<i>M. tuberculosis</i> arabinogalactan	Purified arabinogalactan from <i>Mycobacterium tuberculosis</i> , Strain H37Rv (BEI Number NR-14852)
18	Pullulan from <i>Pullularia pullulans</i>	Mixed-linked α 1-4, α 1-6 glucose polysaccharide (Megazyme)
19	Curdlan from <i>Alcaligenes faecalis</i>	β 1-3 glucose polysaccharide (dissolved in 50 mM NaOH) (Megazyme)
20	Pustulan from <i>Umbilicaria papulosa</i>	β 1-6 glucose polysaccharide (CalBiochem)

Table 4.1: List of glycan probes included in microarray analyses. The neoglycolipids 1-4 were prepared either *via* coupling of the carboxylic acid moiety with the amino lipid DHPE (1 and 2) or oxime ligation of the reducing end of the glycan with AO (3 and 4). Shaded in yellow are probes printed at 2 and 5 fmol/spot; the rest were printed at 0.03 and 0.1 ng/spot.

NMR Experiments: STD-NMR spectra were recorded on a 600 MHz spectrometer (Bruker BioSpin) equipped with a TXI probe. Non-labeled ZG16p (50 μ M) in PBS (pH 7.4, 10 mM sodium phosphate buffer, 150 mM NaCl 99% D₂O) was used for STD-NMR experiments and 100-fold excess of ligands **14** (Sigma Aldrich), **1** and **2** were titrated into the protein solution. The probe temperature was set to 5 °C. The *on*-resonance spectra were obtained *via* saturation of the protein at 0 or -1 ppm with a 50 ms Gaussian 25 Hz pulse train (N = 60) and reference

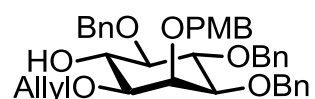
spectra were obtained with irradiation at 40 ppm (*off*-resonance). The *on*-resonance and *off*-resonance spectra were collected in an interleaved manner, and accumulated into two different data sets. Water suppression was achieved using a WATERGATE pulse sequence with a 3-9-19 pulse train. In STD-NMR experiments, 64 scans with 3 repetition loops were required to obtain a good signal to noise ratio, and protein signals were partially suppressed using a $T_{1\rho}$ filter with a 0.3-1.0 ms trim pulse. In binding epitope analyses, which was performed by Dr. Shinya Hanashima (Structural Glycobiology Team, RIKEN, Tokyo) the relative signal intensities were calculated based on the following equation:

$$\text{STD-AF} = \frac{(I_{\text{off}} - I_{\text{on}})}{I_{\text{off}}} \times (\text{ligand excess})$$

, with I_{on} : intensity of *on*-resonance signals and I_{off} : intensity of *off*-resonance signals. The AF values were normalized within each glycan structure with the highest AF value assigned 100%. ^1H -NMR chemical shifts were calibrated according to an external standard chemical shift of singlet 4,4-dimethyl-4-silapentane-1-sulfonic acid, set at 0 ppm. The assignment of all ^1H and ^{13}C NMR signals of phosphoglycan **1** and **2** in deuterated PBS (pH = 7.4) was done by Dr. Shinya Hanashima (Structural Glycobiology Team, RIKEN, Tokyo) using ^1H - ^1H double quantum filtered correlation spectroscopy, ^1H - ^1H NOESY, ^1H - ^{13}C HSQC and ^1H - ^{13}C HSQC-TOCSY experiments measured at 5 °C.

Synthetic Procedures:

1-*O*-Allyl-2-*O*-*para*-methoxy-benzyl-3,4,5-tri-*O*-benzyl-D-*myo*-inositol (**15**)

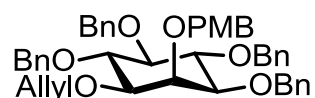


Diol **3** (91 mg, 185 μmol)* and TBAI (68.5 mg, 185 μmol) were dissolved in DMF (2 mL). The solution was cooled down to -20°C using ice/NaCl and NaH (22.3 mg, 927 μmol) was added. The slurry was stirred for 5 min before PMBCl (25.3 μL , 185 μmol) was added. The reaction mixture was stirred for 3h at -20°C before it was quenched with MeOH (200 μL). Water (7 mL) was added and the water phase was extracted with Et_2O (50 mL). The organic layer was washed with sat. NaHCO_3 solution (2x20mL), dried over Na_2SO_4 and evaporated to dryness. The residue was purified using column chromatography (*n*-hexane/ethyl acetate 3:1) to yield **15** as yellow oil (46 mg, 75 μmol , 41%; 38 mg of starting material were recovered):

* Prepared according to procedures described in Chapter 2.3 of this PhD thesis.

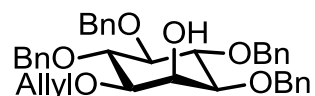
R_f (SiO₂, EtOAc/Hexane 1:2) = 0.55; ¹H NMR (400 MHz, CDCl₃) δ 7.32 – 7.13 (m, 17H), 6.75 (d, J = 8.4 Hz, 2H), 5.81 (ddd, J = 22.5, 10.7, 5.5 Hz, 1H, CH₂=CH-CH₂), 5.19 (d, J = 17.2 Hz, 1H, CH₂=CH-CH₂), 5.10 (d, J = 10.4 Hz, 1H, CH₂=CH-CH₂), 4.88 – 4.49 (m, 8H), 4.07 – 3.84 (m, 5H), 3.71 (s, 3H, OCH₃), 3.29 (t, J = 9.0 Hz, 2H), 3.01 (dd, J = 9.8, 1.6 Hz, 1H), 2.41 (bs, 1H, OH); ¹³C NMR (101 MHz, CDCl₃) δ 159.16, 139.03, 138.96, 138.53, 134.67, 131.04, 129.54, 128.50, 128.42, 128.18, 127.94, 127.73, 127.67, 127.63, 117.42, 113.68, 83.58, 81.55, 81.28, 79.98, 77.48, 77.16, 76.84, 75.93, 75.42, 73.72, 72.96, 72.92, 72.88, 71.20, 55.38. Spectral data were in good agreement with the literature.¹⁷⁵

1-*O*-Allyl-2-*O*-*para*-methoxy-benzyl-3,4,5,6-tetra-*O*-benzyl-*D*-myo-inositol (**16**)

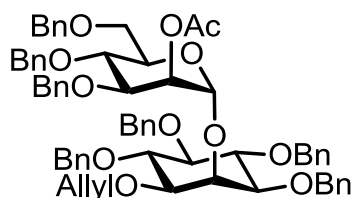


Alcohol **15** (46 mg, 75 μmol) was dissolved in DMF (2 mL). The solution was cooled down to 0°C and NaH (9 mg, 377 μmol) were added. Afterwards BnBr (17.9 μL, 151 μmol) was added and the reaction was stirred at 0 °C for 3 h. The reaction mixture was quenched with MeOH (200 μL) and water (10 mL) was added. The water phase was extracted with Et₂O (40 mL). The organic layer was washed with sat. NaHCO₃ solution (2x20 mL), dried over Na₂SO₄ and evaporated to dryness. The residue was purified using column chromatography (*n*-hexane/ethyl acetate 8:1) to yield **16** as colorless solid (47.5 mg, 68 μmol, 90%): R_f (SiO₂, EtOAc/Hexane 1:6) = 0.44; $[\alpha]_D^{20}$: + 4.7 (c = 1.00, CHCl₃); ATR-FTIR (cm⁻¹): 3033, 2891, 1610, 1510, 1454, 1068; ¹H NMR (400 MHz, CDCl₃) δ 7.38 – 7.21 (m, 27H), 6.84 (d, J = 8.6 Hz, 2H), 6.14 – 5.70 (m, 1H, CH₂=CH-CH₂), 5.30 (d, J = 17.1 Hz, 1H, CH₂=CH-CH₂), 5.17 (d, J = 10.9 Hz, 1H, CH₂=CH-CH₂), 4.93 – 4.85 (m, 4H), 4.84 – 4.75 (m, 4H), 4.62 (q, J = 11.6 Hz, 1H), 4.13 – 3.94 (m, 5H), 3.80 (s, 3H, OCH₃), 3.45 (t, J = 9.2 Hz, 1H), 3.34 (d, J = 10.1 Hz, 1H), 3.24 (d, J = 9.6 Hz, 1H); ¹³C NMR (101 MHz, CDCl₃) δ 159.13, 139.04, 138.61, 135.08, 131.20, 129.57, 128.46, 128.42, 128.26, 128.20, 127.87, 127.64, 127.55, 116.73, 113.66, 83.81, 81.82, 81.07, 80.90, 75.97, 73.76, 72.86, 71.76, 55.39; ESI-MS: m/z [M+Na]⁺ calcd for C₃₈H₄₂O₇ 723.3298, obsd 723.3303.

¹⁷⁵ X. Liu, Y.-U. Kwon, P. H. Seeberger, *J. Am. Chem. Soc.* **2005**, *127*, 5004-5005.

1-*O*-Allyl-3,4,5,6-tetra-*O*-benzyl-*D*-myo-inositol (4)

Fully protected inositol **16** (38.8 mg, 55 μmol) was dissolved in chloroform/TFA (1 mL, 9:1) and stirred for 30 min. The reaction mixture was diluted with toluene (3 mL) and solvents were evaporated. The residue was purified using column chromatography (*n*-hexane/ethyl acetate 4:1) to yield **4** as colorless oil (30 mg, 52 μmol , 93%). R_f (SiO_2 , EtOAc/Hexane 1:6) = 0.21; ^1H NMR (400 MHz, CDCl_3) δ 7.45 – 7.16 (m, 20H), 5.96 (ddd, $J = 22.8, 10.9, 5.7$ Hz, 1H, $\text{CH}_2=\text{CH}-\text{CH}_2$), 5.31 (dd, $J = 17.2, 1.4$ Hz, 1H, $\text{CH}_2=\text{CH}-\text{CH}_2$), 5.21 (d, $J = 10.4$ Hz, 1H, $\text{CH}_2=\text{CH}-\text{CH}_2$), 4.99 – 4.80 (m, 6H), 4.75 (s, 2H), 4.33 – 4.13 (m, 3H), 3.99 (dt, $J = 15.2, 9.5$ Hz, 2H), 3.53 – 3.38 (m, 2H), 3.32 (dd, $J = 9.6, 2.6$ Hz, 1H), 2.50 (bs, 1H, OH); ^{13}C NMR (101 MHz, CDCl_3) δ 138.86, 138.84, 138.83, 138.08, 134.80, 128.59, 128.47, 128.20, 128.14, 127.99, 127.95, 127.72, 127.70, 127.66, 117.57, 114.07, 83.23, 81.32, 81.30, 80.02, 79.73, 76.10, 76.08, 76.05, 72.92, 72.01, 67.81. Spectral data were in good agreement with Ref. [95].

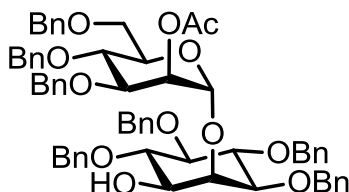
2-*O*-Acetyl-3,4,6-tri-*O*-benzyl- α -*D*-mannopyranosyl-(1 \rightarrow 2)-1-*O*-Allyl-3,4,5,6-tetra-*O*-benzyl-*D*-myo-inositol (6)

Inositol **4** (30 mg, 52 μmol) and phosphate **5**^{*} (50.6 mg, 67 μmol) were coevaporated with toluene (3x2 mL) and placed under HV for 30 min. The residue was dissolved in dry toluene (3 mL) and powdered MS4Å (100 mg) was added. The slurry was stirred at r.t. for 15 min before it was cooled down to -40°C . TMSOTf (12.1 μL , 67 μmol) was added and the reaction was stirred at -40°C for 2 h. The reaction was quenched with TEA (100 μL) and filtered through a pad of Celite®. Solvents were removed in vacuo and the residue was purified using column chromatography (*n*-hexane/ethyl acetate 6:1) to yield **6** as colorless oil (46 mg, 44 μmol , 84%): R_f (SiO_2 , EtOAc/Hexane 1:2) = 0.65; $[\alpha]_D^{20}$: + 26.3 ($c = 1.00$, CHCl_3); ATR-FTIR (cm^{-1}): 3031, 2921, 2864, 1746, 1497, 1454, 1070, 1052; ^1H NMR (400 MHz, CDCl_3) δ

* The glycosylation agent **5** was provided by Y.-H. Tsai and prepared according to Ref. [157].

7.40 – 7.20 (m, 33H), 7.17 – 7.12 (m, 2H), 5.89 (ddt, $J = 17.2, 10.5, 5.2$ Hz, 1H, $\text{CH}_2=\text{CH}-\text{CH}_2$), 5.51 (t, $J = 2.1$ Hz, 1H, Man-2), 5.33 – 5.23 (m, 2H, Man-1, $\text{CH}_2=\text{CH}-\text{CH}_2$), 5.15 (dd, $J = 10.5, 1.6$ Hz, 1H, $\text{CH}_2=\text{CH}-\text{CH}_2$), 4.95 – 4.70 (m, 9H), 4.69 – 4.57 (m, 3H), 4.43 (d, $J = 10.8$ Hz, 1H), 4.37 – 4.29 (m, 2H), 4.23 – 4.17 (m, 1H), 4.15 (dt, $J = 5.1, 1.5$ Hz, 2H), 4.00 – 3.95 (m, 2H), 3.92 – 3.80 (m, 2H), 3.53 – 3.41 (m, 2H), 3.35 – 3.26 (m, 3H), 2.17 (s, 3H, CH_3); ^{13}C NMR (101 MHz, CDCl_3) δ 170.25 (CH_3CO), 138.83, 138.81, 138.77, 138.74, 138.29, 138.09, 134.60, 128.55, 128.51, 128.48, 128.45, 128.44, 128.33, 128.19, 128.09, 128.06, 128.03, 127.85, 127.73, 127.64, 127.60, 127.50, 127.33, 116.74, 110.12, 98.97 (Man-1, $J_{\text{C,H}} = 175.0\text{Hz}$), 83.48, 81.37, 81.24, 80.63, 79.04, 77.82, 76.25, 75.97, 75.87, 75.14, 74.31, 73.54, 72.74, 72.63, 71.96, 71.75, 71.41, 68.89 (Man-2), 68.54, 21.31 (CH_3CO); ESI-MS: m/z $[\text{M}+\text{Na}]^+$ calcd for $\text{C}_{66}\text{H}_{70}\text{O}_{12}$ 1077.4765, obsd 1077.4781.

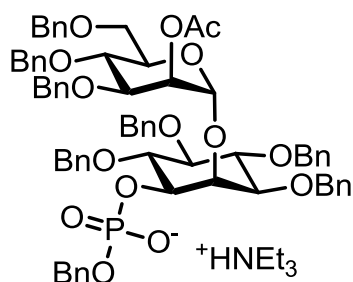
2-*O*-Acetyl-3,4,6-tri-*O*-benzyl- α -D-mannopyranosyl-(1 \rightarrow 2)-3,4,5,6-tetra-*O*-benzyl-D-*myo*-inositol (17**)**



(1,5-Cyclooctadiene)bis(methyldiphenyl-phosphine)iridium(I) PF_6 (3 mg, 3.6 μmol) was dissolved in dry THF (5 mL) and H_2 was bubbled through this solution for 30 min (color change from red to slight yellow). Afterwards dry N_2 was bubbled through this solution for 15 min to get out all H_2 . This solution was then added to a solution of pseudodisaccharide **6** (42 mg, 40 μmol) in dry THF (2 mL). The reaction mixture was stirred for 12 h before 1N HCL (1 mL) was added to cleave the corresponding enol ether. The solution was stirred for 18 h before it was diluted with Et_2O (50 mL). The organic layer was washed with sat. NaHCO_3 solution (3x20 mL), dried over Na_2SO_4 and solvents were removed in vacuo. The residue was purified using column chromatography (*n*-hexane/ethyl acetate 3:1) to yield **17** as colorless oil (37 mg, 36 μmol , 92%): R_f (SiO_2 , $\text{EtOAc}/\text{Hexane}$ 1:2) = 0.44; $[\alpha]_{\text{D}}^{20}$: + 18.9 ($c = 1.00$, CHCl_3); ATR-FTIR (cm^{-1}): 3483, 2925, 2865, 1747, 1454, 1071; ^1H NMR (400 MHz, CDCl_3) δ 7.36 – 7.01 (m, 35H), 5.31 (s, 1H, Man-2), 5.20 (s, 1H, Man-1), 4.95 – 4.80 (m, 3H), 4.79 – 4.59 (m, 6H), 4.51 (d, $J = 10.4$ Hz, 3H), 4.35 (d, $J = 10.7$ Hz, 1H), 4.28 – 4.18 (m, 2H), 4.14 – 4.05 (m, 1H), 3.90 – 3.84 (m, 2H), 3.76 (t, $J = 9.5$ Hz, 1H), 3.65 (t, $J = 9.5$ Hz,

1H), 3.48 – 3.34 (m, 3H), 3.29 (d, $J = 9.8$ Hz, 1H), 3.22 (d, $J = 10.8$ Hz, 1H), 2.18 (bs, 1H, OH), 2.06 (s, 3H, CH₃); ¹³C NMR (101 MHz, CDCl₃) δ 170.37 (CH₃CO), 138.78, 138.66, 138.50, 138.34, 138.30, 138.17, 138.12, 128.88, 128.58, 128.56, 128.47, 128.45, 128.34, 128.32, 128.21, 128.14, 128.09, 128.07, 128.01, 127.87, 127.66, 127.63, 127.60, 127.53, 127.36, 99.21 (Man-1), 83.79, 81.86, 81.24, 79.09, 77.87, 75.96, 75.89, 75.63, 75.21, 74.37, 74.22, 73.54, 72.30, 72.02, 71.57, 68.92, 68.57, 21.32 (CH₃CO); ESI-MS: m/z [M+Na]⁺ calcd for C₆₃H₆₆O₁₂ 1037.4452, obsd 1037.4424.

Triethylammonium 2-O-acetyl-3,4,6-tri-O-benzyl- α -D-mannopyranosyl-(1 \rightarrow 2)-1-O-benzyl-phosphate-3,4,5,6-tetra-O-benzyl-D-*myo*-inositol (8)

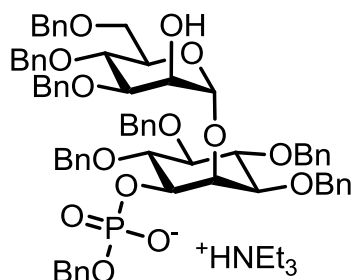


Alcohol **17** (25 mg, 25 μ mol) and H-phosphonate **7*** (10.5 mg, 54 μ mol) were co evaporated with dry pyridine (3x2 mL) and placed under HV for 30 min. The residue was dissolved in dry pyridine (4 mL) and PivCl (10.6 μ L, 86 μ mol) was added. The reaction mixture was stirred for 2 h before water (10 μ L) and iodine (14.4 mg, 57 μ mol) were added. The solution was stirred for 18 h before it was quenched with sat. Na₂S₂O₃ solution (approx. 3 drops), dried with Na₂SO₄ and filtered. Solvents were removed in vacuo and the residue was co evaporated with toluene (3x2 mL). The residue was purified using column chromatography (CHCl₃/MeOH 95:5- \rightarrow 90:10; SiO₂ was deactivated with 1% TEA in CHCl₃) to yield colorless oil. The residue was dissolved in CHCl₃ (30 mL), washed with TEA/CO₂ buffer (3x10 mL), dried over Na₂SO₄ and evaporated to dryness to yield **8** as colorless oil (25 mg, 19 μ mol, 79%): R_f (SiO₂, DCM/MeOH 95:5) = 0.28; [α]_D²⁰: + 32.1 (c = 1.00, CHCl₃); ATR-FTIR (cm⁻¹): 3032, 2926, 1746, 1454, 1236, 1051; ¹H NMR (600 MHz, CDCl₃) δ 12.47 (s, 1H, HN(CH₂CH₃)₃), 7.42 (d, $J = 7.3$ Hz, 2H), 7.36 (d, $J = 7.3$ Hz, 2H), 7.30 – 7.13 (m, 36H), 5.57 – 5.56 (m, 1H, Man-2), 5.55 (s, 1H, Man-1), 5.06 (d, $J = 11.2$ Hz, 1H), 4.97 (dd, $J = 12.3, 6.5$ Hz, 1H), 4.93 (dd, $J = 12.4, 6.5$ Hz, 1H), 4.90 – 4.76 (m, 8H), 4.69 (d, $J = 11.9$ Hz, 1H), 4.58

* The H-phosphonate **7** was provided by Dr. R. Castelli and prepared according to Ref. [158].

– 4.53 (m, 2H), 4.46 (dd, $J = 22.9, 11.5$ Hz, 2H), 4.26 (t, $J = 8.6$ Hz, 1H), 4.22 (d, $J = 12.0$ Hz, 1H), 4.17 (d, $J = 9.5$ Hz, 1H), 3.99 – 3.91 (m, 3H), 3.85 (t, $J = 9.6$ Hz, 1H), 3.49 (t, $J = 9.2$ Hz, 1H), 3.45 – 3.38 (m, 2H), 3.13 (d, $J = 10.6$ Hz, 1H), 2.89 – 2.83 (m, 6H, $\text{HN}(\text{CH}_2\text{CH}_3)_3$), 2.06 (s, 3H, CH_3), 1.15 (t, $J = 7.3$ Hz, 9H, $\text{HN}(\text{CH}_2\text{CH}_3)_3$); ^{13}C NMR (151 MHz, CDCl_3) δ 170.02 (CH_3CO), 139.28, 139.28, 139.01, 138.83, 138.81, 138.63, 138.53, 138.27, 128.54, 128.49, 128.43, 128.42, 128.34, 128.29, 128.27, 128.23, 128.19, 128.19, 128.16, 127.96, 127.94, 127.77, 127.74, 127.64, 127.56, 127.47, 127.28, 127.23, 127.19, 98.85 (Man-1), 83.32, 83.31, 81.24, 80.61, 80.57, 79.49, 78.15, 77.37, 77.16, 76.95, 76.22, 75.80, 75.10, 75.00, 74.34, 74.28, 73.35, 72.45, 71.99, 71.45, 69.04, 68.64, 67.43, 45.41 ($\text{HN}(\text{CH}_2\text{CH}_3)_3$), 21.31 (CH_3CO), 8.55 ($\text{HN}(\text{CH}_2\text{CH}_3)_3$); ^{31}P NMR (243 MHz, CDCl_3) δ - 0.91; ESI-MS: m/z $[\text{M}+\text{Na}]^+$ calcd for $\text{C}_{70}\text{H}_{73}\text{O}_{15}\text{P}$ 1207.4585, obsd 1207.4628.

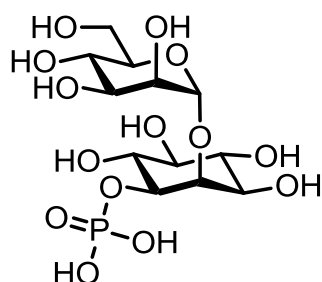
Triethylammonium **3,4,6-tri-*O*-benzyl- α -D-mannopyranosyl-(1 \rightarrow 2)-1-*O*-benzyl-phosphate-3,4,5,6-tetra-*O*-benzyl-D-*myo*-inositol (**12**)**



Triethylammonium salt **8** (25 mg, 19 μmol) was dissolved in dry MeOH (3 mL) and NaH (2.3 mg, 97 μmol) was added. The reaction mixture was stirred for 18 h before it was diluted with CHCl_3 (20 mL) and washed with TEA/ CO_2 buffer (3x10 mL). The organic layer was dried over Na_2SO_4 , filtered and evaporated to dryness to yield **12** yellow oil (24 mg, 19 μmol , 99%): $[\alpha]_{\text{D}}^{20}$: + 32.1 ($c = 1.00$, CHCl_3); ATR-FTIR (cm^{-1}): 3032, 2926, 1746, 1454, 1236, 1051; ^1H NMR (600 MHz, CDCl_3) δ 12.18 (s, 1H, $\text{HN}(\text{CH}_2\text{CH}_3)_3$), 7.32 (d, $J = 7.9$ Hz, 3H), 7.25 (t, $J = 7.6$ Hz, 2H), 7.23 – 7.08 (m, 35H), 5.49 (s, 1H, Man-1), 4.97 (d, $J = 11.1$ Hz, 1H), 4.87 – 4.81 (m, 3H), 4.80 – 4.77 (m, 4H), 4.74 (dd, $J = 10.8, 7.2$ Hz, 2H), 4.70 – 4.63 (m, 3H), 4.49 (d, $J = 12.0$ Hz, 1H), 4.42 (d, $J = 10.9$ Hz, 1H), 4.32 (d, $J = 12.0$ Hz, 1H), 4.16 (d, $J = 12.0$ Hz, 1H), 4.13 (s, 1H), 4.07 (ddd, $J = 9.8, 7.7, 2.1$ Hz, 1H), 4.03 (dt, $J = 10.2, 2.0$ Hz, 1H), 3.93 (t, $J = 9.7$ Hz, 1H), 3.83 – 3.76 (m, 3H), 3.40 (t, $J = 9.3$ Hz, 1H), 3.34 (dd, $J = 10.0, 2.5$ Hz, 1H), 3.32 (dd, $J = 10.9, 2.5$ Hz, 1H), 3.01 (d, $J = 9.8$ Hz, 1H), 2.87 (q, $J = 7.3$ Hz, 6H, $\text{HN}(\text{CH}_2\text{CH}_3)_3$), 1.13 (t, $J = 7.3$ Hz, 9H, $\text{HN}(\text{CH}_2\text{CH}_3)_3$); ^{13}C NMR (151 MHz, CDCl_3) δ

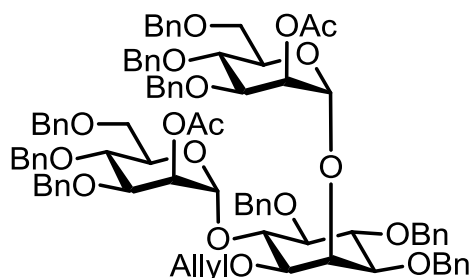
139.23, 138.93, 138.88, 138.83, 138.68, 138.52, 138.39, 128.61, 128.45, 128.43, 128.36, 128.31, 128.25, 128.22, 128.19, 128.13, 128.04, 127.87, 127.67, 127.62, 127.56, 127.55, 127.37, 127.26, 127.15, 127.13, 100.92 (Man-1), 83.38, 81.20, 81.10, 81.05, 79.63, 79.46, 76.24, 75.82, 75.52, 75.14, 74.40, 74.31, 73.31, 72.14, 72.11, 71.10, 68.76, 68.69, 67.23, 67.20, 45.55 (HN(CH₂CH₃)₃), 8.61 (HN(CH₂CH₃)₃); ³¹P NMR (243 MHz, CDCl₃) δ -0.83; ESI-MS: *m/z* [M+HN(CH₂CH₃)₃]⁺ calcd for C₆₈H₇₁O₁₄P 1244.5864, obsd 1244.5867.

α-D-Mannopyranosyl-(1→2)-1-O-phospho-D-*myo*-inositol (*1*)



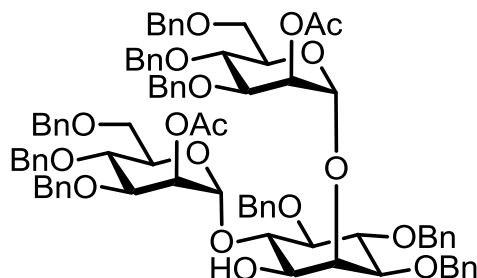
Triethylammonium salt **12** (24 mg, 19 μmol) was dissolved in MeOH (5 mL) and washed Amberlite IR120 H⁺ resin (150 mg) was added. The slurry was stirred for 30 min to remove TEA. The solution was filtered through cotton and solvents were removed in vacuo. The residue was dissolved in MeOH (5 mL) and Pd/C (20.5 mg, 19 μmol, 10wt%) was added. H₂ was bubbled through the solution for 20 min before the reaction mixture was stirred for 18 h under 1 atm H₂. To remove dissolved H₂ dry N₂ was bubbled through the solution for 10 min. The slurry was filtered through a syringe filter and solvents were removed in vacuo. The residue was purified using a G25 size exclusion column (140 mmx10 mm; 5%EtOH in water) to yield **1** as colorless solid (8mg, 19μmol, 98%): [α]_D²⁰: + 28.9 (c = 0.80, H₂O); ATR-FTIR (cm⁻¹): 2929, 2450, 1394, 1032, 983; ¹H NMR (600 MHz, D₂O) δ 5.16 (d, *J* = 1.6 Hz, 1H, Man-1), 4.32 (t, *J* = 2.4 Hz, 1H, Ino-2), 4.11 (dd, *J* = 3.3, 1.9 Hz, 1H, Man-2), 4.05 (td, *J* = 9.7, 1.9 Hz, 1H, Ino-1), 4.01 (ddd, *J* = 10.0, 5.3, 2.3 Hz, 1H, Man-5), 3.88 – 3.83 (m, 2H, Man-6, Man-3), 3.80 – 3.76 (m, 2H, Man-6, Ino-6), 3.69 (t, *J* = 10.0 Hz, 1H, Ino-4), 3.66 – 3.64 (m, 1H, Man-4), 3.62 (dd, *J* = 10.1, 2.4 Hz, 1H, Ino-3), 3.34 (t, *J* = 9.1 Hz, 1H, Ino-5); ¹³C NMR (151 MHz, D₂O) δ 101.31 (Man-1), 78.62 (Ino-2), 76.16 (Ino-1), 74.04 (Ino-5), 72.68 (Man-5), 72.35 (Ino-4), 71.70 (d, *J* = 5.6 Hz, Ino-6), 70.25 (Man-3), 70.03 (Man-2), 69.92 (Ino-3), 66.55 (Man-4), 60.78 (Man-6); ³¹P NMR (243 MHz, D₂O) δ -0.54; ESI-MS: *m/z* [M-H]⁻ calcd for C₁₂H₂₃O₁₄P 421.0752, obsd 421.0831.

2-*O*-Acetyl-3,4,6-tri-*O*-benzyl- α -D-mannopyranosyl-(1 \rightarrow 6)-[2-*O*-acetyl-3,4,6-tri-*O*-benzyl- α -D-mannopyranosyl-(1 \rightarrow 2)]-1-*O*-allyl-3,4,5,-tri-*O*-benzyl-D-*myo*-inositol (9**)**



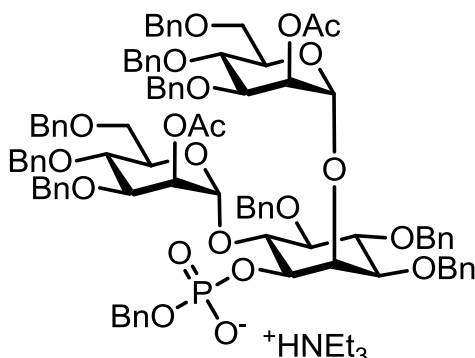
Diol **3** (38 mg, 77 μ mol) and phosphate **5** (152 mg, 201 μ mol) were coevaporated with toluene (3x2 mL) and placed under HV for 30 min. The residue was dissolved in dry toluene (4 mL) and powdered MS4Å (200 mg) was added. The slurry was stirred at r.t. for 15 min before it was cooled down to -40°C . TMSOTf (36.4 μ L, 201 μ mol) was added and the reaction was stirred at -40°C for 2 h. The reaction was quenched with TEA (100 μ L) and filtered through a pad of Celite®. Solvents were removed in vacuo and the residue was purified using column chromatography (*n*-hexane/ethyl acetate 3:1) to yield **9** as yellow oil (69 mg, 48 μ mol, 62%): R_f (SiO₂, EtOAc/Hexane 1:2) = 0.39; $[\alpha]_D^{20}$: + 29.7 ($c = 1.00$, CHCl₃); ATR-FTIR (cm⁻¹): 3031, 2929, 2866, 1745, 1454, 1367, 1235, 1045; ¹H NMR (600 MHz, CDCl₃) δ 7.36 – 6.95 (m, 45H), 5.81 (ddt, $J = 16.2, 10.8, 5.5$ Hz, 1H, CH₂=CH-CH₂), 5.40 (s, 2H), 5.36 (s, 1H), 5.13 (d, $J = 17.2$ Hz, 1H, CH₂=CH-CH₂), 5.08 – 5.04 (m, 2H, CH₂=CH-CH₂), 4.84 (dd, $J = 22.0, 10.6$ Hz, 2H), 4.79 – 4.69 (m, 4H), 4.69 – 4.61 (m, 2H), 4.56 – 4.44 (m, 5H), 4.33 (d, $J = 10.6$ Hz, 2H), 4.26 – 4.18 (m, 2H), 4.13 – 3.92 (m, 7H), 3.91 – 3.83 (m, 4H), 3.76 (t, $J = 9.6$ Hz, 1H), 3.44 (dd, $J = 10.6, 3.0$ Hz, 1H), 3.30 – 3.13 (m, 6H), 2.04 (s, 3H, CH₃), 2.04 (s, 3H, CH₃); ¹³C NMR (151 MHz, CDCl₃) δ 170.42, 169.91 (2xCH₃CO), 139.11, 138.85, 138.51, 138.30, 138.08, 138.06, 134.10, 128.71, 128.53, 128.46, 128.45, 128.43, 128.32, 128.30, 128.27, 128.20, 128.18, 128.17, 128.07, 128.06, 128.02, 127.98, 127.82, 127.78, 127.70, 127.62, 127.60, 127.57, 127.50, 127.47, 127.42, 127.36, 117.66 (CH₂=CH-CH₂), 99.29, 98.65 (2xMan-1; $J_{C,H} = 173.2\text{Hz}$ and $J_{C,H} = 175.7\text{Hz}$), 81.43, 81.02, 78.87, 78.37, 77.50, 76.28, 76.12, 75.80, 75.09, 75.07, 74.27, 74.15, 73.50, 73.42, 72.56, 72.26, 71.79, 71.61, 71.58, 71.55, 71.34, 68.77, 68.61, 68.51, 68.25, 67.49, 67.45, 60.50, 21.28, 21.24 (2xCH₃CO); ESI-MS: m/z [M+Na]⁺ calcd for C₈₈H₉₄O₁₈ 1461.6338, obsd 1461.6364.

2-*O*-Acetyl-3,4,6-tri-*O*-benzyl- α -D-mannopyranosyl-(1 \rightarrow 6)-[2-*O*-acetyl-3,4,6-tri-*O*-benzyl- α -D-mannopyranosyl-(1 \rightarrow 2)]-3,4,5,-tri-*O*-benzyl-D-*myo*-inositol (10**)**



Pseudotriscaccharide **9** (68 mg, 47 μ mol) was dissolved in dry DCM/MeOH (1.4mL; 1:1) and PdCl₂ (4.2 mg, 24 μ mol) was added. The slurry was stirred for 12 h at r.t. before it was filtered over Celite® and evaporated to dryness. The residue was purified using column chromatography (*n*-hexane/ethyl acetate 2:1) to yield **10** as yellow oil (42mg, 30 μ mol, 64%): R_f (SiO₂, EtOAc/Hexane 2:3) = 0.17; [α]_D²⁰: + 43.4 (c = 1.00, CHCl₃); ATR-FTIR (cm⁻¹): 3470, 3031, 2925, 2862, 1745, 1454, 1236, 1048; ¹H NMR (400 MHz, CDCl₃) δ 7.41 – 7.12 (m, 45H), 5.51 (s, 1H), 5.38 (s, 1H), 5.35 – 5.29 (m, 2H), 4.98 – 4.89 (m, 2H), 4.86 (d, *J* = 10.9 Hz, 2H), 4.82 – 4.68 (m, 4H), 4.64 – 4.49 (m, 6H), 4.45 (dd, *J* = 10.9, 1.5 Hz, 2H), 4.33 (dd, *J* = 12.1, 4.7 Hz, 2H), 4.24 – 4.20 (m, 1H), 4.20 – 4.07 (m, 2H), 4.07 – 3.95 (m, 4H), 3.84 (dd, *J* = 20.3, 10.0 Hz, 2H), 3.65 (d, *J* = 8.9 Hz, 1H), 3.57 (dd, *J* = 10.8, 3.0 Hz, 1H), 3.52 – 3.26 (m, 5H), 3.13 (bs, 1H, OH), 2.15 (s, 3H, CH₃), 2.13 (s, 3H, CH₃); ¹³C NMR (101 MHz, CDCl₃) δ 170.92, 170.31 (2xCH₃CO), 138.83, 138.73, 138.59, 138.55, 138.36, 138.12, 138.03, 138.01, 128.58, 128.54, 128.48, 128.45, 128.37, 128.35, 128.33, 128.30, 128.09, 128.07, 128.06, 127.99, 127.88, 127.81, 127.78, 127.70, 127.61, 127.48, 99.65, 96.22 (2xMan-1), 81.41, 80.76, 79.40, 78.66, 77.86, 77.69, 77.36, 76.51, 75.87, 75.73, 75.15, 74.96, 74.44, 74.22, 73.52, 73.49, 72.28, 72.18, 71.78, 71.76, 71.73, 71.67, 69.45, 68.79, 68.60, 21.31, 21.26 (2xCH₃CO); ESI-MS: *m/z* [M+H]⁺ calcd for C₈₅H₉₀O₁₈ 1399.6205, obsd 1399.6206.

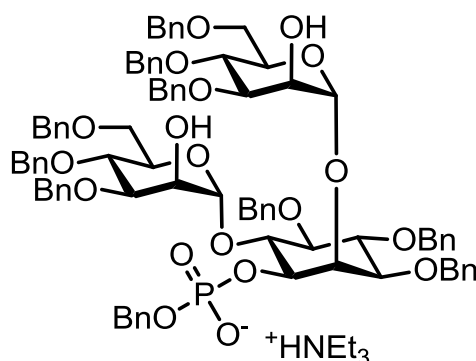
Triethylammonium 2-O-Acetyl-3,4,6-tri-O-benzyl- α -D-mannopyranosyl-(1 \rightarrow 6)-[2-O-acetyl-3,4,6-tri-O-benzyl- α -D-mannopyranosyl-(1 \rightarrow 2)]-1-O-benzyl-phosphate-3,4,5-tri-O-benzyl-D-myoinositol (11**)**



Alcohol **10** (42 mg, 30 μ mol) and H-phosphonate **7** (11.7 mg, 60 μ mol) were coevaporated with dry pyridine (3x2 mL) and placed under HV for 30 min. The residue was dissolved in dry pyridine (3 mL) and PivCl (12.9 μ L, 105 μ mol) were added. The reaction mixture was stirred for 2 h before water (10 μ L) and iodine (16 mg, 63 μ mol) were added. The solution was stirred for 18 h before it was quenched with sat. Na₂S₂O₃ solution (approx. 3 drops), dried with Na₂SO₄ and filtered. Solvents were removed in vacuo and the residue was co evaporated with toluene (3x2 mL). The residue was purified using column chromatography (CHCl₃/MeOH 97:3; SiO₂ was deactivated with 1% TEA in CHCl₃) to yield colorless oil. The residue was dissolved in CHCl₃ (30 mL), washed with TEA/CO₂ buffer (3x10 mL), dried over Na₂SO₄ and evaporated to dryness to yield **11** as colorless oil (31.8 mg, 20 μ mol, 68%): R_f (SiO₂, DCM/MeOH 95:5) = 0.33; $[\alpha]_D^{20}$: + 34.2 (c = 1.00, CHCl₃); ATR-FTIR (cm⁻¹): 2926, 2855, 1745, 1497, 1455, 1367, 1100, 1057; ¹H NMR (600 MHz, CDCl₃) δ 12.41 (s, 1H, HN(CH₂CH₃)₃), 7.36 (d, *J* = 7.3 Hz, 2H), 7.30 (d, *J* = 7.1 Hz, 2H), 7.24 – 7.04 (m, 42H), 6.99 (dd, *J* = 6.6, 2.9 Hz, 2H), 6.96 (t, *J* = 7.6 Hz, 2H), 5.63 (s, 1H), 5.55 (s, 1H), 5.52 (s, 1H), 5.41 (s, 1H), 4.89 (d, *J* = 7.1 Hz, 2H), 4.83 (t, *J* = 9.9 Hz, 2H), 4.77 – 4.65 (m, 7H), 4.57 – 4.40 (m, 6H), 4.35 (d, *J* = 10.9 Hz, 1H), 4.32 (d, *J* = 10.9 Hz, 1H), 4.17 – 4.04 (m, 5H), 4.01 (d, *J* = 9.7 Hz, 1H), 3.96 (dd, *J* = 9.5, 3.1 Hz, 1H), 3.93 (dd, *J* = 9.5, 3.0 Hz, 1H), 3.87 (dd, *J* = 20.9, 9.9 Hz, 2H), 3.79 (t, *J* = 9.6 Hz, 1H), 3.38 (dd, *J* = 11.0, 2.6 Hz, 2H), 3.34 – 3.24 (m, 3H), 3.04 (dd, *J* = 11.0, 1.4 Hz, 1H), 2.81 (q, *J* = 7.3 Hz, 6H, HN(CH₂CH₃)₃), 1.94 (s, 3H), 1.92 (s, 3H), 1.09 (t, *J* = 7.3 Hz, 9H, HN(CH₂CH₃)₃); ¹³C NMR (151 MHz, CDCl₃) δ 170.00, 169.76 (2xCH₃CO), 139.24, 139.03, 138.66, 138.62, 138.51, 138.29, 138.20, 128.75, 128.48, 128.40, 128.34, 128.32, 128.26, 128.23, 128.19, 128.18, 128.13, 128.09, 128.00, 127.92, 127.84, 127.81, 127.67, 127.54, 127.51, 127.47, 127.45, 127.40, 127.34, 127.30, 127.25, 99.51, 98.48 (2xMan-1), 81.60, 79.60, 78.66, 77.92, 76.76, 76.74, 76.12, 75.79, 75.37, 75.04, 75.00, 74.32,

74.19, 73.36, 72.14, 71.66, 71.64, 71.56, 71.47, 68.55, 67.33, 45.33 (HN(CH₂CH₃)₃), 21.34, 21.21 (2xCH₃CO), 8.54 (HN(CH₂CH₃)₃); ³¹P NMR (243 MHz, CDCl₃) δ -0.36; ESI-MS: *m/z* [M+Na]⁺ calcd for C₉₂H₉₇O₂₁P 1591.6158, obsd 1591.6152.

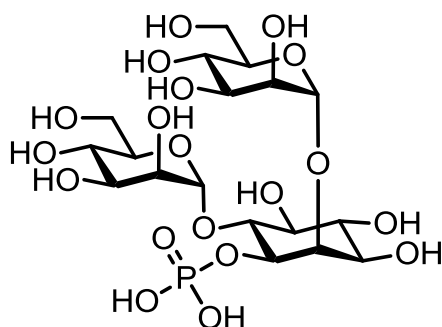
Triethylammonium 3,4,6-Tri-*O*-benzyl- α -D-mannopyranosyl-(1 \rightarrow 6)-[3,4,6-tri-*O*-benzyl- α -D-mannopyranosyl-(1 \rightarrow 2)]-1-*O*-benzyl-phosphate-3,4,5,-tri-*O*-benzyl-D-*myo*-inositol (13)



Phosphate **11** (31 mg, 19 μ mol) was dissolved in dry MeOH (5 mL) and NaH (2.2 mg, 93 μ mol) was added. The solution was stirred for 48 h at r.t. before it was diluted with CHCl₃ (25 mL) and washed with TEA/CO₂ buffer (3x10 mL). The organic layer was dried with Na₂SO₄ and evaporated to dryness. The residue was purified using column chromatography (CHCl₃/MeOH 95:5- \rightarrow 90:10; SiO₂ was deactivated with 1% TEA in CHCl₃) to yield colorless oil. The residue was dissolved in CHCl₃ (30 mL), washed with TEA/CO₂ buffer (3x10 mL), dried over Na₂SO₄ and evaporated to dryness to yield **13** as colorless oil (23 mg, 14 μ mol, 78%): R_f (SiO₂, DCM/MeOH 90:10) = 0.14; [α]_D²⁰: + 51.6 (c = 1.00, CHCl₃); ATR-FTIR (cm⁻¹): 3319, 3030, 2930, 2863, 1454, 1363, 1210, 1048; ¹H NMR (600 MHz, CDCl₃) δ 7.46 (d, *J* = 7.4 Hz, 2H), 7.41 (d, *J* = 7.4 Hz, 2H), 7.37 – 7.13 (m, 42H), 7.12 – 7.06 (m, 4H), 5.56 (s, 1H), 5.53 (s, 1H), 5.04 (d, *J* = 6.7 Hz, 2H), 4.91 (dd, *J* = 10.6, 6.0 Hz, 2H), 4.82 (d, *J* = 10.8 Hz, 1H), 4.80 – 4.75 (m, 3H), 4.72 (d, *J* = 11.4 Hz, 1H), 4.66 (t, *J* = 9.8 Hz, 4H), 4.58 (d, *J* = 11.7 Hz, 1H), 4.51 – 4.44 (m, 4H), 4.41 – 4.35 (m, 2H), 4.28 – 4.20 (m, 2H), 4.19 – 4.09 (m, 4H), 4.01 – 3.84 (m, 6H), 3.43 – 3.37 (m, 2H), 3.33 (t, *J* = 9.3 Hz, 1H), 3.29 (dd, *J* = 10.8, 2.0 Hz, 1H), 3.24 (d, *J* = 10.4 Hz, 1H), 3.15 (d, *J* = 10.5 Hz, 1H), 2.94 (qd, *J* = 7.2, 2.3 Hz, 6H, HN(CH₂CH₃)₃), 1.23 (t, *J* = 7.3 Hz, 9H, HN(CH₂CH₃)₃); ¹³C NMR (151 MHz, CDCl₃) δ 139.10, 138.91, 138.68, 138.45, 138.29, 128.64, 128.39, 128.34, 128.33, 128.31, 128.29, 128.20, 128.19, 128.18, 128.11, 128.09, 127.98, 127.90, 127.86, 127.64, 127.59, 127.51, 127.40, 127.35, 127.28, 127.21, 100.67 (2xMan-1; overlapping signals were resolved in

^1H , ^{13}C -HSQC experiment), 81.49, 81.45, 79.79, 79.59, 79.28, 77.72, 77.68, 76.14, 75.75, 75.07, 74.60, 74.48, 74.42, 74.26, 73.39, 73.22, 71.98, 71.90, 71.38, 71.04, 68.70, 68.66, 68.44, 68.35, 67.47, 67.44, 45.58 ($\text{HN}(\text{CH}_2\text{CH}_3)_3$), 8.71 ($\text{HN}(\text{CH}_2\text{CH}_3)_3$); ^{31}P NMR (243 MHz, CDCl_3) δ -1.29; ESI-MS: m/z $[\text{M}-\text{H}+2\text{Na}]^+$ calcd for $\text{C}_{88}\text{H}_{93}\text{O}_{19}\text{P}$ 1529.5771, obsd 1529.5772.

α -D-Mannopyranosyl-(1 \rightarrow 6)-[α -D-mannopyranosyl-(1 \rightarrow 2)]-1-O-phospho-3,4,5,-D-myoinositol (2)



Pseudotriscarbohydrate **13** (23 mg, 14 μmol) was dissolved in MeOH (5 mL) and washed Amberlite IR120 H⁺ resin (150 mg) was added. The slurry was stirred for 30 min to remove TEA. The solution was filtered through cotton and solvents were removed in vacuo. The residue was dissolved in MeOH (5 mL) and Pd/C (15.4 mg, 14 μmol , 10wt%) was added. H_2 was bubbled through the solution for 20 min before the reaction mixture was stirred for 18 h under 1 atm H_2 . To remove dissolved H_2 dry N_2 was bubbled through the solution for 10 min. The slurry was filtered through a syringe filter and solvents were removed in vacuo. The residue was purified using a G25 size exclusion column (140 mmx10 mm; 5%EtOH in water) to yield **2** as colorless solid (7.8 mg, 13 μmol , 92%): $[\alpha]_{\text{D}}^{20}$: + 120.2 ($c = 0.80$, H_2O); ATR-FTIR (cm^{-1}): 3302, 2977, 1387, 1152, 1010, 809; ^1H NMR (600 MHz, D_2O) δ 5.18 (d, $J = 1.6$ Hz, 2H, 2xMan-1), 4.32 (t, $J = 2.3$ Hz, 1H, Ino-2), 4.16 – 4.14 (m, 2H, 2xMan-2), 4.13 (dd, $J = 9.5, 2.0$ Hz, 1H, Ino-1), 4.05 – 4.00 (m, 2H, 2xMan-5), 3.91 – 3.77 (m, 7H, Ino-6{3.90}, 2xMan-3, 2xMan-6), 3.76 – 3.66 (m, 3H, 2xMan-4, Ino-4{3.68}), 3.62 (dd, $J = 10.2, 2.6$ Hz, 1H, Ino-3), 3.38 (t, $J = 9.2$ Hz, 1H, Ino-5); ^{13}C NMR (101 MHz, D_2O) δ 101.29, 101.17 (2xMan-1), 78.54 (Ino-2), 77.86 (d, $J = 6.2$ Hz, Ino-6), 76.28 (d, $J = 5.5$ Hz, Ino-1), 72.88 (Ino-5), 72.67, 72.58, 72.53, 70.23, 70.21, 70.04, 69.90, 69.74, 66.55, 66.36 (2xMan-4), 60.78, 60.57 (2xMan-6); ^{31}P NMR (243 MHz, D_2O) δ -0.83; ESI-MS: m/z $[\text{M}-\text{H}]^-$ calcd for $\text{C}_{18}\text{H}_{33}\text{O}_{19}\text{P}$ 583.1280, obsd 583.1286.

List of References

1. B. G. Davis, A. J. Fairbanks, in *Carbohydrate Chemistry*, (Ed: S. G. Davies), OXFORD UNIVERSITY PRESS, New York (NY), 2008, Chapter 9.
2. V. Hascall, J. D. Esko, in *Essentials of Glycobiology 2nd Ed.*, (Eds: A. Varki, R. D. Cummings, J. D. Esko, H.H. Freeze, P. Stanley, C. R. Bertozzi, G. W. Hart, M. E. Etzler), Cold Spring Harbor Laboratory Press, Cold Spring Harbor (NY), 2009, Chapter 15.
3. R. G. Spiro, *Glycobiology* **2002**, *12*, 43-56.
4. R. G. Spiro, *Glycoproteins. Adv. Protein Chem* **1973**, *27*, 349–467.
5. A. Seko, M. Kotetsu, M. Nishizono, Y. Enoki, H. R. Ibrahim, L. R. Juneja, M. Kim, T. Yamamoto, *Biochim. Biophys. Acta.* **1997**, *1335*, 23–32.
6. M. A. Hollingsworth, B. J. Swanson, *Nat. Rev. Cancer* **2004**, *4*, 45-60.
7. G. W. Hart, C. Slawson, G. Ramirez-Correa, O. Lagerlof, *Annu. Rev. Biochem* **2011**, *80*, 825–858.
8. K. Jacobson, O. G. Mouritsen, R. G. W. Anderson, *Nat. Cell Biol.* **2007**, *9*, 7-14.
9. T. Debeer, J. F. G. Vliegthart, A. Loffler, J. Hofsteenge, *Biochemistry* **1995**, *34*, 11785–11789.
10. P. Lafite, R. Daniellou, *Nat. Prod. Rep.* **2012**, *29*, 729-738.
11. K. Julenius, *Glycobiology* **2007**, *17*, 868-876.
12. P. A. Haynes, *Glycobiology* **1998**, *8*, 1–5.
13. M. G. Low, *Biochim. Biophys. Acta* **1989**, *988*, 427-454.
14. Y. Maeda, Y. Tashima, T. Houjou, M. Fujita, T. Yoko-o, Y. Jigami, R. Taguchi, T. Kinoshita, *Mol. Biol. Cell* **2007**, *18*, 1497-1506.
15. I. A. Rooney, J. E. Heuser, J. P. Atkinson, *J. Clin. Invest.* **1996**, *97*, 1675-1686.
16. M. Fujita, Y. Maeda, M. Ra, Y. Yamaguchi, R. Taguchi, T. Kinoshita, *Cell* **2009**, *139*, 352-365.
17. M. A. Ferguson, *J. Cell Sci.* **1999**, *112*, 2799-2809.
18. Y. Ueda, R. Yamaguchi, M. Ikawa, M. Okabe, E. Morii, Y. Maeda, T. Kinoshita, *J. Biol. Chem.* **2007**, *282*, 30373–30380.
19. A. M. Almeida, Y. Murakami, D.M. Layton, P. Hillmen, G.S. Sellick, Y. Maeda, S. Richards, S. Patterson, I. Kotsianidis, L. Mollica, D.H. Crawford, A. Baker, M. Ferguson, I. Roberts, R. Houlston, T. Kinoshita, A. Karadimitris, *Nat. Med.* **2006**, *12*, 846-851.

20. J. S. Thorson, V. Thomas, in *Carbohydrate-Based Drug Discovery*, (Ed. C.-H. Wong), Wiley-VCH Verlag GmbH & Co. KGaA, Weinheim, 2005, Chapter 25.
21. E. F. Neufeld, V. Ginsburg, *Annu. Rev. Biochem.* **1965**, *34*, 97–312.
22. C. B. Hirschberg, P. W. Robbins, C. Abeijon, *Annu. Rev. Biochem.* **1998**, *67*, 49–69.
23. L. V. Bindschedler, E. Wheatley, E. Gay, J. Cole, A. Cottage, G. P. Bolwell, *Plant Mol. Biol.* **2005**, *57*, 285-301.
24. J. C. Paulson, K. J. Colley, *J. Biol. Chem.* **1989**, *264*, 17615-17618.
25. C. J. Waechter, *Annu. Rev. Biochem.* **1976**, *45*, 95-112.
26. H. Schachter, *Glycoconjugate J.* **2000**, *17*, 465-483.
27. L. A. Tabak, *Annu. Rev. Physiol.* **1995**, *57*, 547–564.
28. J. D. Esko, S. B. Selleck, *Annu. Rev. Biochem.* **2002**, *71*, 435-471.
29. J. L. Funderburgh, *IUBMB Life* **2002**, *54*, 187-194.
30. T. Kinoshita, M. Fujita, Y. Maeda, *J. Biochem.* **2008**, *144*, 287-294.
31. Y. Maeda, T. Kinoshita, *Prog. Lipid Res.* **2011**, *50*, 411–424.
32. T. Kolter, R. L. Proia, K. Sandhoff, *J. Biol. Chem.* **2002**, *277*, 25859–25862.
33. A. Varki, *Glycobiology* **1993**, *3*, 97-130.
34. A. Helenius, M. Aebi, *Annu. Rev. Biochem.* **2004**, *73*, 1019-1049.
35. D. Chappell, M. Jacob, K. Hofmann-Kiefer, M. Rehm, U. Welsch, P. Conzen, B. F. Becker, *Cardiovasc. Res.* **2009**, *83*, 388-396.
36. A. Varki, T. Angata, *Glycobiology* **2006**, *16*, 1-27.
37. K. Drickamer, M. E. Taylor, *Annu. Rev. Cell Biol.* **1993**, *9*, 237-264.
38. M. L. Phillips, E. Nudelman, F. C. Gaeta, M. Perez, A. K. Singhal, S. I. Hakomori, J. C. Paulson, *Science*, **1990**, *250*, 1130-1132.
39. H. L. Cash, C. V. Whitham, C. L. Behrendt, L. V. Hooper, *Science* **2006**, *313*, 1126-1130.
40. A. H. Courtneya, E. B. Puffera, J. K. Pontrellob, Z.-Q. Yangb, L. L. Kiessling, *Proc. Natl. Acad. Sci.* **2009**, *106*, 2500-2505.
41. M. S. Macauley, F. Pfrengle, C. Rademacher, C. M. Nycholat, A. J. Gale, A. von Drygalski, J. C. Paulson, *J. Clin. Invest.* **2013**, *123*, 3074-3083.
42. G. Szolnok, Z. Bata-Csörgö, A. S. Kenderessy, M. Kiss, A. Pivarcsi, Z. Novák, K. N. Newman, G. Michel, T. Ruzicka, L. Maródi, A. Dobozy, L. Kemény, *J. Invest. Dermatol.* **2001**, *117*, 205-213.
43. L. S. Kreisman, B. A. Cobb, *Glycobiology* **2012**, *22*, 1019-1030.

44. C. R. Raetz, C. M. Reynolds, M.S. Trent, R.E. Bishop, *Annu. Rev. Biochem.* **2007**, *76*, 295-329.
45. J. van Heijenoort, *Glycobiology* **2001**, *11*, 25-36.
46. C. Weidenmaier, A. Peschel, *Nat. Rev. Microbiol.* **2008**, *6*, 276-287.
47. C. Raetz, C. Whitfield, *Annu. Rev. Biochem.* **2002**, *71*, 635–700.
48. I. S. Roberst, *Annu. Rev. Biochem.* **1996**, *50*, 285–315.
49. J. W. Greenberg, W. Fischer, K. A. Joiner, *Infect. Immun.* **1996**, *64*, 3318-3325.
50. N. Ahmad, W. L. Drew, J. J. Plorde, in *Sherris Medical Microbiology 5th Ed.*, (Eds: K. J. Ryan, C. G. Ray), McGraw-Hill Companies, Inc., New York (NY), 2010, Chapter 27.
51. V. Bhowruth, L. J. Alderwick, A. K. Brown, A. Bhatt, G. S. Besra, *Biochem. Soc. Trans.* **2008**, *36*, 555-565.
52. A. K. Mishra, N. N. Driessen, B. J. Appelmelk, G. S. Besra, *FEMS Microbiol. Rev.* **2011**, *35*, 1126-1157.
53. J. D. Barry, R. McCulloch, *Adv. Parasitol.* **2001**, *49*, 1-70.
54. X.-L. He, M. E. Grigg, J. C. Boothroyd, K. C. Garcia, *Nat. Struct. Biol.* **2002**, *9*, 606-611.
55. N. Azzouz, H. Shams-Eldin, S. Niehus, F. Debierre-Grockiego, U. Bieker, J. Schmidt, C. Mercier, M. F. Delauw, J.-F. Dubremetz, T. K. Smith, R. T. Schwarz, *Int. J. Biochem. Cell. Biol.* **2006**, *38*, 1914-1925.
56. A. Imberty, H. Lortat-Jacob, S. Pérez, *Carbohydr. Res.* **2007**, *342*, 430–439.
57. T. Horlacher, P. H. Seeberger, *Chem. Soc. Rev.* **2008**, *37*, 1414-1422.
58. G. Safina, *Anal. Chim. Acta.* **2012**, *712*, 9-29.
59. A. Velázquez-Campoy, H. Ohtaka, A. Nezami S. Muzammil, E. Freire, *Curr. Protoc. Cell Biol.* **2004**, *17*, 1-24.
60. A. Koizumi, I. Matsuo, M. Takatani, A. Seko, M. Hachisu, Y. Takeda, Y. Ito, *Angew. Chem. Int. Ed.* **2013**, *52*, 7426–7431.
61. Z. Wang, Z. S. Chinoy, S. G. Ambre, W. Peng, R. McBride, R. P. de Vries, J. Glushka, J. C. Paulson, G.-J. Boons, *Science* **2013**, *341*, 379-383.
62. T.-I Tsai, H.-Y. Lee, S.-H. Chang, C.-H. Wang, Y.-C. Tu, Y.-C. Lin, D.-R. Hwang, C.-Y. Wu, C.-H. Wong, *J. Am. Chem. Soc.* **2013**, *135*, 14831–14839.
63. C. D. Rillahan, E. Schwartz, R. McBride, V. V. Fokin, J. C. Paulson, *Angew. Chem. Int. Ed.* **2012**, *51*, 11014-11018.
64. M. A. Johnson, D. R. Bundle, *Chem. Soc. Rev.* **2013**, *42*, 4327-4344.

65. F. Debierre-Grockiego, *Trends Parasitol.* **2010**, *26*, 404–411.
66. F. A. Hunter, L. D. Sibley, *Nat. Rev. Microbiol.* **2012**, *10*, 766–778.
67. P. S. Mead, L. Slutsker, V. Dietz, L. F. McCaig, J. S. Bresee, C. Shapiro, P. M. Griffin, R. V. Tauxe, *Emerg. Infect. Dis.* **1999**, *5*, 607-625.
68. C. Silveira, N. Gargano, A. Kijlstra, E. Petersen, *Expert Rev. Anti Infect. Ther.* **2009**, *7*, 905-908.
69. F. Debierre-Grockiego, R. T. Schwarz, *Glycobiology* **2010**, *20*, 801–811.
70. B. J. Luft, J. S. Remington, *Clin. Infect. Dis.* **1992**, *2*, 211-222.
71. Remington, J.S., in *Infectious Diseases of the Fetus and Newborn Infant (6th edition)*, (Ed: J. S. Remington, J. O. Klein, C. B. Wilson, C. J. Baker), Elsevier Saunders, Philadelphia (PA), 2006, Chapter 31.
72. E. Jongert, C. W. Roberts, N. Gargano, E. Förster-Waldl, E. Petersen, *Mem. I. Oswaldo Cruz* **2009**, *104*, 252-266.
73. B. Striepen, C. F. Zinecker, J. B. Damm, P. A. Melgers, G. J. Gerwig, M. Koolen, J. F. Vliegthart, J. F. Dubremetz, R. T. Schwarz, *J. Mol. Biol.* **1997**, *266*, 797-813.
74. S. D. Sharma, J. Mullenax, F. G. Araujo, H. A. Erlich, J. S. Remington, *J. Immunol.* **1983**, *131*, 977-983.
75. Y.-H. Tsai, X. Liu, P. H. Seeberger, *Angew. Chem. Int. Ed.* **2012**, *51*, 11438-11456.
76. O. T. Avery, W. F. Goebel, *J. Exp. Med.* **1929**, *50*, 533–550.
77. P. H. Seeberger, R. L. Soucy, Y. U. Kwon, D. A. Snyder, T. Kanemitsu, *Chem. Commun.* **2004**, 1706-1707.
78. F. Kamena, M. Tamborrini, X. Y. Liu, Y. U. Kwon, F. Thompson, G. Pluschke, P. H. Seeberger, *Nat. Chem. Biol.* **2008**, *4*, 238-240.
79. N. Stahl, M. A. Baldwin, R. Hecker, K. M. Pan, A. L. Burlingame, S. B. Prusiner, *Biochemistry* **1992**, *31*, 5043-5053.
80. Y.-L. Huang, C.-Y. Wu, *Expert Rev. Vaccines* **2010**, *9*, 1257–1274.
81. A. V. Nikolaev, N. Al-Maharik, *Nat. Prod. Rep.* **2011**, *28*, 970-1020.
82. Z. W. Guo, J. Xue, *J. Am. Chem. Soc.* **2003**, *125*, 16334-16339.
83. X. M. Wu, Z. W. Guo, *Org. Lett.* **2007**, *9*, 4311-4313.
84. S. V. Ley, D. K. Baeschlin, A. R. Chaperon, V. Charbonneau, L. G. Green, U. Lucking, E. Walther, *Angew. Chem. Int. Ed.* **1998**, *37*, 3423-3428.
85. S. V. Ley, D. K. Baeschlin, A. R. Chaperon, L. G. Green, M. G. Hahn, S. J. Ince, *Chem.-Eur. J.* **2000**, *6*, 172-186.

86. U. E. Udodong, R. Madsen, C. Roberts, B. Fraser-Reid, *J. Am. Chem. Soc.* **1993**, *115*, 7886-7887.
87. P. G. M. Wuts, T. W. Greene, in *Greene's Protective Groups in Organic Synthesis (4th edition)*, John Wiley & Sons, Inc., Hoboken (NJ), 2007, Chapter 2.
88. C. Murakata, T. Ogawa, *Tetrahedron Lett.* **1991**, *32*, 671-674.
89. A. Ali, R. A. Vishwakarma, *Tetrahedron* **2010**, *66*, 4357-4369.
90. Y.-U. Kwon, R. L. Soucy, D. A. Snyder, P. H. Seeberger, *Chem. Eur. J.* **2005**, *11*, 2493-2504.
91. S. L. Beaucage, R. P. Iyer, *Tetrahedron* **1992**, *48*, 2223-2311.
92. G. Grundler, R. R. Schmidt, *Liebigs Ann. Chem.* **1984**, 1826-1847.
93. Z. J. Jia, L. Olsson, B. Fraser-Reid, *J. Chem. Soc., Perkin Trans. I* **1998**, 631-632.
94. X. Liu, B. L. Stocker, P. H. Seeberger, *J. Am. Chem. Soc.* **2006**, *128*, 3638-3648.
95. S. Boonyarattanakalin, X. Liu, M. Michieletti, B. Lepenies, P. H. Seeberger, *J. Am. Chem. Soc.* **2008**, *130*, 16791-16799.
96. R. J. Ferrier, S. Middleton, *Chem. Rev.* **1993**, *93*, 2779-2831.
97. H. Takahashi, H. Kittaka, S. Ikegami, *J. Org. Chem.* **2001**, *66*, 2705-2716.
98. G. Zemplén, E. Pacsu, *Ber. Dtsch. Chem. Ges.* **1929**, *62*, 1613-1614
99. R.-B. Yan, F. Yang, Y. Wu, L.-H. Zhang, X.-S. Ye, *Tetrahedron Lett.* **2005**, *46*, 8993-8995.
100. J. Zhang, P. Kováč, *J. Carbohydr. Chem.* **1999**, *18*, 461-469.
101. R. R. Schmidt, J. Michel, *Angew. Chem. Int. Ed.* **1980**, *19*, 731-732.
102. J. Park, S. Kawatkar, J.-H. Kim, G.-J. Boons, *Org. Lett.* **2007**, *9*, 1959-1962.
103. Y.-U. Kwon, X. Y. Liu, P. H. Seeberger, *Chem. Commun.* **2005**, 2280-2282.
104. Y.-H. Tsai, S. Götze, I. Vilotijevic, M. Grube, D. Varón Silva, P. H. Seeberger, *Chem. Sci.* **2013**, *4*, 468-481.
105. J. J. Oltvoort, C. A. A. van Boeckel, J. H. De Koning, J. H. van Boom, *Synthesis* **1981**, 305-308.
106. B. M. Swarts, Z. W. Guo, *J. Am. Chem. Soc.* **2010**, *132*, 6648-6650.
107. B. M. Swarts, Z. W. Guo, *Chem. Sci.* **2011**, *2*, 2342-2352.
108. A. J. Birch, *J. Chem. Soc.* **1944**, 430-436.
109. V. Gracias, K. E. Frank, G. L. Milligan, J. Aubé, *Tetrahedron* **1997**, *53*, 16241-16252.
110. Y.-H. Tsai, S. Götze, N. Azzouz, H. S. Hahm, P. H. Seeberger, D. Varón Silva, *Angew. Chem. Int. Edit.* **2011**, *50*, 9961-9964.
111. T. Francis, W. S. Tillett, *J. Exp. Med.* **1930**, *52*, 573-585.

112. M. Heidelberger, M. M. Dilapi, M. Siegel, A. W. Walter, *J. Immunol.* **1950**, *65*, 535–541.
113. J. B. Robbins, R. Austrian, C.-J. Lee, S. C. Rastogi, G. Schiffman, J. Henrichsen, P. H. Mäkelä, C. V. Broome, R. R. Facklam, R. H. Tiesjema RH, J. C. Parker Jr., *J. Infect. Dis.* **1983**, *148*, 1136-1159.
114. M. E. Rogers, O. V. Sizova, M. A. Ferguson, A. V. Nikolaev, P. A. Bates PA, *J. Infect. Dis.* **2006**, *194*, 512-518.
115. I. J. Krauss, J. G. Joyce, A. C. Finnefrock, H. C. Song, V. Y. Dudkin, X. Geng, J. D. Warren, M. Chastain, J. W. Shiver, S. J. Danishefsky, *J. Am. Chem. Soc.* **2007**, *129*, 11042-11044.
116. N. Gaidzik, A. Kaiser, D. Kowalczyk, U. Westerlind, B. Gerlitzki, H. P. Sinn, E. Schmitt, H. Kunz, *Angew. Chem. Int. Ed.* **2011**, *50*, 9977-9981.
117. L. Schofield, M. C. Hewitt, K. Evans, M. A. Siomos, P. H. Seeberger, *Nature* **2002**, *418*, 785–789.
118. G. T. Hermanson, in *Bioconjugate Techniques (1st edition)*, (Ed: G. T. Hermanson), Academic Press, San Diego (CA), 1996, Chapter 5.
119. M. Bröker, P. M. Dull, R. Rappuoli, P. Costantino, *Vaccine* **2009**, *27*, 5574-5580.
120. K. Hu, J. Johnson, L. Florens, M. Fraunholz, S. Suravajjala, C. DiLullo, J. Yates, D. S. Roos, J. M. Murray, *PLoS Pathog.* **2006**, *2*, e13.
121. S. D. Sharma, J. Mullenax, F. G. Araujo, H. A. Erlich, J. S. Remington, *J. Immunol.* **1983**, *131*, 977-983.
122. B. Striepen, C. F. Zinecker, J. B. Damm, P. A. Melgers, G. J. Gerwig, M. Koolen, J. F. Vliegenthart, J. F. Dubremetz, R. T. Schwarz, *J. Mol. Biol.* **1997**, *266*, 797-813.
123. A. Hölemann, B. L. Stocker, P. H. Seeberger, *J. Org. Chem.* **2006**, *71*, 8071-8088.
124. J. G. Montoya, O. Liesenfeld, *Lancet* **2004**, *363*, 1965-1976.
125. E. Stillwaggon, C. S. Carrier, M. Sautter, R. McLeod, *PLoS Negl. Trop. Dis.* **2011**, *5*, e1333.
126. A. Dao, N. Azzouz, C. Eloundou Nga, J. F. Dubremetz, R. T. Schwarz, B. Fortier, *Eur. J. Clin. Microbiol. Infect. Dis.* **2003**, *22*, 418-421.
127. A. Linden, *J. Eval. Clin. Pract.* **2006**, *12*, 132-139.
128. F. Jacob, D. R. Goldstein, N. V. Bovin, T. Pochechueva, M. Spengler, R. Caduff, D. Fink, M. I. Vuskovic, M. E. Huflejt, V. Heinzelmann-Schwarz, *Int. J. Cancer* **2012**, *130*, 138-146.
129. U. Cronshagen, P. Volland, H. F. Kern, *Eur. J. Cell Biol.* **1994**, *65*, 366-377.

130. H. Tateno, R. Yabe, T. Sato, A. Shibazaki, T. Shikanai, T. Gonoi, H. Narimatsu, J. Hirabayashi, *Glycobiology* **2012**, *22*, 210-220.
131. R. Kleene, H. Dartsch, H. F. Kern, *Eur. J. Cell Biol.* **1999**, *78*, 79-90.
132. K. Kumazawa-Inoue, T. Mimura, S. Hosokawa-Tamiya, Y. Nakano, N. Dohmae, A. Kinoshita-Toyoda, H. Toyoda, K. Kojima-Aikawa, *Glycobiology* **2012**, *22*, 258-266.
133. Kanagawa, M.; Satoh, T.; Ikeda, A.; Nakano, Y.; Yagi, H.; Kato, K.; Kojima-Aikawa, K.; Yamaguchi, Y. *Biochem. Biophys. Res. Commun.* **2011**, *404*, 201-205.
134. K. Drickamer, *Curr. Opin. Struct. Biol.* **1999**, *9*, 585-560.
135. C. G. Figdor, Y. van Kooyk, G. J. Adema, *Nat. Rev. Immunol.* **2002**, *2*, 77-84.
136. T. B. Geijtenbeek, S. I. Gringhuis, *Nat. Rev. Immunol.* **2009**, *9*, 465-479.
137. C. A. Wells, J. A. Salvage-Jones, X. Li, K. Hitchens, S. Butcher, R. Z. Murray, A. G. Beckhouse, Y. L. Lo, S. Manzanero, C. Cobbold, K. Schroder, B. Ma, S. Orr, L. Stewart, D. Lebus, P. Sobieszczuk, D. A. Hume, J. Stow, H. Blanchard, R. B. Ashman, *J. Immunol.* **2008**, *180*, 7404-7413.
138. S. Yamasaki, M. Matsumoto, O. Takeuchi, T. Matsuzawa, E. Ishikawa, M. Sakuma, H. Tateno, J. Uno, J. Hirabayashi, Y. Mikami, K. Takeda, S. Akira, T. Saito, *Proc. Natl. Acad. Sci. U S A* **2009**, *106*, 1897-1902.
139. E. Ishikawa, T. Ishikawa, Y. S. Morita, K. Toyonaga, H. Yamada, O. Takeuchi, T. Kinoshita, S. Akira, Y. Yoshikai, S. Yamasaki, *J. Exp. Med.* **2009**, *206*, 2879-2888.
140. L. de Witte, A. Nabatov, M. Pion, D. Fluitsma, M. A. de Jong, T. de Gruijl, V. Piguet, Y. van Kooyk, T. B. Geijtenbeek, *Nat. Med.* **2007**, *13*, 367-371.
141. H. Tateno, K. Ohnishi, R. Yabe, N. Hayatsu, T. Sato, M. Takeya, H. Narimatsu, J. Hirabayashi, *J. Biol. Chem.* **2010**, *285*, 6390-6400.
142. R. A. Childs, K. Drickamer, T. Kawasaki, S. Thiel, T. Mizuochi, T. Feizi, *Biochem. J.* **1989**, *262*, 131-138.
143. E. Laurine, X. Manival, C. Montgelard, C. Bideau, J. L. Berge-Lefranc, M. Erard, J. M. Verdier, *Biochim. Biophys. Acta* **2005**, *1727*, 177-187.
144. H. L. Cash, C. V. Whitham, C. L. Behrendt, L. V. Hooper, *Science* **2006**, *313*, 1126-1130.
145. J. Iovanna, J. M. Frigerio, N. Dusetti, F. Ramare, P. Raibaud, J. C. Dagorn, *Pancreas* **1993**, *8*, 597-601.
146. M. R. Ho, Y. C. Lou, S. Y. Wei, S. C. Luo, W. C. Lin, P. C. Lyu, C. Chen, *J. Mol. Biol.* **2010**, *402*, 682-695.

147. Y. Liu, R. A. Childs, A. S. Palma, M. A. Campanero-Rhodes, M. S. Stoll, W. Chai, T. Feizi, *Methods Mol. Biol.* **2012**, *808*, 117-136.
148. M. Gilleron, V. F. Quesniaux, G. Puzo, *J. Biol. Chem.* **2003**, *278*, 29880-29889.
149. N. N. Driessen, R. Ummels, J. J. Maaskant, S. S. Gurcha, G. S. Besra, G. D. Ainge, D. S. Larsen, G. F. Painter, C. M. Vandembroucke-Grauls, J. Geurtsen, B. J. Appelmelk, *Infect. Immun.* **2009**, *77*, 4538-4547.
150. A. S. Palma, T. Feizi, Y. Zhang, M. S. Stoll, A. M. Lawson, E. Díaz-Rodríguez, M. A. Campanero-Rhodes, J. Costa, S. Gordon, G. D. Brown, W. Chai, *J. Biol. Chem.* **2006**, *281*, 5771-5779.
151. P. S. Patil, S. C. Hung, *Chem. Eur. J.* **2009**, *15*, 1091-1094.
152. A. Ali, M. R. Wenk, M. J. Lear, *Tetrahedron Lett.* **2009**, *50*, 5664-5666.
153. B. S. Dyer, J. D. Jones, G. D. Ainge, M. Denis, D. S. Larsen, G. F. Painter, *J. Org. Chem.* **2007**, *72*, 3282-3288.
154. G. D. Ainge, J. Hudson, D. S. Larsen, G. F. Painter, G. S. Gill, J. L. Harper, *Bioorg. Med. Chem.* **2006**, *14*, 5632-5642.
155. A. Stadelmaier, R. R. Schmidt, *Carbohydr. Res.* **2003**, *338*, 2557-2569.
156. C. J. J. Elie, C. E. Dreef, R. Verduyn, G. A. van der Marel, J. H. van Boom, *Tetrahedron* **1989**, *45*, 3477-3486.
157. A. Ravidà, X. Liu, L. Kovacs, P. H. Seeberger, *Org. Lett.* **2006**, *8*, 1815-1818.
158. L. Knerr, X. Pannecoucke, G. Schmitt, B. Luu, *Tetrahedron Lett.* **1996**, *37*, 5123-5126.
159. M. Mayer, B. Meyer, *J. Am. Chem. Soc.* **2001**, *123*, 6108-6117.
160. M. Mayer, B. Meyer, *Angew. Chem. Int. Ed.* **1999**, *38*, 1784-1788.
161. B. Meyer, T. Peters, *Angew. Chem. Int. Ed.* **2003**, *42*, 864-890.
162. A. Ardá, P. Blasco, D. Varón Silva, V. Schubert, S. André, M. Bruix, F. J. Cañada, H. J. Gabius, C. Unverzagt, J. Jiménez-Barbero, *J. Am. Chem. Soc.* **2013**, *135*, 2667-2675.
163. C. A. Lepre, J. M. Moore, J. W. Peng, *Chem. Rev.* **2004**, *104*, 3641-3676.
164. M. P. Williamson, *Prog. Nucl. Magn. Reson. Spectrosc.* **2013**, *73*, 1-16.
165. D. M. Zajonc, G. D. Ainge, G. F. Painter, W. B. Severn, I. A. Wilson, *J. Immunol.* **2006**, *177*, 4577-4583.
166. K. Schmidt, M. Schrader, H. F. Kern, R. Kleene, *J. Biol. Chem.* **2001**, *276*, 14315-14323.

167. K. Hase, K. Kawano, T. Nochi, G. S. Pontes, S. Fukuda, M. Ebisawa, K. Kadokura, T. Tobe, Y. Fujimura, S. Kawano, A. Yabashi, S. Waguri, G. Nakato, S. Kimura, T. Murakami, M. Iimura, K. Hamura, S. Fukuoka, A. W. Lowe, K. Itoh, H. Kiyono, H. Ohno, *Nature* **2009**, *462*, 226-230.
168. T. Horlacher, C. Noti, J. L. de Paz, P. Bindschädler, P.; M.-L. Hecht, D. F. Smith, M. N. Fukuda, P. H. Seeberger, *Biochemistry* **2011**, *50*, 2650-2659.
169. Y. Tsujii-Hayashi, M. Kitahara, T. Yamagaki, K. Kojima-Aikawa, I. Matsumoto, *J. Biol. Chem.* **2002**, *277*, 47493-47499.
170. K. Kojima, H. K. Ogawa, N. Seno, K. Yamamoto, T. Irimura, T. Osawa, I. Matsumoto, *J. Biol. Chem.* **1992**, *267*, 20536-20539.
171. S. Fukuoka, S. D. Freedman, H. Yu, V. P. Sukhatme, G. A. Scheele, *Proc. Natl. Acad. Sci. U S A* **1992**, *89*, 1189-1193.
172. T. Satoh, Y. Chen, D. Hu, S. Hanashima, K. Yamamoto, Y. Yamaguchi, *Mol. Cell* **2010**, *40*, 905-916.
173. K. Hayashi, C. Kojima, *J. Biomol. NMR* **2010**, *48*, 147-155.
174. Y. Liu, T. Feizi, M. A. Campanero-Rhodes, R. A. Childs, Y. Zhang, B. Mulloy, P. G. Evans, H. M. Osborn, D. Otto, P. R. Crocker, W. Chai, *Chem. Biol.* **2007**, *14*, 847-859.
175. X. Liu, Y.-U. Kwon, P. H. Seeberger, *J. Am. Chem. Soc.* **2005**, *127*, 5004-5005.

List of Publications

Parts of this PhD thesis have already been published:

1. **Chemical Synthesis of GPI Anchors and GPI-Anchored Molecules.** I. Vilotijevic, S. Götze, P. H. Seeberger, D. Varón Silva, in *Modern Synthetic Methods in Carbohydrate Chemistry: From Monosaccharides to Complex Glycoconjugates*, (Eds: D. B. Werz, and S. Vidal), Wiley-VCH Verlag GmbH & Co. KGaA, Weinheim, 2013, Chapter 12.
2. **A General and Convergent Synthesis of Diverse Glycosylphosphatidylinositol Glycolipids.** Y.-H. Tsai, S. Götze, I. Vilotijevic, M. Grube, D. Varón Silva, P. H. Seeberger, *Chem. Sci.* **2013**, *4*, 468-481.
3. **A General Method for Synthesis of GPI Anchors Illustrated by the Total Synthesis of the Low-Molecular-Weight Antigen from *Toxoplasma gondii*.** Y.-H. Tsai, S. Götze, N. Azzouz, H. S. Hahm, P. H. Seeberger, D. Varón Silva, *Angew. Chem. Int. Edit.* **2011**, *50*, 9961-9964.

**Der Lebenslauf ist in der Online-Version aus Gründen des
Datenschutzes nicht enthalten.**

Der Lebenslauf ist in der Online-Version aus Gründen des Datenschutzes nicht enthalten.

*Betrachte nicht müßig den Steinhafen,
sondern frage dich,
wen du damit bewerfen kannst.*

Persisches Sprichwort[†]

[†] Alle Zitate, die in dieser Doktorarbeit angeführt sind, können nachgelesen werden in: D. Bittrich, *Böse Sprüche für jeden Tag 3. Auflage*, Deutscher Taschenbuch Verlag GmbH & Co. KG, München, 2004, Kapitel 1.

Appendix

A. Characterization of the Interaction between the Chemokine CCL20 and Synthetic Heparins

Introduction:

Asthma is a common disease characterized by chronic airway inflammation, mucus hypersecretion and airway hyperreactivity against inhaled allergens.¹⁷⁶ Accumulation of T lymphocytes in the lung in allergic asthma causes Th2 mediated pulmonary inflammation. The asthmatic inflammatory response is orchestrated by a T cell trafficking network present in lung tissue, blood circulation, secondary lymphoid organs and peripheral tissue.^{177,178} Of note, the significant increase of T cells in the airway in asthma is mostly due to T cell recruitment from regional lymph nodes rather than their proliferation at the inflamed site.¹⁷⁹ Therefore, a therapeutic approach that shuts off the trafficking pathway of pathogenic T cells should significantly inhibit the Th2 mediated inflammation in allergic asthma.

It is well known that the destination of the T cell trafficking pathway is tightly restricted by the profile of chemokines, lipid chemoattractants, and T cell chemokine receptors.^{180,181} As a part of immune surveillance, naïve T cells and central memory T cells constantly access secondary lymphoid organs from blood circulation *via* specialized HEV. The interaction between T cells and HEV cells includes in a stepwise manner, L-selectin-dependent tethering and rolling, activation, firm arrest, and transendothelial migration. Besides 6-sulfo sialyl Lewis X as a L-selectin ligand, HEV constitutively express chemokines CCL21 as well as CCL19 and attract T cells, which express its cognate receptor CCR7. In contrast to this homeostatic homing, circulating T cells interact with inflamed blood vessels in the lung after asthmatic exposure to an inhaled allergen. Among numerous combinations of chemokines and their receptors, there is considerable evidence that CCL20 and its cognate receptor CCR6 may

¹⁷⁶ W.W. Busse, R.F. Lemanske, Jr., *N. Engl. J. Med.* **2001**, *344*, 350-362.

¹⁷⁷ B. D. Medoff, S. Y. Thomas, A. D. Luster, *Annu. Rev. Immunol.* **2008**, *26*, 205-232.

¹⁷⁸ S. A. Islam, A. D. Luster, *Nat. Med.* **2012**, *18*, 705-715.

¹⁷⁹ N. L. Harris, V. Watt, F. Ronchese, G. Le Gros, *J. Exp. Med.* **2002**, *195*, 317-326.

¹⁸⁰ P.G. Holt, D. H. Strickland, M. E. Wikstrom, F. L. Jahnsen, *Nat. Rev. Immunol.* **2008**, *8*, 142-152.

¹⁸¹ T. M. Handel, Z. Johnson, S. E. Crown, E. K. Lau, A. E. Proudfoot, *Annu. Rev. Biochem.* **2005**, *74*, 385-410.

contribute to the pathogenesis of asthma.^{182,183} CCL20-CCR6 plays a key role in the recruitment of Th17 cells and Th2 cells.¹⁸⁴ Indeed, CCL20 is highly enriched on inflammatory epithelium¹⁸⁵ and CCR6 is expressed on memory T cells infiltrated in the lung during allergic inflammation¹⁸⁶. In addition, CCR6-deficient mice have decreased airway responsiveness, and reduced recruitment of eosinophils into lung.¹⁸⁷ These findings suggest that the CCL20-CCR6 axis is a putative target for the treatment of asthma.

Cumulative evidence *in vivo* and *in vitro* indicates that chemokines cannot be functionally active in HEV and inflamed sites without their interaction with heparan sulfate.^{181,188} Heparan sulfate protects chemokines from proteolysis¹⁸⁹, immobilizes them on the endothelium surface and produces chemokine gradients in the vasculature¹⁹⁰. Previous reports have indicated that the sulfation patterns in heparan sulfate are more conserved than expected¹⁹¹ and that the sulfation pattern is associated with respiratory distress¹⁹² and asthma¹⁹³. It is believed that there are specific interactions between heparan sulfate and chemokines.¹⁹⁴ Nevertheless, the non-template nature of long carbohydrate chains (< 25,000 disaccharide units) and conformational plasticity still make it difficult to identify common sequences of heparan sulfate, which display affinity to specific chemokines. In this regard, a heparin-glycan microarray system^{195,196} was used as a powerful tool to elucidate heparan sulfate structural motifs that are important for CCL20 binding and to find a possible inhibitor for the CCL20-CCR6 interaction.

¹⁸² N. W. Lukacs, D. M. Prosser, M. Wiekowski, S. A. Lira, D. N. Cook, *J. Exp. Med.* **2001**, 194, 551-555.

¹⁸³ S. Y. Thomas, A. Banerji, B. D. Medoff, C. M. Lilly, A. D. Luster, *J. Immunol.* **2007**, 179, 1901-1912.

¹⁸⁴ M. Weckmann, A. Collison, J. L. Simpson, M. V. Kopp, P. A. Wark, M. J. Smyth, H. Yagita, K. I. Matthaei, N. Hansbro, B. Whitehead, P. G. Gibson, P. S. Foster, J. Mattes, *Nat. Med.* **2007**, 13, 1308-1315.

¹⁸⁵ M.-C. Dieu-Nosjean, C. Massacrier, B. Homey, B. Vanbervliet, J. J. Pin, A. Vicari, S. Lebecque, C. Dezutter-Dambuyant, D. Schmitt, A. Zlotnik, C. Caux, *J. Exp. Med.* **2000**, 192, 705-718.

¹⁸⁶ F. Liao, R. L. Rabin, C. S. Smith, G. Sharma, T. B. Nutman, J. M. Farber, *J. Immunol.* **1999**, 162, 186-194.

¹⁸⁷ S. K. Lundy, S. A. Lira, J. J. Smit, D. N. Cook, A. A. Berlin, N. W. Lukacs, *J. Immunol.* **2005**, 174, 2054-2060.

¹⁸⁸ C. R. Parish, *Nat. Rev. Immunol.* **2006**, 6, 633-643.

¹⁸⁹ R. Sadir, A. Imberty, F. Baleux, H. Lortat-Jacob, *J. Biol. Chem.* **2004**, 279, 43854-43860.

¹⁹⁰ J. Middleton, A. M. Patterson, L. Gardner, C. Schmutz, B. A. Ashton, *Blood* **2002**, 100, 3853-3860.

¹⁹¹ J. T. Gallagher, *J. Clin. Invest.* **2001**, 108, 357-361.

¹⁹² G. Fan, L. Xiao, L. Cheng, X. Wang, B. Sun, G. Hu, *FEBS Lett.* **2000**, 467, 7-11.

¹⁹³ R. I. Zuberi, X. N. Ge, S. Jiang, N. S. Bahaie, B. N. Kang, R. M. Hosseinkhani, E. M. Frenzel, M. M. Fuster, J. D. Esko, S. P. Rao, P. Sriramarao, *J. Immunol.* **2009**, 183, 3971-3979.

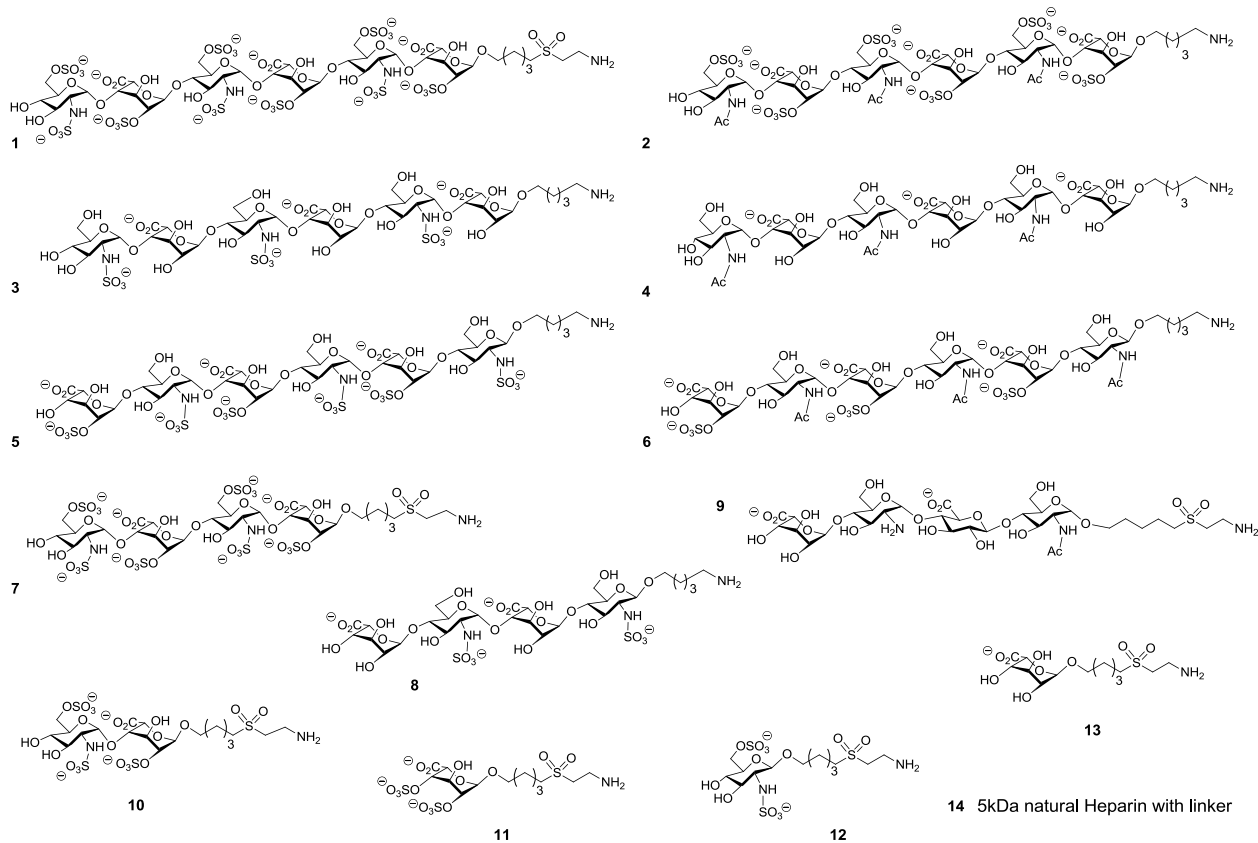
¹⁹⁴ H. Lortat-Jacob, A. Grosdidier, A. Imberty, *Proc. Natl. Acad. Sci. USA* **2002**, 99, 1229-1234.

¹⁹⁵ J. L. de Paz, E. A. Moseman, C. Noti, L. Polito, U. H. von Andrian, P.H. Seeberger, *ACS Chem. Biol.* **2007**, 2, 735-744.

¹⁹⁶ J. L. de Paz, C. Noti, F. Böhm, S. Werner, P. H. Seeberger, *Chem. Biol* **2007**, 14, 879-887.

Results:

The binding profile of CCL20 to a heparin-like carbohydrate library, which is immobilized on a microarray and contains carbohydrates with various sulfation patterns ranging from monosaccharides to hexasaccharides, was investigated (Scheme A.1).



Scheme A.1: Structures of the heparin-like oligosaccharides **1-14**, which were printed on a microarray.

The screening results showed that CCL20 strongly bound to hexasaccharides **1**, **2**, and moderately to hexasaccharide **5** and tetrasaccharide **7**, indicating that the affinity of CCL20 becomes higher as number of sulfations increases (Figure A.1A, page 173). Noteworthy, CCL20 exhibited high affinity to disaccharide **10** and even monosaccharide **11**. Observed fluorescent intensities indicated that CCL20 binds almost with equal affinity to 5 kDa natural heparin **14** and to the small and highly charged carbohydrates **10** and **11** (Figure A.1C). In addition it could be shown, that binding was completely inhibited by performing the experiment in the presence of 5 mM natural heparin underlining the specific interaction of CCL20 with this type of glycosaminoglycan (Figure A.1B).

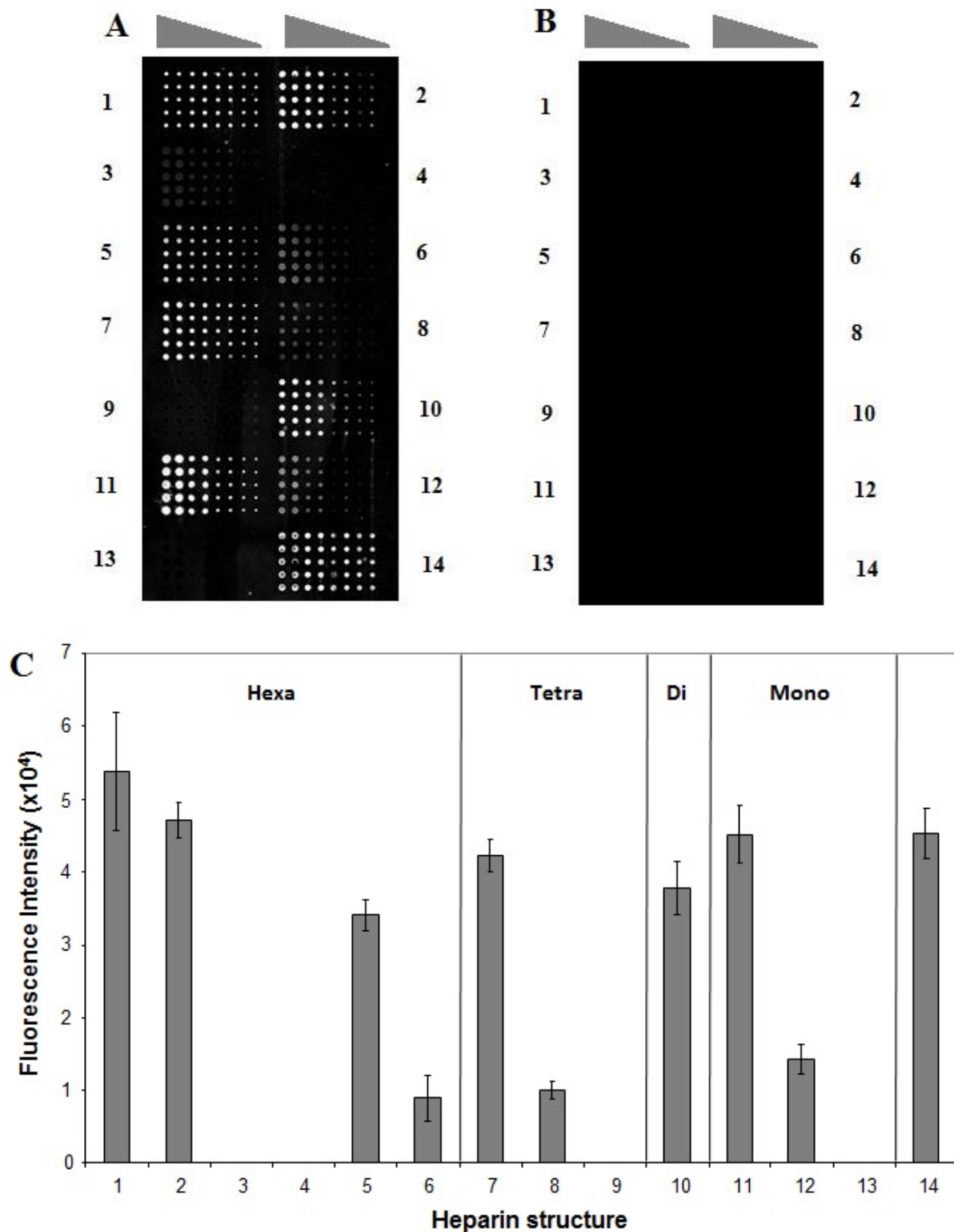


Figure A.1: (A) Binding of recombinant human CCL20 to the heparin library on a microarray. The triangles indicate the concentration decrease of the printed compounds from left to right. Position of the different compounds is annotated. Each sugar was printed on the slide at four different concentrations ranging from 1000, 250, 63, and 16 μM in 10 replicas. (B) Addition of natural heparin inhibits binding of CCL20 to the surface immobilized carbohydrates. (C) Quantification of the binding of CCL20 to the different heparin structures shown in Scheme A.1 ($n = 10$; concentration = 250 μM).

Monosaccharide **11** is a 2,4-*O*-di-sulfated iduronic acid, which consists of two axial sulfate groups. Compound **11** is an unnatural synthetic monosaccharide that has never been reported from a natural source. Therefore the interaction of **11** with CCL20 was further characterized in more detail. The data from SPR showed that CCL20 binds to immobilized IdoA derivative **11** in a concentration dependent manner. Analysis of the kinetic constants using a simple 1:1 binding model generated a K_D value of approximately 2.9 μM , which is in the expected range for the interaction of a protein with a monosaccharide presented in a multivalent fashion (Figure A.2A).¹⁹⁷ Performing the same experiment in the presence of 5 mM 5kDa natural heparin disabled binding of the protein and validated the microarray data (Figure A.2B).

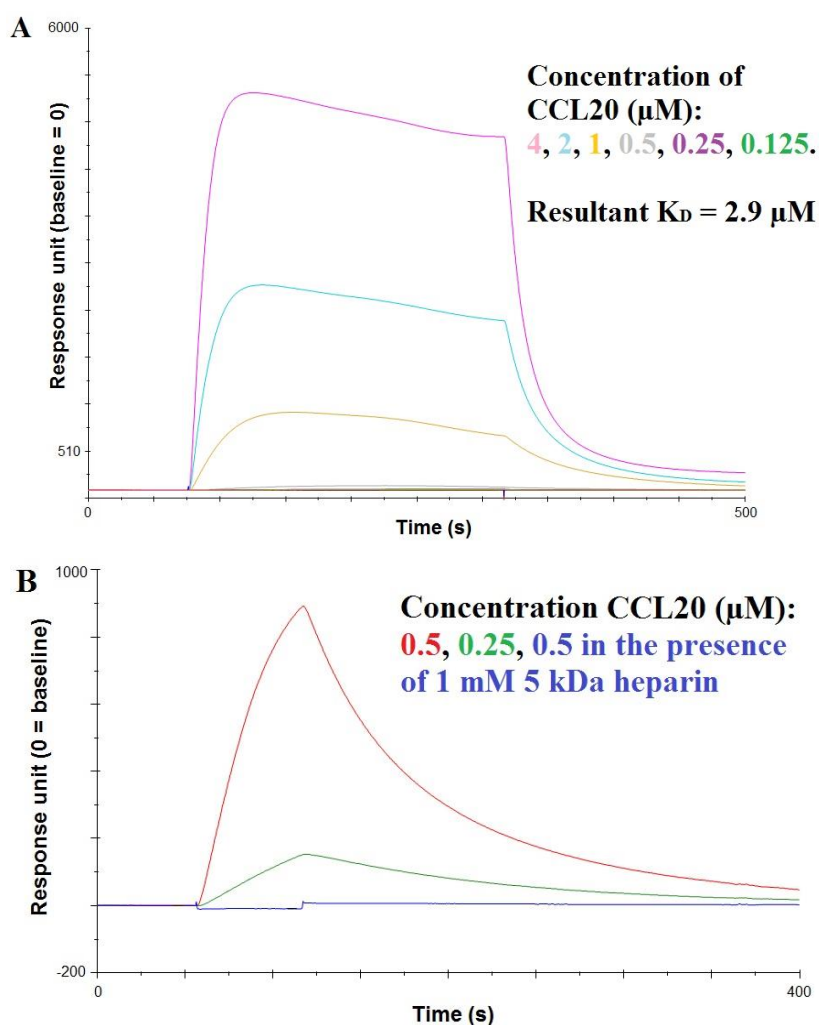


Figure A.2: (A) SPR sensorgrams for characterization of the CCL20-monosaccharide **11** interaction. A 1:1 binding model was used for the determination of the K_D value. The sensorgrams indicate a more complex mode of interaction, for which reason the calculated kinetic and thermodynamic constants have to be validated by other methods. (B) SPR sensorgrams of the inhibition experiment using 1 mM heparin from natural sources.

¹⁹⁷ M.-L. Hecht, B. Rosental, T. Horlacher, O. Hershkovitz, J. L. De Paz, C. Noti, S. Schauer, A. Porgador, P. H. Seeberger, *J. Proteome Res.* **2009**, *8*, 712-720.

Conclusion:

A novel binding partner of the chemokine CCL20 was identified. The monosaccharide Di-S-IdoA **11** was further investigated by our collaboration partners (Prof. Minoru Fukuda and Dr. Motohiro Nonaka, Sanford-Burnham Medical Research Institute, La Jolla, USA) in different *in vitro* and *in vivo* experiments. It could be shown that **11** is a potent inhibitor of CCL20. In addition lymphocyte recruitment into allergen challenged lung inflammation sites was attenuated in a mouse model by simple inhalation of a dispersed solution containing monosaccharide **11**. Pulmonary inhalation drug delivery of this compound may help to reduce asthmatic symptoms by suppressing chemokine-mediated inflammatory responses, mucus production, and airway responsiveness.

Materials and Methods:

Glycan Microarray. Microarrays were fabricated as previously reported.¹⁹⁷ The microarray slide was first blocked for 1 h with PBS-buffer containing BSA (2.5%). Afterwards the microarray slide was incubated for 1 h at room temperature under mild shaking with 100 μ L HBS-N-buffer (GE Healthcare, pH = 7.4) containing 5 μ g of rhCCL20 (R&D Systems) and 0.01% Tween-20 by placing a cover slip onto the slide. The slide was washed three times with HBS-N-buffer and dried by centrifugation [inhibition solution contained 5 mM 5kDa heparin (Santa Cruz Biotechnology)]. The slide was then incubated with 100 μ L HBS-N-buffer containing 2 μ g of anti-hCCL20 goat IgG (R&D Systems) for 1 h, followed by incubation with anti-goat Alexa Fluor 594 antibody (Invitrogen, in HBS-N-buffer, dilution 1:100) for 1 h. The slide was washed three times with HBS-N-buffer before it was dried *via* centrifugation. The slide was scanned with a GenePix 4300A Microarray scanner and analyzed by GenePix® Pro Software.

SPR immobilization. Compound **11** was covalently bound to the sensor surface using primary amine coupling and a Biacore T100 (GE Healthcare). HBS-N containing 0.005% (v/v) P20 was employed as running buffer. The carboxymethylated dextran matrix (CM5 chip, GE Healthcare) was first activated at a flow rate of 10 μ L/min using an 8 min injection pulse of an aqueous solution containing NHS (0.05 M, GE Healthcare) and N-(3-dimethylaminopropyl)-N'-ethylcarbodiimide hydrochloride (EDC · HCL, 0.2 M, GE Healthcare). Next, a solution of the oligosaccharide (50 μ g/mL) containing 1 mM hexadecyltrimethylammonium chloride (Sigma Aldrich) was flowed over the activated surface for 8 min at 5 μ L/min. Remaining reactive groups on the chip surface were quenched by injection of a 1 M ethanolamine hydrochloride (pH 8.5, GE Healthcare) solution for 7.5 min at 10 μ L/min. A parallel flow cell

was coupled with HS/heparin **9** as a reference cell. The following binding levels were established (in response units, RU): HS/heparin **11**, 299; HS/heparin **9**, 407.

Kinetic analysis by SPR. For K_D determination between immobilized **11** and rhCCL20, the following protein concentrations were injected at a flow rate of 30 $\mu\text{L}/\text{min}$ and 25 $^{\circ}\text{C}$: 0.125, 0.250, 0.5, 1, 1.82 and 4 μM . Running buffer was then flowed over the sensor surface for 10 min to enable dissociation. The sensor surface was regenerated for the next sample using 0.1% SDS and 0.085% H_3PO_4 injected for 1 min at a flow rate of 80 $\mu\text{L}/\text{min}$. The signal from the reference flow cell containing oligosaccharide **9** was subtracted to correct for the contribution of nonspecific interactions and systematic errors. Kinetic analysis was performed using the BIAevaluation software for T100. Association and dissociation phase data were globally fitted to a simple 1:1 interaction model ($A + B = AB$).

B. Determination of the Binding Motif of the Monoclonal Antibody my2F12

Introduction:

Based on population surveys and computer modeling, the WHO has estimated that there were 8.7 million new incident cases and 1.4 million deaths due to TB, which is caused mainly by the pathogenic mycobacteria *M. tuberculosis*, in 2011, occurring primarily in the developing countries of Africa and Asia.¹⁹⁸ While TB is a treatable disease with an 85% success rate for primary infections, only two-thirds of the total estimated incident cases were reported to national healthcare programs, suggesting that management of TB in endemic regions is hampered by the lack of effective diagnostic methodologies. Current methods for the microbiological diagnosis of TB include nucleic acid amplification tests, sputum culture or smear microscopy, all of which have significant drawbacks for use in developing countries. Sputum culture, which is the current gold standard diagnostic assay for pulmonary TB, requires up to two weeks for a definitive result.¹⁹⁹ Nucleic acid amplification tests, which have near equivalent sensitivity to sputum culture, have high costs that limit their broader application.²⁰⁰ The most widely utilized diagnostic test remains the sputum smear which relies upon the microscopic observation of stained mycolic acids in acid-fast mycobacteria. While rapid, the sensitivity of this assay has been reported to range from 80% to 20% and is highly dependent on the skills and experience of the person performing the test.²⁰¹ It also has reduced sensitivity in HIV positive cohorts and cannot distinguish between different mycobacterial species-in particular those that are pathogenic versus non-pathogenic.²⁰²

Antibody-based detection of disease-specific biomarkers is a diagnostic methodology that has the potential to be developed into a point-of-care test that is rapid, sensitive, specific, cheap and requires minimal training and infrastructure to operate; and hence offers significant improvements for TB diagnosis. One suitable biomarker for TB is LAM, a membrane glycolipid present on the surface of all species of mycobacteria and reportedly found in the

¹⁹⁸ WHO (2012) Global Tuberculosis Report 2012 (Geneva).

¹⁹⁹ WHO (2006) Diagnostics for Tuberculosis: Global demand and market potential.

²⁰⁰ B. Kambashi, G. Mbulo, R. McNerney, R. Tembwe, A. Kambashi, V. Tihon, P. Godfrey-Faussett, *Int. J. Tuberc. Lung Dis.* **2001**, *5*, 364-369.

²⁰¹ K. R. Steingart, V. Ng, M. Henry, P. C. Hopewell, A. Ramsay, J. Cunningham, R. Urbanczik, M. D. Perkins, M. A. Aziz, M. Pai, *Lancet Infect. Dis.* **2006**, *6*, 664-674.

²⁰² A. M. Elliott, K. Namaambo, B. W. Allen, N. Luo, R. J. Hayes, J. O. Pabee, K. P. McAdam, *Tuber. Lung Dis.* **1993**, *74*, 191-194.

blood, sputum and urine of TB patients.^{203,204} Structural studies have shown that while the LAM backbone is ubiquitous in mycobacteria, the LAM produced by pathogenic slow growing mycobacteria such as *M. tuberculosis* have a unique mannose sugar capping motif comprised of $\alpha 1 \rightarrow 2$ mannose linkages (hence termed ManLAM), making this an ideal target for a candidate diagnostic antibody.²⁰⁵ An additional advantage of LAM as a biomarker is its inherent heat-tolerance that allows a simple sterilization procedure for infectious clinical samples. While the detection of LAM in urine with LAM specific antibody-based assays have been studied extensively, its clinical utility remains in doubt due to its low sensitivity, especially in the HIV negative cohort which comprises the majority of TB patients globally.²⁰⁶

In this study, we characterized the binding motif of a ManLAM-specific human antibody (my2F12) that was derived from an antibody-phage display library for directed epitope targeting*. A microarray system containing high-mannose structures (**1-7**)²⁰⁷, PIMs (**17-23**)²⁰⁸, arabinomannan oligosaccharides (**8-10**)¹²³ and simple nutrition related carbohydrates (**13-16**)²⁰⁹ was used to validate the Man $\alpha 1 \rightarrow 2$ Man specificity of the engineered antibody my2F12, which was employed in the development of a sandwich ELISA to identify smear negative TB patients (Scheme B.1, page 179).

²⁰³ E. Sada, D. Aguilar, M. Torres M, T. Herrera, *J. Clin. Microbiol.* **1992**, *30*, 2415-2418.

²⁰⁴ K. Dheda, V. Davids, L. Lenders, T. Roberts, R. Meldau, D. Ling, L. Brunet, R. van Zyl Smit, J. Peter, C. Green, M. Badri, L. Sechi, S. Sharma, M. Hoelscher, R. Dawson, A. Whitelaw, J. Blackburn, M. Pai, A. Zumla, *PLoS One* **2010**, *5*, e9848.

²⁰⁵ J. Nigou, M. Gilleron, G. Puzo, *Biochimie* **2003**, *85*, 153-166.

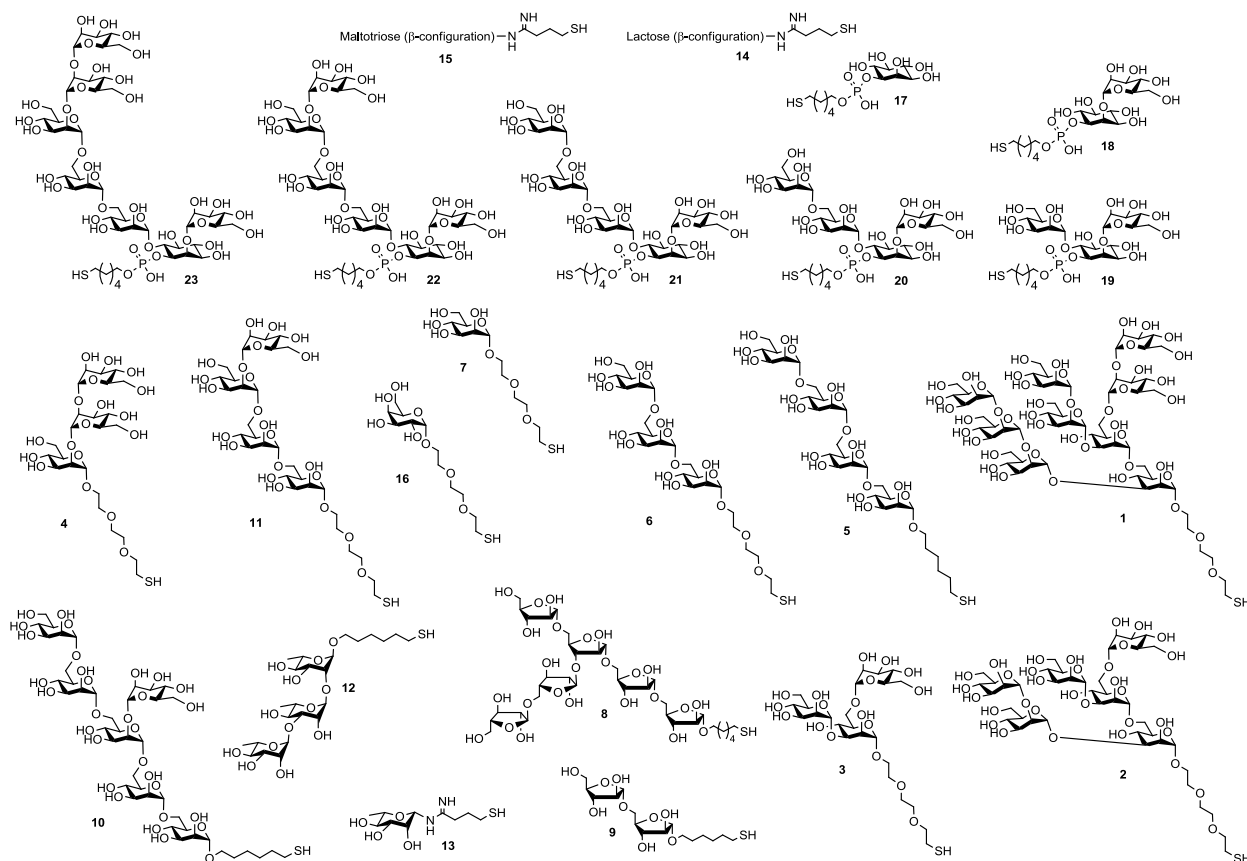
²⁰⁶ J. Minion, E. Leung, E. Talbot, K. Dheda, M. Pai, D. Menzies, *Eur. Respir. J.* **2011**, *38*, 1398-1405.

* The antibody was created by Dr. C. E. Chan (Department of Microbiology, National University of Singapore, Laboratory of Prof. Paul A. MacAry).

²⁰⁷ E. W. Adams, D. M. Ratner, H. R. Bokesch, J. B. McMahon, B. R. O'Keefe, P. H. Seeberger, *Chem. Biol.* **2004**, *11*, 875-881.

²⁰⁸ S. Boonyarattanakalin, X. Liu, M. Michieletti, B. Lepenies, P. H. Seeberger, *J. Am. Chem. Soc.* **2008**, *130*, 16791-16799.

²⁰⁹ T. Horlacher, M. A. Oberli, D. B. Werz, L. Kröck, S. Bufali, R. Mishra, J. Sobek, K. Simons, M. Hirashima, T. Niki, P. H. Seeberger, *ChemBioChem* **2010**, *11*, 1563 – 1573.



Scheme B.1: Structures of oligosaccharides **1-23** that are related to mycobacterial cell wall carbohydrates.

Results and Conclusion:

All thiol modified carbohydrates (**1-23**) were printed at four different concentrations (1 mM, 0.25 mM, 62.5 μ M and 15.6 μ M) in replicates of ten on maleimide functionalized slides. This printing pattern ensures reproducibility of the results and enables the investigation of concentration dependent binding (Figure B.1).

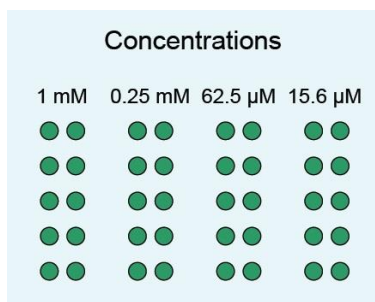


Figure B.1: General printing pattern of all sugars on the microarray. The concentration decreases from left to right.

The antibody showed concentration dependent binding to oligosaccharides containing terminal Man α 1 \rightarrow 2Man linkages (**1, 4, 11, 22** and **23**). The only exception was mannoside **2**

that consists of multiple branches with only one of them featuring the Man α 1 \rightarrow 2Man linkage (Figure B.2A). Given that sugar **2** is sterically crowded the epitope is possibly shielded by other side branches of the molecule making interactions with the antibody unfeasible. The internal Man α 1 \rightarrow 2Man linkage present in hexasaccharide **10**, which is a substructure of the polysaccharide mannan that is present in the capsule material of many mycobacteria, was also not recognized by the antibody exhibiting the exclusive binding preference for terminal mannose caps. No binding was observed for other saccharides related to the mycobacterial cell wall e. g. arabinosides (**8** and **9**), rhamnoses (**12** and **13**) as well as PIMs lacking the terminal Man α 1 \rightarrow 2Man linkage (**17-21**). Nutrition related negative controls such as lactose **14**, maltotriose **15** and monosaccharides **6** and **17** showed also no interaction with the antibody. Furthermore inhibition experiments with isolated ManLAM, PILAM and mannan clearly demonstrated that binding of my2F12 to the glycans presented on the microarray was only abrogated when ManLAM was used as a competing binder (Figure B.2B-C).

These results validated the expected specificity of the antibody as Man α 1 \rightarrow 2Man motifs are the sole type of linkage found in the cap of ManLAM.⁵²

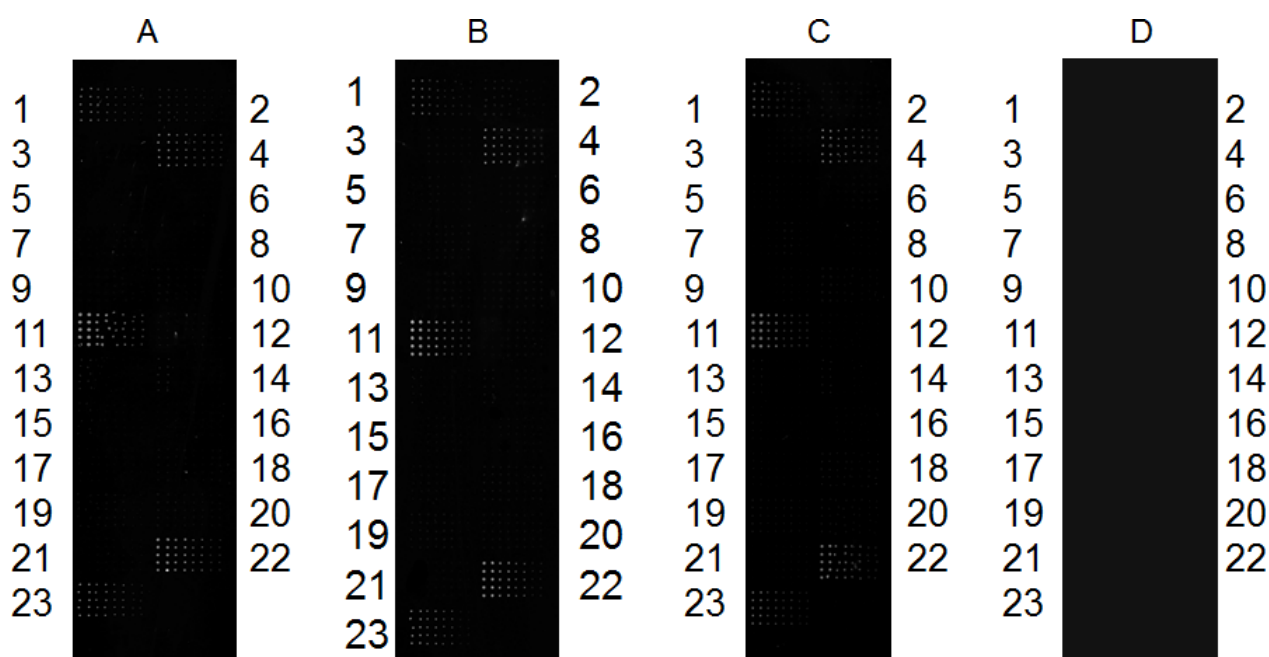


Figure B.2: (A) Binding of the mAb my2F12 to carbohydrates **1-23** presented on a microarray. Inhibition experiments with (B) mannan, (C) PILAM and (D) ManLAM. Binding was only inhibited in the presence of ManLAM.

Materials and Methods:

Glycan Microarray. Microarrays were fabricated as previously reported.²⁰⁹ The microarray slide was first blocked for 1 h with 100 μ L NWB-buffer (20 mM Tris·HCl pH 7.4, 1 mM CaCl₂, 150 mM NaCl) containing BSA (2.5%). Afterwards the slide was washed two times

with NWB-buffer and dried *via* centrifugation. Afterwards the slide was incubated with 100 μ L NWB-buffer containing 5 μ g of mAb (my2F12), which was engineered by Dr. Conrad E. Chan, and BSA (1%) (inhibition experiments additionally contained 30 μ g of mannan (Sigma Aldrich) or isolated ManLAM or PILAM, which was provided by our collaboration partner Prof. Paul A. MacAry) for 1 h at room temperature under mild shaking by placing a cover slip onto the slide. The slide was washed three times with NWB-buffer and dried by centrifugation. The slides were then incubated with 100 μ L NWB-buffer containing 1 μ L of anti-human IgG Alexa Fluor 647 (Invitrogen) and BSA (1%) for 1 h. The slides were washed three times with NWB-buffer and dried by centrifugation. The slides were finally scanned with a GenePix 4300A Microarray scanner and analyzed by GenePix® Pro Software.

C. Development of a Fully Synthetic Glycolipid Vaccine Targeted against the Cancer Associated T_N-antigen

Introduction:

Until recently, vaccines have had little influence on the fight against cancer. However, in the past few years many vaccines have been approved or are being investigated to prime the immune system into fighting this disease.²¹⁰ In most cases, the epitopes are peptide-based, but glycopeptide vaccines are slowly emerging.^{211,212}

The expressed carbohydrate epitopes on cancer cells are often similar to self-carbohydrates. Therefore, a cancer vaccine would have to activate the immune system more strongly than a regular vaccine, in order to break the immunological self-tolerance to the tumor-associated self-antigens. It is thus of prime importance for carbohydrate-based anti-cancer vaccines to include a strategy to strongly activate the immune system against the carbohydrate antigens.

The glycolipid GSL, also known as KRN7000 or α -GalCer, is a synthetic derivative of a glycolipid found in marine sponges, and identified as an immune activator that lowered the tumor burden of mice.²¹³ This glycolipid is known to be presented by antigen-presenting cells by loading it onto the protein CD1d. After having been loaded with the glycolipid, CD1d will interact with an invariant T-cell receptor of invariant natural killer T cells (iNKT cells), resulting in the activation of the iNKT cells, expansion of their population, and secretion of a plethora of cytokines. Also, GSL or analogs are being investigated in many contexts as vaccine adjuvants. The Wong group has recently used a α -GalCer analog as an adjuvant for boosting the response to a protein-based vaccine.²¹⁴ This work was followed by the use of another analog as an adjuvant for protein-carbohydrate vaccines.²¹⁵

However, all published work on the adjuvant effects of α -GalCer and analogs have focused on their use as a physical mixture adjuvant. No work has focused on covalently linking KRN 7000 and an antigen. Such a novel approach has several potential advantages. First of all a covalent system would focus the immune response against the desired antigen by perfectly localizing the antigen and the adjuvant in space. Secondly, α -GalCer and its derivatives can

²¹⁰ J. Schlom, *J. Natl. Cancer. I.* **2012**, *104*, 599-613.

²¹¹ C. C. Liu, X. S. Ye, *Glycoconjugate J.* **2012**, *29*, 259-271.

²¹² N. Gaidzik, U. Westerlind, H. Kunz, *Chem. Soc. Rev.* **2013**, *42*, 4421-4442.

²¹³ E. Kobayashi, K. Motoki, T. Uchida, H. Fukushima, Y. Koezuka, *Oncol. Res.* **1995**, *7*, 529-534.

²¹⁴ X. M. Li, M. Fujio, M. Imamura, D. Wu, S. Vasan, C.-H. Wong, D. D. Ho, M. Tsuji, *Proc. Natl. Acad. Sci. USA* **2010**, *107*, 13010-13015.

²¹⁵ Y. L. Huang, J. T. Hung, S. K. C. Cheung, H. Y. Lee, K. C. Chu, S. T. Li, Y. C. Lin, C. T. Ren, T. J. Cheng, T. L. Hsu, A. L. Yu, C. Y. Wu, C.-H. Wong, *Proc. Natl. Acad. Sci. USA* **2013**, *110*, 2517-2522.

be incorporated into liposomes that offer a multivalent presentation of haptens, which is necessary to activate B cells on the path to antibody production. Finally, such a system could eliminate the need for protein-carbohydrate conjugate vaccines, and replace them with glycolipid-carbohydrate conjugates. As the protein and peptide parts of vaccines are known to be temperature-sensitive, this could open a new route to heat-stable vaccines.²¹⁶

The fully synthetic glycolipid vaccine **1** was envisioned *via* coupling of the tumor associated T_N-antigen derivative **2**²¹⁷ with *p*-nitrophenol carbamate **3** (Figure C.1). This strategy offers the opportunity to couple different amine or hydrazone modified carbohydrates to the immunomodulatory GSL moiety to form a diverse set of carbohydrate-based vaccines against different diseases besides cancer. The received glycolipid can then be incorporated into liposomes to form a stable vaccine.

Here the synthesis of antigen **2**, GSL derivative **3** and the resultant glycolipid **1** is described.

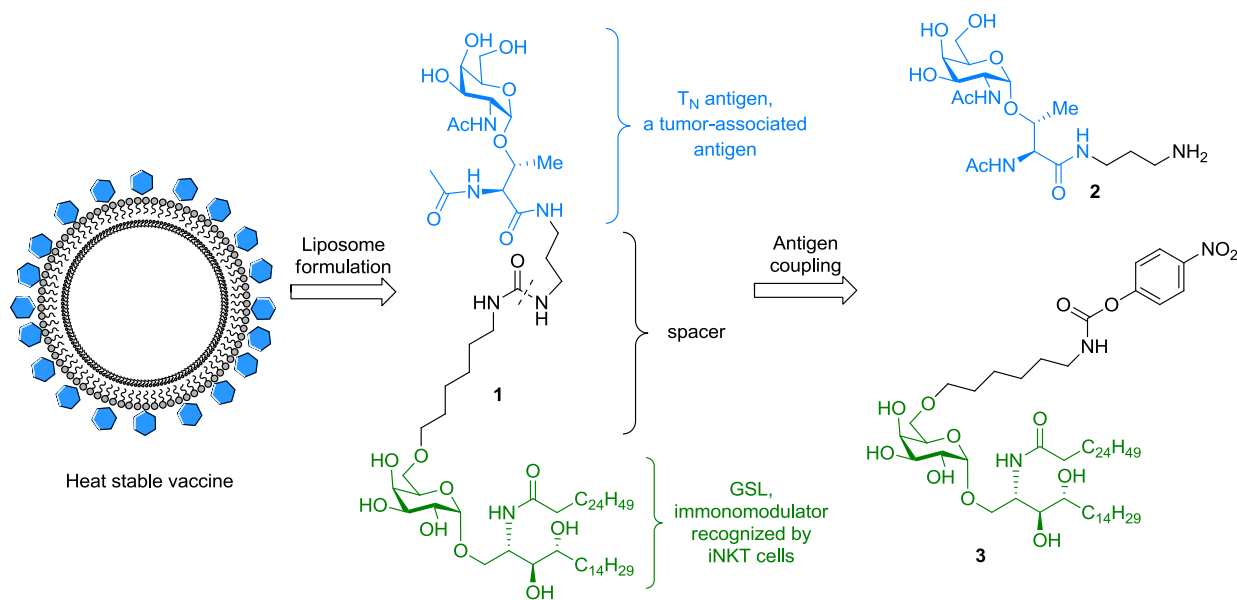


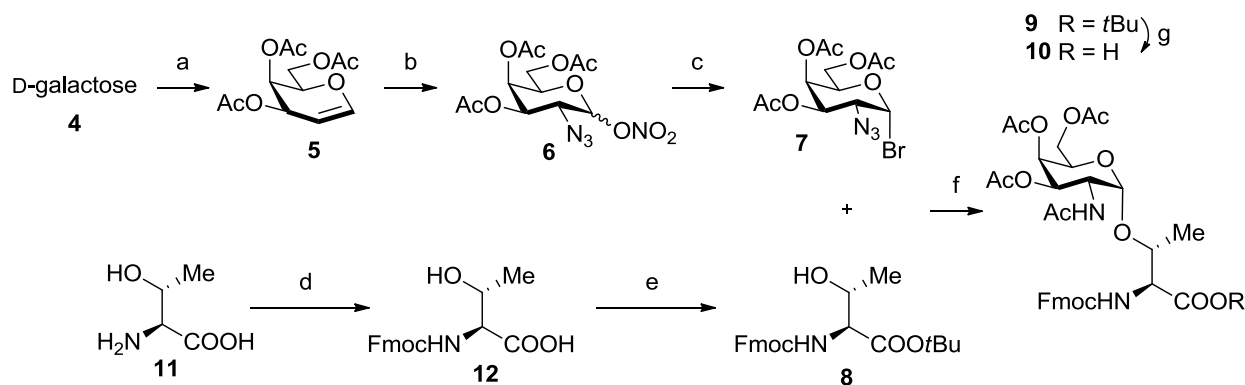
Figure C.1: Design of a fully synthetic vaccine against cancer.

²¹⁶ X. D. Chen, D. Kristensen, *Expert Rev. Vaccines* **2009**, *8*, 547-57.

²¹⁷ T. Buskas, S. Ingale, G.-J. Boons, *Angew. Chem. Int. Ed.* **2005**, *44*, 5985-5988.

Results:

The synthesis of the T_N-antigen **2** was performed according to literature known procedures.^{217,218} D-Galactose (**4**) was acetylated under acidic conditions and brominated with HBr in acetic acid (Scheme C.1). The resulting bromide was reduced to galactal **5** using activated zinc at -20 °C in 95% yield over three steps. Azidonitratization²¹⁹ with sodium azide and CAN yielded an inseparable anomeric mixture of nitrates **6**, which was directly converted into the corresponding bromide **7** using LiBr in acetonitrile. Glycosylation of orthogonally protected L-threonine **8** with bromide **7** promoted by silver carbonate and silver perchlorate yielded the glycosylated amino acid as an inseparable mixture of anomers (α/β – 9:1). Reduction of the azide and *in situ* acetylation gave the fully protected T_N-antigen **9** in 61% over two steps. Final removal of the ester with 50% TFA in DCM using anisole as a scavenger provided SPPS-ready T_N-building block **10** in 87% yield and multigram scale.

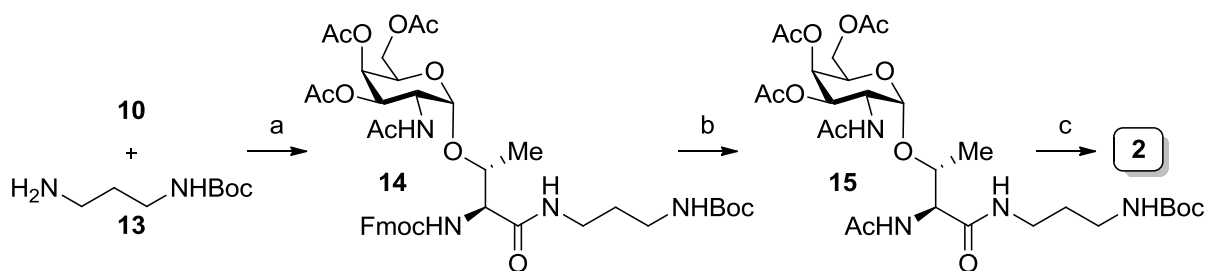


Scheme C.1: Synthesis of building block **10**. *Reagents and conditions:* (a) i. Ac₂O, HClO₄, 0 °C; ii. PBr₃, H₂O, 0 °C; iii. Zn, CuSO₄, AcOH/water (2:3), -20 °C, 95% over 3 steps; (b) NaN₃, CAN, MeCN, -20 °C, (α/β - 6:5), 26%; (c) LiBr, MeCN, 94%; (d) Fmoc-OSu, NaHCO₃, acetone/water (1:1); (e) CuCl, DCC, *t*BuOH, 0 °C, 62% over 2 steps; (f) i. Ag₂CO₃, AgClO₄, toluene/DCM (1:1), MS 4 Å; ii. Zn, CuSO₄, THF/Ac₂O/HOAc (3:2:1) 61% over 2 steps; (g) DCM/TFA (1:1), anisole, 87%.

Further modification of the protected building block **10** was performed according to a procedure developed by Boons and co-workers.²¹⁷ HBTU promoted coupling of **10** with *tert*-butyl-(3-aminopropyl)-carbamate (**13**) lead to the formation of amide **14** in 44% yield (Scheme C.2, page 185). Exchange of the Fmoc protecting group with an acetamide furnished precursor **15** over two steps in 90% yield. Final mild deacetylation using hydrazine monohydrate in MeOH followed by acidic removal of the *N*-Boc group gave the deprotected antigen **2** in almost quantitative yield without the need for purification.

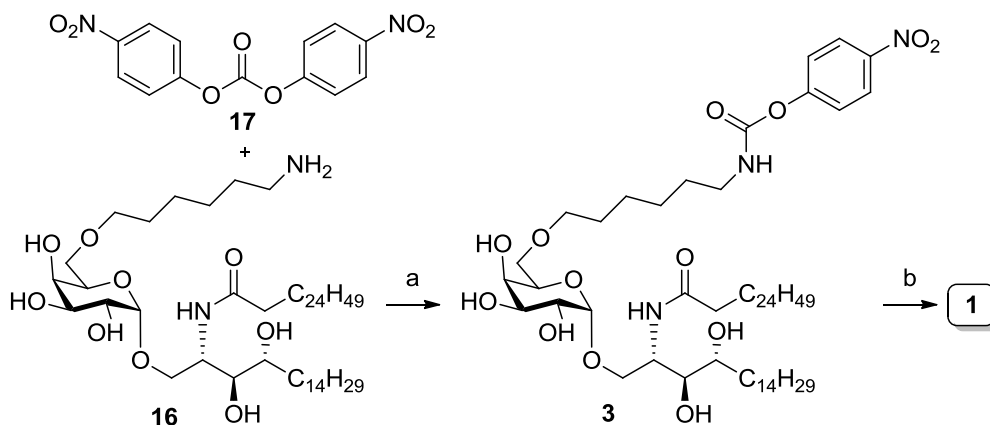
²¹⁸ H. Cai, Z.-H. Huang, L. Shi, P. Zou, Y.-F. Zhao, H. Kunz, Y.-M. Li, *Eur. J. Org. Chem.* **2011**, 3685–3689.

²¹⁹ R. U. Lemieux, R. M. Ratcliffe, *Can. J. Chem.* **1979**, *57*, 1244-1251.



Scheme C.2: Synthesis of fully deprotected antigen **2**. *Reagents and conditions:* a) HBTU, HOBT, THF, **13**, 44%; b) i. DMF/piperidine, (4:1; (v/v)); ii. Pyridine/Ac₂O (1:1; (v/v)), 0 °C, 90% over two steps; c) i. hydrazine, MeOH; ii. TFA/DCM (1:1; (v/v)), 98% over two steps.

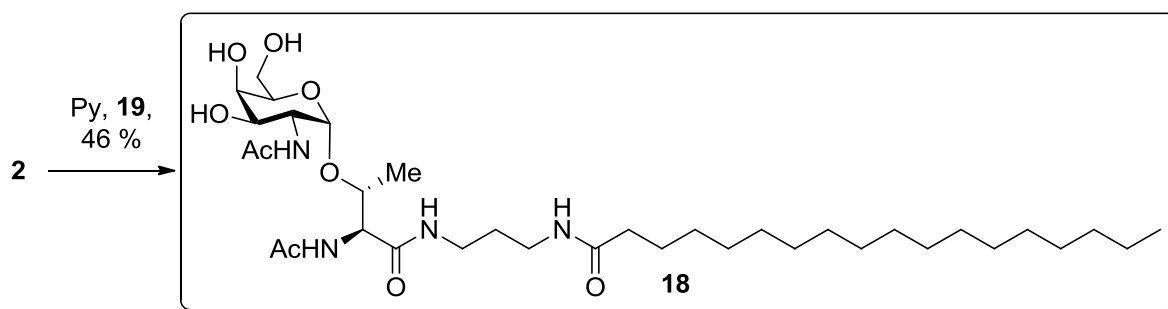
In the last steps of the synthesis α -GalCer derivative **16**^{*} was converted into activated carbamate **3** using bis(4-nitrophenyl)carbonate (**17**), which was subsequently coupled with antigen **2** to finally yield target molecule **1** (Scheme C.3).



Scheme C.3: Synthesis of fully synthetic anti-cancer vaccine candidate **1**. *Reagents and conditions:* (a) **17**, TEA, pyridine, 79%; b) **2**, TEA, pyridine, 42%.

In addition, glycolipid **18**, which features only a stearic acid amide, was prepared by simple condensation of stearyl chloride (**19**) with **2** (Scheme C.4, page 186). This glycolipid is capable of forming liposomes and can be used as a control in immunization studies. Should the synthetic vaccine **1** produce a robust immune response against **2**, compound **18** will be used in a control experiment to investigate if the GSL moiety is responsible for the immunological response or if the multivalent presentation of an antigen on a liposome is enough to elicit the observed effect.

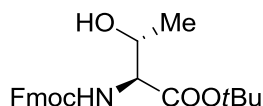
* Compound **16**, **3** and **1** were synthesized by Dr. J. Hudon. See page 195 for details.



Scheme C.4: Synthesis of control glycolipid **18**.

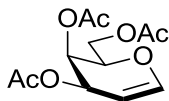
Synthetic Procedures:

N-(9*H*-Fluoren-9-yl-methoxycarbonyl)-*L*-threonine-*tert*-butylester (**8**)

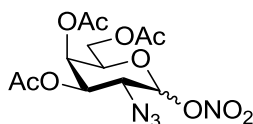


L-Threonine (**II**) (1.5 g, 12.6 mmol) and NaHCO₃ (1.06 g, 12.6 mmol) were dissolved in acetone/water (60 mL; 1:1). Fmoc-OSu (4.25 g, 12.6 mmol) was added and the reaction was stirred for 20 h. The pH was adjusted to 2 with 1 N HCl and acetone was removed in vacuo. Afterwards DCM (100 mL) was added and the organic layer was washed with 1 N HCl (2x100 mL) and sat. brine (2x100 mL). The solution was dried over Na₂SO₄ and solvents were removed in vacuo. The residue was dissolved in dry DCM (20 mL) and was added slowly at 0 °C to a solution of *tert*-butanol (5.14 mL, 53.8 mmol), DCC (8.51 g, 41.3 mmol) and CuCl (124 mg, 1.3 mmol), which was already stirred under light exclusion for 5 days and diluted with dry DCM (25 mL). The ice bath was removed and the solution was stirred for 1 h. Afterwards the solution was cooled down to 0 °C and filtered over Celite® to remove urea. The filter cake was washed with ice cold DCM (5x50 mL). The combined organic layers were washed with sat. NaHCO₃ solution (2x100 mL) and sat. brine (2x100 mL). The organic layer was dried over Na₂SO₄ and solvents were removed in vacuo. Flash column chromatography of the residue (cyclohexane/EtOAc 4:1) yielded **8** as white foam (3.08 g, 7.8 mmol, 62% over 2 steps): R_f (SiO₂, EtOAc/Hexane 1:2) = 0.48; ¹H NMR (400 MHz, CDCl₃) δ 7.77 (d, *J* = 7.6 Hz, 2H), 7.61 (d, *J* = 7.3 Hz, 2H), 7.40 (td, *J* = 7.6, 0.5 Hz, 2H), 7.31 (tt, *J* = 7.4, 1.3 Hz, 2H), 5.57 (d, *J* = 8.5 Hz, 1H, NH), 4.42 (d, *J* = 7.1 Hz, 2H, CH₂ of Fmoc), 4.34 – 4.18 (m, 3H, T^α, T^β, CH of Fmoc), 2.04 (bs, 1H, OH), 1.49 (s, 9H, *t*Bu), 1.25 (d, *J* = 6.2 Hz, 3H, T^γ); ¹³C NMR (101 MHz, CDCl₃) δ 170.33 (COOH), 156.85 (CONH), 143.90, 141.45, 127.85, 127.21, 125.26, 120.12, 120.11, 82.82 (C(CH₃)₃), 68.48 (T^β), 67.32 (CH₂ of Fmoc), 59.65 (T^α), 47.33 (CH₂ of Fmoc), 28.17 (C(CH₃)₃), 20.07 (T^γ); ESI-MS: *m/z* [M+Na]⁺ calcd for C₂₃H₂₇NO₅ 420.2, obsd 420.1. Spectral data were in good agreement with the literature.²²⁰

²²⁰ A. Kaiser, Dissertation, Johannes Gutenberg-Universität Mainz, 2009.

3,4,6-Tri-*O*-acetyl-D-galactal (5)

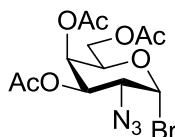
D-galactose (**4**) (63.5 g, 252 mmol) was added in small portions to acetic anhydride (300 mL) and perchloric acid (60%; 1.7 mL). The solution was cooled using an ice bath and kept below 20 °C during addition of the sugar. The reaction mixture was stirred for 3 h. Afterwards the solution was cooled down again to 0 °C and PBr₃ (60 mL, 636 mmol) was added. Subsequently water (35 mL, 1.94 mol) was slowly added using a dropping funnel. The solution was kept below 20 °C during addition and was afterwards stirred for 3 h. The reaction mixture was afterwards poured into ice water (500 mL) and DCM (250 mL). The organic layer was washed with ice water (200 mL), sat. NaHCO₃ solution (5x250 mL) and sat. brine (250 mL). The solution was dried over Na₂SO₄ and concentrated in vacuo (approx. 100 mL). This solution was added to pre cooled slurry (-18 °C) consisting of water (350 mL), acetic acid (250 mL), zinc (100 g, 1.5 mol) and copper(II)sulfate pentahydrate (10 g, 40 mmol). The slurry was stirred at this temperature for 2 h using a mechanic stirrer. After warming to r.t. the solution was filtered over Celite®. The filter cake was washed with DCM (200 mL), the organic layer was washed with ice water (2x200 mL), sat. NaHCO₃ solution (2x250 mL) and dried with Na₂SO₄. Solvents were removed in vacuo to yield **5** as a colorless syrup (91 g, 252 mmol, 95%), which was pure enough for the next step. R_f (SiO₂, EtOAc/Hexane 1:3) = 0.27; ¹H NMR (400 MHz, CDCl₃) δ 6.45 (dd, *J* = 6.3, 1.7 Hz, 1H, Gal-1), 5.60 – 5.50 (m, 1H, Gal-3), 5.41 (dt, *J* = 4.5, 1.6 Hz, 1H, Gal-4), 4.71 (ddd, *J* = 6.3, 2.7, 1.4 Hz, 1H, Gal-2), 4.42 – 4.15 (m, 3H, Gal-5, Gal-6), 2.11 (s, 3H, CH₃), 2.07 (s, 3H, CH₃), 2.01 (s, 3H, CH₃); ¹³C NMR (101 MHz, CDCl₃) δ 170.64, 170.37, 170.22 (3xCOCH₃), 145.52 (Gal-1), 98.95 (Gal-2), 72.91, 64.00, 63.87, 62.03, 20.91, 20.86, 20.76 (3xCOCH₃); ESI-MS: *m/z* [M+Na]⁺ calcd for C₁₂H₁₆O₇ 295.1, obsd 295.0. Spectral data were in good agreement with the literature.²²¹

3,4,6-Tri-*O*-acetyl-2-azido-2-desoxy- α/β -D-galactopyranosylnitrate (6)

²²¹ R. Bukowski, L. M. Morris, R. J. Woods, T. Weimar, *Eur. J. Org. Chem.* **2001**, 2697-2705.

Galactal **5** (19.7 g, 72.4 mmol) was dissolved in dry MeCN (250 mL). The resulting solution was cooled down to -20 °C before CAN (119 g, 217 mmol) and NaN₃ (7.06 g, 109 mmol) were added. The slurry was stirred at -20 °C for 7 h. Afterwards the reaction mixture is diluted with cold Et₂O (200 mL), ice water (100 mL) and was stirred at -20 °C for 10 min. Afterwards the organic phase was washed with water (3x100 mL), dried over Na₂SO₄ and evaporated to dryness. The residue was purified with column chromatography (cyclohexane/n-hexane 3:1) to yield nitrate **6** as yellow oil (7.00 g, 18.60 mmol, 26%; 6:5 mixture of inseparable α/β anomers; product hydrolyzes quickly and should be used immediately for the next step): R_f (SiO₂, EtOAc/Hexane 1:3) = 0.36; ¹H NMR (400 MHz, CDCl₃) δ 6.34 (d, *J* = 4.1 Hz, 1H, Gal-1 α), 5.57 (d, *J* = 8.8 Hz, 1H, Gal-1 β), 5.50 (dd, *J* = 3.2, 0.5 Hz, 1H, Gal-4 α), 5.39 (d, *J* = 3.3 Hz, 1H, Gal-4 β), 5.25 (dd, *J* = 11.3, 3.3 Hz, 1H, Gal-3 α), 4.96 (dd, *J* = 10.6, 3.3 Hz, 1H, Gal-3 β), 4.36 (t, *J* = 6.6 Hz, 1H, Gal-5 α), 4.22 – 4.01 (m, 6H, Gal-2 α , Gal-6 α/β , Gal-5 β), 3.82 (dd, *J* = 10.5, 9.0 Hz, 1H, Gal-2 β), 2.17 (s, 6H, CH₃), 2.09 – 2.06 (m, 6H, CH₃), 2.06 – 2.01 (m, 6H, CH₃). Spectral data were in good agreement with Ref. [221].

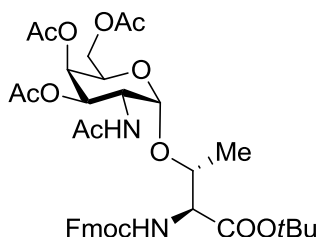
3,4,6-Tri-*O*-acetyl-2-azido-2-desoxy- α -D-galactopyranosylbromide (**7**)



Dry MeCN (100 mL) was added to LiBr (11.31 g, 130 mmol). To this slurry nitrate **6** (7 g, 18.6 mmol) dissolved in dry MeCN (20 mL) was added and the resulting reaction mixture was stirred for 15 h. Afterwards Et₂O (100 mL) was added to the solution and the organic layer was washed with brine (2x100 mL). The organic layer was dried over Na₂SO₄ and solvents were removed in vacuo to yield **7** as yellow solid (6.9 g, 17.5mmol, 94%; product hydrolyzes quickly and should be used immediately for the next step): ¹H NMR (400 MHz, CDCl₃) δ 6.47 (d, *J* = 3.7 Hz, 1H, Gal-1), 5.51 (dd, *J* = 3.2, 1.4 Hz, 1H), 5.35 (dd, *J* = 10.8, 3.2 Hz, 1H), 4.48 (t, *J* = 6.9 Hz, 1H), 4.18 (dd, *J* = 11.4, 6.4 Hz, 1H), 4.11 (dd, *J* = 11.4, 6.8 Hz, 1H), 3.99 (dd, *J* = 10.8, 3.8 Hz, 1H), 2.16 (s, 3H, CH₃), 2.07 (s, 3H, CH₃), 2.06 (s, 3H, CH₃); ¹³C NMR (101 MHz, CDCl₃) δ 170.42, 169.84, 169.61 (3xCOOCH₃), 88.99 (Gal-1), 71.55, 69.99, 66.65, 60.87, 58.78, 20.77, 20.70, 20.69 (3xCOOCH₃). Spectral data were in

good agreement with the literature.²²² Further analytical data can be found in: H. Paulsen, A. Richter, V. Sinnwell, W. Stenzel, *Carbohydr. Res.* **1978**, *64*, 339-364.

***N*-(9*H*-Fluoren-9-yl-methoxycarbonyl)-*O*-(3,4,6-tri-*O*-acetyl-2-azido-2-desoxy- α -D-galactopyranosyl)-*L*-threonine-*tert*-butylester (**9**)**

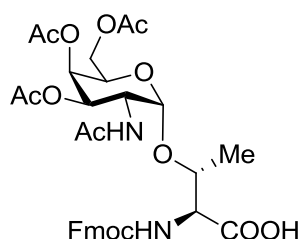


Threonine **8** (6.96 g, 17.5 mmol) was dissolved in a mixture of dry DCM and toluene (1:1; 120 mL) and molecular sieves (17 g, powdered 4Å) was added. The resulting slurry was stirred for 1 h at r.t. and was afterwards cooled down to 0 °C. Ag₂CO₃ (6.27 g, 22.76 mmol) and AgClO₄ (0.762 g, 3.68 mmol) were added under light exclusion and the mixture was stirred for further 15 min at 0 °C. Then galactopyranosylbromide **7** (6.9 g, 17.50 mmol) in dry DCM and toluene (1:1; 120 mL) was added dropwise over 15 min at 0 °C. After addition of the bromide the reaction mixture could rise to r.t. and was stirred for 3 d under light exclusion. The solution was filtered over Celite® and washed with sat. NaHCO₃ solution (2x100 mL) and with sat. brine (100 mL). The organic layers were dried over Na₂SO₄ and solvents were removed in vacuo. The residue was purified with column chromatography (cyclohexane/*n*-hexane 4:1, R_f (SiO₂, EtOAc/Hexane 1:2) = 0.58) to yield an inseparable mixture of anomers (α/β – 9:1) and unreacted amino acid. The crude product (12 g) was dissolved in THF/Ac₂O/HOAc (3:2:1; 860 mL). To this solution zinc (14.1 g, 215 mmol), which was pre activated in an aqueous CuSO₄ solution (5%, 170 mL) and dried with EtOAc (3x40 mL), was added and the black solution was stirred for 24 h. The solution was filtered over Celite® and the solvents were removed in vacuo. The residue was co evaporated with toluene (2x30 mL), dissolved in DCM (400 mL) and washed with sat. NaHCO₃ solution (3x150 mL) and water (2x150 mL). The organic layer was dried over Na₂SO₄ and solvents were removed in vacuo. The residue was purified with column chromatography (EtOAc/*n*-hexane 3:1) to yield **9** as white solid (7.3 g, 10.1 mmol, 61% over two steps): R_f (SiO₂, EtOAc/Hexane 1:1) = 0.12; ¹H NMR (400 MHz, CDCl₃) δ 7.78 (d, *J* = 7.5 Hz, 2H), 7.64 (d, *J*

²²² T. Reipen, H. Kunz, *Synthesis* **2003**, 2487-2502 .

= 7.3 Hz, 2H), 7.44 – 7.39 (m, 2H), 5.96 – 5.87 (m, 2H), 5.92 (d, $J = 9.8$ Hz, 1H, NH of Fmoc), 5.44 (d, $J = 9.3$ Hz, 1H, NH), 5.40 (d, $J = 2.1$ Hz, 1H, Gal-4), 5.09 (dd, $J = 11.2, 2.8$ Hz, 1H, Gal-3), 4.90 (d, $J = 3.3$ Hz, 1H, Gal-1), 4.63 (td, $J = 10.8, 3.4$ Hz, 1H, Gal-2), 4.46 (p, $J = 10.6$ Hz, 2H, CH₂ of Fmoc), 4.36 – 4.02 (m, 6H, Gal-5, Gal-6, CH of Fmoc, T^α, T^β), 2.17 (s, 3H), 2.04 (s, 6H), 2.01 (s, 3H), 1.33 (d, $J = 6.2$ Hz, 3H, T^γ); ESI-MS: m/z [M+Na]⁺ calcd for C₃₇H₄₆N₂O₁₃ 749.3, obsd 749.1. Spectral data were in good agreement with the literature.²²³

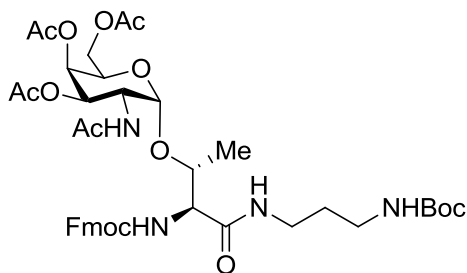
***N*-(9*H*-Fluoren-9-yl-methoxycarbonyl)-*O*-(2-acetamido-3,4,6-tri-*O*-acetyl-2-desoxy- α -D-galactopyranosyl)-L-threonine (**10**)**



Fully protected T_N-antigen **9** (1.8 g, 2.48 mmol) was dissolved in DCM (15 mL) and TFA (15 ml). Anisole (2.5 mL, 22.9 mmol) was added and the reaction was stirred for 1 h. The color of the reaction mixture changed from yellow to black in 10 min. Afterwards the solution was diluted with toluene (40 mL) and the solvents were removed in vacuo. The residue was co evaporated toluene (3x40 mL) and the crude product was purified by column chromatography (CHCl₃/MeOH with 1 % HOAc starting from 0% MeOH to 5% MeOH) to yield **10** as yellow solid (1.44 g, 2.15 mmol, 87%): ¹H NMR (400 MHz, DMSO-d₆) δ 7.87 (d, $J = 7.5$ Hz, 2H), 7.69 (d, $J = 7.4$ Hz, 2H), 7.39 (t, $J = 7.4$ Hz, 2H), 7.30 (t, $J = 7.4$ Hz, 2H), 5.26 (d, $J = 2.8$ Hz, 1H, Gal-4), 4.97 (dd, $J = 11.5, 3.2$ Hz, 1H, Gal-3), 4.82 (d, $J = 3.5$ Hz, 1H, Gal-1), 4.50 – 4.11 (m, 6H, CH of Fmoc, Gal-5, Gal-6, Gal-2, T^β), 4.05 – 3.86 (m, 3H, CH₂ of Fmoc, T^α), 2.07 (s, 3H), 1.95 (s, 3H), 1.86 (s, 3H), 1.83 (s, 3H), 1.11 (d, $J = 6.4$ Hz, 3H, T^γ); ¹³C NMR (101 MHz, DMSO-d₆) δ 171.65, 170.02, 169.93, 169.86 (4x COCH₃), 156.42 (CONH of Fmoc), 143.79, 140.75, 140.72, 127.61, 127.05, 125.23, 125.15, 120.12, 98.50 (Gal-1), 79.17 (T^β), 75.50, 68.17 (Gal-3), 67.32 (Gal-4), 66.41, 65.51 (Gal-6), 61.97 (CH₂ of Fmoc), 58.77 (T^α), 46.76, 46.65, 22.72, 20.54, 20.48, 18.24 (Me of Thr); ESI-MS: m/z [M+H]⁺ calcd for C₃₃H₃₈N₂O₁₃ 671.3, obsd 671.2. Spectral data were in good agreement with Ref. [220].

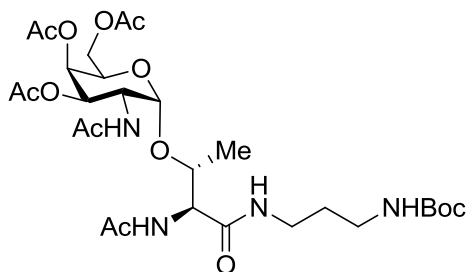
²²³ B. Liebe, H. Kunz, *Helv. Chim. Acta* **1997**, *80*, 1473-1482.

***N*-(9*H*-Fluoren-9-yl-methoxycarbonyl)-*O*-(2-acetamido-3,4,6-tri-*O*-acetyl-2-desoxy- α -D-galactopyranosyl)-*L*-threonine-*tert*-butyl-(3-amidopropyl)-carbamate (**14**)**



Free carboxylic acid **10** (203 mg, 0.30 mmol) was dissolved in THF (10 mL) and HOBt monohydrate (354 mg, 2.31 mmol) and HBTU (148 mg, 0.39 mmol) were added. After stirring for 10 min *tert*-butyl-(3-aminopropyl)-carbamate (**13**) (Sigma Aldrich) (54 mg, 0.31 mmol) was added to this solution and stirred for 12 h at r.t. before the solvent was removed in vacuo. The crude product was purified by column chromatography (CHCl₃/MeOH starting from 0% MeOH to 5% MeOH) to yield **14** as white solid (110 mg, 0.13 mmol, 44%): R_f (SiO₂, DCM/MeOH 9:1) = 0.59; ¹H NMR (400 MHz, CDCl₃) δ 7.18-7.81 (m, 8H), 5.41 (d, 1H), 5.04-5.11 (m, 2H), 4.62 (dd, 1H), 4.43-4.51 (m, 2H, CH₂ of Fmoc), 4.07-4.28 (m, 6H), 3.48-3.50 (m, 1H), 3.17-3.27 (m, 3H), 2.18 (s, 3H), 2.06 (s, 3H), 2.05 (s, 3H), 1.99 (s, 3H), 1.46-1.61 (m, 2H, CH₂ of Linker), 1.42 (s, 9H, Boc), 1.27 (d, 3H, Me of Thr). Spectral data were in good agreement with Ref. [217].

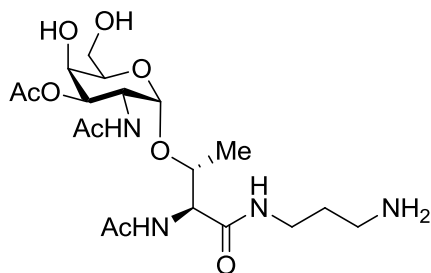
***N*-Acetamido-*O*-(2-acetamido-3,4,6-tri-*O*-acetyl-2-desoxy- α -D-galactopyranosyl)-*L*-threonine-*tert*-butyl-(3-amidopropyl)-carbamate (**15**)**



Glycosylated amino acid **14** (88 mg, 0.11 mmol) was dissolved in DMF (1.6 mL) and piperidine (400 μ L, 4.05 mmol) was added. The solution was stirred for 2 h. The solvent was evaporated in vacuo and the crude residue was dissolved in pyridine (500 μ L). Ac₂O (500 μ L) was added dropwise at 0 °C to this solution. Afterwards the solution was allowed to warm slowly to r.t. and was stirred for 12 h. The solvents were removed in vacuo and the residue

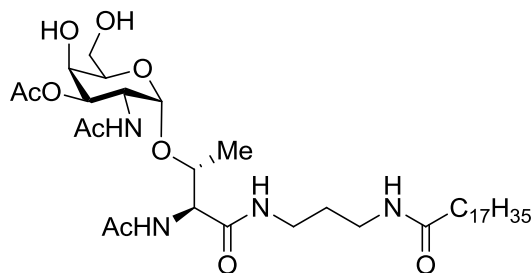
was coevaporated with toluene (3x 2mL). The crude product was purified by column chromatography (CHCl₃/MeOH starting from 0% MeOH to 5% MeOH) to yield **15** as beige amorphous powder (62 mg, 0.10 mmol, 90% over two steps): ¹H NMR (400 MHz, CDCl₃) δ 5.38 – 5.35 (m, 1H), 5.06 (dd, J = 11.5, 3.2 Hz, 1H), 4.97 (d, J = 3.6 Hz, 1H, GalNAc-1), 4.62 – 4.53 (m, 2H), 4.28 – 4.18 (m, 2H), 4.14 – 4.01 (m, 2H), 3.46 – 3.35 (m, 1H), 3.31 – 3.09 (m, 4H), 2.15 (s, 3H), 2.13 (s, 3H), 2.02 (s, 6H), 1.96 (s, 3H), 1.65 – 1.50 (m, 2H, CH₂ of Linker), 1.42 (s, 9H, Boc), 1.24 (d, J = 6.3 Hz, 1H, Me of Thr). Spectral data were in good agreement with Ref. [217].

***N*-Acetamido-*O*-(2-acetamido-2-desoxy- α -D-galactopyranosyl)-L-threonine-(3-aminopropyl)-amide (**2**)**

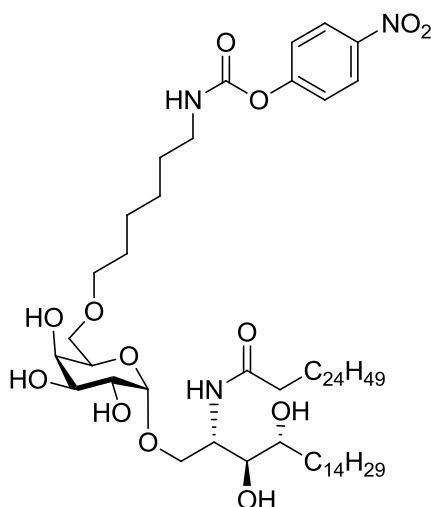


Glycosylated amino acid **15** (4.7 mg, 7.26 μ mol) was dissolved in MeOH (0.5 mL) and hydrazine monohydrate (1 drop, 64wt%) was added to this solution. The solution was stirred for 14 h before it was diluted with toluene (1 mL) and concentrated in vacuo. The residue was coevaporated with toluene (2x 1 mL) and was dissolved in DCM/TFA (1:1, 0.6 mL). The solution was stirred for 1.5 h before it was evaporated to dryness and redissolved in MeOH (1 mL). Amberlite IRA-400(OH) (basic resin, 10 mg) was added to this solution and stirred for 30 min. The slurry was filtered and evaporated to dryness to yield **2** (3 mg, 7.1 μ mol, 98%) as white amorphous solid: ¹H NMR (400 MHz, D₂O) δ 4.87 (d, J = 3.4 Hz, 1H, GalNAc-1), 4.39 (d, J = 2.8 Hz, 1H), 4.38 – 4.30 (m, 1H), 4.08 (dd, J = 11.1, 3.7 Hz, 1H), 4.00 (t, J = 6.1 Hz, 1H), 3.95 (d, J = 2.6 Hz, 1H), 3.84 (dd, J = 11.0, 3.0 Hz, 1H), 3.76 – 3.69 (m, 2H), 3.32 – 3.21 (m, 1H, CH_{2B} of linker), 3.20 – 3.10 (m, 1H, CH_{2A} of linker), 2.65 (t, J = 7.2 Hz, 2H, CH₂-NH₂), 2.11 (s, 3H), 2.03 (s, 3H), 1.69 – 1.57 (m, 2H, CH₂ of linker), 1.24 (d, J = 6.3 Hz, 3H, Me of Thr). Spectral data were in good agreement with Ref. [217].

***N*-Acetamido-*O*-(2-acetamido-2-desoxy- α -D-galactopyranosyl)-L-threonine-(3-amidopropyl)-stearamide (**18**)**



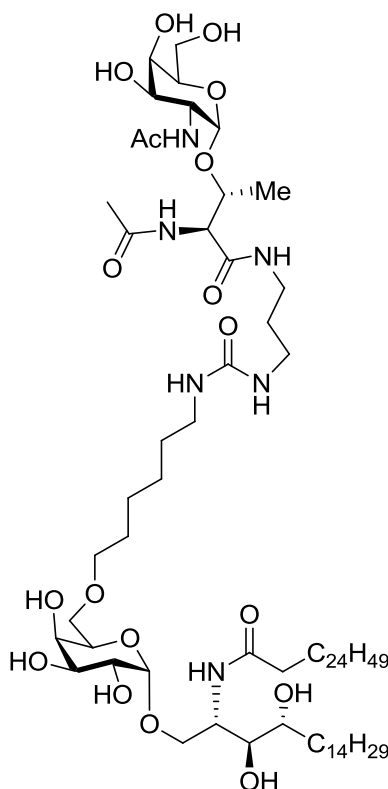
Deprotected T_N-antigen **2** (4 mg, 9.5 μ mol) was dispersed in pyridine (0.7 mL) and stearoyl chloride (7.1 μ L, 19 μ mol, purity \geq 90%) was added to this slurry. The reaction mixture was stirred for 2 h at room temperature till all solids were dissolved. LC-MS analysis showed absence of starting material and formation of the desired glycolipid. The reaction was quenched with MeOH (0.5 mL) and all solvents were evaporated to dryness. The residue was co-evaporated with toluene (3x 2 mL) and purified using silica gel flash column chromatography (5 cm high pipette column, 10% \rightarrow 20% MeOH in CHCl₃) to yield glycolipid **18** (3 mg, 4.4 μ mol, 46%) as white solid: R_f (SiO₂, CDCl₃/MeOH 4:1) = 0.54; ¹H NMR (400 MHz, CDCl₃/CD₃OD – 1:1) δ 4.84 (d, J = 3.7 Hz, 1H, GalNAc-1), 4.46 (d, J = 2.5 Hz, 1H, α -Thr), 4.28 – 4.22 (m, 1H, β -Thr), 4.19 (dd, J = 10.9, 3.7 Hz, 1H, GalNAc-2), 3.96 (d, J = 2.5 Hz, 1H), 3.87 (t, J = 5.8 Hz, 1H), 3.80 – 3.70 (m, 3H, GalNAc-6, GalNAc-3), 3.32 – 3.28 (m, 1H, buried in solvent peak, NH-CH₂-CH₂-CH₂-NH), 3.23 – 3.16 (m, 1H, NH-CH₂-CH₂-CH₂-NH), 3.16 – 3.03 (m, 2H, CH₂, NH-CH₂-CH₂-CH₂-NH), 2.19 – 2.14 (m, 2H, CO-CH₂-CH₂), 2.11 (s, 3H), 2.05 (s, 3H), 1.67 – 1.53 (m, 4H, CO-CH₂-CH₂, NH-CH₂-CH₂-CH₂-NH), 1.36 – 1.17 (m, 31H, 14x CH₂ of lipid, Me of Thr), 0.85 (t, J = 6.9 Hz, 3H, Me of lipid); ¹³C NMR (151 MHz, CDCl₃/CD₃OD – 1:1) δ 176.09, 173.82, 173.00, 171.53 (4x amide), 100.12 (GalNAc-1), 76.56 (β -Thr), 71.42, 70.15, 69.79 (GalNAc-3), 62.40 (GalNAc-6), 58.00 (α -Thr), 50.86 (GalNAc-2), 49.86, 37.03, 36.89, 32.48, 30.22, 30.19, 30.09, 29.93, 29.89, 29.71, 26.55, 23.19, 22.96, 22.69, 18.71 (Me of Thr), 14.30 (Me of lipid); ESI-MS: *m/z* [M+Na]⁺ calcd for C₃₅H₆₆N₄O₉ 709.4722, obsd 709.4724.

Activated carbamate (**3**)^{*}

GSL derivative **16**²²⁴ (3.9 mg, 4.1 μmol) was dissolved in pyridine (0.5 mL). Bis(4-nitrophenyl) carbonate (**17**) (6.1 mg, 20 μmol) was added to this solution followed by TEA (25 μl , 0.179 mmol). The resulting yellow solution was stirred at room temperature for 12 h before it was evaporated to dryness. The crude product was purified by column chromatography (SiO_2 , $\text{CH}_2\text{H}_2/\text{MeOH}$ 0% \rightarrow 20% MeOH) to yield glycolipid **3** (3.6 mg, 3.2 μmol , 79% yield) as pale yellow oil: ^1H NMR (400 MHz, pyridine- d_5) δ 9.02 (t, $J = 5.6$ Hz, 1H, NH of carbamate), 8.49 (d, $J = 8.7$ Hz, 1H, NH of amide), 8.26 (d, $J = 9.2$ Hz, 2H), 7.54 (d, $J = 9.2$ Hz, 2H), 5.56 (d, $J = 3.8$ Hz, 1H, Gal-1), 5.30 – 5.24 (m, 2H), 4.73 – 4.61 (m, 2H), 4.51 (t, $J = 6.0$ Hz, 1H), 4.45 – 4.38 (m, 3H), 4.37 – 4.31 (m, 2H), 4.10 (dd, $J = 9.8, 5.7$ Hz, 1H), 4.02 (dd, $J = 9.8, 6.5$ Hz, 1H), 3.52 (td, $J = 9.2, 2.7$ Hz, 2H), 3.45 (dd, $J = 13.0, 6.9$ Hz, 2H), 2.46 (t, $J = 7.2$ Hz, 2H), 2.36 – 2.23 (m, 1H), 1.97 – 1.79 (m, 4H), 1.74 – 1.65 (m, 3H), 1.64 – 1.54 (m, 2H), 1.48 – 1.18 (m, 74H), 0.87 (t, $J = 6.7$ Hz, 6H, Me of lipids); ^{13}C NMR (101 MHz, pyridine- d_5) δ 173.64 (amide), 157.84 (carbamate), 154.59, 145.15, 125.85, 123.03, 101.96 (Gal-1), 77.09, 72.99, 71.95, 71.92, 71.56, 71.34, 71.29, 70.65, 69.22, 51.76, 42.07, 37.28, 34.78, 32.63, 32.62, 30.89, 30.67, 30.56, 30.52, 30.50, 30.48, 30.44, 30.42, 30.40, 30.35, 30.28, 30.13, 30.12, 27.53, 27.02, 26.91, 26.69, 23.45, 14.79 (Me of lipids); ESI-MS: m/z $[\text{M}+\text{Na}]^+$ calcd for $\text{C}_{63}\text{H}_{115}\text{N}_3\text{O}_{13}$ 1144.8323, obsd 1144.8373.

^{*} Compound **3** was synthesized by Dr. J. Hudon.

²²⁴ The GSL derivative **16** was synthesized by Dr. J. Hudon and prepared according to: Carbohydrate-Glycolipid Conjugate Vaccines, P. H. Seeberger, P. Stallforth, G. De Libero, M. Cavallari, WO2013139803.

T_N-Antigen-GSL glycolipid (1**)^{*}**

Activated GSL **3** (9.1 mg, 8.11 μmol) was dissolved in pyridine (0.8 mL). Amine **2** (4.8 mg, 11 μmol) was added to this solution. Afterwards TEA (2.5 μl , 18 μmol) was added to the reaction mixture, which was stirred for 18 h. The reaction mixture was evaporated to dryness and redissolved in MeOH/CH₂Cl₂ (1 mL, 1:1). DOWEX 50WX-8 acidic resin (25 mg) was added and the slurry was stirred for 15 minutes to remove any excess amine. The filtrate was evaporated to dryness and the residue purified was purified by column chromatography (SiO₂, CH₂H₂/MeOH 0% -> 20% MeOH) to yield glycolipid **1** (4.8 mg, 3.4 μmol , 42% yield) as white powder: ¹H NMR (600 MHz, CDCl₃/CD₃OD, 1:1) δ 5.12 (d, J = 3.8 Hz, 1H, GalNAc-1), 5.09 (d, J = 3.8 Hz, 1H, Gal-1), 4.71 (d, J = 2.5 Hz, 1H, α -Thr), 4.52 – 4.43 (m, 2H, Gal-2, β -Thr), 4.41 (dd, J = 9.9, 4.2 Hz, 1H), 4.18 – 4.08 (m, 4H), 4.04 (dd, J = 10.0, 3.8 Hz, 1H, GalNAc-2), 4.02 – 3.92 (m, 4H), 3.88 (dd, J = 10.2, 5.3 Hz, 1H), 3.86 – 3.81 (m, 2H), 3.81 – 3.77 (m, 1H), 3.75 – 3.70 (m, 2H), 3.47 – 3.28 (m, 6H, 3x C(=O)NH-CH₂), 2.44 (t, J = 7.6 Hz, 2H, HNC(=O)-CH₂ of fatty acid), 2.35 (s, 3H, Me of Ac), 2.29 (s, 3H, Me of Ac), 1.89 – 1.78 (m, 6H), 1.75 – 1.69 (m, 2H) 1.64 – 1.44 (m, 79H), 1.11 (t, J = 7.0 Hz, 6H, 2x Me of lipids); ¹³C NMR (151 MHz, CDCl₃/CD₃OD, 1:1) δ 174.99, 173.67, 172.89, 171.37 (4x amide), 160.63 (carbamide), 100.40 (GalNAc-1), 100.15 (Gal-1), 76.69 (β -Thr), 74.83, 72.52, 72.10, 71.91, 70.90, 70.79, 70.52, 70.03, 69.74, 69.51 (GalNAc-2), 68.03, 62.22, 57.90 (α -

^{*} Compound **1** was synthesized by Dr. J. Hudon.

Thr), 50.99, 50.89, 49.57, 40.47, 37.31, 36.98, 32.65, 32.48, 30.67, 30.55, 30.27, 30.21, 30.03, 29.92, 28.65, 27.07, 26.51, 26.46, 26.31, 23.20, 22.96 (2x Me of NHAc), 18.65 (Me of Thr), 14.32 (Me of lipids); ESI-MS: m/z $[M+Na]^+$ calcd for $C_{74}H_{142}N_6O_{18}$ 1426.0273, obsd 1426.0300.

D. Synthetic Substructures of GPI-Anchors as NMR probes for the Investigation of the Torsion of the Conserved GPI Core

Introduction:

In a recent study, the torsion of the ManIII- α (1 \rightarrow 2)-ManII- α and ManII- α (1 \rightarrow 6)-ManI- α linkages, which are conserved motifs in all GPIs characterized to date, were investigated using a computational method.²²⁵ The results from this numerical study revealed that the conformational properties of both linkages are primarily determined by their two connecting carbohydrate moieties. These data were confirmed by NMR studies of mannoses 1-3 (Figure D.1).

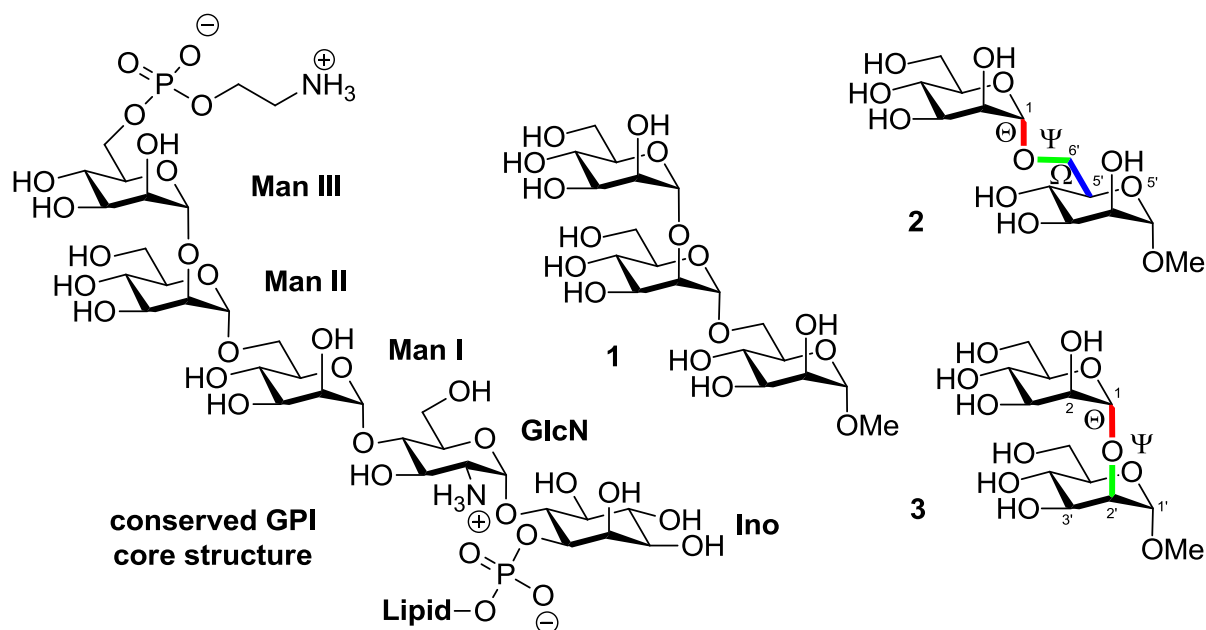


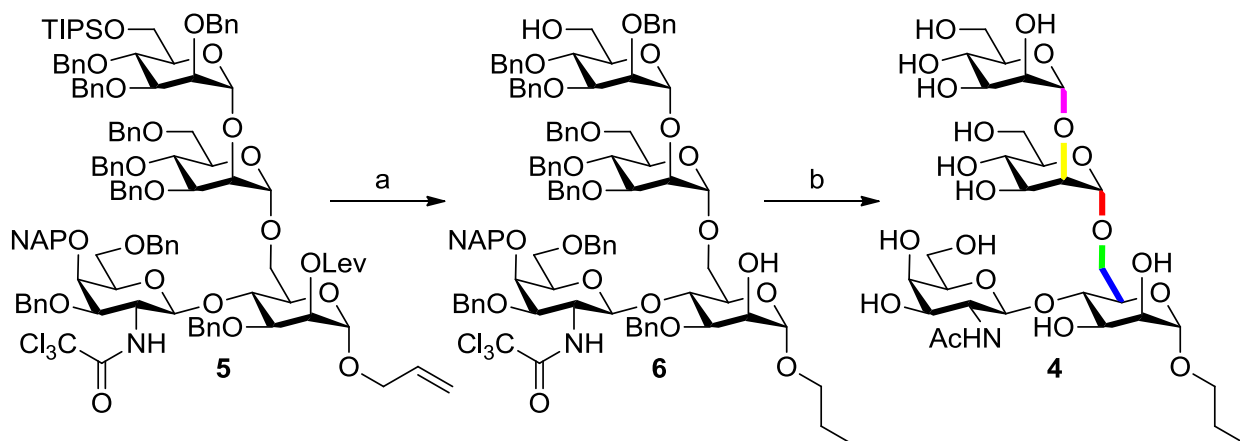
Figure D.1: Conserved GPI core structure and the compounds 1-3, which were used in NMR experiments. Investigated linkages are highlighted in the colors red, green and blue and torsion angles are termed Θ , Ψ and Ω .

The effect of a carbohydrate side branch, which can be attached to ManI either *via* O-3 or O-4, on the aforementioned linkages and torsion angles is still undisclosed. Therefore, we prepared two substructures of GPIs, which are related to parasitic glycolipids and feature different side branches, and investigated their conformation in solution using various NMR techniques. The obtained data in combination with computer simulation techniques will provide valuable insights into the conformational behavior of branched GPI-anchors. Here the synthesis of both GPI substructures as well as their detailed NMR analysis is described.

²²⁵ M. Wehle, I. Vilotijevic, R. Lipowsky, P. H. Seeberger, D. Varon Silva, M. Santer, *J. Am. Chem. Soc.* **2012**, *134*, 18964–18972.

Results:

The synthesis of tetrasaccharide **4**, which features a GalNAc β (1 \rightarrow 4)ManI linkage and is one of the most common side branches in mammalian and non-mammalian GPIs⁷⁵, started from sugar **5** (Scheme D.1). Acidic hydrolysis of the silyl ether in wet acetonitrile followed by hydrazinolysis and simultaneous reduction of the allyl moiety proceeded smoothly in 67% yield using a one pot protocol. Diol **6** was afterwards hydrogenated over palladium on charcoal to provide **4** in 79% yield.



Scheme D.1: Synthesis of oligosaccharide **4**. Linkages that are of interest in the combined NMR-computational study are indicated in different colors. *Reagents and conditions:* (a) i. Sc(OTf)₃, water, MeCN; ii. hydrazine, 67%; (b) Pd/C, H₂, MeOH, THF 79%.

All proton and carbon signals of compound **4** (Table D.1, page 201) could be assigned through the use of 2D-NMR experiments (COSY, TOCSY, ROESY, HSQC, HMBC and TOCSY-HSQC). Interestingly to note is that correlations of all three mannoses in the TOCSY spectrum were identical to the COSY experiment and only showed a cross peak between the anomeric proton and its corresponding H2 (Figure D.2, page 200). The exception was the *N*-acetylgalactosamine moiety, which exhibited additional correlations between the anomeric proton and H3, H5 as well as H6.

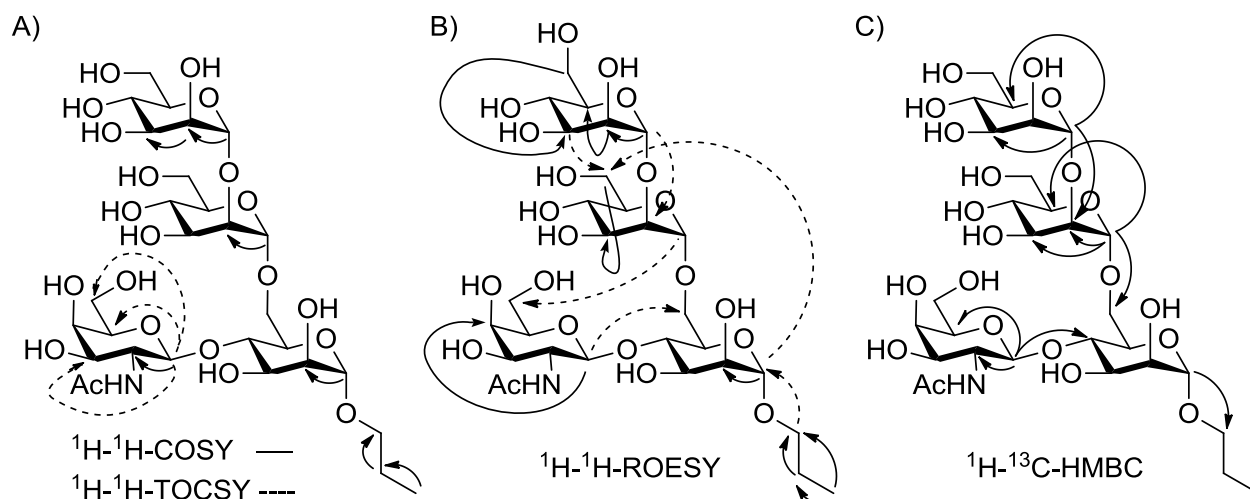


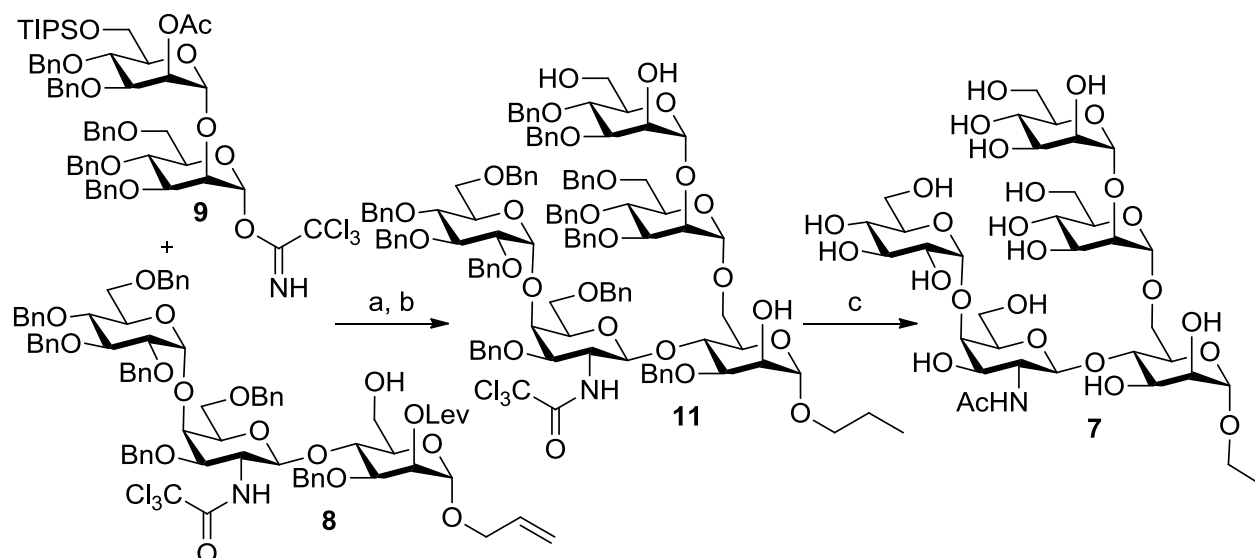
Figure D.2: Relevant 2D-NMR correlations for tetrasaccharide **4**. Dashed lines in figure 1B indicate correlations between different spin-systems whereas straight arrows are used for ROESY-contacts in the same spin-system.

$^1\text{H}/^{13}\text{C}$	δ_{H} (ppm) 600 MHz, D ₂ O	δ_{C} (ppm) 151 MHz, D ₂ O
ManI		
CH-1	4.87 (d, 1H, $J = 1.5$ Hz)	102.03
CH-2	4.02 (dd, 1H, $J = 3.1, 1.8$ Hz)	72.04
CH-3	{3.82}	72.60
CH-4	{3.86}	79.02
CH-5	{3.94($J_{\text{H6}} = 9.4$ Hz; extracted from HSQC)}	71.98
CH-6	{3.87 and 3.81($J_{\text{H6}} = 9.4$ Hz; extracted from HSQC)}	68.62
ManII		
CH-1	5.19 (d, 1H, $J = 1.5$ Hz)	101.23
CH-2	4.04 (dd, 1H, $J = 3.1, 1.8$ Hz)	81.17
CH-3	{3.73}	75.87
CH-4	{3.72}	69.57
CH-5	{3.96}	72.76
CH-6	{3.97 and 3.95}	63.79
ManIII		
CH-1	5.05 (d, 1H, $J = 1.5$ Hz)	104.85
CH-2	4.09 (dd, 1H, $J = 3.1, 1.8$ Hz)	72.57
CH-3	{3.78}	75.83
CH-4	{3.68}	69.39
CH-5	{3.87}	72.95
CH-6	{3.91 and 3.86}	63.66
GalNAc		
CH-1	4.51 (d, $J = 8.4$ Hz, 1H)	104.14
CH-2	{3.94}	55.27
CH-3	{3.96}	70.33
CH-4	{3.76}	78.03
CH-5	{3.78}	73.18
CH-6	{3.80}	63.70
Me of NHAc	2.10 (s, 3H)	24.95
C=O of NHAc	-	177.30
<i>n</i> -propyl		
Me of <i>n</i> -propyl	0.94 (t, $J = 7.4$ Hz, 3H)	12.53
CH ₂ of <i>n</i> -propyl	1.68 – 1.61 (m, 2H)	24.56
O-CH ₂ of <i>n</i> -propyl	3.58 – 3.52 (m, 1H) and {3,67}	72.43

Table D.1: NMR data of tetrasaccharide **4**. Chemical shifts in curly brackets indicate overlapping with other signals. Therefore a multiplicity could not be assigned.

To further investigate the influence of the side chain on the trimannose moiety pentasaccharide **7** that bears a $\text{Glc}\alpha(1\rightarrow4)\text{GalNAc}\beta(1\rightarrow4)$ disaccharide linked to ManI and is part of the GPI anchor of *T. gondii*¹²² was prepared (Scheme D.2). Glycosylation of trisaccharide **8** with imidate **9** yielded pentasaccharide **10** in 66% yield. Acidic hydrolysis of the silyl ether in wet acetonitrile followed by hydrazinolysis of the remaining esters and

simultaneous reduction of the allyl moiety proceeded smoothly using a one pot protocol. Triol **11** was finally hydrogenated over Pd/C to furnish **7** in 92% yield.



Scheme D.2: Synthesis of oligosaccharide **7**. Reagents and conditions: (a) TMSOTf, toluene, 0 °C, MS4Å, 66%; (b) i. Sc(OTf)₃, water, MeCN; ii. hydrazine, 34%; (c) Pd/C, H₂, MeOH, 92%.

Almost all proton and carbon signals of compound **7** (Table D.2, see page 204) could be assigned through the use of 2D-NMR experiments (COSY, TOCSY, ROESY, HSQC, HMBC and TOCSY-HSQC) and relevant correlations are indicated in Figure D.3 (see page 203).

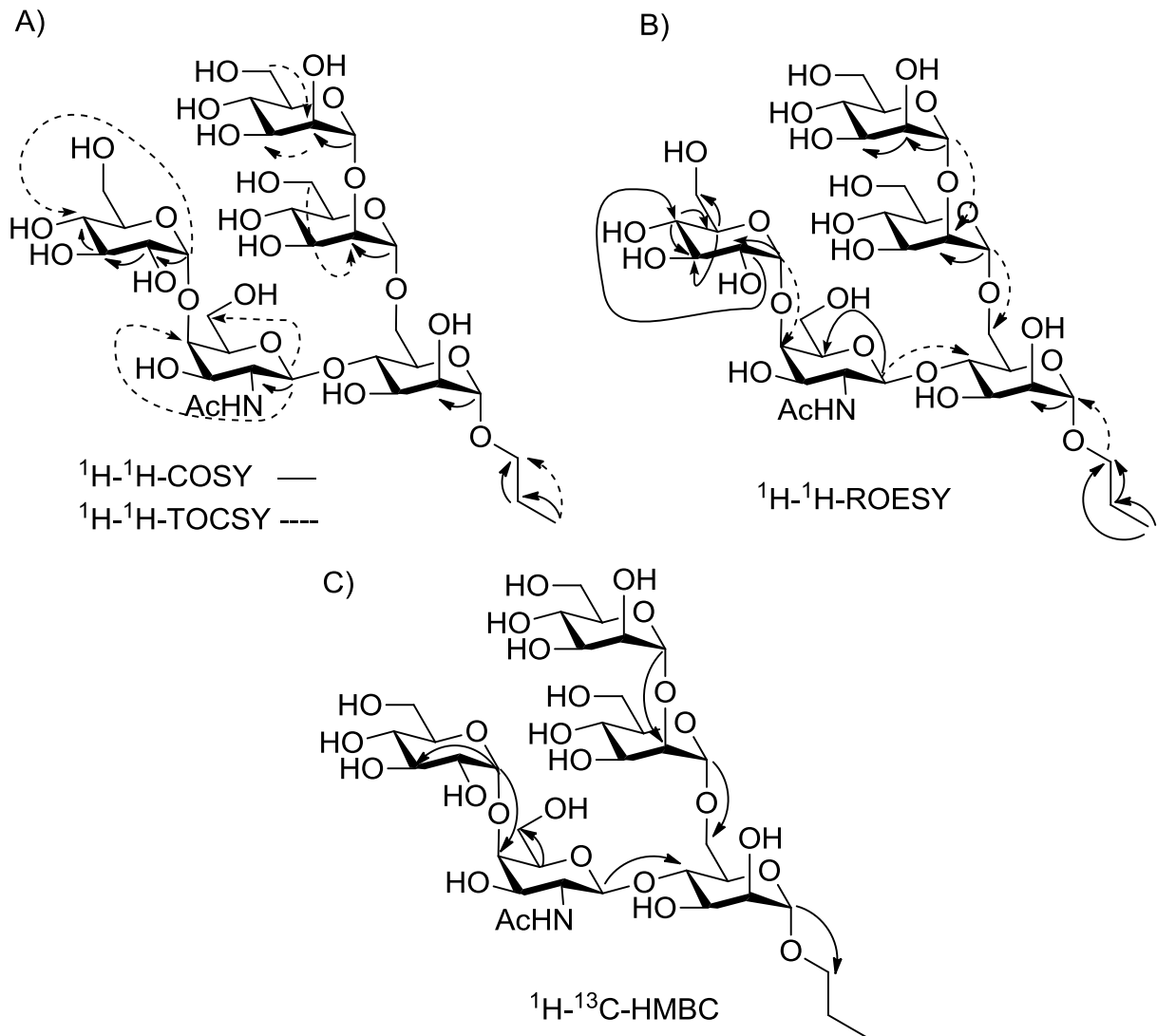


Figure D.3: Relevant 2D-NMR correlations for pentasaccharide 7.

$^1\text{H}/^{13}\text{C}$	δ_{H} (ppm) 600 MHz, D_2O	δ_{C} (ppm) 151 MHz, D_2O
ManI		
CH-1	4.87 (d, 1H, $J = 1.7$ Hz)	101.94
CH-2	{4.00}	72.13
CH-3	{3.79}	75.86
CH-4	{3.84}	79.59
CH-5	{3.92}	72.04
CH-6	{3.80 and 3.82}	68.65
ManII		
CH-1	5.19 (d, $J = 1.6$ Hz)	101.22
CH-2	4.05 – 4.03 (m, 1H)	81.16
CH-3	n.d.	n.d.
CH-4	n.d.	n.d.
CH-5	n.d.	n.d.
CH-6	{3.80 and 3.96}	63.78
ManIII		
CH-1	5.05 (d, $J = 1.6$ Hz)	104.84
CH-2	4.09 (dd, $J = 3.2, 1.8$ Hz)	72.56
CH-3	{3.86}	72.94
CH-4	{3.68}	69.39
CH-5	{3.72}	69.55
CH-6	{3.78 and 3.92}	63.68
GalNAc		
CH-1	4.57 (d, $J = 8.4$ Hz)	104.55
CH-2	{4.00}	55.12
CH-3	{3.95}	72.77
CH-4	4.06 (d, $J = 2.8$ Hz)	79.30
CH-5	{3.82}	78.09
CH-6	{3.88 and 3.99}	62.97
Me of NHAc	2.09 (s)	24.93
C=O of NHAc	-	177.29
Glc		
CH-1	4.96 (d, $J = 3.9$ Hz)	102.83
CH-2	{3.58}	74.41
CH-3	{3.84}	75.29
CH-4	3.49 (dd, $J = 10.1, 9.3$ Hz)	71.80
CH-5	4.12 (dt, $J = 10.5, 2.9$ Hz)	74.55
CH-6	{3.74 and 3.83}	62.51
<i>n</i> -propyl		
Me of <i>n</i> -propyl	0.94 (t, $J = 7.4$ Hz, 3H)	12.55
CH ₂ of <i>n</i> -propyl	1.68 – 1.60 (m, 2H)	24.56
O-CH ₂ of <i>n</i> -propyl	{3.67 and 3.55}	72.39

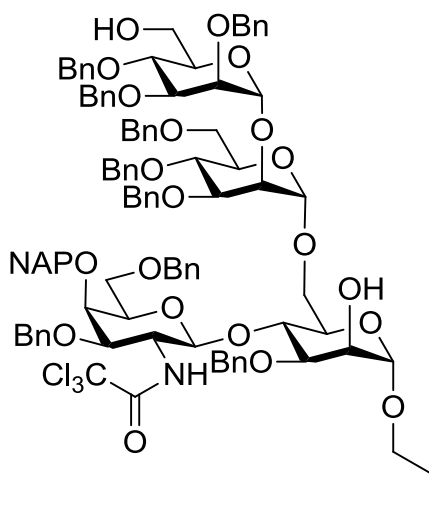
Table D.2: NMR data of pentasaccharide 7. Chemical shifts in curly brackets indicate overlapping with other signals. Therefore a multiplicity could not be assigned. (n.d. = not determined).

Materials and Methods:

2D-ROESY NMR experiments: Tetrasaccharide **4** (20 mM) and pentasaccharide **7** (10 mM) were dissolved in degassed D₂O (ROTH) under an argon atmosphere and measured at 25 °C on a *Varian PremiumCOMPACT 600* (600 MHz) spectrometer. Mixing time for the experiments was set to 600 ms and relaxation delay (d1) to 4 s.

Synthetic Procedures:

n-Propyl 2,3,4-tri-*O*-benzyl- α -D-mannopyranosyl-(1 \rightarrow 2)-3,4,6-tri-*O*-benzyl- α -D-mannopyranosyl-(1 \rightarrow 6)-3-*O*-benzyl-4-*O*-(3,6-di-*O*-benzyl-4-*O*-2-naphthylmethyl-2-deoxy-2-trichloroacetamido- β -D-galactopyranosyl)- α -D-mannopyranoside (**6**)

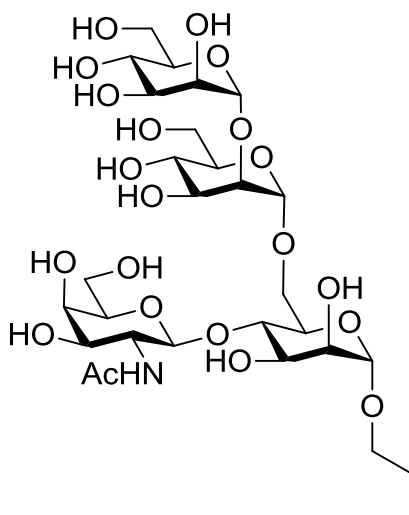


Tetrasaccharide **5**^{*} (60 mg, 0.029 mmol) was dissolved in MeCN (4 mL) and water (2 drops). Sc(OTf)₃ (14.4 mg, 0.029 mmol) was added to the solution, which was heated up to 50 °C for 2.5 h (*R_f* (SiO₂, *n*-hexane/ethyl acetate 2:1) = 0.17 of the mono alcohol). Hydrazine monohydrate (100 μ L, 2.04 mmol, 64wt%) was added to the solution, which was stirred for 18 h at r.t. and was exposed to air. The reaction mixture was diluted with ethyl acetate (25 mL), washed with 0.1 N HCl (2x 20 mL) and sat. sodium bicarbonate solution (2x 20 mL), dried over sodium sulphate, filtered and evaporated to dryness. The residue was purified using flash column chromatography to give diol **6** (35 mg, 0.019 mmol, 67% yield) as colorless amorphous solid: *R_f* (SiO₂, *n*-hexane/ethyl acetate 3:2) = 0.33; $[\alpha]_{20}^D$: + 28.9 (*c* = 3.5, CHCl₃); ATR-FTIR (cm⁻¹): 3431, 3089, 3063, 3030, 2924, 2872, 1719, 1454, 1364, 1052, 1028, 982; ¹H NMR (600 MHz, CDCl₃) δ 7.82 – 7.77 (m, 1H), 7.70 (dt, *J* = 6.8, 5.9 Hz, 2H), 7.64 (s,

* For the preparation of this compound see chapter 2 of this PhD thesis.

1H), 7.48 – 7.40 (m, 3H), 7.35 (d, $J = 7.0$ Hz, 2H), 7.33 – 7.13 (m, 41H), 7.12 – 7.08 (m, 2H), 5.12 – 5.05 (m, 3H, GalNAc-1), 4.97 (d, $J = 11.6$ Hz, 1H), 4.90 (d, $J = 11.1$ Hz, 1H), 4.85 (dd, $J = 11.1, 4.5$ Hz, 2H), 4.81 (s, 1H), 4.69 (dd, $J = 12.0, 8.4$ Hz, 2H), 4.64 (dd, $J = 11.3, 6.5$ Hz, 2H), 4.58 (t, $J = 12.0$ Hz, 2H), 4.55 – 4.42 (m, 7H), 4.39 (d, $J = 11.3$ Hz, 1H), 4.30 (d, $J = 11.6$ Hz, 1H), 4.17 (d, $J = 11.6$ Hz, 1H), 4.10 – 4.03 (m, 3H), 4.02 – 3.96 (m, 2H), 3.92 – 3.80 (m, 9H), 3.79 – 3.60 (m, 10H), 3.56 (dt, $J = 9.6, 6.8$ Hz, 1H), 3.46 (dd, $J = 8.5, 4.9$ Hz, 1H), 3.36 (dt, $J = 9.7, 6.5$ Hz, 1H), 2.30 (bs, 2H, 2x OH), 1.61 – 1.50 (m, 2H, CH₂ of *n*-propyl), 0.89 (t, $J = 7.4$ Hz, 3H, Me of *n*-propyl); ¹³C NMR (151 MHz, CDCl₃) δ 162.21 (amide), 138.70, 138.68, 138.63, 138.57, 138.55, 138.44, 138.43, 137.95, 137.76, 136.05, 133.28, 133.10, 128.58, 128.55, 128.46, 128.42, 128.40, 128.36, 128.34, 128.19, 128.12, 128.02, 128.00, 127.91, 127.89, 127.87, 127.87, 127.83, 127.81, 127.79, 127.76, 127.73, 127.71, 127.64, 127.61, 127.54, 127.50, 127.49, 126.87, 126.45, 126.12, 125.95, 99.67, 99.28, 99.26, 98.81, 92.78 (CCl₃), 80.30, 79.74, 78.30, 77.77, 75.50, 75.28, 75.26, 75.08, 75.02, 74.76, 74.58, 73.70, 73.64, 73.49, 73.36, 72.89, 72.56, 72.48, 72.42, 72.33, 72.30, 72.18, 72.08, 70.52, 69.57, 69.49, 68.78, 68.74, 66.75, 62.93, 56.42, 22.79 (CH₂ of *n*-propyl), 10.87 (Me of *n*-propyl); ESI-MS: m/z [M+Na]⁺ calcd for C₁₀₃H₁₁₀Cl₃NO₂₁ 1825.6567, obsd 1825.6507.

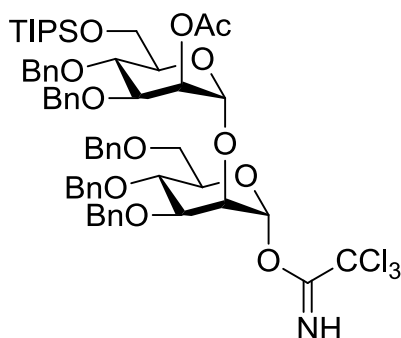
***n*-Propyl α -D-mannopyranosyl-(1 \rightarrow 2)- α -D-mannopyranosyl-(1 \rightarrow 6)-4-*O*-(2-deoxy-2-acetamido- β -D-galactopyranosyl)- α -D-mannopyranoside (4)**



Diol **6** (35 mg, 0.019 mmol) was dissolved in MeOH (3 mL) and THF (1 mL). Pd/C (31 mg, 0.029 mmol, 10 wt%) was added and hydrogen was bubbled through the slurry for 5 min. Afterwards the slurry was stirred for 18 h under hydrogen atmosphere before it was filtered through a syringe filter and evaporated to dryness. The residue was submitted to SEC

chromatography (Sephadex-G10, 5% EtOH in water, prepacked column from GE Healthcare) to yield tetrasaccharide **4** (11.5 mg, 0.015 mmol, 79%) as white solid: ^1H NMR (600 MHz, D_2O) δ 5.19 (d, $J = 1.5$ Hz, 1H, ManII-1), 5.05 (d, $J = 1.5$ Hz, 1H, ManIII-1), 4.87 (d, $J = 1.5$ Hz, 1H, ManI-1), 4.51 (d, $J = 8.4$ Hz, 1H, GalNAc-1), 4.09 (dd, $J = 3.1, 1.8$ Hz, 1H, ManIII-2), 4.04 (dd, $J = 3.1, 1.8$ Hz, 1H, ManII-2), 4.01 (dd, $J = 3.2, 1.8$ Hz, 1H, ManI-2), 3.98 – 3.70 (m, 20H), 3.69 – 3.64 (m, 2H), 3.57 – 3.52 (m, 1H, O- CH_2 of *n*-propyl), 2.09 (s, 3H, Me of NHAc), 1.68 – 1.59 (m, 2H, CH_2 of *n*-propyl), 0.93 (t, $J = 7.4$ Hz, 3H, Me); ^{13}C NMR (151 MHz, D_2O) δ 177.30 (amide), 104.85 (ManIII-1), 104.14 (GalNAc-1), 102.03 (ManI-1), 101.23 (ManII-1), 81.17, 79.02, 78.03, 75.87, 75.83, 73.18, 72.95, 72.76, 72.60, 72.57, 72.43 (O- CH_2 of *n*-propyl), 72.04, 71.98, 70.33, 69.57, 69.39, 68.62, 63.79, 63.70, 63.66, 55.27, 24.95 (Me of NHAc), 24.56 (CH_2 of *n*-propyl), 12.53 (Me); ESI-MS: m/z $[\text{M}+\text{Na}]^+$ calcd for $\text{C}_{29}\text{H}_{51}\text{NO}_{21}$ 772.2846, obsd 772.2867.

2-*O*-Acetyl-3,4-di-*O*-benzyl-6-*O*-triisopropylsilyl- α -D-mannopyranosyl-(1 \rightarrow 2)-3,4,6-tri-*O*-benzyl- α -D-mannopyranosyl trichloroacetimidate (9**)**

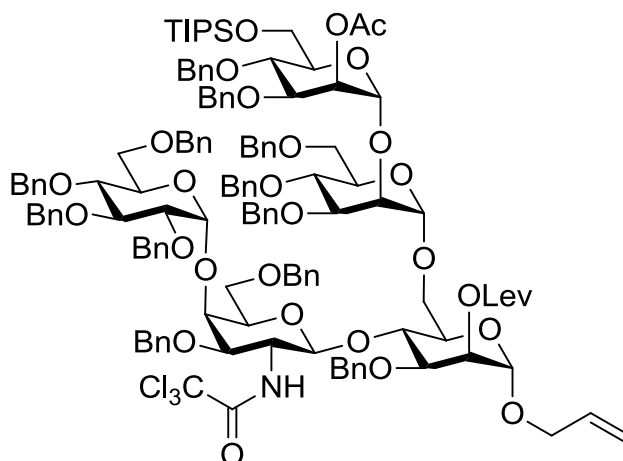


Allyl 2-*O*-acetyl-3,4-di-*O*-benzyl-6-*O*-triisopropylsilyl- α -D-mannopyranosyl-(1 \rightarrow 2)-3,4,6-tri-*O*-benzyl- α -D-mannopyranoside²²⁶ (74 mg, 0.072 mmol) was dissolved in MeOH (2 mL) and DCM (0.5 mL). PdCl_2 (4 mg, 0.023 mmol) was added to this solution. The reaction was stirred for 5 h [R_f (SiO_2 , *n*-hexane/ethyl acetate 2:1) = 0.67 of the lactol], before it was diluted with ethyl acetate (20 mL) and washed with sat. sodium bicarbonate solution (3x 20 mL). The organic layer was dried over sodium sulphate, filtered and evaporated to dryness. The residue was dissolved in DCM (1 mL) and 2,2,2-trichloroacetonitrile (72 μL , 0.718 mmol) was added. The solution was cooled down to 0°C and DBU (1.1 μL , 7.2 μmol) was added to the solution. The reaction mixture was stirred for 1 h at 0°C , before the solvents were evaporated to yield

²²⁶ The dimannoside was provided by Y.-H. Tsai and prepared according to F. John, T. L. Hendrickson, *Org. Lett.* **2010**, *12*, 2080-2083.

brown oil, which was purified using flash column chromatography on deactivated silica gel (+ 0.5% TEA) to give imidate **9** (48 mg, 0.042 mmol, 59% yield over two steps) as yellow oil: R_f (SiO_2 , *n*-hexane/ethyl acetate 10:1) = 0.28; $[\alpha]_{20}^D$: + 29.4 ($c = 0.80 \text{ CHCl}_3$); ATR-FTIR (cm^{-1}): 3065, 3032, 2892, 2865, 1745, 1672, 1455, 1368, 1102, 1050, 1028; $^1\text{H NMR}$ (400 MHz, CDCl_3) δ 8.53 (s, 1H, NH), 7.39 – 7.13 (m, 25H), 6.29 (d, $J = 1.9 \text{ Hz}$, 1H), 5.51 – 5.49 (m, 1H, =CH), 4.90 (d, $J = 3.3 \text{ Hz}$, 1H), 4.87 (d, $J = 3.3 \text{ Hz}$, 1H), 4.72 – 4.59 (m, 6H), 4.50 (d, $J = 12.1 \text{ Hz}$, 1H), 4.44 (d, $J = 11.1 \text{ Hz}$, 1H), 4.12 (t, $J = 2.4 \text{ Hz}$, 1H), 4.09 – 3.86 (m, 8H), 3.83 – 3.77 (m, 2H), 3.73 – 3.68 (m, 1H), 2.11 (s, 3H, Me of Ac), 1.17 – 1.02 (m, 21H, TIPS); $^{13}\text{C NMR}$ (101 MHz, CDCl_3) δ 170.32 (ester), 160.27 (imine), 138.93, 138.54, 138.36, 138.30, 138.10, 128.57, 128.50, 128.47, 128.42, 128.41, 128.31, 128.24, 128.07, 128.01, 127.91, 127.87, 127.72, 127.67, 127.63, 127.54, 99.31, 97.07, 91.11 (CCl_3), 78.99, 78.16, 75.51, 75.35, 75.01, 74.10, 74.04, 73.69, 73.45, 72.46, 72.44, 72.16, 69.08, 68.90, 62.55, 45.99, 21.12, 18.19 (TIPS), 18.12 (TIPS), 12.25 (TIPS); ESI-MS: m/z $[\text{M}+\text{Na}]^+$ calcd for $\text{C}_{60}\text{H}_{74}\text{Cl}_3\text{NO}_{12}\text{Si}$ 1158.3927, obsd 1158.3992.

Allyl 2-*O*-acetyl-3,4-di-*O*-benzyl-6-*O*-triisopropylsilyl- α -D-mannopyranosyl-(1 \rightarrow 2)-3,4,6-tri-*O*-benzyl- α -D-mannopyranosyl-(1 \rightarrow 6)-3-*O*-benzyl-4-*O*-(2,3,4,6-tetra-*O*-benzyl- α -D-glucopyranosyl-(1 \rightarrow 4)-3,6-di-*O*-benzyl-2-deoxy-2-trichloroacetamido- β -D-galactopyranosyl)-2-*O*-levulinyl- α -D-mannopyranoside (10**)**

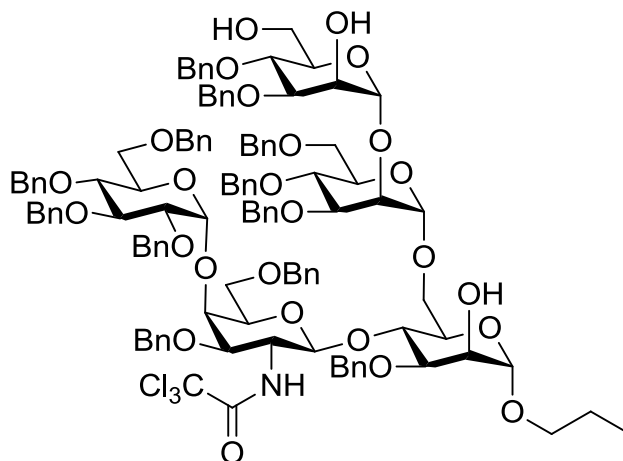


A mixture of trichloroacetimidate **9** (43.3 mg, 0.038 mmol) and trisaccharide **8**^{*} (45 mg, 0.032 mmol) was co-evaporated with toluene (3x2 mL). The residue was then dissolved in toluene (1 mL). Molecular sieves (4Å, 100 mg) was added and the slurry was stirred for 20 min.

^{*} The trisaccharide was provided by Y.-H. Tsai and prepared according to Ref. [104].

Afterwards the reaction mixture was cooled down to 0°C and TBSOTf (2 μ L, 8.7 μ mol) was added. After 1 h, TEA (50 μ L) was added and the reaction mixture was filtered through a pad of Celite®. The filtrate was evaporated to dryness to give a yellow oil that was purified by silica gel column chromatography to afford pentasaccharide **10** (50 mg, 0.021 mmol, 66% yield) as white foam: R_f (SiO₂, EtOAc/Hexane 1:2) = 0.49; $[\alpha]_D^{20} = +42.3$ (c = 2.30, CHCl₃); ATR-FTIR (cm⁻¹): 3088, 3064, 3030, 2926, 2866, 1742, 1719, 1454, 1363, 1236, 1139, 1072, 1051, 1028, 1012; ¹H NMR (400 MHz, CDCl₃) δ 7.42 – 6.97 (m, 60H), 5.84 – 5.72 (m, 1H, =CH), 5.47 (s, 1H), 5.27 (s, 1H), 5.23 – 5.06 (m, 4H), 4.98 (d, J = 3.1 Hz, 1H, Glc-1), 4.91 – 4.80 (m, 3H), 4.78 – 4.44 (m, 15H), 4.42 – 4.27 (m, 4H), 4.23 – 3.78 (m, 23H), 3.75 – 3.62 (m, 5H), 3.60 – 3.56 (m, 1H), 3.52 (dd, J = 9.9, 3.1 Hz, 1H, Glc-2), 3.46 (dd, J = 9.5, 5.8 Hz, 1H), 3.23 (d, J = 9.9 Hz, 1H), 3.09 (dd, J = 14.0, 6.9 Hz, 1H), 2.88 (d, J = 10.1 Hz, 1H), 2.50 – 2.31 (m, 4H, CH₂ of Lev), 2.05 (s, 3H), 1.98 (s, 3H), 1.15 – 1.02 (m, 21H); ¹³C NMR (101 MHz, CDCl₃) δ 206.05 (ketone), 172.08, 170.19 (2x ester), 161.95 (amide), 139.06, 138.91, 138.66, 138.61, 138.54, 138.52, 138.39, 138.35, 138.33, 138.28, 138.03, 133.33, 128.51, 128.47, 128.45, 128.42, 128.37, 128.33, 128.31, 128.26, 128.20, 127.99, 127.94, 127.83, 127.77, 127.75, 127.68, 127.64, 127.62, 127.55, 127.48, 127.44, 127.33, 127.17, 118.31, 100.09 (Glc-1, $J_{C,H} = 171$ Hz), 98.95 (GalNAc-1, $J_{C,H} = 164$ Hz), 98.91 ($J_{C,H} = 175$ Hz), 98.53 ($J_{C,H} = 172$ Hz), 96.32 ($J_{C,H} = 170$ Hz), 92.67 (CCl₃), 82.15, 80.69, 80.18, 78.10, 77.87, 77.36, 76.61, 75.53, 75.39, 75.29, 74.98, 74.75, 73.97, 73.89, 73.64, 73.60, 73.52, 73.42, 73.33, 73.24, 72.89, 72.31, 71.97, 71.85, 71.46, 70.80, 70.07, 69.67, 69.37, 68.96, 68.02, 67.84, 67.65, 66.34, 62.66, 56.40, 37.88, 31.76, 29.81, 29.71, 28.11, 21.08, 18.22, 18.13, 12.24; ESI-MS: m/z [M+Na]⁺ calcd for C₁₃₅H₁₅₆Cl₃NO₂₉Si 2412.9513, obsd 2412.9582.

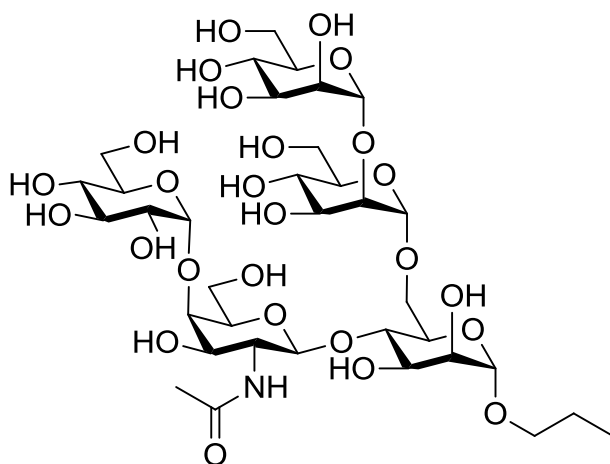
Propyl **3,4-di-*O*-benzyl- α -D-mannopyranosyl-(1 \rightarrow 2)-3,4,6-tri-*O*-benzyl- α -D-mannopyranosyl-(1 \rightarrow 6)-3-*O*-benzyl-4-*O*-(2,3,4,6-tetra-*O*-benzyl- α -D-glucopyranosyl-(1 \rightarrow 4)-3,6-di-*O*-benzyl-2-deoxy-2-trichloroacetamido- β -D-galactopyranosyl)- α -D-mannopyranoside (**11**)**



Fully protected pentasaccharide **10** (50 mg, 0.021 mmol) was dissolved in MeCN (1 mL) and water (1 drop) was added. Sc(OTf)₃ (10.3 mg, 0.021 mmol) was added and the resulting solution was heated to 50°C for 5 h [R_f (SiO₂, *n*-hexane/ethyl acetate 2:1) = 0.18]. Afterwards hydrazine monohydrate (103 μ L, 2.091 mmol, 64wt%) was added and the solution was stirred for 18 h at r.t. exposed to air. The solution was diluted with chloroform (20 mL) and washed with 1 N HCl (2x 20 mL). The organic layer was dried over magnesium sulphate, filtered and evaporated to dryness. The residue was purified by silica gel column chromatography to afford triol **11** (15 mg, 7.4 μ mol, 34% yield over three steps) as colorless oil: R_f (SiO₂, EtOAc/*n*-hexane 3:2) = 0.32; $[\alpha]_D^{20} = + 52.7$ ($c = 0.10$, CHCl₃); ATR-FTIR (cm⁻¹): 3089, 3064, 3031, 2927, 2873, 1715, 1454, 1101, 1069, 1028; ¹H NMR (400 MHz, CDCl₃) δ 7.35 – 7.05 (m, 60H), 6.94 – 6.90 (m, 1H), 5.14 (d, $J = 8.2$ Hz, 1H, GalNAc-1), 5.06 (d, $J = 1.7$ Hz, 1H), 5.05 – 5.01 (m, 2H), 4.83 (dd, $J = 11.0, 2.5$ Hz, 2H), 4.80 – 4.64 (m, 9H), 4.62 – 4.49 (m, 7H), 4.47 – 4.39 (m, 2H), 4.34 (d, $J = 11.5$ Hz, 1H), 4.29 (d, $J = 10.6$ Hz, 1H), 4.22 – 3.96 (m, 10H), 3.94 – 3.60 (m, 18H), 3.59 – 3.49 (m, 3H), 3.37 (dd, $J = 11.1, 2.3$ Hz, 1H), 3.35 – 3.29 (m, 1H), 2.96 (d, $J = 9.1$ Hz, 1H), 1.59 – 1.47 (m, 2H, CH₂ of *n*-propyl), 0.86 (t, $J = 7.4$ Hz, 3H, Me of *n*-propyl); ¹³C NMR (101 MHz, CDCl₃) δ 162.05 (amide), 139.15, 138.95, 138.81, 138.56, 138.51, 138.45, 138.42, 138.33, 138.30, 138.22, 138.12, 138.02, 128.72, 128.61, 128.58, 128.54, 128.50, 128.41, 128.39, 128.27, 128.13, 128.07, 128.04, 128.00, 127.97, 127.90, 127.82, 127.78, 127.73, 127.69, 127.66, 127.58, 127.54, 127.49, 127.42, 127.10, 101.07, 100.16, 99.04, 98.82, 98.45, 92.65 (CCl₃), 82.05, 80.58, 80.20, 80.11, 78.28, 77.89, 77.48, 77.36, 77.16, 76.84, 76.36, 75.34, 75.15, 74.80, 74.47, 73.59, 73.42, 73.24, 72.44,

72.36, 72.32, 72.19, 71.86, 71.70, 70.98, 70.75, 69.38, 68.74, 68.33, 67.98, 67.34, 62.59, 56.21, 22.77 (CH₂ of *n*-propyl), 10.89 (Me of *n*-propyl); ESI-MS: *m/z* [M+Na]⁺ calcd for C₁₁₉H₁₃₀Cl₃NO₂₆ 2118.7856, obsd 2118.7838.

***n*-Propyl** **α-D-mannopyranosyl-(1→2)-α-D-mannopyranosyl-(1→6)-4-O-(α-D-glucopyranosyl-(1→4)-2-deoxy-2-acetamido-β-D-galactopyranosyl)-α-D-mannopyranoside (7)**



Triol **11** (15 mg, 7.2 μmol) was dissolved in MeOH (2 mL). Pd/C (10.7 mg, 10.2 μmol, 10 wt%) was added and hydrogen was bubbled through the slurry for 5 min. Afterwards the slurry was stirred for 18 h under hydrogen atmosphere before it was filtered through a syringe filter and evaporated to dryness. The residue was submitted to SEC chromatography (Sephadex-G10, 5% EtOH in water, prepacked column from GE Healthcare) to yield pentasaccharide **7** (6 mg, 6.6 μmol, 92%) as white solid: ¹H NMR (600 MHz, D₂O) δ 5.19 (d, *J* = 1.6 Hz, 1H), 5.05 (d, *J* = 1.6 Hz, 1H), 4.96 (d, *J* = 3.9 Hz, 1H, Glc-1), 4.87 (d, *J* = 1.7 Hz, 1H), 4.57 (d, *J* = 8.4 Hz, 1H, GalNAc-1), 4.14 – 4.10 (m, 1H), 4.09 (dd, *J* = 3.2, 1.8 Hz, 1H), 4.06 (d, *J* = 2.8 Hz, 1H), 4.05 – 4.03 (m, 1H), 4.01 – 3.98 (m, 3H), 3.98 – 3.94 (m, 2H), 3.94 – 3.85 (m, 6H), 3.85 – 3.74 (m, 10H), 3.74 – 3.71 (m, 2H), 3.70 – 3.62 (m, 2H), 3.59 – 3.53 (m, 2H), 3.51 – 3.47 (m, 1H), 2.09 (s, 3H, NHAc), 1.68 – 1.60 (m, 2H, CH₂ of *n*-propyl), 0.94 (t, *J* = 7.4 Hz, 3H, Me); ¹³C NMR (151 MHz, D₂O) δ 177.29, 104.84, 104.55, 102.83, 101.94, 101.22, 81.16, 79.59, 79.30, 78.09, 75.86, 75.83, 75.29, 74.55, 74.41, 72.94, 72.87, 72.77, 72.67, 72.56, 72.39, 72.13, 72.04, 71.80, 69.55, 69.39, 68.65, 63.78, 63.68, 62.97, 62.51, 55.12, 24.93, 24.56, 12.55; ESI-MS: *m/z* [M+Na]⁺ calcd for C₃₅H₆₁NO₂₆ 934.3380, obsd 934.3387.